1983

Theory and application of collision integrals for rigid ovaloids

Robert G. Cole
Iowa State University

INFORMATION TO USERS

This reproduction was made from a copy of a document sent to us for microfilming. While the most advanced technology has been used to photograph and reproduce this document, the quality of the reproduction is heavily dependent upon the quality of the material submitted.

The following explanation of techniques is provided to help clarify markings or notations which may appear on this reproduction.

1. The sign or "target" for pages apparently lacking from the document photographed is "Missing Page(s)". If it was possible to obtain the missing page(s) or section, they are spliced into the film along with adjacent pages. This may have necessitated cutting through an image and duplicating adjacent pages to assure complete continuity.

2. When an image on the film is obliterated with a round black mark, it is an indication of either blurred copy because of movement during exposure, duplicate copy, or copyrighted materials that should not have been filmed. For blurred pages, a good image of the page can be found in the adjacent frame. If copyrighted materials were deleted, a target note will appear listing the pages in the adjacent frame.

3. When a map, drawing or chart, etc., is part of the material being photographed, a definite method of "sectioning" the material has been followed. It is customary to begin filming at the upper left hand corner of a large sheet and to continue from left to right in equal sections with small overlaps. If necessary, sectioning is continued again—beginning below the first row and continuing on until complete.

4. For illustrations that cannot be satisfactorily reproduced by xerographic means, photographic prints can be purchased at additional cost and inserted into your xerographic copy. These prints are available upon request from the Dissertations Customer Services Department.

5. Some pages in any document may have indistinct print. In all cases the best available copy has been filmed.

University
Microfilms
International
300 N. Zeeb Road
Ann Arbor, MI 48106

Cole, Robert G.

THEORY AND APPLICATION OF COLLISION INTEGRALS FOR RIGID OVALOIDS

Iowa State University PH.D. 1983

Theory and application of collision integrals for rigid ovaloids

by

Robert G. Cole

A Dissertation Submitted to the

Graduate Faculty in Partial Fulfillment of the

Requirements for the Degree of

DOCTOR OF PHILOSOPHY

Department: Chemistry
Major: Physical Chemistry

Approved:

Signature was redacted for privacy.

In Charge of Major Work

Signature was redacted for privacy.

For the Major Department

Signature was redacted for privacy.

For the Graduate College

Iowa State University
Ames, Iowa

1983

TABLE OF CONTENTS

I. INTRODUCTION

In 1872, Ludwig Boltzmann (1) proposed an equation governing the evolution of the singlet distribution function (i.e., a probability density for locating a particle of the system in a particular phase at a given time) for a dilute gas. This equation, which now bears his name, is a nonlinear integrodifferential equation. A solution to the Boltzmann equation, one which would reproduce or possibly even extend the understanding of macroscopic physics of the day, proved extremely difficult to secure.

A satisfactory method of obtaining a solution to this equation for general systems was not found until some forty years later. At that time, Chapman (2) and Enskog (3) independently developed a method which yields successive approximations to the solution of the Boltzmann equation (BE). This method allowed for successive approximations to the hydrodynamic equations to be written. That is, the Chapman-Enskog method successively generates the nondissipative Euler, linear phenomenological Navier-Stokes, Burnett, and higher order hydrodynamic equations. Consequently, the Chapman-Enskog (C-E) solution has successfully allowed for the calculation of the transport properties of dilute gases (4,5).

In 1921, Enskog empirically modified the BE appropriate to rigid spheres in order to account for high density effects (6). The Enskog equation (EE), because it is very similar in structure to the Boltzmann equation, can be handled using the C-E method. Experimental and theoretical comparisons have shown that the EE successfully incorporates (to first order) high density effects (4,5).

The great successes in calculating the transport properties of atomic systems provided the motivation to generalize these methods to the study of polyatomic fluids. Curtiss and his collaborators (7,8) extended the classical Boltzmann equation, allowing for the examination of phenomena peculiar to nonspherical molecules. This polyatomic BE, and its high density counterpart, the polyatomic EE, have been applied to the simplest of polyatomic systems (i.e., the loaded sphere and the rough sphere) by Dahler and associates (9,10). In 1969, Hoffman (11) demonstrated that it is a fairly simple matter to obtain numerical results from the BE for systems interacting through any general rigid convex potential. Since that time, Hoffman and co-workers have utilized the above mentioned techniques to study gas phase transport properties for various model systems. These systems include simple systems composed of linear (12) and spherical top molecules (13), and diatom-diatom (14) and spherical top-spherical top (15) mixtures. Also, viscosities and thermal conductivities of dense fluids composed of rigid ellipsoids and rigid ellipsoids surrounded by a square well have been calculated by Dahler and Theodosopulu (16).

These techniques have proven extremely useful in that they allow for a relatively simple and inexpensive calculation of transport properties for rather complex systems. In brief, these methods assume that the dynamics of the system are adequately determined by the impulsive part of the molecular potential. The impulsive core is assumed to have a rigid convex geometry. Furthermore, it is assumed that the phases of any two particles in the fluid are dynamically uncorrelated prior to

their collision. Thus, complicated n-body collision events are neglected and the time evolution of the many body system is determined by means of the collision dynamics of two isolated molecules. Finally, the two body dynamics are assumed to be chatterless. A chattering collision is a recollision event between two rigid, nonspherical bodies without the intervention of a third body.

It is the objective of this work to examine further applications of these methods. Specifically, gas phase studies of (1) Senftleben-Beenakker effects in simple systems composed of symmetric top molecules (Chapter III) and (2) chiral molecules in the presence of an external magnetic field (Chapter IV) are carried out. Due to the complicated structure of these molecules, the models and methods discussed in the previous paragraphs represent the only existing methods which are feasible for calculating the transport properties of these systems. Later chapters are devoted to liquid phase studies of (1) orientational relaxation phenomena in atom-diatom fluids (Chapter V) and (2) shear-orientational couplings in simple diatomic fluids, as measured by the Rytov parameter obtained from Depolarized Light Scattering (DPLS) (Chapter VI). Finally, a discussion of chattering events is given (Chapter VII), along with possible methods for the incorporation of these events into kinetic theory calculations.

We begin our study by discussing, in Chapter II, the derivation of and methods of solution to the Boltzmann and the Enskog equations. This treatment will serve as a guide to the following chapters.

II. THEORY OF THE BOLTZMANN AND ENSKOG EQUATIONS FOR RIGID OVALOIDS

A. Derivations

We will (unless explicitly stated otherwise) consider only a single component fluid of N molecules having rotational structure. The generalization of our discussion to mixtures is obvious. The N molecule Hamiltonian is

$$H^{(N)}(\underline{x}^N) = \sum_{i=1}^{N} \{K_i(\underline{p}_i, \underline{L}_i) + \phi_i(\underline{r}_i, \underline{\alpha}_i)\} + \sum_{i \neq j} V_{ij}(\underline{r}_i \underline{\alpha}_i ; \underline{r}_j \underline{\alpha}_j) \qquad (2.1)$$

where K_i is the kinetic energy of molecule i, ϕ_i is the potential energy of particle i due to the presence of an external field, and V_{ij} is the intermolecular potential acting between i and j. Throughout this work, $\underline{r}_i$ represents the Cartesian coordinates of the center of mass of molecule i, $\underline{\alpha}_i$ represents its set of Eulerian angles, and $\underline{p}_i$ and $\underline{L}_i$ its linear and angular momentum, respectively. Furthermore, we define $\underline{i}$ as the set $(\underline{\alpha}_i, \underline{p}_i, \underline{L}_i)$, $\underline{x}_i$ as the phase of molecule i (i.e., $\underline{r}_i, \underline{\alpha}_i, \underline{p}_i, \underline{L}_i$), and $\underline{x}^s$ as the set $(\underline{x}_1, \underline{x}_2, \ldots, \underline{x}_s)$.

We begin the derivation of the kinetic equation with the basic equation of statistical mechanics, the Liouville equation

$$\frac{\partial}{\partial t} F^{(N)}(\underline{x}^N, t) = -iL^{(N)} F^{(N)}(\underline{x}^N, t) \quad . \qquad (2.2)$$

Here, $F^{(N)}(\underline{x}^N, t)$ is the full N particle distribution function normalized to unity, $L^{(N)}$ is the N particle Liouville operator defined by

$$L^{(N)} = i\{H^{(N)}, \ \} \quad , \qquad (2.3)$$

with {A,B} denoting the Poisson Bracket. For a system interacting through a pairwise additive potential, the macroscopic quantities which characterize the fluid can be expressed as averages in terms of the singlet and pair distribution functions. Reduced distribution functions, $f^{(s)}(\underline{x}^s,t)$, are defined in terms of $F^{(N)}(\underline{x}^N,t)$ by

$$f^{(s)}(\underline{x}^s,t) = [N!/(N-s)!] \int \prod_{i=1}^{N} d\underline{x}_i F^{(N)}(\underline{x}^N,t) \tag{2.4}$$

where $f^{(s)}(\underline{x}^s,t)d\underline{x}^s dt$ is the probability of finding any s particles of the original N, in phase $\underline{x}^s$, regardless of the positions and momenta of the remaining N-s particles. By integration of Liouville's equation over $\underline{x}_{s+1}$ through $\underline{x}_N$, the reduced distribution functions can be shown to obey the equations

$$\{\frac{\partial}{\partial t} + iL^{(s)}\}f^{(s)}(\underline{x}^s,t) = \sum_{j=1}^{s} \int d\underline{x}_{s+1}\{V_{j,s+1}, f^{(s+1)}(\underline{x}^{s+1},t)\} \tag{2.5}$$

which express the evolution of $f^{(s)}$ in terms of $f^{(s+1)}$. This set of coupled equations is known as the BBGKY hierarchy (17-20). The first equation of this hierarchy is

$$\{\frac{\partial}{\partial t} + iL^{(1)}\}f^{(1)}(\underline{x},t) = J_{12}(f^{(2)}) \tag{2.6}$$

where

$$J_{ij}(f^{(2)}) = \int d\underline{x}_j \{V_{ij}, f^{(2)}\} \quad . \tag{2.7}$$

Defining the Liouville operator for free streaming as

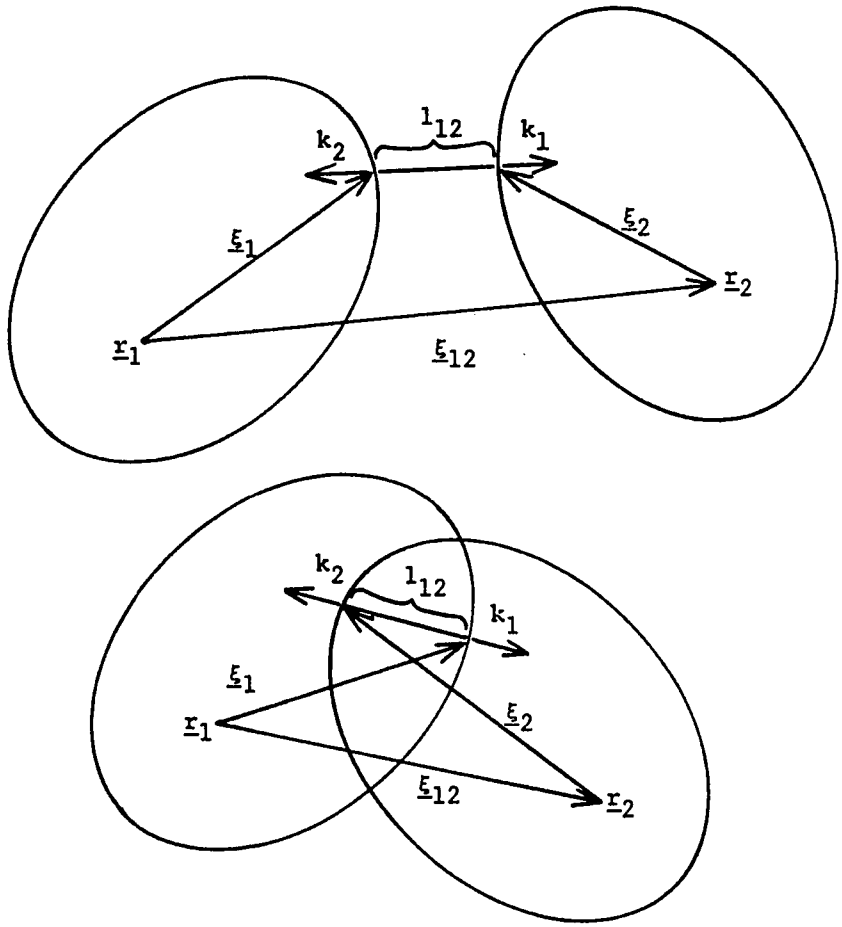

Figure 2.1. Collision geometry for rigid ovaloids in nonoverlapping and overlapping configurations

$$L_0^{(s)} = i\{H_0^{(s)}, \} \quad , \tag{2.8}$$

allows $J_{12}(f^{(2)})$ to be expressed as

$$J_{12}(f^{(2)}) = -\int d\underline{x}_2 (iL^{(2)} - iL_0^{(2)}) f^{(2)}(\underline{x}_1 \underline{x}_2 t) \tag{2.9}$$

or

$$J_{12}(f^{(2)}) = \lim_{\varepsilon \to 0_+} \varepsilon^{-1} \int d\underline{x}_2 (e^{-iL^{(2)}\varepsilon} - e^{-iL_0^{(2)}\varepsilon}) f^{(2)}(\underline{x}_1 \underline{x}_2 t) \quad . \tag{2.10}$$

In Eq. (2.8), $H_0^{(s)}$, the interactionless s particle Hamiltonian, is defined by

$$H_0^{(s)} = \sum_{i=1}^{s} \{K_i(\underline{x}_i) + \phi_i(x_i)\} \quad . \tag{2.11}$$

The quantities $\exp \pm iL^{(2)}\varepsilon$ and $\exp \pm iL_0^{(2)}\varepsilon$ are the two particle interacting and noninteracting streaming operators. The -(+) sign refers to backward (forward) streaming.

For a system composed of rigid convex ovaloids, the intermolecular potential is given by

$$V_{ij}(\underline{r}_i \alpha_i ; \underline{r}_j \alpha_j) = \begin{cases} \infty & \text{if } \ell_{ij} \leq 0 \\ 0 & \text{if } \ell_{ij} > 0 \end{cases} \tag{2.12}$$

where ℓ_{ij} is the minimum distance between the surfaces of bodies i and j. For overlapping configurations, ℓ_{ij} is defined as the maximum distance between the overlapping portions of the surfaces of bodies i and j (refer to Figure 2.1). Due to the geometry of this potential, it is

convenient to carry out the volume integration in Eq. (2.10) as an integral over ℓ_{12} and $\hat{k}_1$. From Figure 2.1, $\underline{r}_{ij}$ $(= \underline{r}_j - \underline{r}_i)$, is seen to equal

$$\underline{r}_{12} = \underline{\xi}_{12} + \ell_{12}\hat{k}_1 \tag{2.13}$$

where $\underline{\xi}_{ij} = \underline{\xi}_i - \underline{\xi}_j$ and $\underline{\xi}_i$ is defined as the vector extending from the center of mass of body i to the point on the surface which is closest to (for nonoverlapping configurations) or farthest from (for overlapping configurations) the surface of the jth body. The Jacobian of the transformation from $\underline{r}_{12}$ to $(\ell_{12},\hat{k}_1)$, required for the variable transformation,

$$d\underline{r}_{12} = d\ell_{12}d\hat{k}_1 S \tag{2.14}$$

can be shown from Eq. (2.13) to equal (21)

$$S = \left|\partial(\underline{\xi}_{12} + \ell_{12}\hat{k}_1)/\partial\hat{k}_1\right|_{\perp\hat{k}_1} , \tag{2.15}$$

which is the determinate of $\partial(\underline{\xi}_{12} + \ell_{12}\hat{k}_1)/\partial(\hat{k}_1)$ in the subspace orthogonal to $\hat{k}_1$. Using the above transformation, $J_{12}(f^{(2)})$ becomes

$$J_{12}(f^{(2)}) = \lim_{\varepsilon \to 0_+} \varepsilon^{-1} \int d\underline{2}d\hat{k}Sd\ell_{12}(e^{-iL^{(2)}\varepsilon} - e^{-iL_0^{(2)}\varepsilon})f^{(2)} . \tag{2.16}$$

Because the interaction in a single impulsive hit is instantaneous, the integrand is zero except in the region $-|\dot{\ell}_{12}|\varepsilon \le \ell_{12} \le |\dot{\ell}_{12}|\varepsilon$, for a vanishingly short time ε, where $\dot{\ell}$ is the time rate of change of ℓ. On the precollisional surface of the excluded volume (the excluded volume

being defined as the volume excluded to the center of mass of body two in configuration $\underline{\alpha}_2$ due to the presence of body one in configuration $\underline{\alpha}_1$ at position $\underline{r}_1$) the only contribution to the integral is from the region $-|\dot{\ell}|\varepsilon \leq \ell \leq 0$. Here, the action of the streaming operators on $f^{(2)}$ is

$$(e^{-iL^{(2)}\varepsilon} - e^{-iL_0^{(2)}\varepsilon})f^{(2)}(\underline{x}_1,\underline{x}_2,t) = -f^{(2)}(\underline{x}_1,\underline{x}_2,t) \tag{2.17}$$

where we have used the result that $\exp - iL^{(2)}\varepsilon f^{(2)}(\underline{x}_1,\underline{x}_2,t)$ vanishes in this region. This is due to the fact that for two colliding molecules to have penetrated essentially requires (1) an infinite relative momentum because of energy conservation and (2) that $f^{(2)}(\underline{x}_1,\underline{x}_2,t)$ approaches zero as the momentum of particles one and/or two approach infinity. Similarly, on the postcollisional surface, the contribution is from the region $0 \leq \ell < |\dot{\ell}|\varepsilon$. Here,

$$(e^{-iL^{(2)}\varepsilon} - e^{-iL_0^{(2)}\varepsilon})f^{(2)}(\underline{x}_1,\underline{x}_2,t) = f^{(2)}(\underline{x}_1',\underline{x}_2',t) \tag{2.18}$$

where it is assumed that $f^{(2)}$ vanishes identically for overlapping configurations. The primes in Eq. (2.18) denote the prehit momentum (i.e., the momentum just prior to the impulse). Utilizing these results, along with the Mean Value Theorem of Calculus, we find that $J_{12}(f^{(2)})$ becomes

$$J_{12}(f^{(2)}) = \int d\underline{2}d\hat{k}S\dot{\ell}f^{(2)^*}(\underline{r}_1,\underline{1};\ \underline{r}_1+\underline{\xi}_{12},\underline{2},t) \tag{2.19}$$

where

$$f^{(2)^*}(\underline{x}_1,\underline{x}_2,t) = \begin{cases} f^{(2)}(\underline{x}_1,\underline{x}_2,t) & \text{if } \dot{\ell} < 0 \\ f^{(2)}(\underline{x}_1',\underline{x}_2',t) & \text{if } \dot{\ell} > 0 \end{cases} . \tag{2.20}$$

Furthermore, we obtain

$$\{\frac{\partial}{\partial t} + iL^{(1)}\}f^{(1)}(\underline{x}_1,t) = \int d\underline{2}d\hat{k}S\hat{k}\cdot g\ f^{(2)^*}(\underline{r}_1,\underline{1};\ \underline{r}_1+\underline{\xi}_{12},\underline{2},t) \tag{2.21}$$

by writing $\dot{\ell}$ as $\hat{k}\cdot g$, where g is the relative velocity of the contact points, i.e.,

$$g = \underline{v}_2 - \underline{v}_1 + \underline{\omega}_2 \times \underline{\xi}_2 - \underline{\omega}_1 \times \underline{\xi}_1 . \tag{2.22}$$

Here, $\underline{v}_i$ and $\underline{\omega}_i$ are the linear and angular velocity of molecule i, respectively. This equation was first derived by Curtiss and Dahler (8) using identical techniques. It should be noted that Eq. (2.21) is an exact consequence of the Liouville equation for rigid convex ovaloids. An alternate derivation of Eq. (2.21) as found in Chapter VII.

In order to obtain a closed equation for $f^{(1)}$, various approximations must be made on Eq. (2.21). One approximation we choose to make at this point is to ignore the existence of chattering collisions, i.e., multiple hit events between isolated pairs of molecules. The existence of such events is obviously related to the nonspherical nature of the interaction potential, which permits the collision, or encounter, to consist of one or more hits. (See Chapter VII for a discussion of chattering events.) The neglect of chattering allows the interpretation of $f^{(2)^*}$ as a function of the precollisional state of molecules one and two (as opposed to a prehit state, see Chapter VII). One further assumption must be made. It will be assumed that $f^{(2)^*}$ factorizes as

$$f^{(2)*}(\underline{r}_1,\underline{1};\ \underline{r}_1+\underline{\xi}_{12},\underline{2},t) = \chi(\underline{r}_1\underline{\alpha}_1,\underline{r}_1+\underline{\xi}_{12},\underline{\alpha}_2)f^{(1)*}(\underline{r}_1\underline{1}t)f^{(1)*}(\underline{r}_1+\underline{\xi}_{12},\underline{2}t) \tag{2.23}$$

where χ represents a nonequilibrium radial distribution function which is independent of the momentum of particles one and two. Equation (2.23) implies that prior to a collision the states of the two particles are dynamically uncorrelated, which is a generalization of Boltzmann's assumption of molecular chaos.

The traditional factorization of $f^{(2)*}$ (6), leading to the Enskog equation, treats χ as having the form of the equilibrium radial distribution function dependent on the nonequilibrium density at a particular space point, i.e.,

$$\begin{aligned}\chi(\underline{r}_1\underline{\alpha}_1,\underline{r}_2\underline{\alpha}_2,t) &= \chi^{(E)}(\underline{r}_1\underline{\alpha}_1,\underline{r}_2\underline{\alpha}_2|n(\underline{R},t)) \\ &= W(\underline{r}_1\underline{\alpha}_1,\underline{r}_2\underline{\alpha}_2)\{1 + n(\underline{R},t)\int d\underline{r}_3 d\underline{\alpha}_3\ Z(\underline{r}_1\underline{\alpha}_1,\underline{r}_2\underline{\alpha}_2|\underline{r}_3\underline{\alpha}_3) \\ &\quad + \frac{1}{2!}n^2(\underline{R},t)\int d\underline{r}_3 d\underline{\alpha}_3 d\underline{r}_4 d\underline{\alpha}_4\ Z(\underline{r}_1\underline{\alpha}_1,\underline{r}_2\underline{\alpha}_2|\underline{r}_3\underline{\alpha}_3\underline{r}_4\underline{\alpha}_4) \\ &\quad + \ldots\}\ .\end{aligned} \tag{2.24}$$

Here, $\underline{R}$ is some "reasonable" point between the mass centers of the two particles. For hard spheres of equal size, $\underline{R}$ is obviously the point of contact, but for general hard ovaloid systems identification of $\underline{R}$ is not obvious. Also, $W(\underline{r}_1\underline{\alpha}_1,\underline{r}_2\underline{\alpha}_2)$ and $Z(\underline{r}_1\underline{\alpha}_1,\underline{r}_2\underline{\alpha}_2|\underline{r}_3\underline{\alpha}_3)$ are defined in terms of the Mayer functions, f_{ij} ($f_{ij} = \exp -\beta V_{ij} - 1$), as

$$W(\underline{r}_i\underline{\alpha}_i,\underline{r}_j\underline{\alpha}_j) = 1 + f_{ij} \tag{2.25}$$

and

$$Z(\underline{r}_i\underline{\alpha}_i, \underline{r}_j\underline{\alpha}_j | \underline{r}_k\underline{\alpha}_k) = f_{ik}f_{jk} \quad . \tag{2.26}$$

For a listing of the higher order $Z(\underline{r}_i\underline{\alpha}_i, \underline{r}_j\underline{\alpha}_j | \underline{r}_k\underline{\alpha}_k \ \ldots \ \underline{r}_n\underline{\alpha}_n)$, the reader is referred to the literature (22,23). However, this choice for χ is inconsistent with the force-flux relations of nonequilibrium thermodynamics (24).

To remedy this inconsistency, Van Beijeren and Ernst (25) have chosen χ to be the equilibrium radial distribution function for a fluid with a nonuniform density. Thus, they expand $\chi(\underline{r}_i\underline{\alpha}_i, \underline{r}_j\underline{\alpha}_j)$ as (26)

$$\begin{aligned}\chi^{(ME)}(\underline{r}_1\underline{\alpha}_1, \underline{r}_2\underline{\alpha}_2, t) = W(\underline{r}_1\underline{\alpha}_1, \underline{r}_2\underline{\alpha}_2)\{1 + \int d\underline{r}_3 d\underline{\alpha}_3 n(\underline{r}_3, t)\ Z(\underline{r}_1\underline{\alpha}_1, \underline{r}_2\underline{\alpha}_2 | \underline{r}_3\underline{\alpha}_3) \\ + \frac{1}{2!}\int d\underline{r}_3 d\underline{\alpha}_3 d\underline{r}_4 d\underline{\alpha}_4 n(\underline{r}_3 t) n(\underline{r}_4 t) \\ \times Z(\underline{r}_1\underline{\alpha}_1, \underline{r}_2\underline{\alpha}_2 | \underline{r}_3\underline{\alpha}_3, \underline{r}_4\underline{\alpha}_4) + \ldots\} \quad .\end{aligned} \tag{2.27}$$

Using Eq. (2.27) for χ, we obtain what is referred to as the Modified Enskog equation which is consistent with nonequilibrium thermodynamics (27). An expansion of the densities in a Taylor series about some point $\underline{R}$ and insertion of the result into $\chi^{(ME)}$ produces an expansion of $\chi^{(ME)}$ in terms of gradients of the density,

$$\begin{aligned}\chi^{(ME)}(\underline{r}_1\underline{\alpha}_1, \underline{r}_2\underline{\alpha}_2, t) = \chi^{(E)}(\underline{r}_1\underline{\alpha}_1, \underline{r}_2\underline{\alpha}_2 | n(\underline{R}, t)) + \int d\underline{r}_3 d\underline{\alpha}_3 \\ \times H(\underline{r}_1\underline{\alpha}_1, \underline{r}_2\underline{\alpha}_2, \underline{r}_3\underline{\alpha}_3 | n(\underline{R}, t))(\underline{r}_3 - \underline{R}) \cdot \frac{\partial}{\partial \underline{R}} n(\underline{R}, t) \\ + O(\nabla^2)\end{aligned} \tag{2.28}$$

where

$$H(\underline{r}_1\underline{\alpha}_1,\underline{r}_2\underline{\alpha}_2,\underline{r}_3\underline{\alpha}_3|n(\underline{R},t)) = Z(\underline{r}_1\underline{\alpha}_1,\underline{r}_2\underline{\alpha}_2|\underline{r}_3\underline{\alpha}_3) + n(\underline{R},t)\int d\underline{r}_4 d\underline{\alpha}_4 \times Z(\underline{r}_1\underline{\alpha}_1,\underline{r}_2\underline{\alpha}_2|\underline{r}_3\underline{\alpha}_3,\underline{r}_4\underline{\alpha}_4) + \ldots \quad . \tag{2.29}$$

This expansion suggests that the "best" $\underline{R}$ to choose is the one which satisfies the equation

$$\underline{R} = \int d\underline{r}_3 d\underline{\alpha}_3 \; H(\underline{r}_1\underline{\alpha}_1,\underline{r}_2\underline{\alpha}_2,\underline{r}_3\underline{\alpha}_3 \; n(\underline{R},t))\underline{r}_3 \quad , \tag{2.30}$$

(Van Beijeren and Ernst show this choice of $\underline{R}$ to be $\underline{r}_1 + \frac{1}{2}\underline{r}_{12}$ for the case of identical spheres (25)) since, for this choice, $\chi^{(ME)}$ and $\chi^{(M)}$ agree through first order in the gradients.

Neglecting the existence of chattering events and factoring $f^{(2)^*}$ as described above, we have that

$$\{\frac{\partial}{\partial t} + iL^{(1)}\}f^{(1)}(\underline{r}_1,\underline{1},t) = \int d\underline{2}d\hat{k}S\hat{k}\cdot g \; \chi^{(E)}(\underline{r}_1\underline{\alpha}_1,\underline{r}_1+\underline{\xi}_{12}\underline{\alpha}2|n(\underline{R},t)) \times f^{(1)^*}(\underline{r}_1,\underline{1},t)f^{(1)^*}(\underline{r}_1+\underline{\xi}_{12},\underline{2},t) \tag{2.31}$$

which is the Enskog equation appropriate to rigid ovaloids. Assuming the spatial gradients in the fluid to be small, we can expand $\chi^{(E)}$ and $f^{(1)^*}(\underline{r}_1+\underline{\xi}_{12})$ about $\underline{r}_1$ to obtain

$$\chi^{(E)}(\underline{r}_1\underline{\alpha}_1,\underline{r}_1+\underline{\xi}_{12}\underline{\alpha}_2|n(\underline{R},t)) = \chi^{(E)}(\underline{\alpha}_1,\underline{\alpha}_2,k|n(\underline{r}_1,t)) + \underline{\xi}_R \cdot \frac{\partial}{\partial \underline{r}_1}\chi^{(E)}(\underline{\alpha}_1,\underline{\alpha}_2,k|n(\underline{r}_1,t)) + \ldots \tag{2.32}$$

and

$$f^{(1)*}(\underline{r}_1+\underline{\xi}_{12},\underline{2},t) = f^{(1)*}(\underline{r}_1,\underline{2},t) + \underline{\xi}_{12}\cdot\frac{\partial}{\partial\underline{r}_1} f^{(1)*}(\underline{r}_1,\underline{2},t) + \ldots \tag{2.33}$$

where $\underline{\xi}_R = \underline{R} + \underline{r}_1$. Inserting these expansions into Eq. (2.31) gives, to first order in the gradients,

$$\begin{aligned}\{\frac{\partial}{\partial t} + iL^{(1)}\}f^{(1)}(\underline{r}_1,\underline{1},t) &= \int d\underline{2}d\hat{k}S\hat{k}\cdot g\ \chi(\underline{\alpha}_1,\underline{\alpha}_2,k|n(\underline{r}_1,t)) \\ &\times f^{(1)*}(\underline{r}_1,\underline{1},t)f^{(1)*}(\underline{r}_1,\underline{2},t) + \int d\underline{2}d\hat{k}S\hat{k}\cdot g\ f^{(1)}(\underline{r}_1,\underline{1},t) \\ &\times \{\chi(\underline{\alpha}_1,\underline{\alpha}_2,\hat{k}|n(\underline{r}_1,t))\underline{\xi}_{12}\cdot\frac{\partial}{\partial\underline{r}_1} f^{(1)}(\underline{r}_1,\underline{2}^*,t) \\ &+ f^{(1)}(\underline{r}_1,\underline{2}^*,t)\underline{\xi}_R\cdot\frac{\partial}{\partial\underline{r}_1}\chi(\underline{\alpha}_1,\underline{\alpha}_2,\hat{k}|n(\underline{r}_1,t))\}\ .\end{aligned} \tag{2.34}$$

This is the form of the Enskog equation which is used in the applications discussed in Chapter V.

The Boltzmann equation, which is applicable to the special case of a dilute gas, can be obtained as a limiting form of the Enskog equation. In the limit of infinite dilution, two simplifications to Eq. (2.34) are immediate. Firstly, in a dilute gas, all many body effects vanish; therefore, we can set $\chi = 1$. Secondly, inhomogeneities in the gas are negligible over distances on the order of a few molecular diameters and, therefore, the gradient terms appearing in Eq. (2.34) drop out. Thus, the dilute gas equation is

$$\{\frac{\partial}{\partial t} + iL^{(1)}\}f^{(1)}(\underline{r}_1,\underline{1},t) = \int d\underline{2}d\hat{k}S\hat{k}\cdot g\ f^{(1)}(\underline{r}_1,\underline{1}^*,t)f^{(1)}(\underline{r}_1,\underline{2}^*,t)\ . \tag{2.35}$$

However, this equation is not yet in the form of the well-known Boltzmann equation, because the second assumption made in this paragraph places rather severe restrictions on the solutions of Eq. (2.35), which are consistent with a simpler equation. We wish to make these restrictions explicit. By ignoring all spatial variations on the order of r_0 ($r_0 \sim$ molecular diameter), we are simultaneously neglecting all phenomena which vary rapidly wrt time scales $O(r_0/\langle v_{12}\rangle) \sim t_c$, where $\langle v_{12}\rangle$ is the average relative velocity. Thus, this assumption allows us to replace Eq. (2.35) with a simpler equation, obtained by averaging Eq. (2.35) over a time $O(t_c)$. This is equivalent to integrating out all of the rapidly varying quantities. This yields

$$\{\frac{\partial}{\partial t} + \overline{iL^{(1)}}\}f^{(1)}(\underline{r}_1,\overline{\underline{1}},t) = \int d\underline{\eta}_1 d\underline{\eta}_2 \int d\underline{2}d\hat{k}\hat{S}\hat{k}\cdot g\, f^{(1)}(\underline{r}_1,\overline{\underline{1}}^*,t) \times f^{(1)}(\underline{r}_1,\overline{\underline{2}},t) \qquad (2.36)$$

where $f^{(1)}(\underline{r}_1,\underline{1},t)$ has been replaced with $\Delta_1^{-1}f^{(1)}(\underline{r}_1,\overline{\underline{1}},t)$, with $\Delta_i = \int d\underline{\eta}_i$. Here, $\underline{\eta}_i$ represents the set of rapidly varying molecular quantities, and i represents the remaining molecular variables hereafter referred to as the free flight invariants. The function $f^{(1)}(\underline{r}_1,\overline{\underline{1}},t)$, referred to as the Boltzmann distribution function, is the time average of $f^{(1)}(\underline{x}_1,t)$ over a period τ, such that $\tau \gtrsim t_c$. (For convenience, the symbol $f^{(1)}$ will be used for both the time averaged and nonaveraged singlet distribution functions. The function meant will be clear by its context. Where the two must be distinguished, the function arguments $(\underline{r}_1,\overline{\underline{1}},t)$ or $(\underline{x}_1,t)$ will be given.) For a system of rigid polyatomic molecules, the set, $\underline{\eta}_i$, generally contains the angular coordinates and

the set, $\underline{\bar{i}}$, generally denotes the linear and angular momenta. However, the situation is complicated somewhat in the case of symmetric top molecules where there exists an additional free flight invariant, namely the projection of the angular momentum onto the symmetry axis of the molecule. This situation is discussed more fully in Chapter II. Equation (2.36) is the well-known Boltzmann equation. It is explicit in Eq. (2.36) that the solution of the Boltzmann equation is a function of the free flight invariants alone.

This concludes the derivations of the Enskog (Eq. (2.31)) and the Boltzmann (Eq. 2.36)) equations. For a more complete discussion of these equations for simple fluids, the reader is referred to the literature (4,5,28,29). For a thorough discussion of the derivation and formal properties of the Boltzmann equation appropriate to a system of rigid ovaloids, the reader is referred to the article by Hoffman and Dahler (30).

B. Solutions

In this section, we will discuss the methods by which approximate solutions to the kinetic equations are obtained. The first method we discuss, that of Chapman (2) and Enskog (3), relies on the distinction of two time scales on which the fluid relaxes to equilibrium (4). These two time scales, denoted by t_k and t_h, are related to the mean free time between collisions and the typical time required for a particle to transverse distances comparable to the dimension of the fluid, respectively. The Chapman-Enskog (C-E) method is essentially a perturbation expansion in t_k/t_h. For this reason, it is applicable only when

the fluid density is high enough so that $t_k/t_h \ll 1$. Under this condition, the fluid is assumed to approach equilibrium in two states. For a time of $O(t_k)$, the fluid is in the process of equilibriating locally. During this process, occurring during the so-called kinetic stage, the time evolution of the fluid is governed by the full singlet distribution function as determined from the initial condition at the beginning of the stage. For times long compared to t_k, the molecules have undergone several collisions establishing a local equilibrium which is characterized by the hydrodynamical fields, i.e., $n(\underline{r},t)$, $\underline{u}(\underline{r},t)$, and $T(\underline{r},t)$, the number density, streaming velocity, and temperature, respectively. For times $O(t_h)$, the local fields characterizing the fluid relax according to the equations of hydrodynamics; the distribution function is determined by the hydrodynamic fields in this relaxation process. Thus, "memory" of the initial conditions, except for the hydrodynamics fields, which correspond to the first three moments of the distribution, are lost in this stage.

An alternate solution to the kinetic equations was developed by Grad (31). Grad's method of moments depends on the existence of a contraction in the number of moments of the distribution necessary to adequately describe the system as the fluid equilibriates. The method involves expansion of the solution to the Enskog or Boltzmann equation in terms of the contracted set of functions corresponding to these moments. Since such a contraction occurs for a wide variety of phenomena, this method is broadly applicable, whereas the C-E method is appropriate to fluids with small gradients and densities which are not too low. In

philosophy, there is, however, a close correspondence between the methods.

For the sake of generality, we will work with the Enskog equation

$$\{\frac{\partial}{\partial t} + iL^{(1)}\}f^{(1)} = \hat{J}(F^{(1)}|f^{(1)}) \tag{2.37}$$

where $\hat{J}(f^{(1)}|f^{(1)}$ is the collision operator and $iL^{(1)}$ is explicitly

$$iL^{(1)} = \underline{v}_1 \cdot \frac{\partial}{\partial \underline{r}_1} + \underline{\omega}_1 \cdot i\hat{J}_1 + \underline{F}_1 \cdot \frac{\partial}{\partial \underline{p}_1} + \underline{N}_1 \cdot \frac{\partial}{\partial \underline{L}_1} \quad . \tag{2.38}$$

Here,

$$i\hat{J}_1 = \hat{e}_1 \times \frac{\partial}{\partial \hat{e}_1} \tag{2.39}$$

is the rotation operator, $\underline{F}_1$ represents the force, and $\underline{N}_1$ the torque experienced by molecule one due to the presence of an external field. We will only consider the existence of an external field when discussing dilute gases and then confine our attention to an external magnetic field. For this reason, we will discuss an equation of the form

$$\{\frac{\partial}{\partial t} + \underline{v}_1 \cdot \frac{\partial}{\partial \underline{r}_1} + \underline{\omega}_1 \cdot i\hat{J}_1\}f^{(1)} = -\overline{\hat{F}(f^{(1)})} + \hat{J}(f^{(1)}|f^{(1)}) \tag{2.40}$$

where

$$\overline{F(f^{(1)})} = \overline{\underline{N}}_1 \cdot \frac{\partial}{\partial \underline{L}_1} f^{(1)} \tag{2.41}$$

is the time average of the field operator over a period equal to t_c. Here, the quantity $\overline{\underline{N}}$, the time average torque, is given by

$$\overline{\underline{N}} = \underline{\mu} \times \underline{H} \tag{2.42}$$

where $\underline{H}$ is the applied magnetic field and $\underline{\mu}$ is the molecular magnetic dipole averaged over the rapidly varying molecular quantities (refer to the reduction of the Enskog equation to the Boltzmann equation above).

Not all of the terms in Eq. (2.40) act on the same time scale. In order to scale the individual terms in the Enskog equation, we will transform to dimensionless variables. First, we define

l_h = a characteristic macroscopic length (i.e., dimension of vessel)

r_0 = typical range of molecular interaction

$\langle v_{rel} \rangle$ = average relative velocity $\sim (kT/\mu_{rel})^{1/2}$

$\langle v \rangle$ = average molecular velocity $\sim (kT/m)^{1/2}$

$\langle \omega \rangle$ = average rotational velocity $\sim (kT/I)^{1/2}$ (2.43)

t_{rel} = mean time between collisions $\sim (nr_0^2 \langle v_{rel} \rangle)^{-1}$

t_h = mean travel time for distances $O(l_h)$, $\sim l_h/\langle v \rangle$

t_ω = mean reorientation time $\sim \langle \omega \rangle^{-1}$

t_L = inverse Lamar frequency $= (H\beta_{nucl}/\hbar)$ where β_{nucl} = nuclear magneton

along with the dimensionless quantities (denoted with a tilde)

$$\begin{aligned} t &= t_h \tilde{t} \\ \underline{r} &= l_h \tilde{\underline{r}} \\ \underline{p}/m &= \langle v \rangle \tilde{\underline{v}} \\ \underline{\omega} &= \langle \omega \rangle \tilde{\underline{\omega}} \\ \underline{L} &= \hbar \tilde{\underline{L}} \end{aligned} \tag{2.44}$$

$$\underline{\mu} = \beta_{nucl}\,\tilde{\underline{\mu}}$$
$$g = \langle v_{rel}\rangle \tilde{g}$$
$$S = r_0^2\,\tilde{S}$$
$$f^{(1)}(\underline{x}_1)d\underline{x}_1 = n(m\langle v\rangle\hbar)^{-3}\,\tilde{f}^{(1)}(\tilde{\underline{x}}_1)d\tilde{\underline{x}}_1 \quad .$$

In terms of these dimensionless quantities, the Enskog equation becomes

$$\{\frac{\partial}{\partial \tilde{t}} + \tilde{\underline{v}}_1 \cdot \frac{\partial}{\partial \tilde{\underline{r}}} + \varepsilon_\omega \tilde{\underline{\omega}} \cdot i\hat{J}_1\}f^{(1)} = \varepsilon^{-1}\tilde{\Lambda}(\tilde{f}^{(1)}|\tilde{f}^{(1)}) \tag{2.45}$$

where $\tilde{\Lambda}(\tilde{f}^{(1)}|\tilde{f}^{(1)})$ ($\Lambda(f^{(1)}\ f^{(1)})$ used below is similarly defined) is

$$\tilde{\Lambda}(\tilde{f}^{(1)}|\tilde{f}^{(1)} = -\varepsilon_L \tilde{\underline{\mu}} \times \tilde{H} \cdot \frac{\partial}{\partial \tilde{\underline{L}}}\tilde{f}^{(1)} + \tilde{J}(\tilde{f}^{(1)}|\tilde{f}^{(1)}) \quad , \tag{2.46}$$

$\tilde{J}(\tilde{f}^{(1)}|\tilde{f}^{(1)})$ is simply the collision operator defined entirely in terms of dimensionless quantities, and the marking parameters are

$$\varepsilon = t_{rel}/t_h$$
$$\varepsilon_L = t_{rel}/t_L \tag{2.47}$$
$$\varepsilon_\omega = t_h/t_\omega \quad .$$

Equation (2.45) gives us an indication of the relative importance of the processes in competition in the fluid. The parameter, ε_ω, measures the importance of molecular reorientation in the fluid. For high densities and highly anisotropic geometries, $\varepsilon_\omega \sim 1$. In Chapters V and VI, we will examine orientational correlation times and light scattering phenomena in this regime. For low densities, $\varepsilon_\omega \to 0$; this is the reason the Boltzmann equation is averaged over the rapidly varying quantities. The parameter ε_L is a measure of the competition between

the effects of the magnetic field versus the collisional effects. This competition gives rise to the Senftleben-Beenakker effects to be discussed in Chapter III. Finally, the parameter ε gauges the relative importance of the free streaming versus the collisional relaxation in the fluid. This competition is central to the C-E method of solving Eq. (2.40).

1. Chapman-Enskog

The starting point for the implementation of the Chapman-Enskog method is to rewrite Eq. (2.40) (motivated by Eq. (2.45)) as

$$\{\frac{\partial}{\partial t} + \underline{v}_1 \cdot \frac{\partial}{\partial \underline{r}_1} + \underline{\omega}_1 \cdot i\hat{J}_1\} f^{(1)} = \varepsilon^{-1} \Lambda(f^{(1)}|f^{(1)}) \qquad (2.48)$$

where ε is to be treated as a dimensionless marking parameter. From Eq. (2.47), ε can be interpreted as the ratio of the mean free path to some typical macroscopic length in the system. Next, we assume that $f^{(1)}(\underline{x}_1,t)$ can be expanded in a power series in ε, as

$$f^{(1)}(\underline{x}_1,t) = f_0^{(1)}(\underline{x}_1,t)\{1 + \varepsilon\phi(\underline{x}_1,t) + \theta(\varepsilon^2)\} \quad . \qquad (2.49)$$

The C-E solution follows by substituting this expansion into Eq. (2.48) and equating the coefficients of like powers in ε. Because ϕ is proportional to gradients of the local fields, we are required to associate an ε with each order of the gradients in $J(f^{(1)}|f^{(1)})$ (refer to Eq. (2.34) above). To lowest order, this procedure generates the equation

$$\theta(\varepsilon^{-1}): \int d\underline{2}d\hat{k}\hat{S}k\cdot g \; \chi f_0^{(1)}(\underline{1}) f_0^{(1)}(\underline{2}) = 0 \quad , \qquad (2.50)$$

the solution of which is the Maxwell-Boltzmann (local) equilibrium distribution function given by

$$f_0^{(1)}(\underline{x}_1,t) = An(\underline{r}_1,t)T^{-\alpha/2}(\underline{r}_1,t) \times \exp -\{\frac{(\underline{p}_1 - m\underline{u}(\underline{r}_1,t))^2}{2mkT(\underline{r}_1,t)} + \frac{E_{int}}{kT(\underline{r}_1,t)}\} . \tag{2.51}$$

Here, α is the number of active degrees of freedom of the molecule and A is chosen such that $f_0^{(1)}(\underline{x}_1,t)$ is normalized to the local number density. Also, n, $\underline{u}$, and T are chosen to be the local values of the number density, streaming velocity, and temperature, respectively. This choice forces the distortion, $\varepsilon\phi + \theta(\varepsilon^2)$, to be orthogonal to 1, $\underline{v}$, and $(p - m\underline{u})^2/2m + E_{int}$. It is convenient to impose this condition to every order in ε so that ϕ itself is orthogonal to these quantities. In Eq. (2.51), E_{int} represents the internal energy of the molecule. To second lowest order, we have

$$\theta(\varepsilon^0): \quad \mathcal{D}^{(E)} f_0^{(1)}(\underline{x}_1,t) = -f_0^{(1)}\hat{F}(\phi) - f_0^{(1)}K_E(\phi) = \hat{\Lambda}^{(E)}\phi \tag{2.52}$$

where the inhomogeneous term is (32)

$$\mathcal{D}^{(E)} f_0^{(1)} = \{\frac{\partial_0}{\partial t} + \underline{v}_1 \cdot \frac{\partial}{\partial \underline{r}_1} + \underline{\omega}_1 \cdot i\hat{J}_1\} f_0^{(1)} - \frac{1}{2}\int d\underline{2}d\hat{k}S\hat{k}\cdot g\, f_0^{(1)}(\underline{r}_1,\underline{1}^*,t)$$
$$\times \{2\chi\underline{\xi}_{12} \cdot \frac{\partial}{\partial \underline{r}_1} f_0^{(1)}(\underline{r}_1,\underline{2}^*,t) + f_0^{(1)}(\underline{r}_1,\underline{2}^*,t)\underline{\xi}_{12} \cdot \frac{\partial}{\partial \underline{r}_1}\chi\} \tag{2.53}$$

and the collision term is given by

$$\hat{K}_E\phi = -\int d\underline{2}d\hat{k}S\hat{k}\cdot g\, \chi f_0^{(1)}(\underline{r}_1,\underline{2},t)[\phi(\underline{r}_1,\underline{1}^*,t) + \phi(\underline{r}_1,\underline{2}^*,t)] \quad . \tag{2.54}$$

It is not the full time derivative of $f_0^{(1)}$ which appears in Eq. (2.53). We have indicated this by placing a subscript zero on the time derivative symbol (i.e., $\partial_0/\partial t$). The interpretation of this operation is derived from the solubility conditions on Eq. (2.52) which are discussed below. We are not interested in the expressions obtained from equating higher order terms in ε.

As was already mentioned, the solution to Eq. (2.50) is known and is given by Eq. (2.51). Implicit in the expansion of $f^{(1)}$ about this lowest order solution is the idea that we are seeking a solution to Eq. (2.40) in the hydrodynamic regime, where the fluid is close to a state of local equilibrium. In this regime, $f^{(1)}$ is a functional of the local hydrodynamic fields (33). A solution of this form is termed a "Normal Solution". Such is the case of $f_0^{(1)}$,

$$\mathcal{D}^{(E)} f_0^{(1)} = f_0^{(1)}\{\left(\frac{\partial_0}{\partial t} \ln n + \underline{v}_1 \cdot \frac{\partial}{\partial \underline{r}_1} \ln n\right) + \left[W_1^2 + \Omega_1^2 - \frac{\alpha}{2}\right] \times \left(\frac{\partial_0}{\partial t} \ln T + \underline{v}_1 \cdot \frac{\partial}{\partial \underline{r}_1} \ln T\right) + \sqrt{\frac{2m}{kT}}\, \underline{W}_1 \cdot \left(\frac{\partial_0}{\partial t} \underline{u} + \underline{v}_1 \cdot \frac{\partial}{\partial \underline{r}_1} \underline{u}\right)\} \tag{2.55}$$

where $\underline{W}_i$ and $\underline{\Omega}_i$, the reduced linear and angular momentum, are defined by

$$\underline{W}_i = (\underline{p}_i - m\underline{u})/\sqrt{2mkT} \tag{2.56a}$$

and

$$\underline{\Omega}_i = \underline{L}_i/\sqrt{2IkT} \quad . \tag{2.56b}$$

Now recall that for a solution to a linear equation such as Eq. (2.52) to exist (34), the inhomogeneous term, $\mathcal{D}^{(E)} f_0^{(1)}$, must be orthogonal (35) to the solutions of the adjoint of the corresponding homogeneous equation, $\Lambda^{(E)\dagger}\psi = 0$. These solutions are well-known (4) and are

$$\psi_1 = m_1 \tag{2.57a}$$

$$\underline{\psi}_2 = m_1 \underline{v}_1 \tag{2.57b}$$

and

$$\psi_3 = \frac{1}{2} m v_1^2 + E_{int} \quad . \tag{2.57c}$$

Explicitly these solubility conditions are

$$\int d\underline{1} \psi_i(\underline{x}_1) \mathcal{D}^{(E)} f_0^{(1)}(\underline{x}_1, t) = 0 \tag{2.58}$$

which can be written as

$$\begin{aligned} 0 = {} & \frac{\partial}{\partial t} \{ \int d\underline{1} \psi_i(\underline{1}) f_0^{(1)}(\underline{x}_1, t) \} + \frac{\partial}{\partial \underline{r}_1} \cdot \{ \int d\underline{1} \underline{v}_1 \psi_i(\underline{1}) f_0^{(1)} \} \\ & - \int d\underline{1} d\underline{2} d\hat{k} S\hat{k} \cdot g (\psi_i(\underline{1}^{pre}) - \psi_i(\underline{1}^{post})) \times \{ \frac{1}{2} \chi \underline{\xi}_{12} \cdot \frac{\partial}{\partial \underline{r}_1} f_0^{(1)}(\underline{1}) f_0^{(1)}(2) \\ & + \frac{1}{2} f_0^{(1)}(\underline{1}) f_0^{(1)}(\underline{2}) \underline{\xi}_{12} \cdot \frac{\partial}{\partial \underline{r}_1} \chi \} \end{aligned} \tag{2.59}$$

where the superscripts indicate functions of the pre- or post-collisional momentum.

The three solubility equations obtained from Eq. (2.59) by letting $i = 1$, 2, and 3 determine the reduced time derivatives (i.e., $\partial_0/\partial t$) of

the local fields in $\mathcal{D}^{(E)} f_0^{(1)}(\underline{x},t)$. The three conditions are:

(1) for $\psi_i = m_1$,

$$\frac{\partial_0}{\partial t} \ln n + \underline{u} \cdot \frac{\partial}{\partial \underline{r}} \ln n = - \frac{\partial}{\partial \underline{r}} \cdot \underline{u} \quad , \tag{2.60}$$

(2) for $\psi_i = m\underline{v}_1$,

$$\frac{\partial_0}{\partial t} \underline{u} + \underline{u} \cdot \frac{\partial}{\partial \underline{r}} \underline{u} = - \frac{1}{\rho} \frac{\partial}{\partial \underline{r}} \cdot \underline{\underline{P}}_0 \quad , \tag{2.61}$$

(3) for $\psi_i = \frac{1}{2} m v_1^2 + E_{int}$,

$$\frac{\partial_0}{\partial t} \ln T + \underline{u} \cdot \frac{\partial}{\partial \underline{r}} \ln T = - \frac{P_0}{C_V T} \frac{\partial}{\partial \underline{r}} \cdot \underline{u} \quad . \tag{2.62}$$

Equation (2.60) is just the hydrodynamic Equation of Continuity. Equation (2.61) is Euler's Equation of Motion where $\rho = nm$ and P_0 is the hydrostatic pressure tensor. Explicitly

$$\underline{\underline{P}}_0 = (P_0^{(K)} + P_0^{(V)}) \underline{\underline{U}}^{(3)} \tag{2.63}$$

where $\underline{\underline{U}}^{(3)}$ is the unit tensor (isotropic) and

$$P_0^{(K)} = \frac{1}{3} \int d\underline{1}m \, C_1^2 \, f_0^{(1)} \tag{2.64}$$

$$P_0^{(V)} = - \frac{1}{12} \int d\underline{1}d\underline{2}d\hat{k}Sk \cdot g \, K\chi f_0^{(1)} f_0^{(1)} \hat{k} \cdot \underline{\xi}_{12} \quad . \tag{2.65}$$

Finally, Eq. (2.62) is Euler's Energy Balance Equation written in terms of the temperature, where C_V ($= \alpha/2$ kT) is the heat capacity at constant volume. In deriving Eqs. (2.61) and (2.62), use of the previous solubility conditions was made.

Using the solubility conditions to eliminate the time derivatives in $\mathcal{D}^{(E)} f_0^{(1)}(\underline{x}_1,t)$, we obtain, after much algebra, the final form

$$\mathcal{D}^{(E)} f_0^{(1)}(\underline{x}_1,t) = f_0^{(1)} \{ [\frac{P_0}{\rho}\sqrt{\frac{2m}{kT}}\,(W_1^2 + \Omega_1^2 - \frac{\alpha}{2} - 1)\underline{W}_1 + \underline{\tilde{H}}_T(1)] \cdot \frac{\partial}{\partial \underline{r}} \ln T$$
$$+ [\frac{P_0}{nkT} 2\underline{W}_1\underline{W}_1 - \frac{P_0}{C_V T}(W_1^2 + \Omega_1^2 - \frac{\alpha}{2}) - \frac{P_0}{nkT}\underline{\underline{U}}^{(3)}$$
$$+ \underline{\underline{\tilde{H}}}_u(1)] : \frac{\partial}{\partial \underline{r}}\underline{u}\} \qquad (2.66)$$

for the inhomogeneity, where the functions $\underline{\tilde{H}}_T(1)$ and $\underline{\underline{\tilde{H}}}_u(1)$ are

$$\underline{\tilde{H}}_T = \frac{1}{2kT}\int d\underline{2}d\hat{k}\hat{S}k\cdot g\ \chi f_0^{(1)}(\underline{2})[E_1^* - E_2^*]\underline{\xi}_{12} \qquad (2.67a)$$

and

$$\underline{\underline{\tilde{H}}}_u = \frac{1}{2kT}\int d\underline{2}d\hat{k}\hat{S}k\cdot g\ \chi f_0^{(1)}(\underline{2})Kk\underline{\xi}_{12} \qquad (2.67b)$$

In Eq. (2.67a), E represents the energy of molecule i as measured with respect to a coordinate system moving with the streaming velocity, $\underline{u}(\underline{r},t)$. This expression for $\mathcal{D}^{(E)} f_0^{(1)}$ is identical in form to that first obtained by McCoy et al. (10) for a dense fluid of perfectly rough spheres. As a check on Eq. (2.66), we now take the dilute gas limit, $n \to 0$, in which case $P_0^{(V)}$, $\underline{\tilde{H}}_T$, and $\underline{\underline{\tilde{H}}}_u$ all vanish. This gives

$$\mathcal{D}^{(B)} f_0^{(1)} = f_0^{(1)}\{(W_1^2 + \Omega_1^2 - \frac{\alpha}{2} - 1)\underline{C}_1 \cdot \frac{\partial}{\partial \underline{r}} \ln T + [2\underline{W}_1\underline{W}_1$$
$$- \frac{2}{\alpha}(W_1^2 + \Omega_1^2)\underline{\underline{U}}^{(3)}] : \frac{\partial}{\partial \underline{r}}\underline{u}\} \qquad (2.68)$$

which is the correct dilute gas limit (30).

Using Eq. (2.66) for the inhomogeneity, we find that the equation for the distortion from the C-E method becomes

$$\mathcal{D}^{(E)} f_0^{(1)}(\underline{x}_1,t) = -\hat{\Lambda}(\phi) \tag{2.69}$$

where $\hat{\Lambda}(\phi) \equiv f_0^{(1)}(\underline{1},t)\{\hat{F}(\phi) + \hat{K}_E(\phi)\}$. Since $\hat{\Lambda}$ is a linear operator, the form for the solution can be expanded as

$$\phi = \sqrt{\frac{2kT}{n}}\,\underline{A}\cdot\frac{\partial}{\partial \underline{r}}\ln T + \underline{\underline{B}}:\frac{\partial^0}{\partial \underline{r}}\underline{u} + D\frac{\partial}{\partial \underline{r}}\cdot\underline{u} + \underline{E}\cdot\frac{\partial}{\partial \underline{r}}\times\underline{u} \tag{2.70}$$

where the functions $\underline{A}$, $\underline{\underline{B}}$, D, and $\underline{E}$ must individually satisfy the equations

$$-\tilde{\Lambda}(\underline{A}) = f_0^{(1)}\{\frac{P_0}{nkT}(W_1^2 + \Omega_1^2 - \frac{\alpha}{2} - 1)\underline{W}_1 + \sqrt{\frac{m}{2kT}}\,\underline{\tilde{H}}_T(\underline{1})\}\quad , \tag{2.71a}$$

$$-\tilde{\Lambda}(\underline{\underline{B}}) = f_0^{(1)}\{\frac{P_0}{nkT}\,2\underline{W}_1^0\underline{W}_1 + \underline{\underline{\tilde{H}}}_u(\underline{1})\}\quad , \tag{2.71b}$$

$$-\tilde{\Lambda}(D) = f_0^{(1)}\{\frac{P_0}{nkT}\frac{2}{3}W_1^2 - \frac{P_0}{C_V T}\,W_1^2 + \Omega_1^2 - \frac{\alpha}{2} - \frac{P_0}{nkT} + \frac{1}{3}\underline{\underline{\tilde{H}}}_u(\underline{1}):\underline{\underline{U}}^{(3)}\} \tag{2.71c}$$

and

$$-\tilde{\Lambda}(\underline{E}) = f_0^{(1)}\{\underline{\underline{\tilde{H}}}_u(\underline{1})\,\dot{X}\,\underline{\underline{U}}^{(3)}\}\quad . \tag{2.71d}$$

(Note that ϕ, as given by Eq. (2.70), does not contain a constant term ϕ_0 which satisfies $\tilde{\Lambda}(\phi_0) = 0$. Such a term is ruled out by our requirement that ϕ does not contribute to the hydrodynamic fields.) In the dilute gas limit, these equations reduce to

$$-\tilde{\Lambda}(\underline{A}) = f_0^{(1)}\{W_1^2 + \Omega_1^2 - \frac{\alpha}{2} - 1\}\underline{W}_1 \quad , \tag{2.72a}$$

$$-\tilde{\Lambda}(\underline{\underline{B}}) = f_0^{(1)}\{2\underline{W}_1^0\underline{W}_1\} \quad , \tag{2.72b}$$

$$-\tilde{\Lambda}(D) = f_0^{(1)}\{\frac{2}{3}W_1^2 - \frac{P_0^{(K)}}{C_V T}[W_1^2 + \Omega_1^2 - \frac{\alpha}{2}] - 1\} \tag{2.72c}$$

and

$$-\tilde{\Lambda}(\underline{E}) = 0 \quad . \tag{2.72d}$$

Therefore, the C-E method has reduced the evaluation of $f^{(1)}$, satisfying the nonlinear Enskog equation, Eq. (2.40), to the evaluation of the distortion, ϕ, satisfying a set of inhomogeneous linear integral equations of Eq. (2.71). The methods for solving such equations, when mathematically well-behaved, are well-known. Briefly, the unknowns are expanded in a complete set of polynomials (36) which is then truncated, transforming Eqs. (2.71a)-(2.71d) into a set of matrix equations (37-39). Solving these matrix equations, we obtain expressions for the distortions and, hence, the transport coefficients in terms of quantities known as bracket integrals. Because we will deal only with rigid interactions ignoring chattering, these bracket integrals take the form

$$[\underline{\underline{\xi}},\underline{\underline{\psi}}]_{\mu,\nu}^{i,u} = \frac{1}{n_\mu n_\nu}\int d\underline{1}\, f_0^{(1)}\underline{\underline{\xi}}_1\hat{K}_E\underline{\underline{\psi}} = \left(\frac{2kT}{\mu}\right)^{1/2} B^{(n)}$$
$$\times \int dk d\underline{\alpha}_i d\underline{\alpha}_j S\underline{\underline{S}}_{\xi_i}\underline{\underline{S}}_{\psi_j}\Theta_n^2(u,v)D \tag{2.73}$$

where $\underline{\underline{\xi}}$ and $\underline{\underline{\psi}}$ represent polynomials in which we have expanded the solutions to Eqs. (2.71a)-(2.71d) or Eqs. (2.72a)-(2.72d), the indices μ

and ν are species labels, and the indices i and j label the colliding molecules. Here μ is the reduced mass, n is the number of active degrees of freedom of the colliding pair, $B^{(n)}$ is a constant which depends on (n), and D is a normalization constant. The projection operators, $\underline{\underline{S}}_{\xi_i}$ and $\underline{\underline{S}}_{\xi_j}$, along with the term (u,v) which results from the momentum integrations in the collision operator, are defined in Ref. 11. The form of the bracket integrals is derived in Appendix A. These bracket integrals will appear throughout this work, since we will be able to express all of the transport coefficients or correlation fucntions which we require in terms of them.

2. Grad's method of moments

Grad's method of moments relies on the idea that as the fluid approaches equilibrium, the variables necessary to describe the fluid contract. The initial state of the fluid is adequately given only by the full set of (2f)N coordinates and momenta where f is the number of molecular degrees of freedom. Whereas at equilibrium, a thermodynamic description is adequate. In the hydrodynamic regime, Grad proposes that the singlet distribution can be expanded about equilibrium as

$$f^{(1)}(\underline{x}_1,t) = f_0^{(1)}(\underline{x}_1)\{1 + \phi(\underline{x}_1,t)\} \tag{2.74}$$

where $f_0^{(1)}$ can be understood to represent an absolute equilibrium and $\phi(\underline{x}_1,t)$, the distortion, is normalized to the local fields. The local fields may be the usual hydrodynamic fields, the number density, streaming velocity, or temperature; or they may represent more exotic

fields such as the orientation and angular momentum densities. The choice obviously depends on the phenomenon being described.

Once the appropriate fields are determined, the distortion is expanded in a finite basis set whose moments are the local fields. Substitution of this expansion of $f^{(1)}$ into the kinetic equation, Eq. (2.40), dropping terms bilinear in the distortion (assuming, of course, small distortions), using Eq. (2.50), and taking the appropriate moments, results in a set of linear algebraic equations for the expansion coefficients. The solution of these equations yields the expansion coefficients in terms of the bracket integrals of Eq. (2.73) above. Therefore, the transport coefficients and correlation times calculated using Grad's method are also given in terms of the bracket integrals.

III. SENFTLEBEN-BEENAKKER EFFECTS IN SYMMETRIC TOPS

Senftleben-Beenakker effects were first observed by Senftleben (40) who subjected the paramagnetic gas, oxygen, to an external magnetic field. Senftleben noticed that as the magnetic field strength increased, the values of the transport coefficients decreased. Similar results were observed in the paramagnetic gases, NO (41) and NO_2 (42) as well. It was Beenakker et al. (43) who first observed these effects in diamagnetic gases.

This effect was explained by Gorter (44) using the following simple picture of the gas. Due to the presence of macroscopic gradients, molecular flows are established in the gas. For a dilute gas, these flows determine the values of the transport coefficients (i.e., all transport properties of dilute gases are of a mean free type). Collisions in the system selectively eliminate from the flow particles with large effective cross sections which, in turn, creates a polarization in the angular momentum distribution in the gas. This polarization is such that it minimizes the effective collisional cross sections of the streaming molecules. The introduction of an external field destroys this $\underline{\Omega}$-polarization through Lamar precession, thus increasing the effective molecular cross sections. This, in turn, decreases the mean free path and, hence, decreases the value of the transport coefficients. Because the Senftleben-Beenakker effects depend solely on the anisotropic part of the interactions, they have been the subject of intensive investigation (45).

As mentioned above, the magnitude of this effect is measured by the dimensionless parameter $\varepsilon_L \sim t_{rel}/t_L$ which is proportional to H/n. Here t_{rel} and t_L represent the mean time between collisions for a fluid particle and the Lamar precession time, respectively. Thus, at high densities, for the effects to be measurable, the strength of the field is prohibitively large. Therefore, the Senftleben-Beenakker effects are detectable only at low densities for which the Boltzmann equation can be applied.

Our reason for investigating Senftleben-Beenakker effects for symmetric top molecules lies in the existence of an additional free flight invariant; that being the projection of the angular momentum of the molecule onto its body fixed symmetry axis. The importance of the free flight invariants was eluded to in the derivation of the Boltzmann equation (Chapter II). There it was argued that the dependence of the singlet distribution function for a dilute gas on variables other than the free flight invariants is weak. For this reason, in the Boltzmann equation, the full singlet distribution function can be replaced by its time average. This time averaging over a period, which is long compared to a rotational period but short compared to the mean free time, results in an average distribution that is a function of the free flight invariants alone.

We will first discuss the thermal conductivity and then the viscosity. The discussion of the thermal conductivity will be fairly detailed in order to familiarize the reader with techniques. Since the methods used in calculating the viscosity are nearly identical to those

for the thermal conductivity, the latter discussion will be much abbreviated. Finally, numerical results will be given.

A. Thermal Conductivity

The phenomenological equation describing the heat flow in a system with a nonzero temperature gradient is

$$\underline{q} = - \underline{\underline{\lambda}} \cdot \frac{\partial}{\partial \underline{r}} T \tag{3.1}$$

where $\underline{q}$ is the heat flux vector and $\underline{\underline{\lambda}}$ is the thermal conductivity tensor. This relationship is known as Fourier's Law. The form of $\underline{\underline{\lambda}}$ depends on the symmetry of the system. For an isotropic fluid, $\underline{\underline{\lambda}}$ reduces to a scalar multiple of the unit tensor, $\underline{\underline{U}}^{(3)}$. The introduction of an external field aligned along the $\hat{k}$ axis (i.e., $\underline{H} \| \hat{k}$) destroys the spatial isotropy. In this case, the form of $\underline{\underline{\lambda}}(\underline{H})$ becomes

$$\underline{\underline{\lambda}}(H) = \lambda_{\|} kk + \lambda_{\perp} \underline{\underline{U}}_k^{(2)} + \lambda_{tr} \underline{\underline{V}}_k^{(2)} \tag{3.2}$$

where $\underline{\underline{U}}_k^{(2)} = \underline{\underline{U}}^{(3)} - \hat{k}\hat{k}$, $\underline{\underline{V}}_k^{(2)} = \underline{\underline{U}}^{(3)} \times \hat{k}$, and $\lambda_{\|}$, $\lambda_{\perp}$, and λ_{tr} represent the parallel, perpendicular, and transverse components of $\underline{\underline{\lambda}}(\underline{H})$.

In order to obtain an expression relating $\underline{\underline{\lambda}}$ to the microscopic properties of the fluid, we first write the heat flux vector as

$$\underline{q} = \int d\underline{1}\, f^{(1)}(\underline{x}_1, t)\, E_1\, \underline{C}_1 \tag{3.3}$$

where, in this section on symmetric tops, $d\underline{1}$ is understood to represent $d\underline{p}_1 d\underline{L}_1 d(\cos\theta_1)$, with θ_1 being the angle between the angular momentum and the molecular symmetry axis. Since Fourier's Law is valid only in the

linear regime, we are justified in expanding $f^{(1)}$ as $f_0^{(1)}(1 + \phi_T)$, where ϕ_T is chosen to be the solution of the first order C-E approximation to Boltzmann's equation, Eq. (2.72a). Using the expanded $f^{(1)}$ in Eq. (3.3) and the form for ϕ_T, obtained from Eq. (2.70) by setting all but the temperature gradients to zero, we obtain

$$\underline{q} = n\left(\frac{2kT}{m}\right)^{1/2} \langle E_1 \underline{C}_1, \underline{A} \rangle \cdot \frac{\partial}{\partial \underline{r}} \ln T \tag{3.4}$$

where

$$\langle \chi, y \rangle = n^{-1} \int d\underline{1}\, f_0^{(1)}(\underline{x}_1, t) \chi^{\dagger} y \quad . \tag{3.5}$$

Here, the dagger denotes the tensor adjoint. Finally, comparing Eqs. (3.1) and (3.4), we have that

$$\underline{\underline{\lambda}}(\underline{H}) = nk\left(\frac{2kT}{n}\right) \langle [(\frac{5}{2} - W_1^2) + (\langle \Omega^2 \rangle - \Omega_1^2) + \Gamma(\langle \Omega_C^2 \rangle - \Omega_{C_1}^2)] \underline{W}_1, \underline{A} \rangle \tag{3.6}$$

where the molecular energy has been expressed in the reduced variables

$$E_1 = kT(W_1^2 + \Omega_1^2 + \Gamma \Omega_{C_1}^2) \tag{3.7}$$

with

$$\Omega_{C_1} = (2I_{\perp} kT)^{-1/2} \underline{L}_1 \cdot \hat{e}_3 \tag{3.8}$$

and

$$\Gamma = I_{\perp}/I_{\parallel} - 1 \quad . \tag{3.9}$$

Here, $\hat{e}_3$ is the body fixed symmetry axis and $I_{\parallel}$ and $I_{\perp}$ denote the

moments of inertia parallel and perpendicular to $\hat{e}_3$. Also, we have made use of the orthogonality conditions on ϕ_T (refer to Chapter II). This is the desired microscopic expression for the thermal conductivity tensor; it remains to solve Eq. (2.72a) for $\underline{A}$.

In order to obtain an approximate solution of Eq. (2.72a), $\underline{A}$ is expanded in terms of a set of complete functions of the free flight invariants, i.e., $\underline{W}$, $\underline{\Omega}$, and Ω_c. The literature is vague concerning the appropriate set of functions to use. We choose to expand $\underline{A}$ in the rather unorthodox set

$$\underline{A} = \sum_{pqrst} S^{(r)}_{p+1/2}(W^2) R^{(q)}_s(\Omega^2) R_t(\Omega_c) \times [\underline{W}]^{(p)} [\underline{\Omega}]^{(q)} \odot^{p+q} \underline{\underline{A}}_{pqrst}(\underline{H}) \qquad (3.10)$$

due to the freedom it affords us. Namely, this expansion set allows us to choose the Ω_c dependence of the basis functions independent of the $\underline{\Omega}$ dependence. This is not possible for other more traditional expansion sets (cf. Eq. (3.14)). This is to our advantage, for the purpose of this study is to investigate the Ω_c dependence of the distribution function. Here, $S^{(r)}_{p+1/2}(W^2)$ denotes the Sonine polynomials which satisfy the orthogonality conditions

$$\int_0^\infty dx e^{-x^2} S^{(n)}_m(x^2) S^{(n')}_m(x^2) x^{2m+1} = \delta_{nn'} \Gamma(n+m+1)/2n! \qquad (3.11)$$

where $\Gamma(x)$ is the gamma function and $R^{(q)}_s(\Omega^2)$ represents the Wang Chang-Uhlenbeck polynomials (46) of degree s in Ω^2. The latter are defined through the orthogonality conditions

$$\langle R_s^{(q)}(\Omega^2) R_{s'}^{(q)}(\Omega^2) [\underline{\Omega}]^{(q)} [\underline{\Omega}]^{(q)} \rangle = C_s^{(q)} \delta_{ss'} \underline{\underline{\delta}}^{(q)} \tag{3.12}$$

where $\underline{\underline{\delta}}^{(q)}$ is the unique (idempotent under the multiplication $\underline{\underline{\delta}}^{(q)} \circledcirc^q \underline{\underline{\delta}}^{(q)} = \underline{\underline{\delta}}^{(q)}$) isotropic tensor of rank 2q which is traceless and symmetric on all pairs of first and last q indices. The quantity $C_s^{(q)}$ is a normalization factor defined so that the highest order term of the polynomial in the angular momentum, Ω^{2t}, has a coefficient of unity. The $R_t(\Omega_C)$'s are defined through the orthogonality relations

$$\langle R_t(\Omega_C) R_{t'}(\Omega_C) \rangle = C_t \delta_{tt'} \tag{3.13}$$

where C_t is similarly defined so as to give the leading term Ω_C^t a coefficient of unity. Here, $[\underline{x}]^{(y)}$ is an irreducible Cartesian tensor (47) of weight and rank y constructed from the vector $\underline{x}$, and $\circledcirc^n$ denotes an n-tuple contraction (with the nesting convention for contraction invoked). Finally, $\underline{\underline{A}}_{pqrst}(H)$ is the field dependent expansion coefficient which forms a basis for the totally symmetric representation of the group of rotations about the field. The difficulty with this set of functions lies in the fact that it is not possible to obtain an orthogonality condition between the factored functions $R_s^{(q)}(\Omega^2) R_t(\Omega_C)$ of the form

$$\langle R_s^{(q)}(\Omega^2) R_t(\Omega_C) R_{s'}^{(q)}(\Omega^2) R_{t'}(\Omega_C) [\underline{\Omega}]^{(q)} [\underline{\Omega}]^{(q)} \rangle = C_{st}^{(q)} \delta_{ss'} \delta_{tt'} \underline{\underline{\delta}}^{(q)} \tag{3.14}$$

due to the requirement that $\Omega_C^2 \leq \Omega^2$. However, the general nonorthogonality of the expression set will not present any difficulty in this work. This is due to the fact that the field terms discussed below are orthogonal not only to one another, but also to the nonfield contributing

terms. To obtain a general orthogonality condition, we would be forced to consider a set functions of the form $R_{st}^{(q)}(\Omega^2,\Omega_C)$, but this would not allow consideration of expansion terms commonly found in the literature. Finally, one might believe that an appropriate set of functions in which to expand the Ω_C dependence of $\underline{A}$ is the Legendre polynomials in $\cos\theta$. However, these functions are not orthogonal under the weight $\exp(-\cos^2\theta)$ which is required here. These are precisely the reasons we have chosen to expand $\underline{A}$ as in Eq. (3.10).

The truncated expansion of $\underline{A}$ should contain the terms $(5/2 - W^2)\underline{W}$, $(\langle\Omega^2\rangle - \Omega^2)\underline{W}$, and $(\langle\Omega_C^2\rangle - \Omega_C^2)\underline{W}$ (refer to Eq. (3.6) for $\underline{\underline{\lambda}}(\underline{H})$). In order to observe the S-B effects, nonzero angular momentum polarizations are required. Furthermore, the inversion symmetry of the collision operator (30) forces all of the terms to have a negative parity eigenvalue. Terms both even and odd in $\underline{\Omega}$ should be included for it will be observed that terms odd in $\underline{\Omega}$ cause positive changes in the transport coefficients whereas terms even in $\underline{\Omega}$ cause negative changes. Most importantly, since we initiated this investigation to study the effects of Ω_C, terms containing Ω_C should also be included.

Past work has indicated $\underline{W}\Omega^0\underline{\Omega}$ to be the dominate field term and, thus, we include it in our expansion set. We complete the basis set with the terms $\Omega_C\underline{\Omega}$ and $\Omega_C\underline{\Omega}\underline{W}^0\underline{W}$ which are odd in the angular momentum. A field term, which is odd in the angular momentum and which has often been considered in formal discussion of S-B thermal conductivity effects, is the function $\underline{W}\underline{\Omega}$. However, the contribution of $\underline{W}\underline{\Omega}$ vanishes in the limit of a rigid potential to 2nd order in the nonsphericity; hence, we need

not include this basis function in the expansion. Equation (3.10) then reduces to

$$\underline{\underline{A}} = \underline{\underline{\psi}}_{10100} \cdot \underline{\underline{A}}_{10100} + \underline{\underline{\psi}}_{10010} \cdot \underline{\underline{A}}_{10010} + \underline{\underline{\psi}}_{12000} \circledcirc^2 \underline{\underline{A}}_{12000}$$
$$+ \Gamma\underline{\underline{\psi}}_{10002} \cdot \underline{\underline{A}}_{10002} + \underline{\underline{\psi}}_{10110} \cdot \underline{\underline{A}}_{01001} + \underline{\underline{\psi}}_{21001} \circledcirc^2 \underline{\underline{A}}_{21001} \qquad (3.15)$$

which is abbreviated to

$$\underline{\underline{A}} = \sum_{i=1}^{6} \underline{\underline{\psi}}_i \circledcirc^{n_i} \underline{\underline{A}}_i \qquad (3.16)$$

where in Table 3.1 is listed the basis functions along with their parity and time reversal eigenvalues. We have not considered potential field terms which contain an Ω_C dependence, but do not contain an $\underline{\Omega}$ dependence, for the following reason. For a gas composed of symmetric top molecules, the field operator in Boltzmann's equation is of the form (cf. Eq. (2.41))

$$\overline{\hat{F}\underline{\underline{\psi}}} = (1/\Delta_1) \int d\underline{\eta}_1 \, f_0^{(1)} \underline{\mu} \times \underline{H} \cdot \frac{\partial}{\partial \underline{L}} \underline{\underline{\psi}} \qquad (3.17)$$

where the integration is over the rapidly varying molecular quantities. Consider the function $\underline{\underline{\psi}} = L_C$ $(= \underline{L} \cdot \hat{e}_3)$. The action of the field operator on L_C is

$$\overline{\hat{F}L_C} = (1/\Delta_1) \int d\underline{\eta}_1 \, f_0^{(1)} \underline{\mu} \times \underline{H} \cdot \frac{\partial}{\partial \underline{L}} \underline{L} \cdot \hat{e}_3$$
$$\propto \int d\underline{\eta}_1 \, f_0^{(1)} \hat{L} \times \underline{H} \cdot \hat{e}_3 \qquad (3.18)$$

where we have used the fact that the magnetic dipole moment is parallel to the angular momentum. For a symmetric top molecule $\hat{e}_3$ averages to

$\hat{L}\cos\theta$, where θ is the angle between the angular momentum and the molecular symmetry axis. Therefore, $\hat{F}L_C$ is proportional to

$$\hat{F}L_C \propto \hat{L} \times \underline{H} \cdot \hat{L} \cos\theta = 0 \quad . \tag{3.19}$$

From this result, we conclude that basis functions which are anisotropic solely by virtue of an Ω_C dependence do not contribute to the S-B effects.

The expansion of Eq. (3.16) is inserted into Eq. (3.6) for $\underline{\underline{\lambda}}(\underline{H})$ and the Boltzmann equation, Eq. (2.72a), is then inverted, utilizing the nonsphericity expansion of Cooper and Hoffman (38) or Matzen (39), to obtain the values of the expansion coefficients. This procedure generates a power series expansion of $\underline{\underline{\lambda}}(\underline{H})$ in orders of the nonsphericity. The following results are obtained for the thermal conductivity to second order:

$$\underline{\underline{\lambda}} = \underline{\underline{\lambda}}^{[0]} + \underline{\underline{\lambda}}^{[1]} + \underline{\underline{\lambda}}^{[2]} \tag{3.20}$$

where

$$\underline{\underline{\lambda}}^{[0]} = \frac{k}{2\sqrt{2}} \left(\frac{kT}{m} \right)^{1/2} \{ \frac{25}{4} a + \langle\Omega^2\rangle^2 e + \Gamma^2\langle\Omega_C^2\rangle^2 + \Gamma\langle\Omega^2\rangle\langle\Omega_C^2\rangle[f + h]$$

$$+ \frac{5}{2} [\langle\Omega^2\rangle b + \Gamma\langle\Omega_C^2\rangle c + \langle\Omega^2\rangle d + \Gamma\langle\Omega_C^2\rangle g]\} \tag{3.21}$$

and

$$a = M\{\theta_{22}\theta_{44} - \theta_{24}^2\}$$

$$b = M\{\theta_{24}\theta_{14} - \theta_{12}\theta_{44}\}$$

$$
\begin{aligned}
c &= M\{\theta_{12}\theta_{24} - \theta_{22}\theta_{14}\} \\
d &= M\{\theta_{14}\theta_{24} - \theta_{12}\theta_{44}\} \\
e &= M\{\theta_{11}\theta_{44} - \theta_{14}^2\} \\
f &= M\{\theta_{12}\theta_{14} - \theta_{11}\theta_{24}\} \\
g &= M\{\theta_{12}\theta_{24} - \theta_{14}\theta_{22}\} \\
h &= M\{\theta_{14}\theta_{12} - \theta_{11}\theta_{24}\} \\
i &= M\{\theta_{11}\theta_{22} - \theta_{12}\theta_{12}\}
\end{aligned}
\tag{3.22}
$$

$$
M = \{\theta_{11}[\theta_{22}\theta_{44} - \theta_{24}^2] - \theta_{12}[\theta_{12}\theta_{44} - \theta_{24}\theta_{14}] + \theta_{14}[\theta_{12}\theta_{24} - \theta_{22}\theta_{14}]\} \tag{3.23}
$$

with θ_{ij}, the reduced cross section, defined by

$$
\begin{aligned}
\theta_{ij}\underline{\underline{\delta}}^{(p,q)} &= n^{-2}\left(\frac{\mu}{kT}\right)^{1/2} \int d\underline{1}\, \underline{\underline{\psi}}_i^{\dagger}\, \hat{K}_B\, \underline{\underline{\psi}}_j \\
&= \left(\frac{\mu}{kT}\right)^{1/2} \{[\underline{\underline{\psi}}_i, \underline{\underline{\psi}}_j]_{s,s}^{1,1} + [\underline{\underline{\psi}}_i, \underline{\underline{\psi}}_j]_{s,s}^{1,2}\} \quad .
\end{aligned}
\tag{3.24}
$$

Thus defined, θ_{ij} has units of area. The bracket integrals in Eq. (3.23) are discussed in Appendix A. The rank 2(p+q) tensor, $\underline{\underline{\delta}}^{(p+q)}$, represents the tensor formed by embedding $\underline{\underline{\delta}}^{(p)}$ between the inner two indices of $\underline{\underline{\delta}}^{(q)}$. Here p and q denote the rank of the irreducible tensors made up from $\underline{W}$ and $\underline{\Omega}$, respectively, as contained in the $\underline{\underline{\psi}}_i$ basis functions. The first and second order terms are

$$\underline{\underline{\lambda}}^{[1]} = 0 \tag{3.25}$$

and

$$\underline{\underline{\lambda}}^{[2]} = \underline{\underline{\lambda}}_3^{[2]} + \underline{\underline{\lambda}}_5^{[2]} + \underline{\underline{\lambda}}_6^{[2]} \tag{3.26}$$

where the subscripts denote the basis functions giving rise to the effect, with

$$\underline{\underline{\lambda}}_3^{[2]} = \frac{k}{2\sqrt{2}} \left(\frac{kT}{m} \right)^{1/2} \omega_3 \{5[\theta_{13}a + \theta_{23}b + \theta_{34}c] + 2\langle\Omega^2\rangle[\theta_{13}d + \theta_{23}e + \theta_{34}f] + 2\Gamma\langle\Omega_c^2\rangle[\theta_{13}g + \theta_{23}h + \theta_{34}i] \underline{\underline{Y}}_3$$

$$= \theta_{33} H_3 \underline{\underline{Y}}_3 \tag{3.27}$$

$$\omega_3 = \theta_{13}\{ \frac{5}{4} a + \frac{1}{2} \langle\Omega^2\rangle b + \frac{1}{2} \Gamma\langle\Omega_c^2\rangle c\} + \theta_{23}\{ \frac{5}{4} d + \frac{1}{2} \langle\Omega^2\rangle e + \frac{1}{2} \Gamma\langle\Omega_c^2\rangle f + \theta_{34}\{ \frac{5}{4} g + \frac{1}{2} \langle\Omega^2\rangle h + \frac{1}{2} \Gamma\langle\Omega_c^2\rangle i\} \tag{3.28}$$

$$\underline{\underline{Y}}_3 = \underline{\underline{\delta}}^{(2)} \circledcirc^3 \underline{\underline{X}}_3 \circledcirc^3 \underline{\underline{\delta}}^{(2)} \tag{3.29}$$

$$\underline{\underline{\lambda}}_5^{[2]} = -\frac{k}{2\sqrt{2}} \left(\frac{kT}{m} \right)^{1/2} \omega_5 \{5[\theta_{25}b + \theta_{45}c] + 2\langle\Omega^2\rangle[\theta_{25}e + \theta_{45}f] + 2\Gamma\langle\Omega_c^2\rangle[\theta_{25}h + \theta_{45}i] \underline{\underline{Y}}_5$$

$$= -\theta_{55} H_5 \underline{\underline{Y}}_5 \tag{3.30}$$

$$\omega_5 = \theta_{25}[\frac{5}{4} d + \frac{1}{2} \langle\Omega^2\rangle e + \frac{1}{2} \Gamma\langle\Omega_c^2\rangle f] + \theta_{45}[\frac{5}{4} g + \frac{1}{2} \langle\Omega^2\rangle h + \frac{1}{2} \Gamma\langle\Omega_c^2\rangle i] \tag{3.31}$$

$$\underline{\underline{Y}}_5 = \underline{\underline{\delta}}^{(1)} \cdot \underline{\underline{\chi}}_5 \cdot \underline{\underline{\delta}}^{(1)} \tag{3.32}$$

and

$$\underline{\underline{\lambda}}_6^{[2]} = -\frac{k}{2\sqrt{2}} \left(\frac{kT}{m}\right)^{1/2} \omega_6 \{5[\theta_{61}a + \theta_{62}b + \theta_{64}c]$$

$$+ 2\langle\Omega^2\rangle[\theta_{61}d + \theta_{62}e + \theta_{64}f] + 2\Gamma\langle\Omega_c^2\rangle[\theta_{61}g + \theta_{62}h + \theta_{64}i]\}\underline{\underline{Y}}_6$$

$$= -\theta_{66}H_6\underline{\underline{Y}}_6 \tag{3.33}$$

$$6 = \frac{5}{4}[\theta_{61}a + \theta_{62}d + \theta_{64}g] + \frac{1}{2}\langle\Omega^2\rangle[\theta_{61}b + \theta_{62}e + \theta_{64}h]$$

$$+ \frac{1}{2}\Gamma\langle\Omega_c^2\rangle[\theta_{61}c + \theta_{62}f + \theta_{64}i] \tag{3.34}$$

$$\underline{\underline{Y}}_6 = \underline{\underline{\delta}}^{(2)} \circledcirc^3 \underline{\underline{\chi}}_6 \circledcirc^3 \underline{\underline{\delta}}^{(2)} \quad . \tag{3.35}$$

The symbol $\underline{\underline{\chi}}_i$ is the inverse of the matrix element $(\Lambda^{(0)})_{ii}$ (38,39).

Due to the presence of the external field, the thermal conductivity tensor contains three independent components. Following Cooper and Hoffman (38), we expand $\underline{\underline{\lambda}}$ as

$$\underline{\underline{\lambda}}(\underline{H}) = \lambda_{\parallel}(\underline{H})\underline{\underline{B}}_0^{(a)}(1) + \lambda_{\perp}(\underline{H})\underline{\underline{B}}_1^{(a)}(1) + \lambda_{tr}(\underline{H})\underline{\underline{B}}_1^{(b)}(1) \quad . \tag{3.36}$$

The change in these components due to the introduction of the external field is denoted as

$$\Delta\underline{\underline{\lambda}}(\underline{H}) = \Delta\lambda_{\parallel}\underline{\underline{B}}_0^{(a)}(1) + \Delta\lambda_{\perp}\underline{\underline{B}}_1^{(a)}(1) + \Delta\lambda_{tr}\underline{\underline{B}}_1^{(b)}(1) \tag{3.37}$$

where the $\underline{\underline{B}}_j^{(i)}(k)$ tensors are defined in Ref. 38 (refer also to Eq. (3.2) above). The explicit forms for the change in these components are

Figure 3.1. Geometric field effects arising from the basis functions $\Omega_c \underline{\Omega}\underline{W}^0\underline{W}$, $\Omega_c \underline{\Omega}$, and $\underline{W}\underline{\Omega}^0\underline{\Omega}$ used in the thermal conductivity calculation. The abscissa is the ratio of the magnetic field strength to the pressure (in units of tesla/Pa) and the ordinate denotes the relative change in the components of the $\underline{\underline{\lambda}}$ tensor

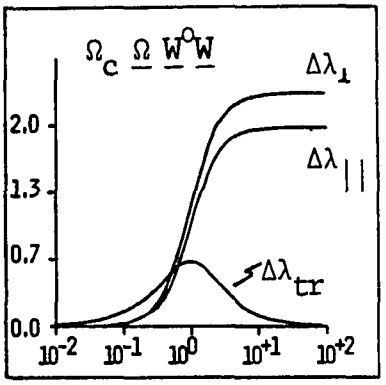
Ω_c $\underline{\Omega}$ $\underline{W}^{\circ}\underline{W}$
$\Delta\lambda_{\perp}$
$\Delta\lambda_{||}$
$\Delta\lambda_{tr}$
2.0
1.3
0.7
0.0
10^{-2} 10^{-1} 10^{0} 10^{+1} 10^{+2}

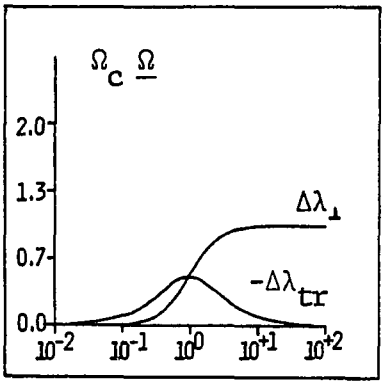
Ω_c $\underline{\Omega}$
$\Delta\lambda_{\perp}$
$-\Delta\lambda_{tr}$
2.0
1.3
0.7
0.0
10^{-2} 10^{-1} 10^{0} 10^{+1} 10^{+2}

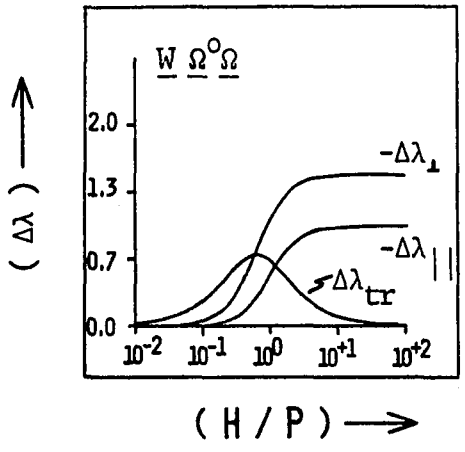
$\underline{W}$ $\underline{\Omega}^{\circ}\underline{\Omega}$
$-\Delta\lambda_{\perp}$
$-\Delta\lambda_{||}$
$\Delta\lambda_{tr}$
2.0
1.3
0.7
0.0
10^{-2} 10^{-1} 10^{0} 10^{+1} 10^{+2}
(Δλ) ⟶
(H / P) ⟶

$$\Delta\lambda_j(\underline{H}) = (\Delta\lambda_j)_3 + (\Delta\lambda_j)_5 + (\Delta\lambda_j)_6 \tag{3.38}$$

with

$$\begin{aligned}(\Delta\lambda_{\parallel})_3 &= -H_3 C_2(\xi_3^{tc}) \\ (\Delta\lambda_{\parallel})_5 &= 0 \\ (\Delta\lambda_{\parallel})_6 &= H_6 2C_2(\xi_6^{tc})\end{aligned} \tag{3.39}$$

$$\begin{aligned}(\Delta\lambda_{\perp})_3 &= -H_3\{\tfrac{1}{2} C_2(\xi_3^{tc}) + C_2(2\xi_3^{tc})\} \\ (\Delta\lambda_{\perp})_5 &= H_5 C_2(\xi_5^{tc}) \\ (\Delta\lambda_{\perp})_6 &= H_6 \tfrac{7}{3} C_2(\xi_6^{tc})\end{aligned} \tag{3.40}$$

and

$$\begin{aligned}(\Delta\lambda_{tr})_3 &= H_3\{\tfrac{1}{2} C_1(\xi_3^{tc}) + C_1(2\xi_3^{tc}) \\ (\Delta\lambda_{tr})_5 &= -H_5 C_1(\xi_5^{tc}) \\ (\Delta\lambda_{tr})_6 &= H_6 \tfrac{4}{3} C_1(\xi_6^{tc}) \quad .\end{aligned} \tag{3.41}$$

The field dependence of Eqs. (3.36)-(3.38) is plotted in Fig. 3.1. The quantities H_3, H_5, and H_6 are defined by Eqs. (3.27), (3.30), and (3.33) above,

$$C_i(x) = x^i/(1 + x^2) \quad , \tag{3.42}$$

and the field parameters are defined by

$$\xi_i^{tc} = \{(\mu kT)^{1/2}\, \beta_n g_\perp / h\theta_{ii}\}\left(\frac{H}{P_0(K)}\right) G_i^{tc} \tag{3.43}$$

Here, μ is the reduced mass, β_n is the Bohr magneton, and $\underline{g}_\parallel$ and $\underline{g}_\perp$ are the parallel and perpendicular components of the rotational Lande tensor. The G_i^{tc}'s are given by

$$G_3^{tc} = \frac{1}{60}\left\{8 + 2\left(1 + \frac{g_\parallel}{g_\perp}\right)\left(\frac{I_\parallel}{I_\perp}\right) + 3\,\frac{g_\parallel}{g_\perp}\left(\frac{I_\parallel}{I_\perp}\right)^2\right\} \tag{3.44a}$$

$$G_5^{tc} = \frac{1}{6}\,\frac{I_\parallel}{I_\perp}\left\{1 + \frac{3}{2}\,\frac{I_\parallel}{I_\perp}\left(\frac{g_\parallel}{g_\perp}\right)\right\} \tag{3.44b}$$

$$G_6^{tc} = \frac{1}{12}\,\frac{I_\parallel}{I_\perp}\,1 + \frac{3}{4}\,\frac{I_\parallel}{I_\perp}\left(1 + \frac{g_\parallel}{g_\perp}\right) \quad . \tag{3.44c}$$

This completes the derivation of the necessary equations.

The nonsphericity expansion was truncated to second order due to the rapid convergence of the series. The two terms, $\underline{\Psi}_5$ and $\underline{\Psi}_6$, which are odd in $\underline{\Omega}$, were included in the expansion because they allow for a positive change in the thermal conductivity by the field. This can be observed from Eqs. (3.39) and (3.40).

B. Viscosity

The methods utilized in this section are identical to those of the preceding section. Therefore, we abbreviate the discussion. The pressure tensor for a dilute gas contains only a kinetic part (see the discussion of Chapter II) and is given explicitly by

$$\underline{\underline{P}}^{(K)} = m \int d\underline{1}\, f^{(1)}(\underline{x}_1, t)\underline{C}_1\underline{C}_1 \quad , \tag{3.45}$$

where the superscript K indicates the kinetic part of the pressure tensor. Confining our attention to a gas near equilibrium, we can expand the distribution function about $f_0^{(1)}$. The insertion of the form for the distortion, ϕ_u, from Eq. (2.70) in this expression for $\underline{\underline{P}}^{(K)}$ yields

$$\underline{\underline{P}}^{(K)} = P_0^{(K)}\{1 + \frac{2}{3}\pi\}\underline{\underline{\delta}}^{(1)} + \overset{0}{\underline{\underline{\pi}}} \tag{3.46}$$

where

$$P_0^{(K)} = nkT \tag{3.47}$$

$$\pi = \frac{1}{3}\langle W^2, \underline{\underline{B}}:\underline{\underline{\delta}}^{(1)}\rangle \frac{\partial}{\partial \underline{r}} \cdot \underline{u} \tag{3.48}$$

$$\overset{0}{\underline{\underline{\pi}}} = 2nkT\langle W^0 W, \underline{\underline{B}}\rangle : \frac{\partial}{\partial \underline{r}}\underline{u} \quad . \tag{3.49}$$

The quantity $\overset{0}{\underline{\underline{\pi}}}$ determines the coefficient of shear viscosity, i.e.,

$$\overset{0}{\underline{\underline{\pi}}} = -2\underline{\underline{\eta}} : \frac{\partial^0}{\partial \underline{r}}\underline{u} \tag{3.50}$$

with $\underline{\underline{\eta}}$ representing the fourth rank shear viscosity tensor. Equating Eqs. (3.49) and (3.50), we find that

$$\underline{\underline{\eta}} = -nkT\langle \underline{\underline{W}}^0 \underline{\underline{W}}, \underline{\underline{B}}\rangle \quad , \tag{3.51}$$

which is the microscopic form of the shear viscosity tensor. For isotropic systems, the shear viscosity tensor reduces to a scalar multiple of $\underline{\underline{\delta}}^{(2)}$, i.e.,

$$\underline{\underline{\eta}} = \eta_0 \underline{\underline{\delta}}^{(2)} \quad , \tag{3.52}$$

where η_0 is the field free viscosity. In the presence of an external magnetic field aligned along $\hat{k}$, the shear viscosity tensor decomposes into five independent components

$$\underline{\underline{\eta}} = \eta_1 \underline{\underline{B}}_0^{(a)}(2) + \eta_2 \underline{\underline{B}}_1^{(a)}(2) + \eta_3 \underline{\underline{B}}_2^{(a)}(2) + \eta_4 \underline{\underline{B}}_1^{(b)}(2) + \eta_5 \underline{\underline{B}}_2^{(b)}(2) \tag{3.53}$$

where the $\underline{\underline{B}}_j^{(i)}(k)$'s are defined in Ref. 38.

In order to obtain an approximate solution of Eq. (2.72b), the distortion, $\underline{\underline{B}}$, is expanded in a complete set of functions (cf. Eq. (3.10) and the expansion of $\underline{A}$). By truncating this expansion to

$$\underline{\underline{B}} = \underline{\underline{\phi}}_1 \circledcirc^2 \underline{\underline{B}}_1 + \underline{\underline{\phi}}_2 \circledcirc^2 \underline{\underline{B}}_2 + \underline{\underline{\phi}}_3 \circledcirc^2 \underline{\underline{B}}_3 \tag{3.54}$$

where the $\underline{\underline{\phi}}$'s are given in Table 3.2, solving for the expansion coefficients, and inserting Eq. (3.54) into Eq. (3.51), we obtain:

$$\underline{\underline{\eta}}^{[0]} = \frac{1}{2} (\mu kT)^{1/2} \theta_{11}^{-1} \underline{\underline{\delta}}(2) = \eta^{[0]} \underline{\underline{\delta}}(2) \tag{3.55}$$

$$\underline{\underline{\eta}}^{[1]} = 0 \tag{3.56}$$

and

$$\begin{aligned} \underline{\underline{\eta}}^{[2]} = \eta^{[0]} \{ & [1 + \Phi_{12} - \Phi_{13} + \tfrac{1}{3} C_2(\xi_3^v)\Phi_{13}] \underline{\underline{B}}_0^{(a)}(2) \\ & + [1 + \Phi_{12} - \Phi_{13} + \tfrac{1}{2} C_2(\xi_3^v)\Phi_{13} - C_2(\xi_2^v)\Phi_{12}] \underline{\underline{B}}_1^{(a)}(2) \\ & + [1 + \Phi_{12} - \Phi_{13} - C_2(\xi_3^v)\Phi_{13} - C_2(2\xi_2^v)\Phi_{12}] \underline{\underline{B}}_2^{(a)}(2) \end{aligned}$$

$$+ [1 + \Phi_{12} - \Phi_{13} + C_1(\xi_2^v)\Phi_{12} - \tfrac{1}{2} C_1(\xi_3^v)\Phi_{13}]\underline{\underline{B}}_1^{(b)}(2)$$

$$+ [1 + \Phi_{12} - \Phi_{13} + C_1(\xi_2^v)\Phi_{12} - \tfrac{1}{2} C_1(\xi_3^v)\Phi_{13}]\underline{\underline{B}}_2^{(b)}(2)\} \quad . \quad (3.57)$$

Here,

$$\Phi_{ij} = \theta_{ij}^2/\theta_{ii}\theta_{jj} \quad (3.58)$$

is a measure of the coupling of the ith and the jth basis functions. The field parameters, ξ_i^v, are defined by

$$\xi_i^v = \{(\mu kT)^{1/2}\beta_n g_\perp/\hbar\theta_{ii}\}\left(\frac{H}{P_0(K)}\right)G_i^v \quad (3.59)$$

where

$$G_2^v = \frac{1}{30}\{8 + 2\left(1 + \frac{g_\parallel}{g_\perp}\right)\frac{l_\parallel}{l_\perp} + 3\frac{g_\parallel}{g_\perp}\left(\frac{l_\parallel}{l_\perp}\right)\} \quad (3.60)$$

and

$$G_3^v = \frac{1}{24}\{2\frac{l_\parallel}{l_\perp} + 3\frac{g_\parallel}{g_\perp}\left(\frac{l_\parallel}{l_\perp}\right)^2\} \quad . \quad (3.61)$$

Finally, defining the change in the coefficient of viscosity due to the introduction of the external field as

$$(\underline{\underline{\eta}}(\underline{H}) - \underline{\underline{\eta}}_0)/\eta_0 = \left(\frac{\Delta\eta_1}{\eta_0}\right)\underline{\underline{B}}_0^{(a)}(1) + \left(\frac{\Delta\eta_2}{\eta_0}\right)\underline{\underline{B}}_1^{(a)}(2) + \left(\frac{\Delta\eta_3}{\eta_0}\right)\underline{\underline{B}}_2^{(a)}(2)$$

$$+ \left(\frac{\Delta\eta_4}{\eta_0}\right)\underline{\underline{B}}_1^{(b)}(2) + \left(\frac{\Delta\eta_5}{\eta_0}\right)\underline{\underline{B}}_2^{(b)}(2) \quad , \quad (3.62)$$

Figure 3.2. Geometric field effects arising from the basis functions $\Omega_c \underline{\underline{\Omega W}}$ and $\underline{\Omega}^0 \underline{\Omega}$ used in the viscosity calculation. The abscissa is the ratio of the magnetic field strength to the pressure (in units of tesla/Pa) and the ordinate denotes the relative change in the components of the $\underline{\underline{\eta}}$ tensor

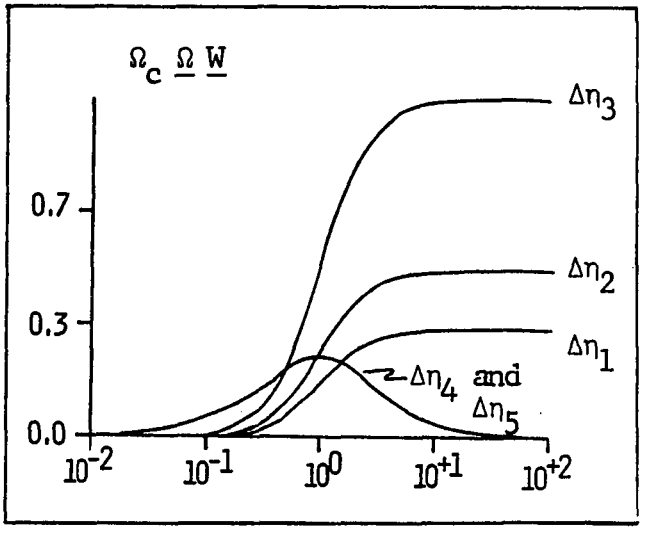
Ω_c Ω W
$\Delta\eta_3$
$\Delta\eta_2$
$\Delta\eta_1$
$\Delta\eta_4$ and $\Delta\eta_5$
0.7
0.3
0.0
10^{-2}
10^{-1}
10^{0}
10^{+1}
10^{+2}

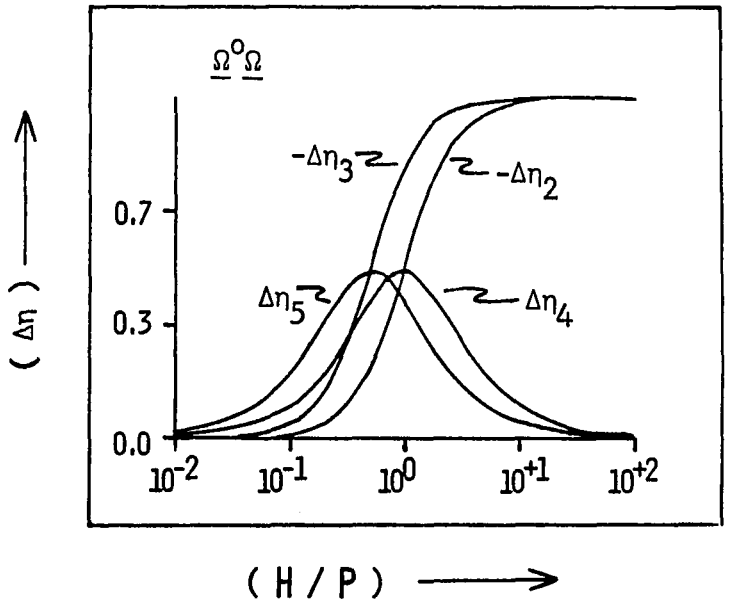
Ω°Ω
$-\Delta\eta_3$
$-\Delta\eta_2$
$\Delta\eta_5$
$\Delta\eta_4$
0.7
0.3
0.0
10^{-2}
10^{-1}
10^{0}
10^{+1}
10^{+2}
(Δη)
(H / P)

we obtain

$$\left(\frac{\Delta n_1}{n_0}\right) = \frac{1}{3} H_3 C_2(\xi_3^v) \tag{3.63a}$$

$$\left(\frac{\Delta n_2}{n_0}\right) = \frac{1}{2} H_3 C_2(\xi_3^v) - H_2 C_2(\xi_2^v) \tag{3.63b}$$

$$\left(\frac{\Delta n_3}{n_0}\right) = H_3 C_2(\xi_3^v) - H_2 C_2(2\xi_2^v) \tag{3.63c}$$

$$\left(\frac{\Delta n_4}{n_0}\right) = H_2 C_1(\xi_2^v) - \frac{1}{2} H_3 C_1(\xi_3^v) \tag{3.63d}$$

$$\left(\frac{\Delta n_5}{n_0}\right) = H_2 C_1(2\xi_2^v) - \frac{1}{2} H_3 C_1(\xi_3^v) \tag{3.63e}$$

with

$$H_2 = \Phi_{12}/(1 + \Phi_{12} - \Phi_{13}) \tag{3.64a}$$

and

$$H_3 = \Phi_{13}/(1 + \Phi_{12} - \Phi_{13}) \quad . \tag{3.64b}$$

The field dependence of Eqs. (3.63a)-(3.63e) is plotted in Fig. 3.2. This completes the derivation of the equations necessary for the viscosity. As in the case of the thermal conductivity, inclusion of the basis function odd in $\underline{\Omega}$ allows for an increase in the value of the transport coefficient in the presence of an external field.

C. Numerical Results

To evaluate the required collision integrals, it is necessary to find a convenient method of specifying the molecular geometries. Such a method is afforded through the use of a supporting function, h, given by

$$h = \underline{\xi} \cdot \hat{k} \tag{3.65}$$

where $\underline{\xi}$ and $\hat{k}$ are defined in Fig. 2.1 above. Equation (3.62) is easily inverted (21) yielding

$$\underline{\xi} = h\hat{k} + \partial h/\partial \hat{k} \quad . \tag{3.66}$$

Hence, h completely specifies the geometry of the molecule. Thus, it is a simple matter to evaluate the bracket integrals given the form of the supporting function (13).

For the purpose of modeling a symmetric top molecule, we choose to use a supporting function of the form (13)

$$h = \alpha + \beta_1 \sum_{i=1,2,4} (k \cdot \hat{e}_i)^3 + \beta_3 (k \cdot \hat{e}_3)^3 - \gamma k \cdot \hat{e}_3 \tag{3.67}$$

where the unit vectors $\hat{e}_i$ extend from the center of a tetrahedron in the direction of the four vertices. The parameter α determines the overall size of the molecule, the β_i's are a measure of the molecular distortions along the corresponding $\hat{e}_i$, and γ locates the center of mass which for a symmetric top is confined to lie along the symmetry axis. We have chosen $\hat{e}_3$ to represent the molecular symmetry axis. In the numerical work on which we report, the quantities α, β_1, β_3, and γ were

treated as free parameters which were varied to fit the available experimental results. A computer program was written to carry out this procedure. In short, the program varied the parameters in search of the minimum of the function

$$F(\alpha,\beta_1,\beta_3,\gamma) = \sum_{i=1}^{n} w_i(y_i - y_i^{exp})^2 \quad , \tag{3.68}$$

where n is the number of experimental measurements available on the system in question (generally n = 3, the field free transport coefficient and either $(\Delta\eta_2/\eta_0)_{sat}$ and $(\Delta\eta_4/\eta_0)_{max}$ for the viscosity or $(\Delta\lambda_{\parallel}/\lambda_0)_{sat}$ and $(\Delta\lambda_{\perp}/\ _0)_{sat}$ for the thermal conductivity). The quantity w_i represents the weight for the experimental results (the field free transport coefficient, rather arbitrarily, was weighted twice that of the remaining two experimental values), and y_i and y_i^{exp} denote the calculated and experimental quantities, respectively. Finally, all of the numerical results reported in this chapter were carried out assuming a temperature of 300°K.

In Table 3.3, we list the systems investigated along with relevant kinematic parameters. The isotopically substituted methane series was chosen in order to observe effects related to varying the kinematic parameters while holding the intermolecular potential fixed (a procedure justified by the Born-Oppenheimer approximation). The molecules CHF_3 and CH_3F were chosen as representative oblate and prolate symmetric tops along with their deuterated counterparts. The molecules NH_3 and ND_3 were chosen because of the unique behavior of the viscosity of these gases in the presence of a magnetic field (45).

Table 3.4 contains the results of optimizing the geometries of the molecules. Two geometries are given for each system, derived separately from the thermal conductivity results and from the viscosity results. For most of the systems, the agreement between the two geometries is poor. However, the two geometries obtained for CH_4 are in reasonable agreement as are also the thermal conductivity derived geometries for CHF_3 and CDF_3. In the previous work of Verlin et al. (13), the optimized geometries for CH_4, obtained from the viscosity and the thermal conductivity experimental results, compared poorly. Our agreement for CH_4 may be the result of the improved fitting methods employed here.

We initiated this study to calculate the effects of field terms containing Ω_C. In Table 3.5, are listed the relative contributions of the three field basis functions for the thermal conductivity. The basis functions are $\underline{W}\underline{\Omega}^0\underline{\Omega}$, $\Omega_C\underline{\Omega}$, and $\Omega_C\underline{\Omega}\underline{W}^0\underline{W}$ and their contributions are proportional to (H_3/λ_0), (H_5/λ_0), and (H_6/λ_0), respectively (cf. Eqs. (3.38)-(3.41)). From Table 3.5, it is obvious that the dominate contribution is from the term $\underline{W}\underline{\Omega}^0\underline{\Omega}$ for all of the systems studied. The contribution of the other two terms is at best two to three orders of magnitude less. The effect of the $\Omega_C\underline{\Omega}$ polarization is generally ten times the effect of the $\Omega_C\underline{\Omega}\underline{W}^0\underline{W}$ polarization on the S-B effects. Intuitively, one would expect the significance of the $\Omega_C\underline{\Omega}$ and $\Omega_C\underline{\Omega}\underline{W}^0\underline{W}$ polarizations to increase with increasing anisotropy of the inertia tensor, a measure of which is the parameter Γ $(= I_\perp/I_\parallel - 1)$. This is found to be true. For the CH_4 series, the contribution of these terms is largest for CH_3T. Overall, the largest contributions are obtained

in the CHF_3 and CDF_3 systems where the effect of the $\Omega_C\underline{\Omega}$ term is approximately one percent of the dominate $\underline{W}\underline{\Omega}^0\underline{\Omega}$ term. We expect that for more highly nonspherical top molecules such as CH_3Cl or CH_3Br, the importance of the $\Omega_C\underline{\Omega}$ and $\Omega_C\underline{\Omega}\underline{W}^0\underline{W}$ terms will further increase.

Overall, the fitting gave very good results for the case of the thermal conductivity parameters as seen in Table 3.6. This is a reflection on our choice of basis functions. The value of λ_0 appears fairly insensitive to the kinematic parameters. The slight decrease in λ_0 down the series reflects the $1/\sqrt{m}$ dependence in Eq. (3.21). As expected, the S-B effects show greater variation. In Table 3.7, we list the characteristic field strengths of the S-B effects.

The two field terms investigated in conjunction with the viscosity are $\underline{\Omega}^0\underline{\Omega}$, known to be the dominate term, and $\Omega_C\underline{\Omega}\underline{W}$, of interest because of its Ω_C dependence. The significance of these basis functions is measured by Φ_{12} and Φ_{13}, respectively (see Eqs. (3.58), (3.63) and (3.64) above). From Table 3.8, it can be seen that $\Omega_C\underline{\Omega}\underline{W}$ is of no importance to the viscosity S-B effects for rigid polyatomics. The whole effect is adequately handled by the inclusion of the $\underline{\Omega}^0\underline{\Omega}$ term (except in the case of NH_3 and ND_3). As expected, the more nonspherical the molecule, the larger is the coupling of $\underline{\Omega}^0\underline{\Omega}$ and $\underline{W}^0\underline{W}$. In the CH_4 series, CH_3T shows the largest effect.

The results of the fitting to the viscosity data for the CH_4 series, and CHF_3 and CH_3F are very good, as seen in Table 3.9. The η_0's in the CH_4 series shows a slight increase due to the $\sqrt{m}$ dependence in Eq. (3.55), whereas the S-B effects show a much greater variation in

this series. Table 3.10 lists the characteristic field strengths of the Senftleben-Beenakker effects for the viscosity.

Unlike the case of the thermal conductivity, the viscosity calculations for NH_3 and ND_3 are very poor. This is not surprising, for it has long been known that an additional mechanism for building up odd in $\underline{\Omega}$ polarizations is at work in NH_3 and ND_3 which cannot be accounted for by rigid impulsive collisions. It could be argued that this anomalous behavior is due to the inversion of NH_3. In order to incorporate this phenomenon into our theory, an inversion term, perhaps of the form

$$\hat{I} f^{(1)}(\underline{p},\underline{L},L_C) = w_I[f^{(1)}(\underline{p},\underline{L},-L_C) - f^{(1)}(\underline{p},\underline{L},L_C)] \tag{3.69}$$

could be included into the RHS of the Boltzmann equation (cf. Eq. (2.40)). Here, w_I represents the inversion frequency of NH_3 (or ND_3). This expression is similar to those found in master equation approaches where $w_I f^{(1)}(\underline{p},\underline{L},-L_C)$ represents a gain term and $w_I f^{(1)}(\underline{p},\underline{L},+L_C)$ represents a loss term. The $\hat{I}$ operator is obviously diagonal within our expansion set. It has two eigenvalues, i.e., $-2w_I$ for functions odd in L_C (or Ω_C) and zero for functions even in L_C. From its eigenvalues, $\hat{I}$ is seen to be seminegative definite (as is the Boltzmann collision operator). Therefore, this term simply adds to the diagonal matrix elements of the collision operator, increasing its apparent magnitude by a factor proportional to w_I. Because the S-B effects are proportional to the inverse of the diagonal matrix elements, a large inversion frequency would tend to diminish the importance of the terms odd in Ω_C such as $\Omega_C\underline{\Omega}$ and $\Omega_C\underline{\Omega}\underline{W}$. For this reason, we expect that some

other process is contributing to the unusually large odd in $\underline{\Omega}$ polarizations existing in the NH_3 system.

In conclusion, reasonable results were obtained for all systems except the viscosity calculations on NH_3 and ND_3. For the viscosity, the $\Omega_C\underline{\Omega}\underline{W}$ term gave essentially no contribution to the S-B effects. For the thermal conductivity calculations, the contributions of the $\Omega_C\underline{\Omega}$ and $\Omega_C\underline{\Omega}\underline{W}^0\underline{W}$ terms, although comparable to one another, are very small. The largest effects were found in the least spherical top molecules such as CH_3T and CHF_3.

Table 3.1. Basis functions, $\underline{\underline{\Psi}}_i$, used in the thermal conductivity calculation with their parity, P, and time reversal, T, eigenvalues

Basis Function	P	T
$\underline{\underline{\Psi}}_1 = (\frac{5}{2} - W^2)\underline{W}$	-1	-1
$\underline{\underline{\Psi}}_2 = (\langle\Omega^2\rangle - \Omega^2)\underline{W}$	-1	-1
$\underline{\underline{\Psi}}_3 = \underline{W}\underline{\Omega}^0\underline{\Omega}$	-1	-1
$\underline{\underline{\Psi}}_4 = (\langle\Omega_c^2\rangle - \Omega_c^2)\underline{W}$	-1	-1
$\underline{\underline{\Psi}}_5 = \Omega_c\underline{\Omega}$	-1	+1
$\underline{\underline{\Psi}}_6 = \Omega_c\underline{\Omega}\underline{W}^0\underline{W}$	-1	+1

Table 3.2. Basis functions, $\underline{\underline{\phi}}_i$, used in the viscosity calculation with their parity, P, and time reversal, T, eigenvalues

Basis Function	P	T
$\underline{\underline{\phi}}_1 = \underline{\underline{W}}^{O}\underline{\underline{W}}$	+1	+1
$\underline{\underline{\phi}}_2 = \underline{\underline{\Omega}}^{O}\underline{\underline{\Omega}}$	+1	+1
$\underline{\underline{\phi}}_3 = \Omega_C\underline{\underline{\Omega W}}$	+1	-1

Table 3.3. Values for the molecular constants μ, $I_\perp$, $I_\parallel$, $g_\perp$, and $g_\parallel$

Molecule	μ (amu)	$I_\perp$ (amu Å^2)	$I_\parallel$ (amu Å^2)	$g_\perp$	$g_\parallel$
CH_4[a]	8.024	3.213	3.213	0.313	0.313
CH_3D[a]	8.528	4.155	3.213	-0.242	0.313
CH_3T[a]	9.032	7.297	3.213	-0.138	0.313
CD_3H[a]	9.536	5.127	6.380	0.199	0.160
CD_4[a]	10.041	6.380	6.380	0.160	0.160
CD_3T[a]	10.545	7.490	6.380	-0.136	0.160
CHF_3[b]	35.01	48.60	88.94	-0.036	-0.031
CDF_3[b]	35.52	50.63	89.11	-0.035	-0.031
CH_3F[b]	17.02	20.25	3.362	-0.062	0.265
CD_3F[b]	18.53	25.31	6.83	-0.050	0.133
NH_3[b]	8.515	1.083	1.70	0.563	0.500
ND_3[b]	10.028	3.28	5.35	0.280	0.250

[a]Source: Ref. 48.

[b]Source: Ref. 49.

Table 3.4. Optimized molecular potential parameters α, β_1, β_3, and γ, obtained from experimental results for the viscosity, v, and the thermal conductivity, tc

Molecule	Data	α (Å)	β_1 (Å)	β_3 (Å)	γ (Å)
CH_4	v	2.00183	-0.03512	-0.03512	0 [a]
	tc	1.89665	0.09209	0.09209	0
CH_3D	v	2.00183	-0.03512	-0.03512	0.064[a]
	tc	1.89665	0.09209	0.09209	0.064
CH_3T	v	2.00183	-0.03512	-0.03512	0.121[a]
	tc	1.89665	0.09209	0.09209	0.121
CD_3H	v	2.00183	-0.03512	-0.03512	-0.060[a]
	tc	1.89665	0.09209	0.09209	-0.060
CD_4	v	2.00183	-0.03512	-0.03512	0 [a]
	tc	1.89665	0.09209	0.09209	0
CD_3T	v	2.00183	-0.03512	-0.03512	0.051
	tc	1.89665	0.09209	0.09209	0.051
CHF_3	v	2.49470	0.09036	0.09565	-0.10058
	tc	2.19359	0.20710	0.16193	-0.12586
CDF_3[b]	tc	2.09084	0.20765	0.15190	-0.12366
CH_3F	v	2.30301	0.03873	0.08834	0.06695
	tc	2.41038	0.08853	0.18545	0.25833
CD_3F[b]	tc	2.21842	0.16444	0.11510	0.13394
NH_3	v	2.12740	-0.00027	0.00061	0.00056
	tc	2.30175	0.01236	0.06857	0.00509
ND_3	v	2.19400	-0.00028	0.00068	0.00064
	tc	2.20711	0.05109	0.03960	0.05273

[a] Source: Ref. 48.

[b] Experimental results for the viscosity not available.

Table 3.5. Theoretically determined contributions of the three field terms $\underline{\underline{\psi}}_3$, $\underline{\underline{\psi}}_5$, and $\underline{\underline{\psi}}_6$, to the S-B effects on the thermal conductivity as measured by (H_3/λ_0), (H_5/λ_0), and (H_6/λ_0), respectively

Molecule	$\left(\frac{H_3}{\lambda_0}\right) \times 10^3$	$\left(\frac{H_5}{\lambda_0}\right) \times 10^3$	$\left(\frac{H_6}{\lambda_0}\right) \times 10^3$
CH_4	1.80	10^{-39}	10^{-8}
CH_3D	1.71	1×10^{-4}	2×10^{-5}
CH_3T	1.13	3×10^{-3}	3×10^{-4}
CD_3H	1.10	5×10^{-4}	3×10^{-7}
CD_4	0.80	10^{-30}	10^{-8}
CD_3T	0.81	1×10^{-4}	5×10^{-6}
CHF_3	1.86	7×10^{-3}	4×10^{-6}
CDF_3	1.77	7×10^{-3}	1×10^{-5}
CH_3F	1.15	1×10^{-3}	1×10^{-4}
CD_3F	1.12	5×10^{-4}	6×10^{-4}
NH_3	0.23	2×10^{-6}	7×10^{-6}
ND_3	0.30	8×10^{-5}	1×10^{-5}

Table 3.6. Comparison of theoretical and experimental (in parentheses when available) results for λ_0, $\lambda_0^{[2]}/\lambda_0^{[0]}$, $\Delta\lambda_{\parallel}$, $\Delta\lambda_{\perp}$, and $\Delta\lambda_{tr}$

Molecule	$\lambda_0 \times 10^5$ (cal/cm·s·°K)	$\left(\frac{\lambda_0^{[2]}}{\lambda_0^{[0]}}\right) \times 10^3$	$\left(\frac{\Delta\lambda_{\parallel}}{\lambda_0}\right)_{sat} \times 10^3$	$\left(\frac{\Delta\lambda_{\perp}}{\lambda_0}\right)_{sat} \times 10^3$	$\left(\frac{\Delta\lambda_{tr}}{\lambda_0}\right)_{max} \times 10^3$
CH_4	8.80 (8.75)[a]	1.80	-1.80 (-1.72)[a]	-2.70 (-2.75)[a]	1.28
CH_3D	8.53	1.71	-1.71	-2.56	1.22
CH_3T	8.29	1.13	-1.13	-1.69	0.80
CD_3H	8.07	1.10	-1.10	-1.65	0.78
CD_4	7.87 (8.77)[a]	0.80	-0.80 (-2.05)[a]	-1.20 (-3.20)[a]	0.57
CD_3T	7.67	0.81	-0.80	-1.21	0.57
CHF_3	3.16 (3.11)[b]	1.86	-1.86 (-1.90)[b]	-2.79 (-2.95)[b]	1.32
CDF_3	3.45 (3.44)[b]	1.77	-1.78 (-1.72)[b]	-2.66 (-2.70)[b]	1.26
CH_3F	3.74 (3.68)[b]	1.15	-1.15 (-0.98)[b]	-1.72 (-1.85)[b]	0.82

CD_3F	4.24 (4.20)[b]	1.12	-1.12 (-1.06)[b]	-1.68 (-1.73)[b]	0.80
NH_3	5.80 (5.83)[b]	0.23	-0.23 (-0.15)[b]	-0.35 (-0.40)[b]	0.16
ND_3	5.81 (5.76)[b]	0.30	-0.30 (-0.24)[b]	-0.46 (-0.50)[b]	0.22

[a]Source: Ref. 50.

[b]Source: Ref. 49.

Table 3.7. Characteristic field strengths for the S-B effects, $(H/P)^i_j$, where i denotes the component of the $\underline{\underline{\lambda}}$ tensor and j denotes the contributing basis function. For i = $\parallel$ or $\perp$, the value quantity listed is the field strength at one-half the saturation value of $\Delta\lambda_i$, and for i = tr the quantity listed is the field strength at the maximum value of $\Delta\lambda_{tr}$

Molecule	$(\frac{H}{P})^{\parallel}_3 \times 10^3$ (tesla/Pa)	$(\frac{H}{P})^{\parallel}_5 \times 10^3$ (tesla/Pa)	$(\frac{H}{P})^{\parallel}_6 \times 10^3$ (tesla/Pa)	$(\frac{H}{P})^{\perp}_3 \times 10^3$ (tesla/Pa)
CH_4	3.64	-	3.93	2.28
CH_3D	11.29	-	0.80	7.05
CH_3T	14.23	-	0.58	8.89
CD_3H	5.65	-	0.79	3.53
CH_4	6.27	-	0.67	3.92
CD_3T	18.96	-	1.50	11.84
CHF_3	21.72	-	12.87	13.57
CDF_3	19.92	-	3.35	12.44
CH_3F	27.08	-	6.45	16.92
CD_3F	29.11	-	3.60	18.19
NH_3	2.97	-	0.52	1.85
ND_3	5.05	-	0.92	3.15

$(\frac{H}{P})_5^{\perp} \times 10^3$ (tesla/Pa)	$(\frac{H}{P})_6^{\perp} \times 10^3$ (tesla/Pa)	$(\frac{H}{P})_3^{tr} \times 10^3$ (tesla/Pa)	$(\frac{H}{P})_5^{tr} \times 10^3$ (tesla/Pa)	$(\frac{H}{P})_6^{tr} \times 10^3$ (tesla/Pa)
0.65	3.93	2.24	0.65	3.93
3.71	0.80	6.94	3.71	0.80
4.32	0.58	8.75	4.32	0.58
0.72	0.79	3.48	0.72	0.78
0.74	0.67	3.86	0.74	0.67
4.04	1.50	11.66	4.04	1.50
3.34	23.87	13.36	3.34	23.87
3.05	3.35	12.25	3.05	3.35
12.87	6.45	16.65	12.87	6.45
84.39	3.60	17.90	84.39	3.60
0.01	0.52	1.82	0.01	0.52
0.27	0.92	3.10	0.27	0.92

Table 3.8. Theoretically derived contributions of the field terms $\underline{\underline{\phi}}_2$ and $\underline{\underline{\phi}}_3$ to the S-B effects on the viscosity as measured by Φ_{12} and Φ_{13}, respectively

Molecule	$\Phi_{12} \times 10^3$	$\Phi_{13} \times 10^3$
CH_4	0.96	10^{-15}
CH_3D	1.56	5×10^{-10}
CH_3T	2.30	2×10^{-9}
CD_3H	1.17	3×10^{-10}
CD_4	0.61	10^{-15}
CD_3T	0.89	1×10^{-10}
CHF_3	1.90	3×10^{-10}
CH_3F	1.05	2×10^{-10}
NH_3	8×10^{-5}	10^{-23}
ND_3	4×10^{-5}	10^{-24}

Table 3.9. Comparison of theoretical and experimental (in parentheses when available) results for η_0, $\eta_0^{[2]}/\eta_0^{[0]}$, $\Delta\eta_1$, $\Delta\eta_2$, $\Delta\eta_3$, η_4, and η_5

Molecule	$\eta_0 \times 10^4$ (gm/cm·s)	$\left(\frac{\eta_0^{[2]}}{\eta_0^{[0]}}\right) \times 10^3$	$\left(\frac{\Delta\eta_1}{\eta_0}\right)_{sat} \times 10^{12}$
CH_4	1.15 (1.09)[a]	0.96	3×10^{-6}
CH_3D	1.19	1.56	0.16
CH_3T	1.22	2.30	0.58
CD_3H	1.26	1.17	9×10^{-2}
CD_4	1.29	0.61	1×10^{-6}
CD_3T	1.32	0.89	3×10^{-2}
CHF_3	1.55 (1.48)[b]	1.90	0.01
CH_3F	1.27 (1.17)[b]	1.05	0.01
NH_3	1.05 (0.98)[b]	8×10^{-5}	3×10^{-15}
ND_3	1.08 (0.98)[b]	4×10^{-5}	2×10^{-15}

[a]Source: Ref. 51.

[b]Source: Ref. 52.

$\left(\frac{\Delta\eta_2}{\eta_0}\right)_{sat} = 10^3$	$\left(\frac{\Delta\eta_3}{\eta_0}\right)_{sat} \times 10^3$	$\left(\frac{\eta_4}{\eta_0}\right)_{max} \times 10^3$	$\left(\frac{\eta_5}{\eta_0}\right)_{max} \times 10^3$
-0.96 (-0.99)[a]	-0.96	0.48 (0.40)[a]	0.48
-1.56	-1.56	0.78	0.78
-2.30	-2.30	1.15	1.15
-1.17	-1.17	0.58	0.58
-0.61	-0.61	0.31	0.31
-0.89	-0.89	0.45	0.45
-1.90 (-1.90)[b]	-1.90	0.95 (0.95)[b]	0.95
-1.05 (-1.05)[b]	-1.05	0.52 (0.53)[b]	0.52
-8×10^{-5} (0.39)[b]	-8×10^{-5}	4×10^{-5} (-0.04)[b]	4×10^{-5}
-4×10^{-5} (0.43)[b]	-4×10^{-5}	2×10^{-5} (-0.04)[b]	2×10^{-5}

Table 3.10. Characteristic field strengths for the S-B effects, $(H/P)_j$, where j denotes the component of the $\underline{\underline{\eta}}$ tensor. For j = 1, 2, and 3, the quantity listed is the field strength at one-half the saturation value of $\Delta\eta_j$, and for j = 4 and 5 the quantity listed is the field strength at the maximum value of $\Delta\eta_j$

Molecule	$(\frac{H}{P})_1$ (tesla/Pa	$(\frac{H}{P})_2 \times 10^4$ (tesla/Pa)	$(\frac{H}{P})_3 \times 10^4$ (tesla/Pa)	$(\frac{H}{P})_4 \times 10^4$ (tesla/Pa)	$(\frac{H}{P})_5 \times 10^4$ (tesla/Pa)
CH_4	-	1.43	0.72	1.43	0.72
CH_3D	0.24	7.52	3.76	7.52	3.76
CH_3T	0.31	14.35	7.18	14.35	7.18
CD_3H	0.07	2.73	1.36	2.73	1.36
CD_4	-	1.58	0.79	1.58	0.79
CD_3T	0.04	7.09	3.55	7.09	3.55
CHF_3	0.31	19.33	9.67	19.33	9.67
CH_3F	3.45	9.52	4.76	9.52	4.76
NH_3	3×10^{-3}	7×10^{-5}	4×10^{-5}	7×10^{-5}	4×10^{-5}
ND_3	6×10^{-3}	7×10^{-5}	4×10^{-5}	7×10^{-5}	4×10^{-5}

IV. THERMAL-VISCOUS EFFECT IN CHIRAL MOLECULES

In this chapter, we will investigate the existence of a thermal-viscous effect in a dilute gas of chiral molecules. The thermal-viscous effect is an example of a cross coupling in the linear phenomenological behavior of the system. Many such effects are conceivable, some are well-known; the most common of these being the thermal-diffusion effect, or equivalently, the Dufour effect. However, many couplings can be shown to vanish in systems having a high degree of molecular and spatial symmetry. The general symmetry arguments used in discussing these effects are embodied in Curie's Principle (53). Examples of these arguments will be given below for the specific problem of a thermal-viscous effect. In order to see these cross effects, certain symmetries of the system must be broken. For example, it will be shown below that systems which are invariant to rotations or systems which are invariant under inversions can have no thermal-viscous couplings. To break these symmetries, we must introduce an external field and consider a gas of chiral molecules.

First, a discussion on the existence of a thermal-viscous effect in a gas of chiral molecules in a magnetic field will be given. Then a calculation of the thermal-viscous coefficient will be carried out along the lines followed in the evaluation of the expressions of the viscosity and thermal conductivity in the previous chapter. Finally, numerical results for the thermal-viscous coupling in model systems will be presented.

A. Theory

The entropy production in systems near equilibrium can be expressed as (54)

$$\frac{d}{dt} S_i = \sum_k J_k X_k \tag{4.1}$$

where S_i is the entropy produced by the system, J_k can be identified as a generalized flux and X_k its corresponding generalized force. Explicitly, for a gas with nonzero temperature and velocity gradients, Eq. (4.1) becomes

$$\frac{d}{dt} S_i = -\frac{1}{T^2} \underline{q} \cdot \underline{\nabla} T - \frac{1}{T} \overset{0}{\underline{\underline{\pi}}}^s : \underline{\nabla}^0 \underline{u} \tag{4.2}$$

where $\underline{q}$ represents the microscopic expression of the heat flux vector defined in the discussion of the thermal conductivity of symmetric top molecules and $\overset{0}{\underline{\underline{\pi}}}$ is the traceless symmetric part of the viscous pressure tensor. In Eq. (4.2), it is assumed that the divergence of the velocity field vanishes. Rewriting Eq. (4.2) in the form

$$\frac{d}{dt} S_i = \underline{J}^v \cdot \underline{X}^v + \underline{\underline{J}}^t : \underline{\underline{X}}^t \quad , \tag{4.3}$$

we find that

$$\underline{J}^v = \underline{q} \tag{4.4a}$$

$$J^t = \overset{0}{\underline{\underline{\pi}}}^s \tag{4.4b}$$

and

$$\underline{X}^{v} = -T^{-2}\underline{\nabla}T \tag{4.5a}$$

$$\underline{\underline{X}}^{t} = -T^{-1}\underline{\nabla}^{0}\underline{u} \quad . \tag{4.5b}$$

The generalized forces and fluxes are related through the linear phenomenological relations

$$\underline{J}^{v} = \underline{\underline{L}}^{vv} \cdot \underline{X}^{v} + \underline{\underline{L}}^{vt} : \underline{\underline{X}}^{t} \tag{4.6a}$$

and

$$\underline{\underline{J}}^{t} = \underline{\underline{L}}^{tv} \cdot \underline{X}^{v} + \underline{\underline{L}}^{tt} : \underline{\underline{X}}^{t} \quad . \tag{4.6b}$$

Here $\underline{\underline{L}}^{vv}$ is a second rank tensor related to the thermal conductivity tensor, $\underline{\underline{L}}^{tt}$ is a fourth rank tensor related to the coefficient of viscosity tensor, and $\underline{\underline{L}}^{vt}$ and $\underline{\underline{L}}^{tv}$, which are third rank tensors, are the thermal-viscous coupling coefficients. Since the two coefficients, $\underline{\underline{L}}^{vt}$ and $\underline{\underline{L}}^{tv}$, are related through Onsager (55)-Casimir (56) relations, we need only to concentrate our efforts towards the calculations of $\underline{\underline{L}}^{vt}$. The method of calculating $\underline{\underline{L}}^{tv}$ is similar to that for calculating $\underline{\underline{L}}^{vt}$. The coefficient $\underline{\underline{L}}^{vt}$ explicitly couples the heat flux to a nonequilibrium distortion proportional to the velocity gradients.

In general, all fluxes can conceivably couple to all forces. However, Curie (53) has shown that many of the $\underline{\underline{L}}$'s vanish in systems with a high degree of spatial symmetry. Consider an orthogonal transformation of the cartesian coordinate frame. This transformation will be represented by the second rank tensor $\underline{\underline{A}}^{\dagger}$. If the microscopic equations of motion for the system are invariant in form under the action

of $\underline{\underline{A}}^{\dagger}$ on the coordinate system, then we say that the transformation $\underline{\underline{A}}^{\dagger}$ reflects a spatial symmetry of the system. For example, the system composed of N molecules in the absence of an external field is invariant under general rotations of the coordinate system. Equivalently, instead of considering a coordinate transformation, we can imagine an actual transformation of the system. The action of this transformation on a vector in the system is given in terms of the transpose of the second rank tensor $\underline{\underline{A}}^{\dagger}$, denoted by $\underline{\underline{A}}$. The tensor $\underline{\underline{A}}$ transforms a vector, say $\underline{T}^{(1)}$, to a new vector $\underline{T}^{(1)'}$, which is related to $\underline{T}^{(1)}$ through the relation

$$\underline{T}^{(1)'} = \underline{\underline{A}} \cdot \underline{T}^{(1)} \quad . \tag{4.7}$$

In general, let $\underline{\underline{T}}^{(n)}$ represent an nth rank tensor. Then the transformation, $\underline{\underline{A}}$, acts on $\underline{\underline{T}}^{(n)}$ as

$$\underline{\underline{T}}^{(n)'} = |\underline{\underline{A}}|^{\varepsilon}(\underline{\underline{A}})^{n}(\cdot)^{n}\underline{\underline{T}}^{(n)} \tag{4.8}$$

where $\underline{\underline{T}}^{(n)'}$ denotes the transformed tensor, $|\underline{\underline{A}}|$ is the determinate of $\underline{\underline{A}}$, and the quantity ε is zero for polar tensors and one for axial tensors. The symbol $(\cdot)^{n}$ denotes a sequential contraction of the right hand indices of each of the n $\underline{\underline{A}}$'s into the n indices of $\underline{\underline{T}}^{(n)}$, i.e.,

$$[(\underline{\underline{A}})^{n}(\cdot)^{n}\underline{\underline{T}}^{(n)}]_{j_1 j_2 \cdots j_n} = \sum_{i_1 i_2 \cdots i_n} A_{j_1 i_1} A_{j_2 i_2} \cdots A_{j_n i_n} T^{(n)}_{i_1 i_2 \cdots i_n} \quad . \tag{4.9}$$

Because the linear phenomenological relations are simply macroscopic manifestations of the microscopic equations of motion, the force-flux

relations of Eq. (4.6) must be invariant to transformations reflecting spatial symmetries of the system. Therefore, if $\underline{\underline{A}}$ (or $\underline{\underline{A}}^{\dagger}$) reflects a spatial symmetry of the system, the coupling coefficients of Eq. (4.6) must satisfy the relations

$$\underline{\underline{L}} = |\underline{\underline{A}}|^{\varepsilon}(\underline{\underline{A}})^{n}(\cdot)^{n}\underline{\underline{L}} \tag{4.10}$$

where n is the tensor rank of $\underline{\underline{L}}$. This equation represents the mathematical formulation of Curie's Principle.

We now wish to discuss the implication of Curie's Principle for a dilute gas. This will be accomplished by considering three examples:

(1) A dilute gas of achiral molecules is invariant under inversions. The transformation corresponding to an inversion can be represented by $\underline{\underline{I}}$, where

$$(\underline{\underline{I}})_{ij} = -\delta_{ij} \tag{4.11}$$

with $\det(\underline{\underline{I}}) = -1$. Applying Curie's Principle in the form of Eq. (4.10) to this system and replacing $\underline{\underline{A}}$ with $\underline{\underline{I}}$ and $\underline{\underline{T}}^{(n)}$ with the coupling coefficients, we obtain

$$\underline{\underline{L}}^{vt} = -\underline{\underline{L}}^{vt} \tag{4.12a}$$

and

$$\underline{\underline{L}}^{tv} = -\underline{\underline{L}}^{tv} \tag{4.12b}$$

where the fact that $\underline{\underline{L}}^{vv}$, $\underline{\underline{L}}^{tt}$, $\underline{\underline{L}}^{tv}$, and $\underline{\underline{L}}^{tt}$ are all polar tensors has been used. Equation (4.12) requires that $\underline{\underline{L}}^{tv} = \underline{\underline{L}}^{vt} = 0$, which allows us to reexpress the linear relations as

$$\underline{J}^{v} = \underline{\underline{L}}^{vv} \cdot \underline{X}^{v} \tag{4.13a}$$

and

$$\underline{\underline{J}}^{t} = \underline{\underline{L}}^{tt} : \underline{\underline{X}}^{t} \quad . \tag{4.13b}$$

These are the familiar expressions (with no cross couplings) of Fourier's Law and Newton's Law of friction, respectively. In systems with parity symmetry, the thermal-viscous couplings vanish.

(2) A dilute gas of chiral molecules has no parity symmetry. However, the system is invariant under general rotations. Denoting the general rotation transformation by $\underline{\underline{R}}(\theta,\phi,\psi)$, where θ, ϕ, and ψ are the usual Euler angles, implementation of Curie's Principle demands

$$(\underline{\underline{R}})^{3}(\cdot)^{3}\underline{\underline{L}}^{vt} = \underline{\underline{L}}^{vt} \quad . \tag{4.14}$$

This implies that $\underline{\underline{L}}^{vt}$ is proportional to the third rank isotropic tensor, $\underline{\underline{\Psi}}$ ($\Psi_{ijk} = \varepsilon_{ijk}$, the Levi-Civita density) where $\underline{\underline{\Psi}}$ is antisymmetric on all pairs of indices. Therefore, the product $\underline{\underline{L}}^{vt} : \underline{\underline{X}}^{t}$, which is proportional to $\underline{\underline{\Psi}} : \underline{\underline{X}}^{t}$, vanishes due to the symmetric nature of $\underline{\underline{X}}^{t}$ (refer to Eq. (4.5)). Similar arguments show the coupling through $\underline{\underline{L}}^{tv}$ to vanish. For this system, the linear relations of the form in Eq. (4.13) hold.

From these first two examples, we see that the thermal-viscous couplings vanish in the presence of either a rotational or an inversional symmetry. In order to observe a thermal-viscous effect, both of these symmetries must be destroyed. This assertion is born out in the last example.

(3) A dilute gas of chiral molecules in the presence of an external magnetic field contains neither inversional or rotational symmetry. The chirality of the molecule has eliminated the parity symmetry and the field has broken the isotropy of the space. The remaining symmetry is the invariance to rotations about the field. Denoting this transformation by $\underline{\underline{R}}(0,\phi,0)$ (where the field is taken to lie along the $\hat{k}$ direction) and applying Curie's Principle to $\underline{\underline{L}}^{vt}$, we find that

$$\underline{\underline{L}}^{vt} = (\underline{\underline{R}}(0,\phi,0))^3(\cdot)^3\underline{\underline{L}}^{vt} \quad . \tag{4.15}$$

This requires $\underline{\underline{L}}^{vt}$ to be proportional to tensors of third rank which are isotropic about the field. All such tensors are formed from the three elementary tensors

$$\hat{k} \tag{4.16a}$$

$$\underline{\underline{U}}_k^{(2)} = \underline{\underline{U}}^{(3)} - \hat{k}\hat{k} \tag{4.16b}$$

and

$$\underline{\underline{V}}_k^{(2)} = -\hat{k} \times \underline{\underline{U}}^{(3)} \tag{4.16c}$$

which are individually isotropic about the $\hat{k}$ direction. Thus, Curie's Principle allows for the existence of a thermal-viscous coupling, but requires the coupling coefficient, $\underline{\underline{L}}^{vt}$, to be a functional of $\hat{k}$, $\underline{\underline{U}}_k^{(2)}$, $\underline{\underline{V}}_k^{(2)}$, i.e.,

$$\underline{\underline{L}}^{vt} = \underline{\underline{L}}^{vt}(\hat{k},\underline{\underline{U}}_k^{(2)},\underline{\underline{V}}_k^{(2)}) \quad . \tag{4.17}$$

At this point, we can now deduce the general form of $\underline{\underline{L}}^{vt}$. Knowing that $\underline{\underline{L}}^{vt}$ is rank 3 and a functional of $\hat{k}$, $\underline{\underline{U}}_k^{(2)}$, and $\underline{\underline{V}}_k^{(2)}$ allows us to write

$$\underline{\underline{L}}^{vt} = A\hat{k}\hat{k}\hat{k} + Bk\underline{\underline{U}}_k^{(2)} + C\underline{\underline{(\hat{k}U)}}_k^{(2)} + D\underline{\underline{U}}_k^{(2)}\hat{k} + Ek\underline{\underline{V}}_k^{(2)} + F\underline{\underline{\hat{k}V}}_k^{(2)} + G\underline{\underline{V}}_k^{(2)}\hat{k} \quad . \tag{4.18}$$

Further, the fact that $\underline{\underline{L}}^{vt}$ is symmetric and traceless on its last pair of indices reduces Eq. (4.18) to

$$\underline{\underline{L}}^{vt} = L_1(\hat{k}\hat{k}\hat{k} - \frac{1}{2}\hat{k}\underline{\underline{U}}_k^{(2)} + L_2(\underline{\underline{U}}_k^{(2)}\hat{k} + \underline{\underline{(\hat{k}U)}}_k^{(2)}) + L_3(\underline{\underline{V}}_k^{(2)}\hat{k} + \underline{\underline{\hat{k}V}}_k^{(2)}) \quad . \tag{4.19}$$

This is the final form for $\underline{\underline{L}}^{vt}$. From Eq. (4.19), the following relations between the components of $\underline{\underline{L}}^{vt}$ are obtained

$$L_{333}^{vt} = -\frac{1}{2}L_{311}^{vt} = -\frac{1}{2}L_{322}^{vt} = L_1 \tag{4.20a}$$

$$L_{113}^{vt} = L_{223}^{vt} = L_{131}^{vt} = L_{232}^{vt} = L_2 \tag{4.20b}$$

and

$$L_{123}^{vt} = -L_{213}^{vt} = L_{132}^{vt} = -L_{231}^{vt} = L_3 \quad . \tag{4.20c}$$

This is identical to the form for $\underline{\underline{L}}^{vt}$ obtained by de Groot and Mazur (54). Also from Eq. (4.19), the components L_1 and L_2 are seen to be odd in the field, whereas the component L_3 is even in the field.

To obtain a microscopic expression for the thermal-viscous coupling coefficient, we proceed in a manner similar to that of the previous

derivations of the coefficients of shear viscosity and thermal conductivity. We begin with the explicit form of the heat flux vector, $\underline{q}$, from Eq. (3.4), namely

$$\underline{q} = - nkT \left(\frac{2kT}{m} \right)^{1/2} \langle \underline{W} \left(\frac{5}{2} - W^2 \right) + \underline{W} (\langle E_{int}/kT \rangle - E_{int}/kT), \Phi \rangle \quad . \tag{4.21}$$

When the distortion,

$$\Phi = \left(\frac{2kT}{m} \right)^{1/2} \underline{A} \cdot \underline{\nabla} \ln T + \underline{\underline{B}} : \underline{\nabla}^0 \underline{u} \tag{4.22}$$

is inserted into this expression, we obtain the microscopic analogue to Eq. (4.6a)

$$\begin{aligned} \underline{J}^v = {} & nkT^2 \left(\frac{2kT}{m} \right) \langle \underline{W} \left(\frac{5}{2} - W^2 \right) + \underline{W} (\langle E_{int}/kT \rangle - E_{int}/kT), \underline{A} \rangle \cdot (- T^{-2} \underline{\nabla} T) \\ & + nkT^2 \left(\frac{2kT}{m} \right)^{1/2} \langle \underline{W} \left(\frac{5}{2} - W^2 \right) + \underline{W} (\langle E_{int}/kT \rangle \\ & - E_{int}/kT), \underline{\underline{B}} \rangle : (- T^{-1} \underline{\nabla}^0 \underline{u}) \quad . \end{aligned} \tag{4.23}$$

Here, E_{int} is the internal energy of the chiral molecule. From Eqs. (4.5), (4.6) and (4.23), we obtain

$$\underline{\underline{L}}^{vt} = nkT^2 \left(\frac{2kT}{m} \right)^{1/2} \langle \underline{W} \left(\frac{5}{2} - W^2 \right) + \underline{W} (\langle E_{int}/kT \rangle - E_{int}/kT), \underline{\underline{B}}^{vt} \rangle \quad . \tag{4.24}$$

where $\underline{\underline{B}}^{vt}$ is required to satisfy the linear equation

$$2 f_0^{(1)} \underline{W}^0 W = - \hat{\Lambda} (\underline{\underline{B}}^{vt}) \tag{4.25}$$

which is derived in Chapter II. Equation (4.24) is the desired microscopic expression for the thermal-viscous coupling coefficient.

The quantity $\underline{\underline{B}}^{vt}$, which satisfies Eq. (4.25), is generated by the methods used in the previous sections. It is expanded in a truncated basis set forming a matrix equation, which can be solved using the inversion technique of Cooper and Hoffman (38). From Eqs. (4.24) and (4.25), it is realized that for a nonzero $\underline{\underline{L}}^{vt}$ to exist, there must be a coupling between basis terms of the form $\underline{W}^{0}\underline{W}$ and $\underline{W}(\langle E\rangle - E)$. Because these terms have different parity symmetries, the coupling would be impossible were it not for the chirality of the molecules (refer to example 1 above). However, the collision operator still commutes with the general rotation operator. Thus, it is impossible to couple these terms through the collision operator alone since they transform as basis elements belonging to different irreducible representations of the full rotation group. Therefore, we must seek a coupling of these two terms through the field operator. This is not surprising; it is exactly what examples 2 and 3 prepared us for. After all, it requires both the molecular chirality and the presence of the external field in order to observe a thermal-viscous coupling.

Because the field effects are at best 2nd order in the nonsphericity, $\underline{\underline{L}}^{vt}$ also is at best a 2nd order effect. The expansion set must contain an element, say $\underline{\underline{X}}$, such that

$$\underline{W}^{0}\underline{W} \longleftrightarrow \underline{\underline{X}} \longleftrightarrow \underline{W}(\langle E\rangle - E) \tag{4.26}$$

where the two headed arrows represent a coupling. However, no such $\underline{\underline{X}}$ exists. For example, let $\underline{\underline{X}}$ be a basis function whose tensorial structure is given by $\underline{W}\underline{W}$. Due to the rotational symmetry of the collision

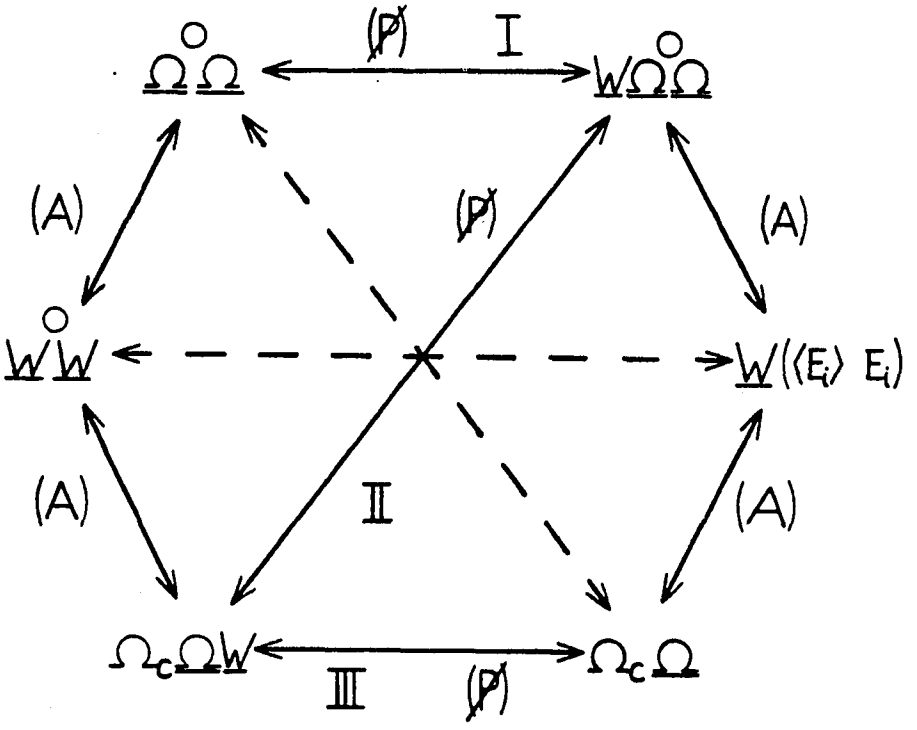

Figure 4.1. The various thermal-viscous coupling routes contained in the basis set listed in Table 4.1

operator (30), the bracket integral of two tensor functions is zero unless their direct product contains a basis element belonging to the totally symmetric representation of the rotation group. Both the direct products of $\underline{W}^0\underline{W}$ with $\underline{WW}$ and $\underline{W}$ with $\underline{WW}$ contain such a basis element. However, for rigid chatterless interactions, the integrand of the bracket integral of $\underline{W}$ with $\underline{WW}$ is proportional to $\hat{k} \cdot \hat{k} \times \hat{k}$ which vanishes identically. Therefore, the term, $\underline{WW}$, does not give rise to a second order coupling. Similar arguments show that other plausible choices for $\underline{\underline{X}}$ also do not give rise to a second order coupling. Because of this, the best we can hope for is a third order coupling, i.e.,

$$\underline{W}^0\underline{W} \longleftrightarrow \underline{\underline{X}}_1 \longleftrightarrow \underline{\underline{X}}_2 \longleftrightarrow \underline{W}(\langle E \rangle - E) \quad . \tag{4.27}$$

We will investigate three such couplings. These three avenues are contained in the following expansion of $\underline{\underline{B}}^{vt}$

$$\underline{\underline{B}}^{vt} = \underline{\underline{\phi}}_1 \circledcirc^2 \underline{\underline{B}}_1 + \underline{\underline{\phi}}_2 \circledcirc^2 \underline{\underline{B}}_2 + \underline{\underline{\phi}}_3 \circledcirc^3 \underline{\underline{B}}_3 + \underline{\phi}_4 \cdot \underline{\underline{B}}_4 + \underline{\phi}_5 \cdot \underline{\underline{B}}_5 + \underline{\phi}_6 \cdot \underline{\underline{B}}_6 + \underline{\underline{\phi}}_7 \circledcirc^2 \underline{\underline{B}}_7 \tag{4.28}$$

with the $\underline{\underline{\phi}}_i$'s given in Table 4.1 along with their parity and time reversal eigenvalues. The three possible couplings in the expansion above are shown diagrammatically in Fig. 4.1. The dashed lines in Fig. 4.1 denote couplings forbidden because their direct products do not contain a basis for the totally symmetric representation of the rotation group. The solid lines denote possible couplings, where the letter in parentheses indicates the mode of coupling. For instance,

($\not{P}$) represents a coupling due to the chirality of the molecular potential, whereas the term (A) denotes a coupling through the anisotropy of the interaction. The Roman numerals indicate the various pathways. Below, terms with a superscript I, II, or III will refer to the pathway I, II, or III, respectively.

Insertion of the expression for B, Eq. (4.28), into the microscopic expression for $\underline{\underline{L}}^{vt}$, Eq. (4.24), results in

$$\underline{\underline{L}}^{vt} = \frac{kT^2}{4\sqrt{2}} \{5\underline{\underline{B}}_4 + 3\underline{\underline{B}}_5\} \quad . \tag{4.29}$$

The $\underline{\underline{B}}_i$'s can be expanded as

$$\underline{\underline{B}}_i = \underline{\underline{B}}_i^{I} + \underline{\underline{B}}_i^{II} + \underline{\underline{B}}_i^{III} \quad , \quad i = 4, 5 \tag{4.30}$$

due to the three possible coupling routes. Solving Eq. (4.25) for $\underline{\underline{B}}_4$ and $\underline{\underline{B}}_5$, using standard techniques, we find that:

$$\underline{\underline{B}}_4^{I} = (\Delta/\theta_{33}\theta_{22})(\theta_{55}\theta_{43}\theta_{32}\theta_{21} - \theta_{45}\theta_{53}\theta_{32}\theta_{21})\underline{\underline{\Gamma}}_I \tag{4.31a}$$

$$\underline{\underline{B}}_5^{I} = (\Delta/\theta_{33}\theta_{22})(\theta_{44}\theta_{53}\theta_{32}\theta_{21} - \theta_{45}\theta_{43}\theta_{32}\theta_{21})\underline{\underline{\Gamma}}_I \tag{4.31b}$$

$$\begin{aligned}\underline{\underline{\Gamma}}_I = {} & [4C_1(\xi_3)]\{\hat{k}\hat{k}\hat{k} - \tfrac{1}{2}\hat{k}\underline{\underline{U}}_k^{(2)}\} + [2C_1(2\xi_3)C_0(\xi_2) - C_1(\xi_3)C_0(\xi_2) - C_1(\xi_2) \\ & - C_0(\xi_3)C_1(\xi_2)]\{\underline{U}_k^{(2)}\hat{k} + \underline{\underline{(\hat{k})}}_k^{(2)}\} + [C_0(\xi_2) + C_0(\xi_3)C_0(\xi_2) \\ & - 2C_0(2\xi_3)C_0(\xi_2) - C_1(\xi_3)C_1(\xi_2) + \tfrac{5}{3}C_1(2\xi_3)C_1(\xi_2)]\{\underline{V}_k^{(2)}k + \underline{\underline{\hat{k}\hat{k}}}_k^{(2)}\}\end{aligned}$$

$$= L_1^{I}\{\hat{k}\hat{k}\hat{k}\hat{k} - \tfrac{1}{2}\,\hat{k}\underline{\underline{U}}_k^{(2)}\} + L_2^{I}\{\underline{\underline{U}}_k^{(2)}\hat{k} + \underline{\underline{\hat{k}\underline{U}}}_k^{(2)}\} + L_3^{I}\{\underline{\underline{V}}_k^{(2)}\hat{k} + \underline{\underline{\hat{k}\underline{V}}}_k^{(2)}\}\ , \quad (4.32)$$

$$\underline{\underline{B}}_4^{II} = (\Delta/\theta_{33}\theta_{77})(\theta_{55}\theta_{43}\theta_{37}\theta_{71} - \theta_{45}\theta_{53}\theta_{37}\theta_{71})\underline{\underline{\Gamma}}_{II} \quad (4.33a)$$

$$\underline{\underline{B}}_5^{II} = (\Delta/\theta_{33}\theta_{77})(\theta_{44}\theta_{53}\theta_{37}\theta_{71} - \theta_{45}\theta_{43}\theta_{37}\theta_{71})\underline{\underline{\Gamma}}_{II} \quad (4.33b)$$

$$\begin{aligned}\underline{\underline{\Gamma}}_{II} = {} & [-\tfrac{2}{3}C_1(\xi_3) - \tfrac{1}{3}C_1(\xi_3)C_0(\xi_7) + \tfrac{2}{3}C_1(\xi_7) + C_0(\xi_3)C_1(\xi_7)] \\ & \times \{\hat{k}\hat{k}\hat{k}\hat{k} - \tfrac{1}{2}\,\hat{k}\underline{\underline{U}}_k^{(2)}\} + [-\tfrac{1}{4}C_1(\xi_3) - C_1(2\xi_3) + \tfrac{1}{2}C_1(\xi_3)C_0(\xi_7) \\ & + \tfrac{1}{2}C_1(2\xi_3)C_0(\xi_7) + \tfrac{1}{4}C_1(\xi_7) + \tfrac{1}{2}C_0(\xi_3)C_1(\xi_7) + \tfrac{1}{2}C_0(2\xi_3)C_1(\xi_7)] \\ & \times \{\underline{\underline{U}}_k^{(2)}\hat{k} + \ {}_k^{(2)}\} + [\tfrac{1}{4}C_0(\xi_3) + C_0(2\xi_3) - \tfrac{1}{4}C_0(\xi_7) \\ & - \tfrac{1}{2}C_0(\xi_3)C_0(\xi_7) - \tfrac{1}{2}C_0(2\xi_3)C_0(\xi_7) + \tfrac{1}{2}C_1(\xi_3)C_1(\xi_7) \\ & + \tfrac{1}{2}C_1(2\xi_3)C_1(\xi_7)]\{\underline{\underline{V}}_k^{(2)}\hat{k} + \ {}_k^{(2)}\}\end{aligned}$$

$$= L_1^{II}\{\hat{k}\hat{k}\hat{k}\hat{k} - \tfrac{1}{2}\,k\underline{\underline{U}}_k^{(2)}\} + L_2^{II}\{\underline{\underline{U}}_k^{(2)}\hat{k} + \underline{\underline{\hat{k}\underline{U}}}_k^{(2)}\} + L_3^{II}\{\underline{\underline{V}}_k^{(2)}\hat{k} + \underline{\underline{\hat{k}\underline{V}}}_k^{(2)}\}\ , \quad (4.34)$$

$$\underline{\underline{B}}_4^{III} = -(\Delta/\theta_{66}\theta_{77})(\theta_{45}\theta_{56}\theta_{67}\theta_{71})\underline{\underline{\Gamma}}_{III} \quad (4.35a)$$

$$\underline{\underline{B}}_5^{III} = (\Delta/\theta_{66}\theta_{77})(\theta_{44}\theta_{56}\theta_{67}\theta_{71})\underline{\underline{\Gamma}}_{III} \quad (4.35b)$$

and

$$\underline{\underline{\Gamma}}_{III} = [\tfrac{2}{3} C_1(\xi_7)]\{\hat{k}\hat{k}\hat{k}\hat{k} - \tfrac{1}{2} \hat{k}\underline{\underline{U}}_k^{(2)}\} + \tfrac{1}{2} [C_1(\xi_6)C_0(\xi_7) + C_0(\xi_6)C_1(\xi_7)$$

$$- C_1(\xi_6)]\{\underline{\underline{U}}_k^{(2)}\hat{k} + \underline{\underline{(\hat{k}U)}}_k^{(2)}\} + \tfrac{1}{2} [C_0(\xi_6)(1 - C_0(\xi_7))$$

$$+ C_1(\xi_6)C_1(\xi_7)]\{\underline{\underline{V}}_k^{(2)}\hat{k} + \underline{\underline{\hat{k}V}}_k^{(2)}\}$$

$$= L_1^{III}\{\hat{k}\hat{k}\hat{k}\hat{k} - \tfrac{1}{2} \hat{k}\underline{\underline{U}}^{(2)}\} + L_2^{III}\{\underline{\underline{U}}_k^{(2)}\hat{k} + \underline{\underline{(\hat{k}U)}}_k^{(2)}\} + L_3^{III}\{\underline{\underline{V}}_k^{(2)}\hat{k} + \underline{\underline{\hat{k}V}}_k^{(2)}\}. \tag{4.36}$$

Here, $\Delta = \theta_{11}[\theta_{44}\theta_{55} - \theta_{45}^2]$, and the θ_{ij}'s and the $C_i(x)$ functions are defined in the previous chapter. Equations (4.28)-(4.35) relate the thermal-viscous coupling coefficient to the collision integrals. In the following section, the collision integrals are evaluated for various model systems.

In concluding this section, we remark that the thermal-viscous effect in rigid chatterless systems is third order in the nonsphericity of the potential. For systems interacting through more realistic potentials (i.e., soft potentials or rigid potentials where chattering is considered), the thermal-viscous effect could conceivably be a second order effect. However, the requirement that an external field be present excludes the existence of a thermal-viscous coupling at any order lower than second in molecular nonsphericity.

B. Numerical Results

The theory presented above for the thermal-viscous effect assumes the chiral molecules to behave kinematically like symmetric tops. We

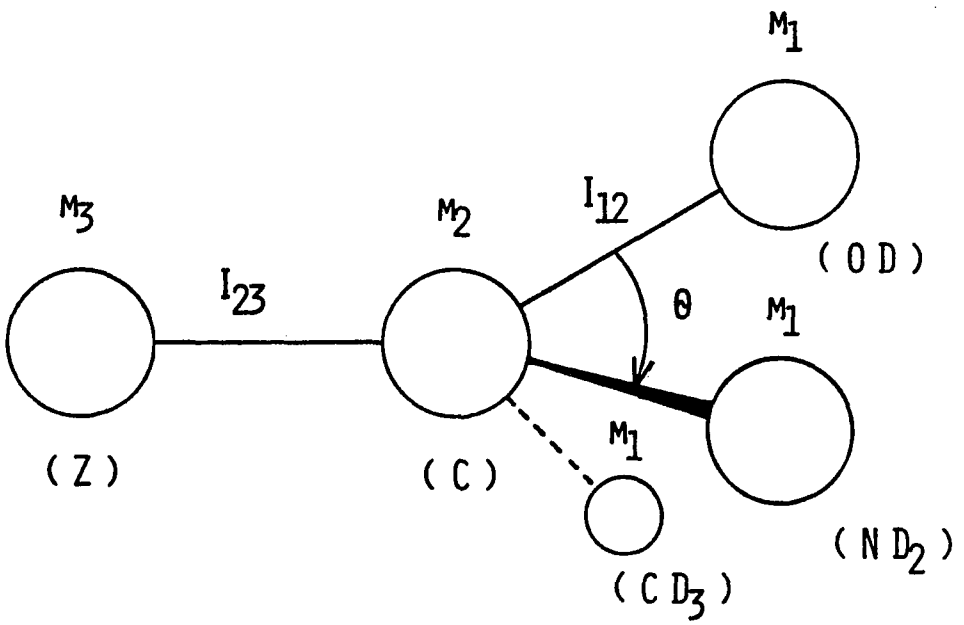

Figure 4.2. Geometry of the chiral molecules used in the calculation of the kinematic parameters in Table 4.2. Here M_1 = 18 amu, M_2 = 12 amu, θ = 1.9114 radians (tetrahedral angle), and ℓ_{12} = 1.48 Å. The values of M_3 and ℓ_{23} depend on the choice of z and are listed in Table 4.2

have chosen to base the numerical work on the molecular system, C Z CD_3 ND_2 OD, where Z will equal H, D, F, Cl, and Br. Setting Z equal to D yields the totally deuterated analogue of 1-amino-ethanol. This chiral molecule is chosen because it is nearly a symmetric top. The approximate geometry of this molecule is given in Fig. 2.2. In Table 2.2, we list the relevant kinematic parameters.

In order to model the geometry of the above system, we use the supporting function (13)

$$h = \alpha + \sum_i \beta_i (\hat{k} \cdot \hat{e}_i)^3 + \gamma(\hat{k} \cdot \hat{e}_3) \tag{4.37}$$

where the quantities in this expression are defined in the numerical section of Chapter III. Due to the lack of experimental results on chiral systems, we will not be able to utilize a fitting program similar to the one used in the symmetric top studies above to determine molecular parameters. For this reason, we will calculate the size of the thermal-viscous coupling for several choices of the β_i parameters in Eq. (4.37). The values of α are chosen to be in reasonable agreement with the values for the symmetric top molecules of the last chapter, and is determined from the molecular geometry in Fig. 4.2. These values for α, the β_i's, and γ are given in Table 4.3, along with the dimensionless parameter, χ,

$$\chi = \left| \prod_{i<j} [(\ell_i - \ell_j)/\alpha] \right| \quad . \tag{4.38}$$

Here, ℓ_i represents the distance from the center of mass to the molecular surface along the ith axis for a system described by the supporting

Figure 4.3. The geometric field dependence of the thermal-viscous coupling coefficient arising from coupling route I for various values of ρ_{37}. The abscissa is the ratio of the magnetic field strength to the pressure (in tesla/Pa) and the ordinate is the magnitude of the L_i's

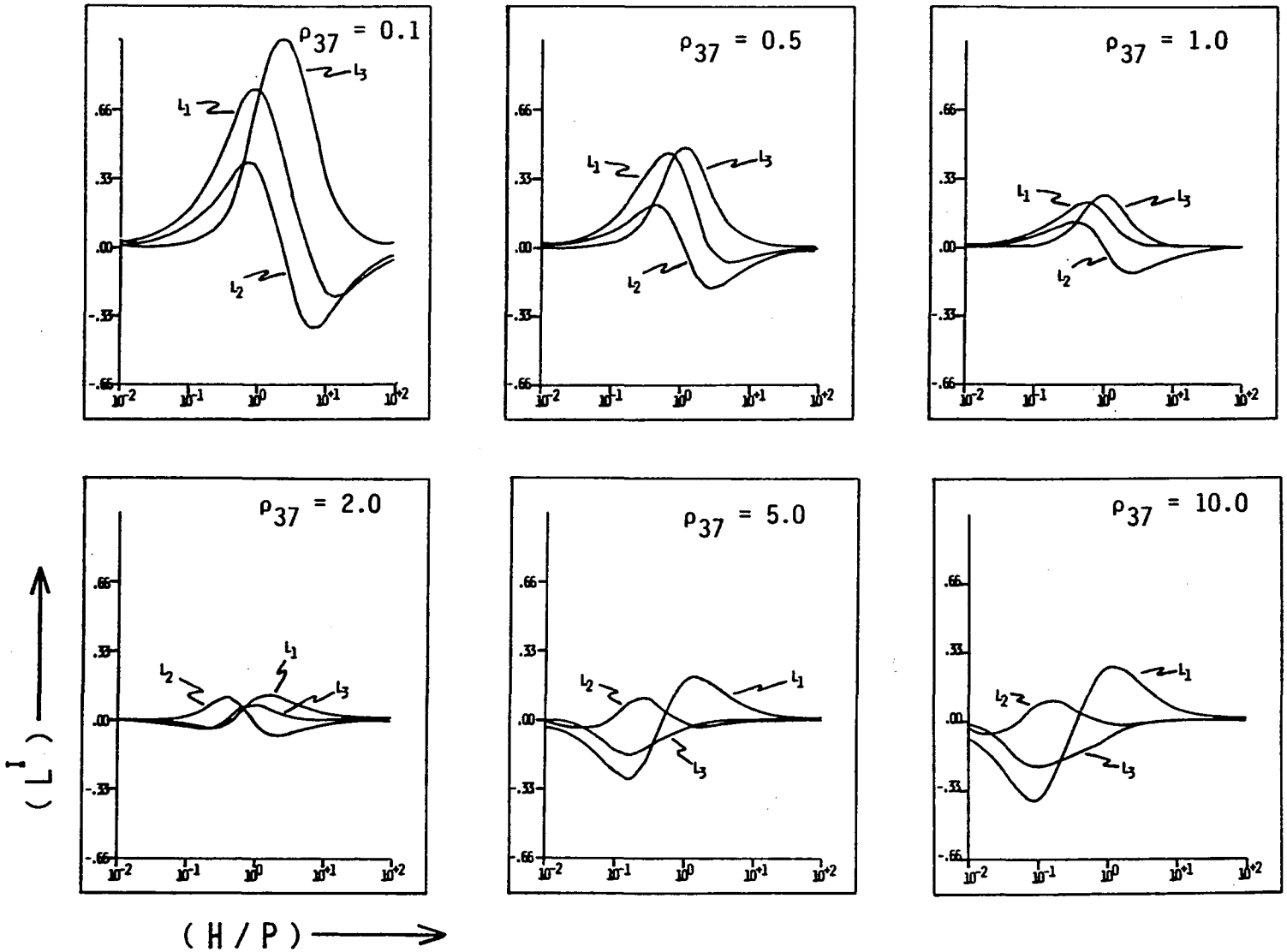
ρ37 = 0.1
ρ37 = 0.5
ρ37 = 1.0
ρ37 = 2.0
ρ37 = 5.0
ρ37 = 10.0
L1
L2
L3
.66
.33
.00
-.33
-.66
10-2
10-1
100
10+1
10+2
(I)
(H / P)

Figure 4.4. The geometric field dependence of the thermal-viscous coupling coefficient arising from coupling route II for various values of ρ_{67}. The abscissa is the ratio of the magnetic field strength to the pressure (in tesla/Pa) and the ordinate is the magnitude of the L_i^{II}'s

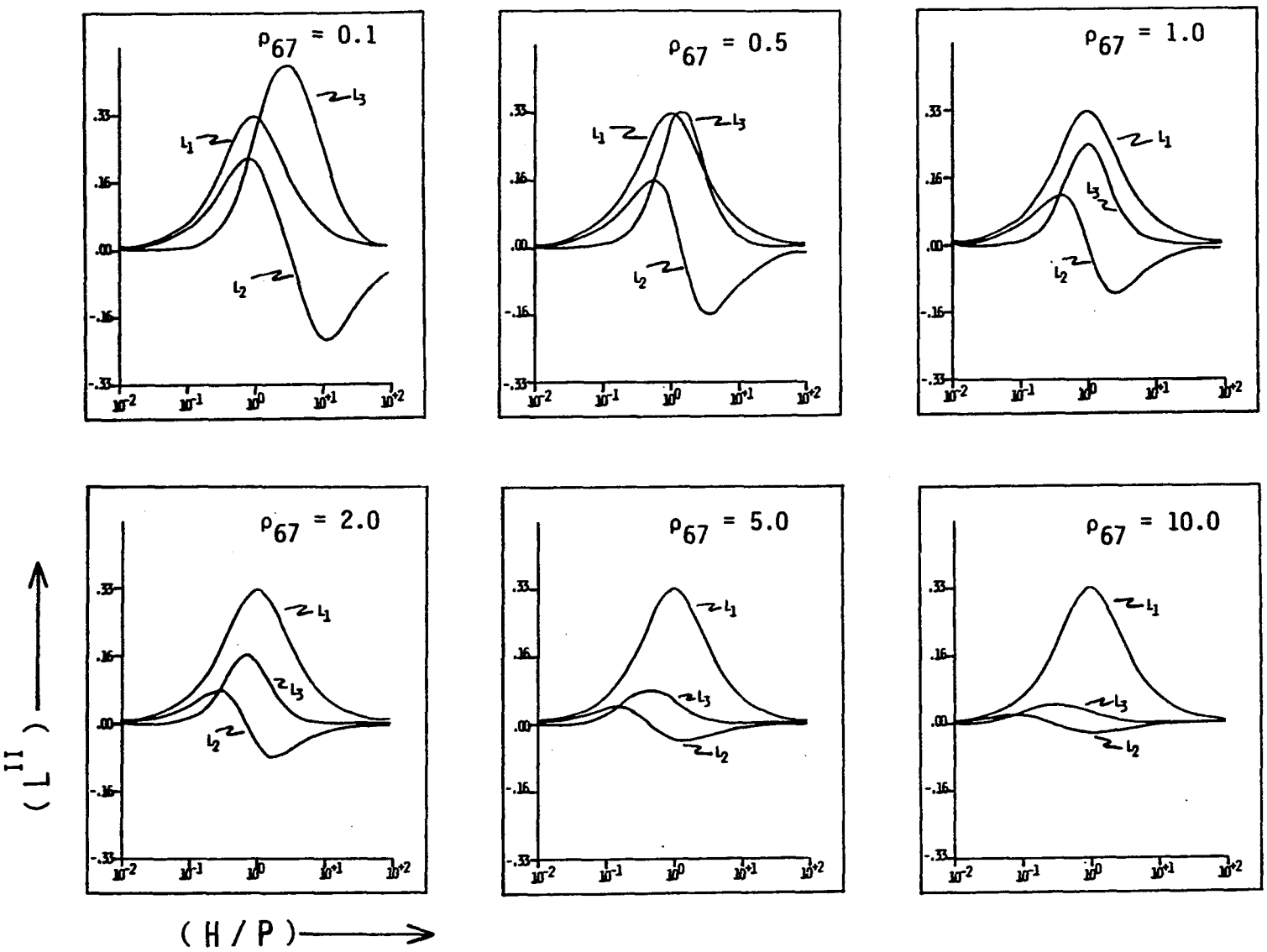
ρ_{67} = 0.1
ρ_{67} = 0.5
ρ_{67} = 1.0
ρ_{67} = 2.0
ρ_{67} = 5.0
ρ_{67} = 10.0
l_1
l_2
l_3
.33
.16
.00
-.16
-.33
10^{-2}
10^{-1}
10^{0}
10^{+1}
10^{+2}
(L I)
(H / P)

Figure 4.5. The geometric field dependence of the thermal-viscous coupling coefficient arising from coupling route III for various values of ρ_{23}. The abscissa is the ratio of the magnetic field strength to the pressure (in tesla/Pa) and the ordinate is the magnitude of the L_i^{III}'s

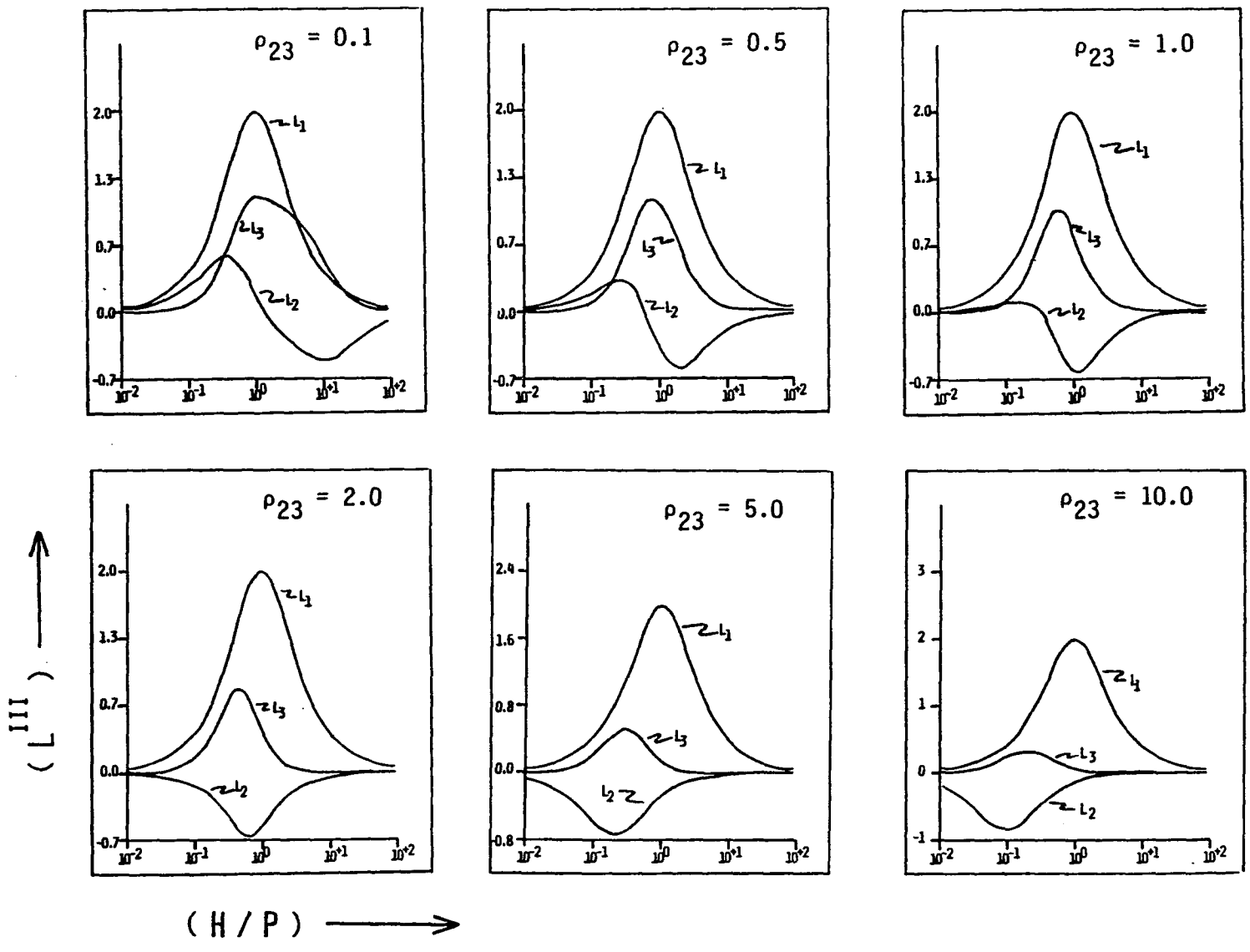
ρ_{23} = 0.1
ρ_{23} = 0.5
ρ_{23} = 1.0
ρ_{23} = 2.0
ρ_{23} = 5.0
ρ_{23} = 10.0
L_1
L_2
L_3
(L^{III})
(H / P)

function in Eq. (4.37). The quantity, χ, is a measure of the molecular chirality.

Finally, we will write the thermal-viscous coupling coefficient, $\underline{\underline{L}}^{vt}$, as

$$\underline{\underline{L}}^{vt} = \sum_{i=1}^{III} L_i^{vt} \underline{\underline{\Gamma}}_i \tag{4.39}$$

where

$$L_i^{vt} = \frac{kT^2}{4\sqrt{2}} \{5B_4^i + 3B_5^i\} \tag{4.40}$$

and B_4^i and B_5^i are given by Eqs. (4.31)-(4.35). Then $\underline{\underline{L}}^{vt}$ will be evaluated as if the $\underline{\underline{\Gamma}}_i$'s are unity. This separates the geometric field dependence from the interaction dependent collision integrals. The form of the field dependence of the $\underline{\underline{\Gamma}}_i$'s, for various values of the ratio of the field parameters (i.e., $\delta_{ij} = \xi_i/\xi_j$), is plotted in Figs. 4.3 through 4.5.

In Table 4.4, the magnitudes of B_4 and B_5 are given for the various systems and geometries. Table 4.5 lists the magnitudes of the L_i^{vt}'s for the three modes of coupling. For all of the systems and all of the geometries, the values of these quantities are seen to be very small. However, as expected, the magnitudes of these quantities increase with increasing χ, the molecular chirality. From Table 4.5, we see that the dominate coupling is through avenue I. The strength of this coupling is approximately two orders of magnitude greater than schemes II and III, whose importance are nearly identical to one another. Avenue I

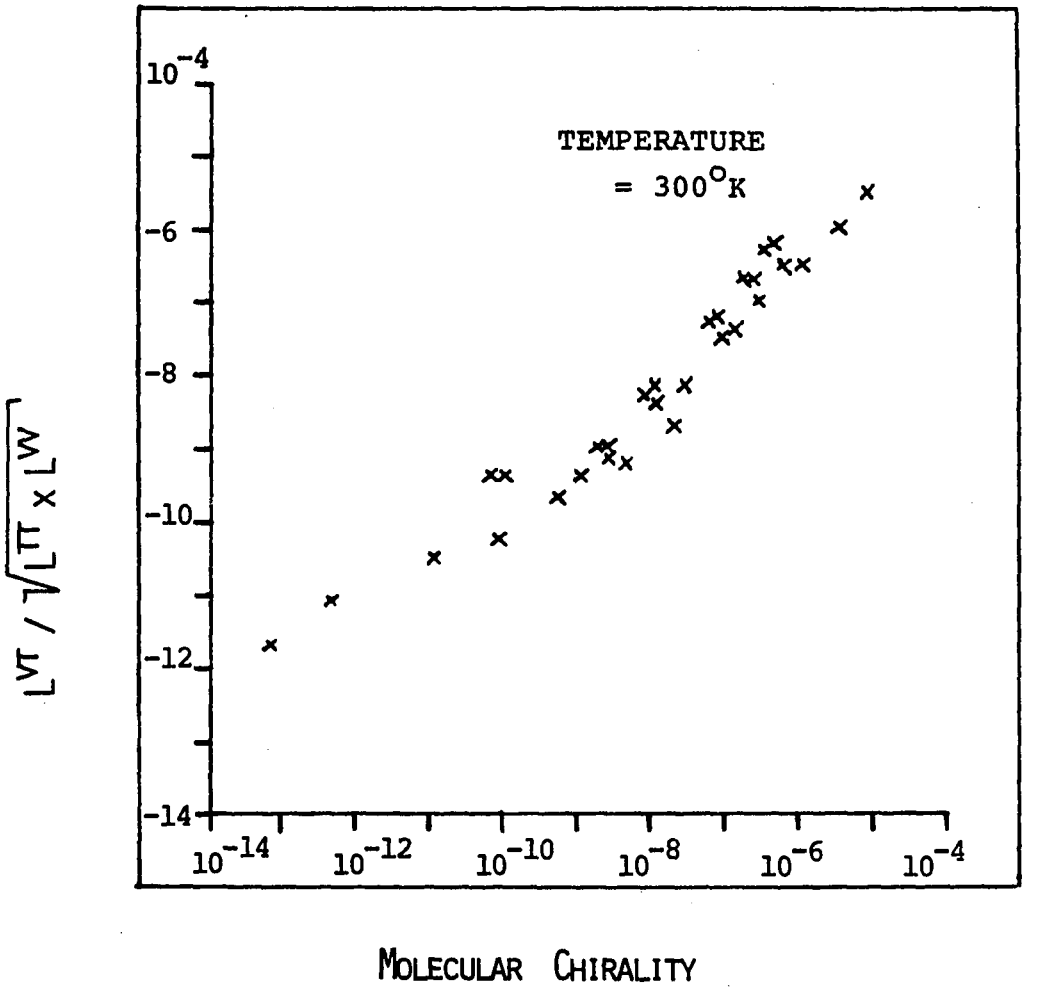

Figure 4.6. The reduced thermal-viscous coupling coefficient, $L^{vt}/\sqrt{L^{tt} \times L^{vv}}$, versus the molecular chirality, χ

couples the heat flux to a shear gradient through the basis functions $\underline{\Omega}^0\underline{\Omega}$ and $\underline{W\Omega}^0\underline{\Omega}$. These terms are the dominate field terms for the viscosity ($\underline{\Omega}^0\underline{\Omega}$) and the thermal conductivity ($\underline{W\Omega}^0\underline{\Omega}$) as was noted in Chapter III.

To appreciate the size of this effect, these quantities should be compared to the values of the coefficients of the viscosity, η (or equivalently $L^{tt} = 2T\eta$), and the thermal conductivity, λ (or equivalently $L^{vv} = T^2\lambda$). The coefficients, η and λ, are easily obtained from these results because the expansion set contains the functions required for their calculation, as indicated in Table 4.1. Table 4.6 displays the values of η, λ, and L^{vt} along with the dimensionless quantity $L^{vt}/\sqrt{L^{vv}L^{tt}}$. The largest values for this ratio are $\sim 10^{-6}$ to 10^{-7}. As a comparison, the smallest Senftleben-Beenakker effect ratios, given as $(L^{tt}(\underline{H}) - L^{tt})/L^{tt}$ for the viscosity and $(L^{vv}(\underline{H}) - L^{vv})/L^{vv}$ for the thermal conductivity, that can be detected experimentally are $\sim 10^{-4}$. Therefore, even in the systems with large chiralities, the thermal-viscous effect is still approximately two orders of magnitude too small to be detected. However, it is conceivable that for more general asymmetric top, chiral molecules, or for systems where a second order coupling exists (cf. Eq. (4.26)) the magnitude of this coupling could be measurable.

Finally, one last point of interest should be mentioned. Figure 4.6 is a plot of the chirality of the molecule, χ, versus the dimensionless quantity, $L^{vt}/\sqrt{L^{vv}L^{tt}}$. From this graph, it can be seen that these two variables are linearly related. Therefore, χ can be

considered as an estimate to the magnitude of the thermal-viscous effect.

Table 4.1. Basis functions, $\underline{\underline{\phi}}_i$, used in the thermal-viscous calculation with their parity, P, and time reversal, T, eigenvalues. Also listed is the relationship to basis functions used in Chapter III

Basis Functions	P	T	Relationship to Previous Work
$\underline{\underline{\phi}}_1 = \underline{W}^0\underline{W}$	+1	+1	$\underline{\underline{\phi}}_1$ (viscosity)
$\underline{\underline{\phi}}_2 = \underline{\Omega}^0\underline{\Omega}$	+1	+1	$\underline{\underline{\phi}}_2$ (viscosity)
$\underline{\underline{\phi}}_3 = \underline{W\Omega}^0\underline{\Omega}$	-1	-1	$\underline{\underline{\psi}}_3$ (thermal conductivity)
$\underline{\underline{\phi}}_4 = \underline{W}(5/2 - W^2)$	-1	-1	$\underline{\underline{\psi}}_1$ (thermal conductivity)
$\underline{\underline{\phi}}_5 = \underline{W}(\langle E_i\rangle_0 - E_i)$	-1	-1	$\underline{\underline{\psi}}_2 + \Gamma\underline{\underline{\psi}}_4$ (thermal conductivity)
$\underline{\underline{\phi}}_6 = \Omega_c\underline{\Omega}$	-1	-1	$\underline{\underline{\psi}}_5$ (thermal conductivity)
$\underline{\underline{\phi}}_7 = \Omega_c\underline{\Omega W}$	+1	+1	$\underline{\underline{\phi}}_3$ (viscosity)

Table 4.2. Values for the molecular constants m_3, ℓ_{23}, μ, $I_\perp$, $I_\parallel$, and the molecular center of mass, c.m. (cf. Fig. 4.5)

Z	m_3 (amu)	ℓ_{23}[a] (Å)	μ (amu)	$I_\perp$ (amu Å^2)	$I_\parallel$ (amu Å^2)	c.m.[b] (Å)
H	1	1.07	33.5	57.1	105.2	-0.382
D	2	1.07	34.0	59.1	105.2	-0.360
F	19	1.35	42.5	100.3	105.2	-0.012
Cl	36	1.77	50.75	164.0	105.2	+0.364
Br	80	1.94	72.95	253.5	105.2	+0.881

[a]Source: Ref. 57.

[b]Quantity listed is the distance of the c.m. from the central C atom along the ℓ_{23} bond.

Table 4.3. Values of the potential parameters for the thermal-viscous calculation

Z	α (Å)	β_1 (Å)	β_2 (Å)	β_3 (Å)	β_4 (Å)	γ (Å)	χ
H	3.1	0.20	0.20	0.05	0.20	-0.382	0
	"	0.19	0.20	0.05	0.21	"	8.7×10^{-11}
	"	0.15	0.20	0.05	0.25	"	1.1×10^{-8}
	"	0.05	0.20	0.05	0.35	"	2.3×10^{-7}
D	3.1	0.20	0.20	0.05	0.20	-0.360	0
	"	0.19	0.20	0.05	0.21	"	6.7×10^{-11}
	"	0.15	0.20	0.05	0.25	"	8.2×10^{-9}
	"	0.05	0.20	0.05	0.35	"	1.8×10^{-7}
F	3.2	0.20	0.20	0.15	0.20	-0.12	0
	"	0.19	0.20	0.15	0.21	"	6.7×10^{-14}
	"	0.15	0.20	0.15	0.25	"	1.0×10^{-11}
	"	0.05	0.20	0.15	0.35	"	4.6×10^{-9}
Cl	3.3	0.20	1.20	0.30	0.20	+0.364	0
	"	0.19	0.20	0.30	0.21	"	1.0×10^{-10}
	"	0.15	0.20	0.30	0.25	"	1.2×10^{-8}
	"	0.05	0.20	0.30	0.35	"	2.9×10^{-7}
Br	3.4	0.20	0.20	0.50	0.20	+0.881	0
	"	0.19	0.20	0.50	0.21	"	1.1×10^{-9}
	"	0.15	0.20	0.50	0.25	"	1.3×10^{-7}
	"	0.05	0.20	0.50	0.35	"	3.6×10^{-6}

Table 4.4. Values of B_4 and B_5 for the individual coupling routes I, II, and III

Z	X	I		II		III	
		B_4 ($\AA^{-2}$)	B_5 ($\AA^{-2}$)	B_4 ($\AA^{-2}$)	B_5 ($\AA^{-2}$)	B_4 ($\AA^{-2}$)	B_5 ($\AA^{-2}$)
H	0	10^{-29}	10^{-29}	10^{-27}	10^{-26}	10^{-26}	10^{-26}
	8.7×10^{-11}	-6×10^{-17}	-1×10^{-16}	-3×10^{-18}	-7×10^{-18}	1×10^{-19}	1×10^{-19}
	1.1×10^{-8}	-7×10^{-15}	-2×10^{-14}	5×10^{-18}	1×10^{-17}	2×10^{-17}	2×10^{-17}
	2.3×10^{-7}	-2×10^{-13}	-6×10^{-13}	5×10^{-16}	1×10^{-15}	6×10^{-16}	6×10^{-16}
D	0	10^{-29}	10^{-29}	10^{-27}	10^{-26}	10^{-26}	10^{-26}
	6.7×10^{-11}	-4×10^{-17}	-1×10^{-16}	-3×10^{-18}	-7×10^{-18}	1×10^{-19}	1×10^{-19}
	8.2×10^{-9}	-6×10^{-15}	-2×10^{-14}	-7×10^{-18}	-2×10^{-17}	2×10^{-17}	2×10^{-17}
	1.8×10^{-7}	-2×10^{-13}	-5×10^{-13}	1×10^{-16}	3×10^{-16}	5×10^{-16}	5×10^{-16}
F	0	10^{-30}	10^{-30}	10^{-29}	10^{-29}	10^{-28}	10^{-28}
	6.7×10^{-14}	-2×10^{-18}	-4×10^{-18}	-3×10^{-20}	-8×10^{-20}	1×10^{-20}	1×10^{-20}
	1.1×10^{-11}	-3×10^{-17}	-7×10^{-17}	-9×10^{-19}	-2×10^{-18}	1×10^{-18}	1×10^{-18}
	4.6×10^{-9}	-8×10^{-16}	-2×10^{-15}	-4×10^{-17}	-1×10^{-16}	7×10^{-17}	7×10^{-17}
Cl	0	10^{-28}	10^{-28}	10^{-27}	10^{-26}	10^{-27}	10^{-27}
	1.0×10^{-10}	-4×10^{-17}	-9×10^{-17}	2×10^{-18}	4×10^{-18}	4×10^{-20}	4×10^{-20}
	1.2×10^{-8}	-4×10^{-15}	-9×10^{-15}	3×10^{-17}	7×10^{-17}	2×10^{-17}	2×10^{-17}
	2.9×10^{-7}	-1×10^{-13}	-3×10^{-13}	8×10^{-16}	2×10^{-15}	7×10^{-17}	7×10^{-17}
Br	0	10^{-27}	10^{-27}	10^{-25}	10^{-25}	10^{-26}	10^{-26}
	1.1×10^{-9}	-4×10^{-16}	-0×10^{-16}	5×10^{-18}	1×10^{-17}	-3×10^{-19}	-3×10^{-19}
	1.3×10^{-7}	-4×10^{-14}	-8×10^{-14}	-6×10^{-16}	-1×10^{-15}	-7×10^{-18}	-7×10^{-18}
	3.6×10^{-6}	-1×10^{-12}	-2×10^{-12}	-2×10^{-14}	-4×10^{-14}	-2×10^{-16}	-2×10^{-16}

Table 4.5. Magnitude of the thermal-viscous coupling through the individual routes I, II, and III

Z	χ	L_{I}^{vt} (gm·°K/s^2)	L_{II}^{vt} (gm·°K/s^2)	L_{III}^{vt} (gm·°K/s^2)
H	0	10^{-24}	10^{-21}	10^{-20}
	8.7×10^{-11}	-2×10^{-11}	-8×10^{-13}	1×10^{-13}
	1.1×10^{-8}	-2×10^{-9}	1×10^{-12}	1×10^{-11}
	2.3×10^{-7}	-7×10^{-8}	1×10^{-10}	4×10^{-10}
D	0	10^{-24}	10^{-21}	10^{-20}
	6.7×10^{-11}	-1×10^{-11}	-7×10^{-13}	9×10^{-14}
	8.2×10^{-9}	-2×10^{-9}	-2×10^{-12}	1×10^{-11}
	1.8×10^{-7}	-5×10^{-8}	3×10^{-11}	4×10^{-10}
F	0	10^{-25}	10^{-24}	10^{-22}
	6.7×10^{-14}	-4×10^{-13}	-9×10^{-15}	1×10^{-14}
	1.1×10^{-11}	-8×10^{-12}	-2×10^{-13}	1×10^{-12}
	4.6×10^{-9}	-2×10^{-10}	-1×10^{-11}	6×10^{-11}
Cl	0	10^{-26}	10^{-24}	10^{-21}
	1.0×10^{-10}	-1×10^{-11}	4×10^{-13}	3×10^{-14}
	1.2×10^{-8}	-1×10^{-9}	8×10^{-12}	1×10^{-12}
	2.9×10^{-7}	-3×10^{-8}	2×10^{-10}	5×10^{-10}
Br	0	10^{-22}	10^{-20}	10^{-21}
	1.1×10^{-9}	-1×10^{-10}	1×10^{-12}	-1×10^{-13}
	1.3×10^{-7}	-9×10^{-9}	-1×10^{-10}	-3×10^{-12}
	3.6×10^{-6}	-3×10^{-7}	-4×10^{-9}	-0×10^{-11}

Table 4.6. Values of η ($= L^{tt}/2T$), λ ($= L^{vv}/T^2$), L^{vt} and the dimensionless quantity $L^{vt}/\sqrt{L^{tt}L^{vv}}$ versus the molecular chirality, χ

Z	χ	η (gm/cm·s)	λ (cal/cm·s·°K)	L^{vt} (gm·°K/s^2)	$L^{vt}/\sqrt{L^{tt}L^{vv}}$
H	0	9.7×10^{-5}	1.6×10^{-5}	10^{-20}	10^{-20}
	8.7×10^{-11}	"	"	-2×10^{-11}	-5×10^{-11}
	1.1×10^{-8}	"	"	-2×10^{-9}	-7×10^{-9}
	2.3×10^{-7}	"	"	-7×10^{-8}	-2×10^{-7}
D	0	9.8×10^{-5}	1.6×10^{-5}	10^{-20}	10^{-20}
	6.7×10^{-11}	"	"	-1×10^{-11}	-4×10^{-11}
	8.2×10^{-9}	"	"	-2×10^{-9}	-5×10^{-9}
	1.8×10^{-7}	"	"	-5×10^{-8}	-2×10^{-7}
F	0	1.0×10^{-4}	1.3×10^{-5}	10^{-22}	10^{-20}
	6.7×10^{-14}	"	"	-4×10^{-13}	-2×10^{-12}
	1.1×10^{-11}	"	"	-7×10^{-12}	-3×10^{-11}
	4.6×10^{-9}	"	"	-2×10^{-10}	-6×10^{-10}
Cl	0	1.1×10^{-4}	1.2×10^{-5}	10^{-23}	10^{-21}
	1.0×10^{-10}	"	"	-1×10^{-11}	-4×10^{-10}
	1.2×10^{-8}	"	"	-1×10^{-9}	-4×10^{-9}
	2.9×10^{-7}	"	"	-3×10^{-8}	-1×10^{-7}
Br	0	1.2×10^{-4}	9.1×10^{-6}	10^{-21}	10^{-19}
	1.1×10^{-9}	"	"	-1×10^{-10}	-4×10^{-10}
	1.3×10^{-7}	"	"	-9×10^{-9}	-4×10^{-8}
	3.6×10^{-6}	"	"	-3×10^{-7}	-1×10^{-6}

V. ORIENTATIONAL CORRELATION TIMES (58)

The problem of calculating the orientational correlation time τ_ℓ for a ℓth rank spherical harmonic of a molecule in a liquid dates back to Debye (59), who assumed the molecular rotation is governed by a diffusion equation. More recent attempts to determine τ_ℓ theoretically follow two approaches: hydrodynamic and kinetic theory. The hydrodynamic calculations set an ellipse (60) in uniform rotation in order to determine the rotational friction constants, defined as the proportionality between the applied torque and the angular velocity. The orientational correlation time then follows, since τ_ℓ and the friction coefficient are linearly related. Both stick (60) and slip (61) boundary conditions have been employed. Comparison with experiment gives stronger support to the slip models.

The alternative approach to molecular rotation is kinetic theory. This is the approach we choose. Until our own work, the existing theory consists of Chandler's rough-sphere Enskog calculation (62). This model has been quite successful in fitting the data; however, there is some ambiguity as to the definition of molecular roughness and its relationship to the nonspherical shape of the molecule.

A. Theory

We propose to calculate the collective orientational correlation time τ_ℓ^c for the ℓth rank Legendre polynomial $P_\ell(\cos\theta)$ for hard ellipsoid molecules in a bath of hard spheres at liquid densities. Here, $\cos\theta = \hat{z} \cdot \hat{e}$, where e is a unit vector along the symmetry axis of the ellipsoid and $\hat{z}$ is a space fixed reference axis. The orientational

correlation time is defined by

$$\tau_\ell^c = \int_0^\infty dt \langle \mathcal{D}_\ell \mathcal{D}_\ell(t) \rangle / \langle \mathcal{D}_\ell^2 \rangle \tag{5.1}$$

where

$$\mathcal{D}_\ell = \sum_{j=1}^{N} P_\ell(\cos\theta_j) \quad . \tag{5.2}$$

The subscripts on the angles here refer to a particular ellipsoid and $\theta(t)$ is the value that θ evolves to in a time t according to the mechanics of the system. The brackets indicate an average over an equilibrium ensemble representing the fluid mixture.

We find it convenient to interpret the brackets as inner products for Dirac vectors, i.e.,

$$\langle GH \rangle = \langle G|H \rangle = \int d\underline{x}^{N+B} \, F_{eq}^{(N+B)} \, GH \quad , \tag{5.3}$$

where $F_{eq}^{(N+B)}$ is the canonical equilibrium distribution function for a system of N ellipsoids and B bath molecules, $\underline{x}^{N+B}$ denotes the complete set of phase variables, and $|G\rangle$ and $|H\rangle$ are Dirac vectors.

One approach for the calculation of the collective orientational correlation time is the single variable Mori formalism (63) (the Mori formalism is outlined in Appendix B, along with other techniques utilized in this paragraph). In this method, as espoused by Kivelson and Keyes (64), we define projection operators P_D and Q_D by

$$P_D = |\mathcal{D}_\ell\rangle\langle\mathcal{D}_\ell| / \langle \mathcal{D}_\ell \mathcal{D}_\ell \rangle \tag{5.4a}$$

and

$$Q_D = 1 - P_D \quad . \tag{5.4b}$$

The Liouville equation for a dynamical ket vector $|G\rangle$ in differential form is

$$\frac{d}{dt}|G(t)\rangle = iL|G(t)\rangle \tag{5.5}$$

where L is the Liouville operator for the system. This equation is equivalent to Eq. (2.2). Following the usual in manipulations, one begins with Eq. (5.5) for $|\mathcal{D}_\ell(t)\rangle$ to extract an exact equation for the $\mathcal{D}_\ell$ time correlation function

$$\frac{d}{dt}\langle\mathcal{D}_\ell|\mathcal{D}_\ell(t)\rangle = -\int_0^t d\tau\{\langle A_\ell|e^{iQL\tau}|A_\ell\rangle/\langle\mathcal{D}_\ell\mathcal{D}_\ell\rangle\}\langle\mathcal{D}_\ell|\mathcal{D}_\ell(t-\tau)\rangle \quad . \tag{5.6}$$

Here

$$|A_\ell\rangle = iL|\mathcal{D}_\ell\rangle = \sum_j \underline{\omega}_j \cdot i\hat{J}_j|P_\ell(\cos\theta_j)\rangle \tag{5.7}$$

is the implicit time derivative of $|\mathcal{D}_\ell\rangle$. Invoking standard arguments about the Markovian behavior of the memory function (Appendix B), one can remove the convolution part of Eq. (5.6) to obtain the simple transport equation

$$\frac{d}{dt}\langle\mathcal{D}_\ell|\mathcal{D}_\ell(t)\rangle = -(1/\tau_\ell^c)\langle\mathcal{D}_\ell|\mathcal{D}_\ell(t)\rangle \tag{5.8}$$

where

$$\tau_\ell^c = \langle\mathcal{D}_\ell|\mathcal{D}_\ell\rangle/\langle A_\ell|A_\ell\rangle\tau_A \tag{5.9}$$

and

$$\tau_A = \int_0^\infty d\tau \langle A_\ell | e^{iQ_D L\tau} | A_\ell \rangle / \langle A_\ell | A_\ell \rangle \quad . \tag{5.10}$$

The validity of this reduction rests on the fact that $\langle A_\ell | \exp iQ_D Lt | A_\ell \rangle$ decays to zero in a time $\tau^{(+)}$ such that $\tau_A < \tau^{(+)} << \tau_\ell^c$, i.e., the time scale for orientational and momentum relaxation are far separated. This time scale separation exists when the density and shape anisotropy of the ellipses are large. Equations (5.8) and (5.9) are restatements of the Kivelson-Keyes findings (64).

Equation (5.9) can be simplified by noting that

$$\langle \mathcal{D}_\ell | \mathcal{D}_\ell \rangle = \frac{4\pi}{2\ell + 1} N g_\ell \quad , \tag{5.11}$$

where g_ℓ, the orientational pair correlation factor, is

$$g_\ell = 1 + \frac{n(2\ell + 1)}{4\pi} \int d\hat{e}_1 d\hat{e}_2 d\underline{r}_{12} \, P_\ell(\cos\theta_1) P_\ell(\cos\theta_2) \chi \quad . \tag{5.12}$$

To calculate $\langle A_\ell | A_\ell \rangle$, we use Eq. (5.7) to obtain

$$\langle A_\ell | A_\ell \rangle = \frac{4\pi NkT}{I} \frac{\ell(\ell + 1)}{2\ell + 1} \quad . \tag{5.13}$$

Inserting Eqs. (5.11) and (5.13) into Eq. (5.9), we obtain

$$\tau_\ell^c = g_\ell I / (kT\ell(\ell + 1)\tau_A) \quad . \tag{5.14}$$

To proceed further, we need τ_A, which we propose to calculate using kinetic theory.

Mori (63) showed that the tcf τ_A can be expressed by (Appendix B)

$$\tau_A = \frac{1}{\langle A_\ell | A_\ell \rangle} \int_0^{\tau^{(+)}} d\tau \langle A_\ell | e^{iL\tau} | A_\ell \rangle \tag{5.15}$$

which is the tcf of A_ℓ over a short initial period. Furthermore, the tcf of A_ℓ (or any variable whose equilibrium average vanishes) can be written

$$\begin{aligned} \langle A_\ell | e^{iLt} | A_\ell \rangle / \langle A_\ell | A_\ell \rangle &= (1/\bar{A}_\ell(0)) \int d\underline{x}^{N+B} A_\ell e^{-iLt} \\ &\quad \times \{F_{eq}^{(N+B)} [1 + A_\ell (\bar{A}_\ell(0)/\langle A_\ell | A_\ell \rangle)]\} \\ &= \bar{A}_\ell(t|A)/\bar{A}_\ell(0) \end{aligned} \tag{5.16}$$

where $\bar{A}_\ell(t|A)$ is the nonequilibrium average of A_ℓ over a distribution which, at $t = 0$, is of the form

$$F_{eq}^{(N+B)} [1 + A_\ell \bar{A}_\ell(0)/\langle A_\ell | A_\ell \rangle] \quad . \tag{5.17}$$

From Eq. (5.15), we have

$$\tau_A = \int_0^{\tau^{(+)}} d\tau \, \bar{A}_\ell(\tau|A)/\bar{A}_\ell(0) \quad . \tag{5.18}$$

Because A_ℓ is the sum of single particle operators, τ_A can computed using the singlet distribution function for ellipsoids by

$$\tau_A = \int_0^{\tau^{(+)}} dt \int d\underline{x}_1 \, A_\ell(\underline{x}_1) f^{(1)}(\underline{x}_1, t) / \int d\underline{x}_1 \, A_\ell(\underline{x}_1) f^{(1)}(\underline{x}_1, t=0) \tag{5.19}$$

where

$$A_\ell(\underline{x}_1) = \underline{\omega}_1 \times \hat{e}_1 \cdot \frac{\partial}{\partial \hat{e}_1} P_\ell(\cos\theta_1) \tag{5.20}$$

is the implicit time derivative of $P_\ell(\cos\theta_1)$. We propose to use the Enskog equation to determine the time evolution of $f^{(1)}(\underline{x}, t)$ in

Eq. (5.19). Because such an equation governs relaxation on the time scale of the fast variables, $\tau^{(+)}$ in Eq. (5.19) can be replaced by infinity.

The singlet distribution for rigid ellipsoids in a bath of rigid spheres satisfies an equation of the form (refer to Chapter II)

$$\{\frac{\partial}{\partial t} + \underline{v}_1 \cdot \frac{\partial}{\partial \underline{r}_1} + \underline{\omega}_1 \cdot i\hat{J}_1\} f^{(1)} = \sum_{\alpha} \int d2_{\alpha} d\hat{k} S_{\alpha} \hat{k} \cdot \underline{g} \chi f^{(1)*}(1) f_{\alpha}^{(1)*}(2) \quad . \tag{5.21}$$

Here, $d\underline{2}_{\alpha}$ is the differential element for the momentum and orientation variable of a molecular species α. For our purposes, we assume that the distortions of $f^{(1)}$ away from the equilibrium, Maxwellian momentum distributions are small; then we can write

$$f_{\alpha}^{(1)}(\underline{x}_1, t) = f_{0,\alpha}^{(1)}(1)\{1 + \phi_{\alpha}(\underline{x}_1, t)\} \tag{5.22}$$

where $\phi_{\alpha}(\underline{x}, t)$ is the nonequilibrium distortion. To complete the calculation of τ_A, we use Grad's methods of moments (31) (refer to Chapter II) and, in particular, the single moment expansion

$$\phi = \lambda_{\ell} A_{\ell} \overline{A}_{\ell}(t) \tag{5.23}$$

where we have assumed that the bath distortion is zero. Here,

$$\lambda_{\ell} = 1(2\ell + 1)/4\pi\ell(\ell + 1)kT \tag{5.24}$$

is a normalization parameter determined by the relation

$$\int d\underline{x}_1 \, A_{\ell}(\underline{x}_1) f_0^{(1)}(1 + \phi(\underline{x}_1, t)) = \overline{A}_{\ell}(t) \quad . \tag{5.25}$$

We do not include a D_ℓ moment in ϕ since we are interested in the relaxation of the fast variables on the time scale $\tau^{(+)}$. [Alternatively, $\exp(iQ_D L\tau)|A_\ell\rangle$ in Eq. (5.10) evolves in a subspace orthogonal to $|D_\ell\rangle$ and, hence, we are not interested in a D_ℓ contribution to ϕ.] Substituting Eqs. (5.22) and (5.23) into Eq. (5.21) and taking the A_ℓ moment, we obtain

$$\frac{d}{dt}\bar{A}_\ell(t) = -\bar{A}_\ell(t)/\tau_A \tag{5.26}$$

where

$$\frac{1}{\tau_A} = -\lambda_\ell n\,[A_\ell,A_\ell]^{1,1}_{d,d} + [A_\ell,A_\ell]^{1,2}_{d,d} - \lambda_\ell n_B[A_\ell,A_\ell]^{1,1}_{a,d} \quad . \tag{5.27}$$

[The identification of τ_A is apparent from comparing Eq. (5.19) and Eq. (5.26).]

In the high density regime and for highly anisotropic molecules, the separation of the time scales of the fast and slow variables is large and a single moment should adequately describe the relaxation dynamics. At low densities and/or for low-friction molecules such as SF_6, CH_4, or N_2, our general treatment requires modification. This would include using more moments in the expansion of ϕ.

The bracket integrals appearing in Eq. (5.27) can be reduced to simple integrals following standard techniques (11,58). As a result of the reduction, we obtain

$$[A_\ell,A_\ell]^{i,j}_{\mu,\nu} = \frac{\ell(\ell+1)}{I\beta(2\ell+1)}\,\frac{4\pi C^2 B}{3}\,\frac{\varepsilon^2}{\sqrt{1+\varepsilon}}\,\sqrt{\frac{kT}{2\pi I}}\,\lambda^{ij}_{\mu\nu}(\ell) \tag{5.28}$$

where

$$\lambda_{\mu\nu}^{ij}(\ell) = \sqrt{\kappa_{\mu\nu}}\ 8B^{(n)}\pi^{1/2(n+2)}\{C^4\varepsilon^2\}^{-1} \int dx_1(dx_2 d\alpha)S_{\mu\nu}D_{\mu\nu}^{-1}\chi_{\mu\nu}h_i'h_j'B_{ij}(\ell)\ . \tag{5.29}$$

By construction, the $\lambda_{\mu\nu}^{ij}$ integrals are dimensionless quantities. Here $\beta = 1/kT$, B and C represent the major and minor axis of the ellipse respectively, and

$$\varepsilon = (B^2 - C^2)/C^2 \tag{5.30}$$

is the shape anisotropy of the ellipse. For the atom-diatom system, the supporting function of the excluded volume H_{ad} is the sum of supporting functions for the atom h_a and the diatom h_d:

$$H_{ad}(x) = h_a + h_d(x) \tag{5.31}$$

where

$$h_a = A \tag{5.32a}$$

and

$$h_d(x) = [C^2 + (B^2 - C^2)x^2]^{1/2}\ . \tag{5.32b}$$

The first and second derivatives of $H_{ad}(x)$ with respect to x are:

$$H_{ad}'(x) = h_d'(x) = C\varepsilon x(1 + \varepsilon x^2)^{-1/2} \tag{5.33a}$$

and

$$H_{ad}''(x) = C[\varepsilon(1 + \varepsilon x^2)^{-1/2} - \varepsilon^2 x^2(1 + \varepsilon x^2)^{-3/2}]\ . \tag{5.33b}$$

The function $D_{ad}(x)$ is

$$D_{ad} = [1 + (\frac{\mu_{ad}}{l})(H'_{ad})^2(1 - x^2)]^{1/2} \tag{5.34}$$

and the surface area function is

$$S_{ad} = [H_{ad} - xH'_{ad}]\{[H_{ad} - xH'_{ad}] + H''_{ad}(1 - x^2)\} \quad . \tag{5.35}$$

The diatom-diatom orientational functions have been given by Cooper and Hoffman (65) and will be summarized here for completeness. In this case,

$$H_{dd} = h_d(x_1) + h_d(x_2) \quad , \tag{5.36}$$

where $h_d(x_j)$, $j = 1, 2$, is defined by Eq. (5.32b). The function D_{dd} is

$$D_{dd} = \{1 + (\frac{\mu_{DD}}{l})[h'_d(x_1)^2(1 - x_1^2) + h'_d(x_2)^2(1 - x_2^2)]\} \tag{5.37}$$

and the surface area function is

$$S_{dd} = \delta_1 + \delta_2 \sin^2\alpha \tag{5.38}$$

where

$$\delta_1 = j^2 + j\{(1 - x_1^2)h''_d(x_1) + (1 - x_2^2)h''_d(x_2)\} \quad , \tag{5.39a}$$

and

$$\delta_2 = h''_d(x_1)h''_d(x_2)(1 - x_1^2)(1 - x_2^2) \quad , \tag{5.39b}$$

using

$$j = H_{dd} - x_1 h_d^1(x_1) - x_2 h_d^1(x_2) \quad . \tag{5.40}$$

The quantity $\kappa_{\mu\nu} = C^2\mu_{\mu\nu}/I$ where $\mu_{\mu\nu}$ is the reduced mass of the colliding μ and ν species, and the quantity $B_{ij}(\ell)$ is

$$B_{ij}(\ell) = \frac{3}{\ell(\ell+1)}\{(1 - x_i^2 - x_j^2 + x_i x_j \hat{e}_i \cdot \hat{e}_j)P^1(\hat{e}_i \cdot \hat{e}_j) + (x_i - \hat{e}_i \cdot \hat{e}_j x_j)(x_j - \hat{e}_i \cdot \hat{e}_j x_i)P^{11}(\hat{e}_i \cdot \hat{e}_j) \tag{5.41}$$

where

$$P_\ell^1(x) = \frac{d}{dx} P_\ell(x) \tag{5.42a}$$

and

$$P_\ell^{11}(x) = \frac{d^2}{dx^2} P_\ell(x) \tag{5.42b}$$

are the derivatives of the ℓth rank Legendre polynomials. The integration variables in Eq. (5.29) are $x_i = \hat{k} \cdot \hat{e}_i$ and α (defined from the relation $\hat{e}_1 \cdot \hat{e}_2 = x_1 x_2 + \sqrt{(1 - x_1^2)(1 - x_2^2)}\cos\alpha$) is the angle between the projections of $\hat{e}_1$ and $\hat{e}_2$ onto the plane orthogonal to $\hat{k}$. Inserting Eq. (5.28) and Eq. (5.27) into (Eq. (5.14) for τ_ℓ^c, we find that

$$\tau_\ell^c = \frac{1}{\ell(\ell+1)} \rho^* \frac{\varepsilon}{\sqrt{1+\varepsilon}} \sqrt{\frac{I}{2\pi kT}} \{X_d(\lambda_{dd}^{11} + \lambda_{dd}^{12}) + X_a \lambda_{ad}^{11}\} \tag{5.43}$$

which is the main result of this analysis. Here

$$\rho^* = (4/3)\pi C^2 B(n_d + n_a) \tag{5.44}$$

is the reduced density of the fluid, n_d and n_a represent the number

densities of the diatoms and bath, respectively, and

$$X_d = n_d/(n_a + n_d) \tag{5.45a}$$

and

$$X_a = n_a/(n_a + n_d) \tag{5.45b}$$

are the number fractions for the diatom and atom species, respectively.

Equations (5.29) and (5.43) complete the formal calculation of the collective particle correlation time. In principle, given the angle-dependent contact radial distribution function, one can now determine the Enskog prediction for τ_ℓ^c.

Before proceeding to the numerical predictions, we wish to discuss several approximations and simple limits of Eqs. (5.29) and (5.43). The simplest limit to consider is that corresponding to an isolated rotor in a bath of spheres (or $X_d = 0$, $X_a = 1$), since only the rotor-bath collision integral appears:

$$\tau_\ell^s = \frac{3\rho^* \epsilon^2}{\sqrt{1+\epsilon}} \sqrt{\frac{I}{2\pi kT}} \frac{\lambda_{ad}^{11}}{\ell(\ell+1)} \quad . \tag{5.46}$$

Writing Eq. (5.46) in terms of angular momentum correlation time τ_J (66),

$$\tau_\ell^s = 1/kT\ell(\ell+1)\tau_J \quad , \tag{5.47}$$

it follows that

$$\frac{1}{\tau_J} = 3\rho^* \sqrt{\frac{kT}{2\pi I}} \frac{\varepsilon^2}{\sqrt{1+\varepsilon}} \lambda_{ad}^{11} \quad . \tag{5.48}$$

To proceed any further, we must perform the λ_{ad}^{11} integral. Although this integral proves to be easily computed numerically, it can only be performed analytically in a few simple limiting cases. For molecules that are large and nearly spherical in a bath of small light spheres, i.e., $\varepsilon \sim 0$,

$$\lambda_{ad}^{11} \sim \frac{4}{15} \kappa_{ad}^{-1/2} \chi_{ad}(0) \quad , \tag{5.49}$$

and so

$$\frac{1}{\tau_J} \sim \frac{4}{5} \rho^* \sqrt{\frac{kT}{2\pi I}} \varepsilon^2 \chi_{ad}(0) \kappa_{ad}^{-1/2} \tag{5.50}$$

which depends on the square of the shape anisotropy. Here, $\chi_{ad}(0)$ represents the radial distribution function for a molecule of species type ν in a fluid composed entirely of species type μ, in the limit of zero separation (i.e., at contact). For a long heavy rod ($\varepsilon >> 1$) in a bath of small light solvent atoms

$$\lambda_{ad}^{11} \sim \chi_{ad}(0) \pi/8\sqrt{\kappa_{ad}\varepsilon} \tag{5.51}$$

so that

$$\frac{1}{\tau_J} \sim \frac{3}{8} \rho^* \sqrt{\frac{\pi kT}{2I}} \varepsilon \chi_{ad}(0) \kappa_{ad}^{-1/2} \tag{5.52}$$

which, in turn, depends linearly on the shape anisotropy parameter.

For the case of a pure (neat) fluid of diatoms, the λ_{ad}^{11} integrals in Eq. (5.43) vanish, and so

$$\tau_{\ell}^{c} = \frac{3\rho^{*} g_{\ell}}{\ell(\ell+1)} \frac{\varepsilon^{2}}{\sqrt{1+\varepsilon}} \sqrt{\frac{I}{2\pi kT}} \left(\lambda_{dd}^{11} + \lambda_{dd}^{12}\right) \quad . \tag{5.53}$$

The single particle correlation time for a pure fluid of diatoms is obtained from Eq. (5.53) by dropping the λ_{dd}^{12} integral. This is equivalent to tagging the nonequilibrium particle one, set in a fluid of identical particles which are in equilibrium (similar to an approach taken when using a Lorentz-Boltzmann equation). Therefore,

$$\tau_{\ell}^{s} = \frac{3\rho^{*}}{\ell(\ell+1)} \frac{\varepsilon^{2}}{\sqrt{1+\varepsilon}} \sqrt{\frac{I}{2\pi kT}} \lambda_{dd}^{11} \quad . \tag{5.54}$$

The use of the high density Hubbard relation (66) Eq. (5.47), Eq. (5.54) provides an expression for the angular momentum relaxation time for a neat fluid of rotors:

$$\frac{1}{\tau_{J}} = 3\rho^{*} \frac{\varepsilon^{2}}{\sqrt{1+\varepsilon}} \sqrt{\frac{kT}{2\pi I}} \lambda_{dd}^{11} \quad . \tag{5.55}$$

Chandler (62) has obtained a similar expression for the angular momentum relaxation time of a partially rough sphere in a neat fluid. Converting Chandler's result to our notation yields

$$\frac{1}{\tau_{J}} = 3\rho^{*} \sqrt{\frac{kT}{2\pi I}} \, a(T) \left[\frac{(16/3)\sqrt{\kappa_{aa}}\, \chi_{aa}(0)}{2 + \kappa_{aa}} \right] \tag{5.56}$$

where a(T) is defined as a temperature dependent function that determines the stickiness of the molecule and ranges from one to zero (the slip

limit). Our definition of a(T) differs from Chandler's in that we have absorbed the stick limit into Eq. (5.56) so that a value of a(T) = 1 predicts the perfectly rough sphere relaxation.

Given the collective and single particle orientational correlation times for neat fluids (Eqs. (5.53) and (5.54), one can construct the ratio, which has come to be known as the Kivelson-Keyes (KK) relation (64). Thus,

$$\tau_{\ell}^{c}/\tau_{\ell}^{s} = g_{\ell}\{1 + \lambda_{dd}^{12}/\lambda_{dd}^{11}\} \quad . \tag{5.57}$$

Equation (5.57) expresses the ratio of correlation times as a static or equilibrium factor (known as the g_2 factor for $\ell = 2$) times a function of the ratio of collision integrals. The KK relation is usually written for $\ell = 2$ as

$$\tau_{2}^{c}/\tau_{2}^{s} = g_{2}/j_{2} \quad , \tag{5.58}$$

Comparing Eq. (5.57) with Eq. (5.58), we find that, for a neat fluid of rotorlike molecules, the dynamic orientational correlation parameter j_2 is given by

$$j_{2} = \{1 + \lambda_{dd}^{12}/\lambda_{dd}^{11}\}^{-1} \quad . \tag{5.59}$$

Because the collision integrals in this expression are both positive, the kinetic theory predicts that the ratio $\tau_{2}^{c}/\tau_{2}^{s}$ will be greater than g_2.

B. Numerical Results

In order to compare the predictions of Eqs. (5.43) and (5.53)-(5.55) to laboratory measured and computer calculated correlation times, we require a numerical value of the radial distribution function at a contact separation $\chi(0)$. For lack of a better result, we use the Carnahan-Starling value (67) for hard spheres:

$$\chi(0) = (2 - \rho^*)2(1 - \rho^*)^3 \quad , \tag{5.60}$$

Equipped with $\chi(0)$, we can determine the correlation times, and these are shown in Tables 5.1 and 5.2. The kinetic theory predictions underestimated the orientational correlation times and overestimated reciprocal quantities (these reciprocal quantities being the rotational diffusion constant or the angular momentum correlation times). The best agreement was found for computer N_2, wherein the error was less than a factor of two. In all other cases, the typical error was of the order of three.

There are several factors that might be responsible for the consistent underestimation of the friction on the rotor. First, one might argue that attractive forces are important and these have been omitted. However, KT also underestimated friction on hard spherocylinders and, in this case, there are no attractive forces. Second, it is obvious that the radial distribution function is not isotropic and this anisotropy might increase the friction on the rotor. Although there is some recent evidence (68) that the contact $\chi(0)$ for hard dumbbells for certain configurations can be greater than the values of χ used in

Tables 5.1 and 5.2, it would seem unlikely that, for all the systems studied, the $\chi(0)$ should be greater than the isotropic χ contact by a factor of two to three. A third possibility, which causes some concern in our calculation, is the neglect of correlated collisions. Both three body collisions and chattering collisions have been ignored. It has been argued that, in condensed phases, a chattering collision is unlikely due to the intervention of the solvent. However, correlated many body interactions are still a problem to address.

In conclusion, our results for τ_2^c are typically a factor of two to three too small. Whether the bulk of this discrepancy is the result of the kinetic theory or of our inability to properly handle the anisotropic effects of the interaction, it is too early to determine. It would be interesting to repeat the calculation when more realistic radial distribution functions are available.

Table 5.1. Comparison of kinetic theory with experiment

System	B (Å)	C (Å)	ε	ρ^*	T (°K)	χ(0)	κ	Theory (ps)	Expt. (ps)
									τ_2^c
CS_2[a] (neat)	3.2	1.65	2.76	0.364	293	3.18	1.5	0.40	1.4[b]
I_2[c] (in CCl_4)	3.45	2.15	1.57	0.415	293	3.96	0.77	0.55	2.3
I_2[c] (in cyclohexane)	3.45	2.15	1.57	0.401	293	3.71	0.77	0.50	1.8
Dicyanoacetylene[d] (neat)	4.54	1.78	5.50	0.468	297.7	5.0	3.00	2.27	5.0
Dicyanoacetylene[d] (in cyclohexane)	4.54	1.78	5.50	0.400	297.7	3.71	3.00	1.72	5.7

[a]Source: Ref. 68.

[b]Recent molecular dynamics calculations (69) on this molecule at 300°K have yielded a correlation time of 1.1 ps, in good agreement with experiment.

[c]Source: Ref. 70.

[d]Source: Ref. 71.

Table 5.2. Comparison of kinetic theory with molecular dynamics

System	B (Å)	C (Å)	ϵ	ρ^*	T (°K)	$\chi(0)$	κ	Theory (ps)	Expt. (ps)
								τ_J	
N_2[a]	2.22	1.67	0.75	0.364	62.8	3.17	0.217	0.32	0.24
N_2[a]	2.22	1.67	0.75	0.325	152.9	2.27	0.217	0.26	0.17
								τ_2[c]	
F_2[b]	2.13	1.41	1.26	0.415	70	4.68	0.518	0.26	1.45
F_2[b]	2.13	1.41	1.26	0.346	120	2.96	0.518	0.09	0.27
CO_2[b]	2.68	1.50	2.19	0.329	273	2.76	0.870	0.14	0.35
								D_R [c]	
Spherocylinder[d]	2.00	1.00	2.00	0.200	--	1.75	1.72	1.94	0.76
Spherocylinder[d]	2.00	1.00	2.00	0.400	--	3.70	1.72	0.46	0.20

[a]Source: Ref. 72.

[b]Source: Ref. 73.

[c]The reported values for the spherocylinder model are dimensionless, single-particle rotational diffusion coefficients $D_R = \sqrt{I/kT}\,\tau_J$, where τ_J is given by Eq. (5.48).

[d]Source: Ref. 74.

VI. DEPOLARIZED LIGHT SCATTERING R PARAMETER

Fluctuations in the dielectric constant of a fluid can induce light scattering. The local dielectric constant of a medium fluctuates because molecules can translate and nonspherical molecules can rotate. Depolarized light scattering (DPLS) of 'small' (nonpolymeric) torsionally rigid molecules in normal room temperature solvents arises almost exclusively from molecular rotations, with inconsequential corrections from direct translational fluctuation effects (75). In the various theories of DPLS in fluids composed of molecules possessing a C_∞ axis, it has been shown that the fluctuations in the dielectric tensor can be related to the second rank spherical harmonics, Y_{2M}, which describe the orientation of the scattering molecules. In particular, the spectrum of scattered light is given by (76,77)

$$I_{if}(\underline{k},\omega) = \int_0^\infty dt\, e^{i\omega t} \langle \hat{n}_i \cdot \underline{\underline{\mathcal{D}}}(\underline{k},t) \cdot \hat{n}_f \hat{n}_i \cdot \underline{\underline{\mathcal{D}}}(-\underline{k},0) \cdot \hat{n}_f \rangle \tag{6.1}$$

where $\underline{k}$ is defined as the difference between the propagating vectors of the incoming beam ($\underline{k}_i$) and that of the outgoing beam ($\underline{k}_f$), i.e., $\underline{k} = \underline{k}_f - \underline{k}_i$, and ω is the frequency offset of the detected beam from that of the laser source. Here, $\hat{n}_i$ and $\hat{n}_f$ are the polarization vectors for the incoming and the outgoing radiation, respectively, and

$$\underline{\underline{\mathcal{D}}}(\underline{k},t) = \sum_j [\hat{e}_j(t)]^{(2)}\, e^{i\underline{k}\cdot\underline{r}_j(t)} \tag{6.2}$$

is the Fourier transform of the orientation density at a time t. The

quantity r_j denotes the position of the center of mass of molecule j and $[\hat{e}_j]^{(2)}$ is the second rank cartesian tensor, $\hat{e}_j\hat{e}_j - 1/3\ \underline{\underline{U}}^{(3)}$, where $\underline{\underline{U}}^{(3)}$ is the unit tensor and $\hat{e}_j$ is a unit vector which is parallel to the symmetry axis of molecule j. The relationship between $I_{if}(\underline{k},\omega)$ and Y_{2M} can be made explicit by expressing $\hat{n}_i \cdot [\hat{e}_j]^{(2)} \cdot \hat{n}_f$ as a linear combination of second rank spherical harmonics. As usual, k ($= |\underline{k}|$) is related to the scattering angle, θ, between the incoming and scattered wavevectors and for quasi-elastic scattering, $k = 2k_i \sin(\theta/2)$. Equation (6.1) relates the spectrum of scattering light for a particular scattering angle to the Fourier transform of the equilibrium time correlation function for the collective orientation density.

In 1968, Stegeman and Stoicheff (78) noticed that the DPLS spectrum for a variety of fluids consisted of a doublet, which appeared to arise from the subtraction of a sharp Lorentzian from a broader Lorentzian. As a result, $I(\underline{k},\omega)$ had a dip at $\omega = 0$. This so-called Rytov dip has been the subject of a significant amount of theoretical activity. Although several theories have been proposed, the version which has survived critical scruntiny is that of Tsay and Kivelson (77). Like the earlier Keyes and Kivelson theory (79), Tsay and Kivelson concluded that for small k and low viscosity solvents, $I_{VH}(k,\omega)$ is given by

$$I_{VH}(k,\omega) \simeq \frac{\tau_2^c}{1 + (\omega\tau_2^c)^2} - \frac{R\cos^2(\theta/2)(\eta k^2)^2\tau_2^c}{\omega^2 + (\eta k^2)^2} \qquad (6.3)$$

where τ_2^c is the collective second rank orientational correlation time

and η, the shear viscosity (divided by the density). The quantity, R, is a dimensionless factor ranging from zero to one and measures the coupling of the orientation density to a shear gradient. The wavevector $\underline{k}$ defines the $\hat{x}$ axis and $\hat{k}_i \times \hat{k}_f$ defines the $\hat{z}$ axis.

Since its inception, R has been the subject of a number of investigations including real experiments, molecular dynamics, and hydrodynamic modeling (80). The parameter R is a dynamic quantity which measures the ability of a system under shear to relieve the shear by reorientation. Experimental measurements of R on flexible alkanes, small rods (such as CS_2), long rods (p-methoxybenzylidene-(p-n-butyl) aniline (MBBA) in the isotropic phase), and nearly spherical molecules indicate that R is roughly 0.4 and, thus, nearly independent of the shape of the molecule. Furthermore, R seems to be only very weakly dependent on the temperature.

The existing theories of R are hydrodynamic ones. Kivelson and Hallum (81) use stick boundary conditions in the Navier-Stokes equations in a version of Jefferies earlier theory to estimate R. Calef and Wolynes (82) employ slip boundary conditions, motivated in part by the recent successes in applying slip boundary conditions to the calculation of single particle orientational correlation times (61). The stick results show a strong dependence on the particle shape anisotropy, whereas the slip results (for small deviations from nonsphericity) are independent of particle shape. Both these approaches avoid calculating the appropriate time correlation functions and are imprecise regarding the collective variables character of R. We

propose an alternative approach in which one determines the appropriate time correlation functions (tcfs) for a simple fluid of N ellipsoids using Enskog methods. The Enskog result for the tcfs is derived following methods outlined by Ernst et al. (83). However, these methods are generalized somewhat in the spirit of the Mori approach (63) towards the calculation of tcfs. Briefly, the tcfs are written in terms of one and two particle distortions. These functions are shown to satisfy the BBGKY hierarchy discussed in Chapter II. The hierarchy is then truncated at the Enskog level. We will first derive the kinetic theory prediction for R, and then present some numerical results.

A. Theory

Tsay and Kivelson (77) derived an expression for R using the Mori formalism (63). Their derivation, which parallels an earlier derivation of Andersen and Pecora (84), is outlined in Appendix C. Two equivalent expressions for R are discussed in Appendix C. These two forms are

$$R = I_{13}I_{31}/\tilde{I}_{11}I_{33} \tag{6.4a}$$

and

$$R = (\tilde{I}_{11} - I_{11})/\tilde{I}_{11} \quad , \tag{6.4b}$$

where

$$I_{13} = \int_0^\infty dt \langle \underline{\underline{\sigma}} : e^{iQ_2 L^{(N)} t} \dot{\underline{\underline{D}}}^0 \rangle \tag{6.5a}$$

$$I_{31} = \int_0^\infty dt \langle \dot{\underline{\underline{\mathcal{D}}}} : e^{iQ_2 L^{(N)} t} \underline{\underline{\sigma}}^0 \rangle \tag{6.5b}$$

$$\tilde{I}_{11} = \int_0^\infty dt \langle \underline{\underline{\sigma}}^0 : e^{iQ_g L^{(n)} t} \underline{\underline{\sigma}}^0 \rangle \tag{6.5c}$$

$$I_{11} = \int_0^\infty dt \langle \underline{\underline{\sigma}}^0 : e^{iQ_2 L^{(n)} t} \underline{\underline{\sigma}}^0 \rangle \tag{6.5d}$$

and

$$I_{33} = \int_0^\infty dt \langle \dot{\underline{\underline{\mathcal{D}}}} : e^{iQ_2 L^{(N)} t} \dot{\underline{\underline{\mathcal{D}}}} \rangle \quad . \tag{6.5e}$$

The functions $\dot{\underline{\underline{\mathcal{D}}}}$ and $\underline{\underline{\sigma}}^0$ represent the irreducible second rank tensors

$$\dot{\underline{\underline{\mathcal{D}}}} = \frac{d}{dt} \underline{\underline{\mathcal{D}}} = \frac{d}{dt} \sum_{j=1}^{N} [\hat{e}_j]^{(2)} \tag{6.6}$$

and

$$\underline{\underline{\sigma}}^0 = iL^{(n)} \sum_{j=1}^{N} \underline{r}_j^0 \underline{p}_j = \sum_j \underline{\underline{\sigma}}^0_{k,j} + \sum_{j,q} \underline{\underline{\sigma}}^0_{v,jq} \tag{6.7}$$

where

$$\underline{\underline{\sigma}}_{k,j} = m^{-1} \underline{p}_j \underline{p}_j \tag{6.8a}$$

and

$$\underline{\underline{\sigma}}_{v,jq} = \frac{1}{2} \underline{r}_{jq} \frac{\partial}{\partial \underline{r}_j} V_{jq} \tag{6.8b}$$

are related to the kinetic and potential parts of the stress tensor, respectively. The projection operators and the remaining quantities are defined in Appendix C. The validity of Eqs. (6.4a) and (6.4b) for R rests on the assumption that the orientation and momentum densities in the fluid relax on a hydrodynamic time scale (refer to the discussions of Chapters II and V on the existence of time scale separations). The requirement that the momentum density relaxes slowly places no restrictions on the types of systems for which Eqs. (6.4a) and (6.4b) can be applied because the momentum density is a hydrodynamic quantity. By assuming that $\underline{\underline{\mathcal{D}}}$ is slowly relaxing, we have restricted our attention to systems where the approximate inequality

$$(|\varepsilon| + 1)^2 \rho^* \gtrsim 1 \tag{6.9}$$

is satisfied (this is related to the requirement that $\varepsilon_\omega \gtrsim 1$ where ε_ω is defined in Chapter II).

Before we proceed with the reduction of the integrated tcfs of Eq. (6.5), we wish to point out that $\tilde{I}_{11}$ and I_{33} are related to two transport properties of general interest. These are the shear viscosity (discussed in Chapter III), given by

$$\eta = (10Vk_BT)^{-1}\tilde{I}_{11} \quad , \tag{6.10}$$

and the collective particle orientational relaxation time (discussed in Chapter V), given by

$$\tau_2^c = (4\pi/5)Ng_2 I_{33}^{-1} \quad , \tag{6.11}$$

where g_ℓ, the orientational pair correlation factor, is defined in Chapter V. The tcf I_{11}, which is related to $\tilde{I}_{11}$, differs from $\tilde{I}_{11}$ only in the different projection operators contained in the propagator, $\exp(iQL^{(N)}t)$. The knowledge that I_{11} and $\tilde{I}_{11}$ are related to the shear viscosity allows us to interpret R as a measure of the effects of molecular orientation densities in the fluid on the magnitude of the shear viscosity.

Typical Mori expressions for the tcfs are of the form (refer to Appendix B)

$$M = \int_0^\infty dt \langle \dot{m}^\dagger e^{iQ_m L^{(N)} t} \dot{m} \rangle \tag{6.12}$$

where Q_m projects out the slowly relaxing variables; thus, the integrand is assumed to decay rapidly to zero. The tcfs of Eqs. (6.5a)-(6.5e) are of this form. In Chapter V, the tcf of Eq. (6.12) was rewritten as

$$M = \int_0^{\tau_{\dot{m}}^+} dt \langle \dot{m} e^{iL^{(N)} t} \dot{m} \rangle \tag{6.13}$$

where $\tau_{\dot{m}}$ is the relaxation time for the molecular quantity $\dot{m}$, and $\tau_{\dot{m}}^+$ satisfies the inequality

$$\tau_{\dot{m}} \lesssim \tau_{\dot{m}}^+ << \tau_m \quad . \tag{6.14}$$

Here, τ_m represents the relaxation time for the slow or hydrodynamic variables. The expression for M of Eq. (6.13), originally due to Mori (63), is shown in Appendix B to rely on the existence of the time scale separation of Eq. (6.14).

We are now ready to reduce the general tcf in Eq. (6.13) using the kinetic theory utilized in the earlier chapters of this work. Equation (6.13) is explicitly

$$M = \int_0^{\tau_{\dot{m}}^+} dt \int d\underline{x}^N \, F_{eq}^{(N)} \dot{m}^\dagger \, e^{-iL^{(N)}t} \, \dot{m} \tag{6.15}$$

where $F_{eq}^{(N)}$ is the equilibrium canonical distribution function for the fluid consisting of N identical rigid rotors. Assuming $\dot{m}$ to have the form

$$\dot{m} = iL^{(N)} m = iL^{(N)} \sum_{j=1}^{N} m_j \quad , \tag{6.16}$$

which is true for the tcfs we are interesting in calculating, Eq. (6.15) can be rewritten as

$$M = - \int_0^{\tau_{\dot{m}}^+} dt \int d\underline{x}^N \, F_{eq}^{(N)} \dot{m}^\dagger \frac{\partial}{\partial t} e^{-iL^{(N)}t} \, m \quad . \tag{6.17}$$

Carrying out the time integral, we obtain

$$M = - \int d\underline{x}^N \, F_{eq}^{(N)} \dot{m}^\dagger [e^{-iL^{(N)}\tau_{\dot{m}}^+} - 1] m \quad . \tag{6.18}$$

Furthermore, by splitting $\dot{m}$ into its kinetic and potential parts, i.e.,

$$m = \sum_j \dot{m}_{k,j} + \sum_{j,q} \dot{m}_{v,jq} \tag{6.19}$$

where

$$iL_0^{(N)}{}_m = \sum_j \dot{m}_{k,j} \tag{6.20a}$$

and

$$iL_v^{(n)}{}_m = \sum_{jq} \dot{m}_{v,jq} \quad , \tag{6.20b}$$

the tcf expression becomes

$$M = -\{\int d\underline{x}_1 \, \dot{m}_{k,1} \, P^{(1)}(\underline{x}_1, \tau_m^+) + \int d\underline{x}_1 d\underline{x}_2 \, \dot{m}_{v,12} \, P^{(2)}(x_1, x_2, \tau_m^+) \quad . \tag{6.21}$$

Here,

$$P^{(s)}(\underline{x}^s, t) = \rho^{(s)}(\underline{x}^s, t) - \rho^{(s)}(\underline{x}^s, 0) \quad , \tag{6.22}$$

and

$$\rho^{(s)}(\underline{x}^s, t) = N!/(N-s)! \int d\underline{x}_{s+1} \ldots d\underline{x}_N \, F_{eq}^{(N)} \, e^{iL^{(N)}t}{}_m \tag{6.23}$$

represent s particle distortions.

Differentiating $\rho^{(s)}$ with respect to time, we obtain

$$\frac{\partial}{\partial t} \rho^{(s)}(\underline{x}^s, t) + iL^{(s)}\rho^{(s)}(\underline{x}^s, t) = \sum_{i=1}^{s} J_{j,s+1}(\rho^{(s+1)}(\underline{x}^{s+1}, t)) \tag{6.24}$$

where

$$J_{ij}(\rho^{(s+1)}(\underline{x}^{s+1}, t)) = \int d\underline{i} d\hat{k}_{ij} S_{ij} \dot{\ell}_{ij} \rho^{(s+1)}(\underline{x}_1, \ldots, \underline{x}_i, \ldots, x_j, \ldots, \underline{x}_{s+1}, t) \quad . \tag{6.25}$$

Here, the subscripts simply refer to the ij collisional pair. The quantities in Eq. (6.25) are defined in Chapter II. Equation (6.24)

represents the BBGKY hierarchy for the $\rho^{(s)}$ distortions. This hierarchy, for the reduced distribution functions, was introduced in Chapter II for the purpose of obtaining a kinetic equation satisfied by $f^{(1)}$. Drawing upon the methods of Chapter II, we write out the first two equations (x = 1 and s = 2) of the hierarchy,

$$\{ \frac{\partial}{\partial t} + iL^{(1)} \}\rho^{(1)}(\underline{x}_1,t) = J_{12}(\rho^{(2)}) \tag{6.26a}$$

and

$$\{ \frac{\partial}{\partial t} + iL^{(2)} \}\rho^{(2)}(\underline{x}_1,\underline{x}_2,t) = J_{13}(\rho^{(3)}) + J_{23}(\rho^{(3)}) \quad . \tag{6.26b}$$

Due to the instantaneous nature of the interaction, only $\rho^{(2)}$ at contact is required in Eq. (6.26a). Integration of Eq. (6.26b) through the collision of particles one and two yields the boundary condition

$$\rho^{(2)}(\underline{x}_1',\underline{x}_2',t) \Big|_{\text{contact}} = \rho^{(2)}(\underline{x}_1,\underline{x}_2,t) \Big|_{\text{contact}} \quad . \tag{6.27}$$

This is simply a statement of the fact that during the time particles one and two interact (a time of duration zero) no third body interferes. Furthermore, proposing that the particles in the fluid are dynamically uncorrelated in the precollisional state (cf. Eq. (2.23)), we factor $\rho^{(2)*}$ as

$$\rho^{(2)*}(\underline{x}_1,\underline{x}_2,t) = \chi\{\rho^{(1)*}(\underline{x}_1,t)f_0^{(1)*}(\underline{2}) + f_0^{(1)*}(\underline{1})\rho^{(1)*}(\underline{x}_2,t)\} \tag{6.28}$$

where the superscript (*) carries its usual meaning. This is the traditional Enskog factorization. Using Eqs. (6.27) and (6.28) in

Eq. (6.26a), we obtain the equation

$$\frac{\partial}{\partial t}\phi^{(1)}(\underline{x}_1,t) + iL^{(1)}\phi^{(1)}(\underline{x}_1,t) = -\hat{K}\phi^{(1)}(\underline{x}_1,t) \tag{6.29}$$

where the distortions, $\phi^{(1)}(\underline{x},t)$ and $\Phi^{(1)}(\underline{x},t)$, are defined by

$$\phi^{(1)}(\underline{x}_1,t) = \rho^{(1)}(\underline{x}_1,t)/f_0^{(1)}(\underline{1}) \tag{6.30a}$$

and

$$\Phi^{(1)}(\underline{x}_1,t) = P^{(1)}(\underline{x}_1,t)/f_0^{(1)}(\underline{1}) \quad . \tag{6.30b}$$

The nonlocal Enskog collision operator, $\hat{K}$, is given by

$$\hat{K}\phi^{(1)}(\underline{x}_1,t) = -\int d\underline{2}d\hat{k}S\chi f_0^{(1)}(\underline{2})\hat{k}\cdot\underline{g}[\phi^{(1)^*}(\underline{r}_1,\underline{1},t) + \phi^{(1)^*}(\underline{r}_1+\underline{\xi}_{12},\underline{2},t)]. \tag{6.31}$$

Equation (6.29) is the linearized form of Eq. (2.21) for $f^{(1)}$ which was derived by Curtiss and Dahler (8).

With the aid of Eqs. (6.22) and (6.23), the equation for the distortion can be easily transformed to a more manageable expression. First using Eq. (6.22), the time derivative of $\phi^{(1)}(\underline{x},t)$ becomes

$$\frac{\partial}{\partial t}\phi^{(1)}(\underline{x}_1,t) = \frac{\partial}{\partial t}\Phi^{(1)}(\underline{x}_1,t) \quad . \tag{6.32}$$

From Eqs. (6.21) and (6.22), we realize that the evaluation of the tcfs requires the solution to Eq. (6.38) in the long time limit. Explicitly, we require the solution for a time $\tau_{\dot{m}}^{+}$, which is long compared to the relaxation time for the molecular quantity $\dot{m}$ (denoted $\tau_{\dot{m}}$) but which is much shorter than the hydrodynamic relaxation times. Because of the

existence of these widely separated time scales, the initial hydrodynamic fields (prescribed by $\phi^{(s)}(\underline{x}^s, t=0)$) are essentially frozen over the period τ_m^+. Therefore, the spatial and orientational gradients of $\phi^{(1)}(\underline{x}_1, \tau_m^+)$ can be replaced by the corresponding gradients of $\phi^{(1)}(\underline{x}_1, 0)$

$$iL^{(1)}\phi^{(1)}(\underline{x}_1, t) = iL^{(1)}\phi^{(1)}(\underline{x}_1, 0) \quad . \tag{6.33}$$

Here, $\phi^{(1)}(\underline{x}_1, 0)$ is a known function obtained from Eq. (6.23). Next, by expanding $\phi^{(1)}(\underline{r}_1+\underline{\xi}_{12}, \underline{2}, t)$ in a Taylor series about $\underline{r}_1$

$$\phi^{(1)}(\underline{r}_1+\underline{\xi}_{12}, \underline{2}, t) = \phi^{(1)}(\underline{r}_1, \underline{2}, t) + \underline{\xi}_{12} \cdot \frac{\partial}{\partial \underline{r}_1} \cdot \frac{\partial}{\partial \underline{r}_1} \phi^{(1)}(\underline{r}_1, \underline{2}, t) + \ldots , \tag{6.34}$$

replacing the derivatives of $\phi^{(1)}(\underline{r}_1, \underline{2}, t)$ with the corresponding derivatives of $\phi^{(1)}(\underline{r}_1, \underline{2}, 0)$ on the RHS of this expansion, and inserting the resulting expansion into Eq. (6.31), we find that

$$\hat{K}\phi^{(1)}(\underline{x}_1, t) = K_E\phi^{(1)}(\underline{x}_1, t) + \underline{\underline{H}}_\phi \quad . \tag{6.35}$$

Here, $\hat{K}_E$, the local Enskog collision operator, is

$$\hat{K}_E \phi^{(1)}(\underline{x}_1, t) = - \int d\underline{2} d\hat{k} S\chi f_0^{(1)}(\underline{2}) \hat{k} \cdot \underline{g}[\phi^{(1)*}(\underline{r}_1, \underline{1}, t) + \phi^{(1)*}(\underline{r}_1, \underline{2}, t)] \tag{6.36}$$

and $\underline{\underline{H}}_\phi$ is defined by

$$\underline{\underline{H}}_\phi = - \int d\underline{2} d\hat{k} S\chi f_0^{(1)}(\underline{2}) \hat{k} \cdot \underline{g}\underline{\xi}_{12} \cdot \frac{\partial}{\partial \underline{r}_1} \phi^{(1)*}(\underline{r}_1, \underline{2}, 0) \quad . \tag{6.37}$$

Utilizing the results of Eqs. (6.32)-(6.37), Eq. (6.29) is transformed to

$$\frac{\partial}{\partial t}\Phi^{(1)}(\underline{x}_1,t) + iL^{(1)}\phi^{(1)}(\underline{x}_1,0) + \underline{\underline{H}}_{\phi} = -\hat{K}_E\phi^{(1)}(\underline{x}_1,t) \quad . \tag{6.38}$$

Recall that we require the solution at a time τ_m^+, where τ_m^+ is a time which is long compared to the relaxation times governed by the Enskog equation but short in comparison to the hydrodynamic time scale. In this long time limit, we assume that

$$\lim_{t \to \text{large}} \frac{\partial}{\partial t}\Phi^{(1)}(\underline{x}_1,t) \to 0 \quad . \tag{6.39}$$

In fact, the existence of a well-defined tcf, as given by Eq. (6.21), requires this assumption to be valid. Therefore, $\phi^{(1)}(\underline{x},t)$, in the long time limit, must satisfy the equation

$$\phi^{(1)}(\underline{x},\infty) = -\hat{K}_E^{-1}\{iL^{(1)}\phi^{(1)}(\underline{x}_1,0) + \underline{\underline{H}}_{\phi}\} \tag{6.40}$$

where the infinity symbol replaces t in the argument of $\phi^{(1)}$ to indicate that this is valid only for long times.

Using the above relations in Eq. (6.21), the tcf reduces to

$$\begin{aligned} M = & -\int d\underline{x}_1 \, f_0^{(1)}(\underline{1}) \, \dot{m}_{K,1} \, \phi^{(1)}(\underline{x},\infty) - \int d\underline{x}_1 d\underline{x}_2 \chi f_0^{(1)} f_0^{(1)} \\ & \times \dot{m}_{V,12}[\phi^{(1)^*}(\underline{x}_1,\infty) + \phi^{(1)^*}(\underline{x}_2,\infty)] + \int d\underline{x}_1 d\underline{x}_2 \chi f_0^{(1)} f_0^{(1)} \\ & \times \dot{m}_{V,12}[\phi^{(1)^*}(\underline{x}_1,0) + \phi^{(1)^*}(\underline{x}_2,0)] \end{aligned} \tag{6.41}$$

where the use of the orthogonality of $\dot{m}_{K,1}$ and m_1 has been made. Equations (6.40) and (6.41) are simply Chapman-Enskog expressions for the transport coefficients (4) (refer to the expressions for $\underline{\underline{\eta}}$ and $\underline{\underline{\lambda}}$

in Chapter III). Finally, the results of applying the above methods to the tcfs of Eqs. (6.5a) and (6.5b) are:

$$I_{13} = V\{- \int d\underline{1} f_0^{(1)}(\underline{1}) \underline{\underline{\sigma}}^0_{K,1} : \underline{\underline{\phi}}_D^{(1)}(\infty) + 5nk_BT\lambda_V(-\underline{\underline{\phi}}_D^{(1)}(\infty))\} \tag{6.42a}$$

$$I_{31} = V\{- \int d\underline{1} f_0^{(1)}(\underline{1}) \dot{\underline{\underline{D}}}_1 : \underline{\underline{\phi}}_{rp}^{(1)}(\infty)\} \tag{6.42b}$$

$$I_{11} = V\{- \int d\underline{1} f_0^{(1)}(\underline{1}) \underline{\underline{\sigma}}^0_{K,1} : \underline{\underline{\phi}}_{rp}^{(1)}(\infty) + 5nk_BT\lambda_V(-\underline{\underline{\phi}}_{rp}^{(1)}(\infty)) + 5nk_BT\lambda_V(\underline{\underline{\phi}}_{rp}^{(1)}(0))\} \tag{6.42c}$$

$$\tilde{I}_{11} = V\{- \int d\underline{1} f_0^{(1)}(\underline{1}) \underline{\underline{\sigma}}^0_{K,1} : \tilde{\underline{\underline{\phi}}}_{rp}^{(1)}(\infty) + 5nk_BT\lambda_V(-\tilde{\underline{\underline{\phi}}}_{rp}^{(1)}(\infty)) + 5nk_BT\lambda_V(\underline{\underline{\phi}}_{rp}^{(1)}(0))\} \tag{6.42d}$$

and

$$I_{33} = V\{- \int d\underline{1} f_0^{(1)}(\underline{1}) \dot{\underline{\underline{D}}}_1 : \underline{\underline{\phi}}_D^{(1)}(\infty)\} \tag{6.42e}$$

where $\underline{\underline{\phi}}_{rp}^{(1)}$ and $\underline{\underline{\phi}}_D^{(1)}$ satisfy

$$\underline{\underline{\phi}}_{rp}^{(1)}(\infty) = - \hat{K}_E^{-1}\{\underline{\underline{\sigma}}^0_{K,1} + \underline{\underline{H}}^0_u\} \tag{6.43a}$$

and

$$\underline{\underline{\phi}}_D^{(1)}(\infty) = - \hat{K}_E^{-1} \dot{\underline{\underline{D}}}_1 \quad . \tag{6.43b}$$

Here, the lamda and $\underline{\underline{H}}_u$ integrals are defined by

$$\lambda_V(\underline{\underline{\psi}}) = (5Vnk_BT)^{-1} \int d\underline{x}_1 d\underline{x}_2 \chi f_0^{(1)} f^{(1)} \underline{\underline{\sigma}}^0_{V,12} : [\underline{\underline{\psi}}^*(\underline{x}_1) + \underline{\underline{\psi}}^*(\underline{x}_2)] \tag{6.44}$$

and

$$\underline{\underline{H}}_u = - \int d\underline{2}d\hat{k}S_\chi f_0^{(1)}(\underline{2})\hat{k} \cdot \underline{\underline{g\xi}}_{12} \cdot \frac{\partial}{\partial \underline{r}_1} \underline{\underline{\phi}}^*_{rp}(\underline{r}_1, \underline{2}, 0) \quad . \tag{6.45}$$

The $\lambda_V(\underline{\underline{\phi}}_D^{(1)}(0))$ terms in Eqs. (6.42a)-(6.42e) have been dropped because they are identically zero. That these terms vanish results from the close similarity of the λ_V integrals to the collision integrals (refer to Appendix A) and to the fact that the orientation is a collisional conserved quantity for rigid systems. The tilde on $\underline{\underline{\tilde{\phi}}}_{rp}^{(1)}$ in Eq. (6.42d) is a remnant of the definition of $\tilde{I}_{11}$ in terms of the Q_g projection operator. The distortion $\underline{\underline{\tilde{\phi}}}_{rp}^{(1)}$ satisfies an equation similar to that satisfied by $\underline{\underline{\phi}}_{rp}^{(1)}$. The distinction between $\underline{\underline{\tilde{\phi}}}_{rp}^{(1)}$ and $\underline{\underline{\phi}}_{rp}^{(1)}$ is once again made explicit below.

The methods for solving Eqs. (6.42)-(6.44) are well-known and are identical to the methods used in Chapters III and VI. It is now necessary to expand ϕ in a finite basis set. The choice of basis functions is determined by first rewriting Eqs. (6.42a) and (6.42b) as

$$\underline{\underline{\phi}}_{rp}^{(1)}(\infty) = - \hat{K}_E^{-1} \, 2k_B T\{(1 + h_u^{(1)})\underline{W}_{-1}^0 \underline{W}_{-1} + h_u^{(2)} \underline{\Omega}_{-1}^0 \underline{\Omega}_{-1}\} \tag{6.46a}$$

and

$$\underline{\underline{\phi}}_D^{(1)}(\infty) = - \hat{K}_E^{-1} \sqrt{\frac{2k_B T}{I}} \quad \underline{\Omega}_1 \times \hat{e}_1^0 \hat{e}_1 \quad . \tag{6.46b}$$

Here,

$$h_u^{(1)} = n(1/240\pi^2) \int d\hat{k}d\hat{e}_1 d\hat{e}_2 S_\chi D^{-2} \hat{k} \cdot \underline{\xi}_{12} \tag{6.47a}$$

and

$$h_u^{(2)} = -n(\mu/240\pi^2 I)\int d\hat{k}de_1de_2 S\chi D^{-2}\hat{k}\cdot\underline{\xi}_{12}\hat{k}\times\underline{\xi}_1\cdot\hat{k}\times\underline{\xi}_1 \quad . \quad (6.47b)$$

From Eqs. (6.46a) and (6.46b), we see that an appropriate basis set for $\underline{\phi}_{rp}^{(1)}(\infty)$ and $\underline{\phi}_D^{(1)}(\infty)$ is $\underline{W}^0\underline{W}$, $\underline{\Omega}^0\underline{\Omega}$, and $\underline{\Omega}\times\hat{e}^0\hat{e}$. However, this conclusion requires slight modification because the basis function $\underline{\Omega}\times\hat{e}^0\hat{e}$ should not be included in the expansion of $\tilde{\phi}_{rp}^{(1)}(\infty)$. To see this, we note that, in the derivation of the expression for the shear viscosity (via the Mori formalism), it is assumed that the only slowly relaxing variables are the conserved hydrodynamic variables, and that the orientation densities play no role in the viscosity calculation. Because $\underline{\Omega}\times\hat{e}^0\hat{e}$ is proportional to the time rate of change of an orientation density, i.e., $\frac{d}{dt}\hat{e}^0\hat{e}$, it would be inconsistent to include this quantity in the calculation of the viscosity at this level of approximation.

Expanding the $\underline{\phi}_\alpha^{(1)}$'s as

$$\underline{\phi}_\alpha^{(1)}(\infty) = \underline{W}^0\underline{W}\, b_\alpha^{(1)} + \underline{\Omega}^0\underline{\Omega}\, b_\alpha^{(2)} + \underline{\Omega}\times\hat{e}^0\hat{e}\, b_\alpha^{(3)} \quad (6.48a)$$

and

$$\tilde{\phi}_{rp}^{(1)}(\infty) = \underline{W}^0\underline{W}\,\tilde{b}_{rp}^{(1)} + \underline{\Omega}^0\underline{\Omega}\,\tilde{b}_{rp}^{(2)} \quad , \quad (6.48b)$$

where α = rp or D, and inserting this expansion into Eqs. (6.42a)-(6.42e), we obtain expressions for the I_{ij}'s in terms of the expansion coefficients. The expansion coefficients are obtained by solving Eqs. (6.43a) and (6.43b) within the limited basis sets using the nonsphericity expansion of Cooper and Hoffman (38). Retaining only

those terms of lowest order in the nonsphericity, and using the resulting forms for the I_{ij} integrals in either Eq. (6.4a) or Eq. (6.4b) for R, we obtain the expression

$$R = -\gamma_{\Omega xee}/(1 + \gamma_{\Omega\Omega} + \gamma_{rp}) \quad . \tag{6.49}$$

Here, γ_{rp} is defined as

$$\gamma_{rp} = (n/k_B T)\lambda_V(\underline{r}^0\underline{p})K_{11}/5(1 + h_u^{(1)})^2 \quad , \tag{6.50}$$

and $\gamma_{\Omega xee}$ and $\gamma_{\Omega\Omega}$, which are the relative (to the $\underline{W}^0\underline{W}$ polarization) contributions of the $\underline{\Omega}$ x $\hat{e}^0\hat{e}$ and $\underline{\Omega}^0\underline{\Omega}$ polarizations, respectively, to the shear viscosity, are

$$\gamma_{\Omega xee} = \lambda_V(\underline{\Omega} \times \hat{e}^0\hat{e})K_{13}/K_{33}(1 + h_u^{(1)}) \tag{6.51a}$$

and

$$\gamma_{\Omega\Omega} = 8\lambda_V(\underline{\Omega}^0\underline{\Omega})h_u^{(2)}K_{11}/15K_{22}(1 + h_u^{(1)})^2 \quad . \tag{6.51b}$$

The matrix elements of the Enskog collision operator, K_{ij}, are given by

$$K_{ij}\underline{\underline{\delta}}^{(2)} = n^{-2}\int d\underline{1}\, f_0^{(1)}(\underline{1})\, \underline{\underline{\Psi}}_i\, \hat{K}_E\, \underline{\underline{\Psi}}_j \quad , \tag{6.52}$$

which, in terms of the bracket integrals, are

$$K_{ij} = \frac{1}{5}\{[\underline{\underline{\Psi}}_i;\underline{\underline{\Psi}}_j]_{dd}^{11} + [\underline{\underline{\Psi}}_i;\underline{\underline{\Psi}}_j]_{dd}^{12}\} \quad . \tag{6.53}$$

Here, $\underline{\underline{\Psi}}_i$ represents a basis function used in the expansion of the $\underline{\underline{\phi}}_\alpha^{(1)}$'s. Reexpressing Eqs. (6.50) and (6.51) in terms of reduced integrals defined in Appendix D, we find that

$$\gamma_{\Omega xee} = \frac{\rho^*}{\sqrt{1+\varepsilon}} \tilde{\lambda}_V (\underline{\Omega} \times \hat{e}^0 \hat{e}) \tilde{K}_{13} / \tilde{K}_{33} \left(1 + \frac{\rho^*}{\sqrt{1+\varepsilon}} \tilde{h}_u^{(1)}\right) \tag{6.54a}$$

$$\gamma_{\Omega\Omega} = 8 \frac{\rho^{*2}}{(1+\varepsilon)} \tilde{\lambda}_V (\underline{\Omega}^0 \underline{\Omega}) \tilde{h}_u^{(2)} \tilde{K}_{11} / 15 \tilde{K}_{22} \left(1 + \frac{\rho^*}{\sqrt{1+\varepsilon}} \tilde{h}_u^{(1)}\right)^2 \tag{6.54b}$$

and

$$\gamma_{rp} = 3 \frac{\rho^{*2}}{(1+\varepsilon)} \tilde{\lambda}_V (\underline{r}^0 \underline{p}) \tilde{K}_{11} / 10\pi \left(1 + \frac{\rho^*}{\sqrt{1+\varepsilon}} \tilde{h}_u^{(1)}\right)^2 \tag{6.54c}$$

where the tilde denotes the reduced integrals. Equation (6.49) is the main result of this chapter. It relates the R parameter to the reduced Enskog collision integrals, and to the lambda and $h_u^{(i)}$ integrals which arise from the potential part of the stress tensor.

Because we wish to apply our results to systems consisting of very nonspherical molecules (such as MBBA), there may exist some concern as to the validity of using an expansion in the nonsphericity. However, we will show that this expansion converges very rapidly even for MBBA. The success of the nonsphericity expansion is determined by the inequality $\Psi_{ij} << 1$, where

$$\Psi_{ij} = K_{ij}^2 / K_{ii} K_{jj} \quad . \tag{6.55}$$

The condition that $\Psi_{ij} << 1$ will be tested for each system and the results will be listed in the numerical section.

From the above analysis, we can also write down expressions for the shear viscosity, Eq. (6.10), and the collective particle orientational relaxation time, Eq. (6.11). The resulting expressions are

$$\eta = \frac{5\sqrt{mk_BT}}{(2C)^2\tilde{K}_{11}}\{[1 + \frac{\rho^*}{\sqrt{1+\varepsilon}}\tilde{h}_u^{(1)}]^2 + \frac{\rho^{*2}}{(1+\varepsilon)}\frac{8\tilde{\lambda}_V(\underline{\Omega}^0\underline{\Omega})\tilde{h}_u^{(2)}\tilde{K}_{11}}{15\,\tilde{K}_{22}}\}$$

$$+ \frac{\rho^{*2}}{(1+\varepsilon)}\frac{3}{2\pi}\frac{\sqrt{mk_BT}}{(2C)^2}\tilde{\lambda}_V(\underline{r}^0\underline{p}) \qquad (6.56)$$

and

$$\tau_2^c = \frac{12}{5}\sqrt{\frac{1}{2k_BT}}\,\kappa_{dd}^{-1/2}\,g_2\,\rho^*\,\frac{\varepsilon^2}{\sqrt{1+\varepsilon}}\,\tilde{K}_{33} \qquad (6.57)$$

where κ_{dd} is defined as $1/\mu C^2$. Equation (6.57) is identical to Eq. (5.53).

Certain limiting forms of R should be noted. First, the coupling of the orientation density to a shearing force, as measured by R, is obviously a high density phenomena. Therefore, it is not surprising to find that R vanishes in the case of a dilute gas. At the opposite extreme, in the limit of high density where the potential contributions to the transport coefficients are expected to dominate, R becomes

$$\lim_{\rho^*\to 1} R \to -\{\frac{\lambda_V(\underline{\Omega}\times\hat{e}^0\hat{e})\tilde{K}_{13}}{\tilde{h}_u^{(1)}\tilde{K}_{33}}\}/\{1 + \frac{8K_{11}\lambda_V(\underline{\Omega}^0\underline{\Omega})\tilde{h}_u^{(2)}}{15\tilde{K}_{22}\tilde{h}_u^{(1)2}} + \frac{3\tilde{K}_{11}\tilde{\lambda}_V(\underline{r}^0\underline{p})}{10\pi\tilde{h}_u^{(1)2}}\}\,, \qquad (6.58)$$

which is seen to be independent of the density. The density dependence of R for various molecular systems is plotted in the numerical results section.

It is also instructive to examine the dependence of R on the shape anisotropy of the molecule. The dependence of R on ε (for various

systems) is plotted in the following section at various densities. In the limit $\varepsilon \to 0$, the reduced integrals in Eqs. (6.54a)-(6.54c) can be evaluated analytically. In this limit, we find that

$$\lim_{\varepsilon \to 0} R \to \{ \frac{96}{105} \alpha \} / \{ 1 + \frac{768}{125\pi} \alpha^2 \}$$

$$\sim 0.91 \alpha / (1 + 1.96 \alpha^2) \qquad (6.59)$$

where

$$\alpha = \chi \rho^* / (1 + \frac{8}{5} \chi \rho^*) \quad . \qquad (6.60)$$

Therefore, R is nearly independent of the shape anisotropy for small anisotropies.

Two alternate expressions for R in the $\varepsilon \to 0$ limit are found in the literature. Both expressions are obtained using hydrodynamic arguments in the investigation of a single ellipsoid in a continuous solvent. Kivelson and Hallum (81), utilizing stick boundary conditions, found that

$$\lim_{\varepsilon \to 0} R_{hyd}^{(stick)} \to \frac{3}{5} \rho_s \lambda \left(\frac{\varepsilon}{2 + \varepsilon} \right)^2 \qquad (6.61)$$

where ρ_s is the number density of the solvent and λ is the Perrin factor (60), which for small ε is approximately one. Here R is found to be strongly dependent on the shape anisotropy in the small ε limit. However, experimental evidence suggests that R is practically independent of the shape anisotropy. The hydrodynamic calculation of Calef and Wolynes (82), who applied slip boundary conditions, yielded

$$\lim_{\varepsilon \to 0} R_{hyd}^{(slip)} \to \frac{16}{15} \rho_s \lambda \tag{6.62}$$

which is independent of ε, in agreement with our result and with experimental evidence. The density dependence of Eqs. (6.59) and (6.62) is not the same. Although the two expressions are similar in the low density regime, the expression in Eq. (6.59) approaches a constant value at high densities, whereas Eq. (6.62) does not. In the double limit of ρ^* large and $\varepsilon \to 0$, Eq. (6.49) becomes

$$\lim_{\varepsilon \to 0} \lim_{\rho^* \to 1} R \sim 0.32 \tag{6.63}$$

where ε is allowed to approach zero only after ρ^* becomes large. The density dependence of Eq. (6.58) at high densities reflects the collective nature of our calculation, whereas Eq. (6.62) is strictly a single particle expression.

Finally, that R does not vanish in the $\varepsilon \to 0$ limit for arbitrary densities, is the result of the definition of R as a ratio of quantities which individually vanish as $\varepsilon \to 0$. This, of course, does not imply that there exists a shear-orientation coupling in the limit of spherical particles, for the theory presented above remains valid only for conditions where the time scale separation arguments apply.

B. Numerical Results

Before we are able to evaluate the necessary integrals, we require the full angle dependent contact radial distribution function. However, at the present time, this function is not available to us. Therefore,

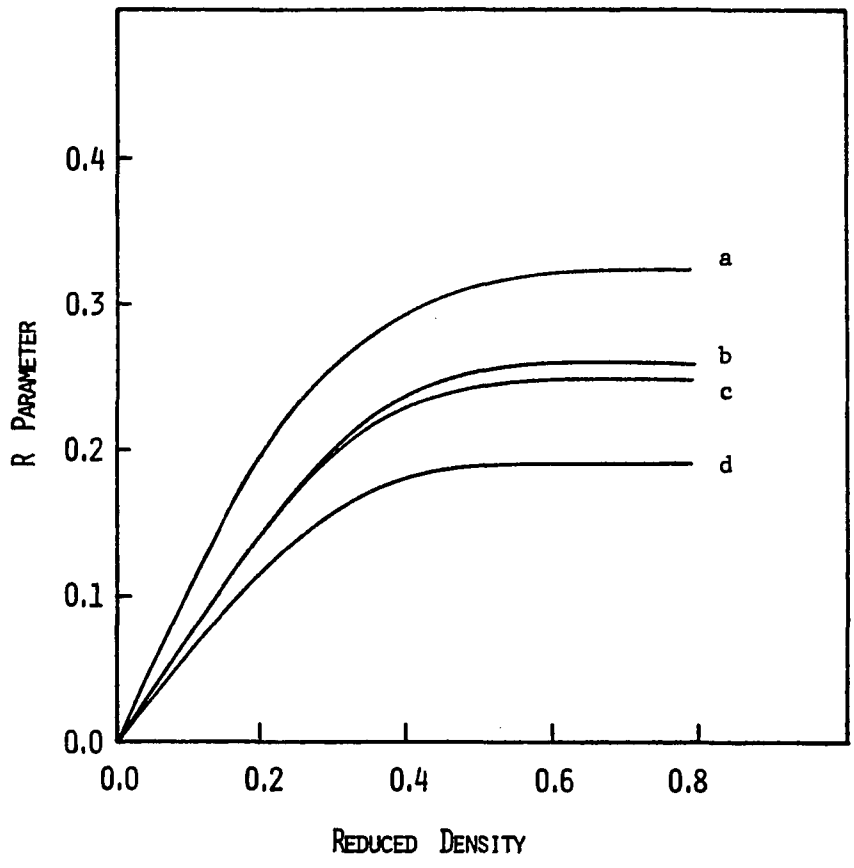

Figure 6.1. Variation of R versus the reduced density holding ε fixed for a) $\varepsilon = 0$ (Eq. (6.89)), b) N_2, c) CS_2 (Table 6.2), and d) MBBA

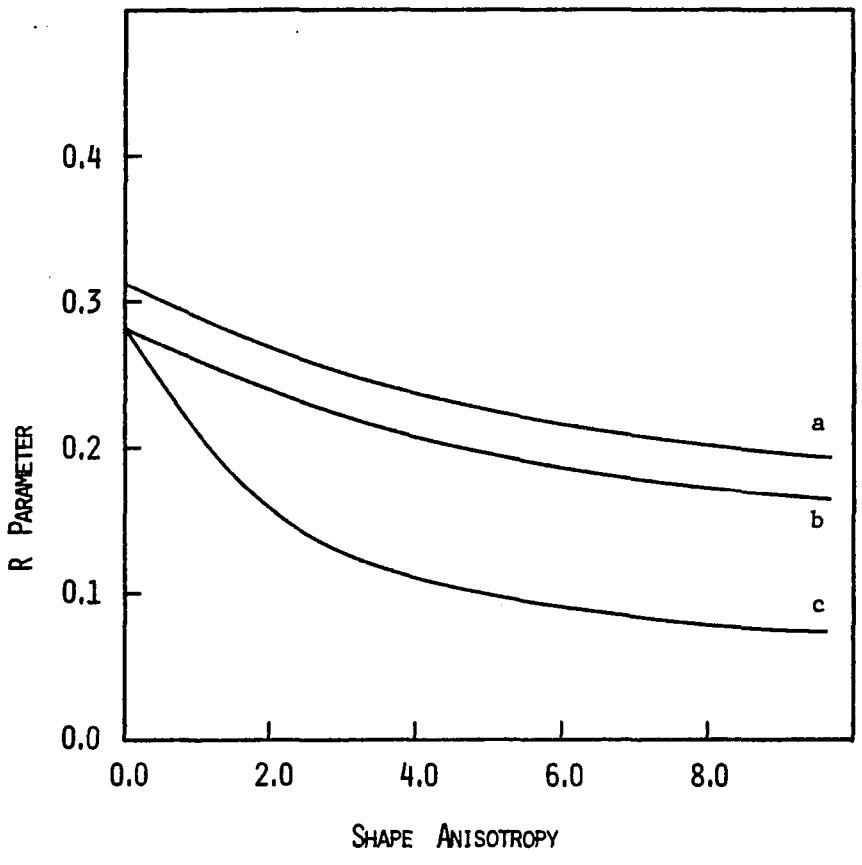

Figure 6.2. Variation of R versus the shape anisotropy holding ρ^* fixed for a) MBBA, b) CS_2 (Table 6.2), and c) N_2. The molecular volume is held fixed while the B/C ratio is varied

we will substitute for χ the Carnahan-Starling (67) approximation for rigid spheres

$$\chi(0) = (2 - \rho^*)/2(1 - \rho^*)^3 \quad , \tag{6.64}$$

as we previously did in Chapter V. At densities for which Eq. (6.64) predicts too large a $\chi(0)$, we assume $\chi(0) = 5.0$.

It is a simple matter to numerically evaluate Eq. (6.49) for R. Table 6.1 compares the results of our kinetic theory (KT) calculation with experimentally determined R values. It is seen that the theoretically determined values are approximately three quarters to one half the values as determined experimentally. The KT values appear to be fairly insensitive to the system studied. The molecules listed in Table 6.1 are large and highly nonspherical. Found in Table 6.2 are the KT results applied to smaller more spherical molecules such as N_2 and F_2. Once again the R values are seen to be fairly insensitive to the systems studied. Typically, KT predicts values in the neighborhood of 0.2, while the experimentally determined values are centered about 0.4.

The dependence of R upon the reduced density for various systems is shown in Fig. 6.1. As mentioned in the previous section, R goes to zero as ρ^* at low densities and becomes independent of density around $\rho^* \sim 0.4\text{-}0.5$. Also evident from Fig. 6.1 is that R apparently decreases with increasing shape anisotropy. This fact is born out in Fig. 6.2 where R is plotted versus ε for systems modeling N_2, CS_2, and MBBA. In Fig. 6.2, the reduced density and molecular volumes were held fixed,

while the B/C ratio was varied. Before we are tempted to draw any conclusions from this plot, we should remind ourselves that in using Eq. (6.64) for $\chi(0)$, we might have drastically altered the dependence or R upon ε.

It is known from a number of studies (80) that R has little or no temperature dependence. The KT result (assuming smooth rigid molecules) for R, from Eqs. (6.49) and (6.54), is seen to be independent of the temperature in agreement with experiment.

At this level of theory, we should not be too concerned that the KT values of R are approximately one half the experimental values. In fact, this could have been predicted from past work. From Eqs. (6.4), (6.10), and (6.11), it is obvious that R is proportional to τ_2^c/η. In Chapter V, a theory similar to this work was applied towards the calculation of τ_2^c. There it was discovered that the KT results for τ_2^c were two to three times smaller than those determined experimentally. Also, it is known that the simple Enskog theory for rigid spheres exaggerates the magnitude of the viscosity at high densities (85). These results indicate that the KT results for R should have been expected to be too small.

In conclusion, the kinetic theory values for R are typically one half the values determined experimentally. The predicted dependence of R on the temperature and the shape anisotropy agrees favorably with experiment. The kinetic theory results indicate that the range of R values is expected to be very small, which is born out experimentally. Furthermore, the dependence of R on the shape anisotropy is in agreement

with the slip hydrodynamic calculations of Calef and Wolynes (82). Finally, we expect that this calculation suffers from the same problems discussed in the orientational correlation time calculation in Chapter V.

Table 6.1. Comparison of kinetic theory with experiment

System	R[a]	B[b] (Å)	C (Å)	ε	ρ*	μ (amu)	I[c] (amu Å^2)	κ_{dd}	T (°K)	Ψ_{13}	Ψ_{12}
CS_2[d]	0.18 (0.35±0.06)	4.66	1.63	7.15	0.59	38.07	155.5	1.53	175	0.019	0.001
MBBA[e]	0.19 (0.36±0.02)	9.03	2.78	9.55	0.58	134.5	∿3100	3	463	0.022	0.001
Pyridine[f]	0.22 (0.35±0.08)	1 76	3.26	-0.71	0.61	39.55	∿72	0.17	243	0.044	0.007
Triphenyl phosphate[g]	0.22 (0.45±0.05)	2.58	4.84	-0.72	0.68	163	∿760	0.2	313	0.047	0.008

[a]The numbers in parentheses represent the experimental values.

[b]The geometries for these systems were derived from the material contained in Table VI of Ref. 86.

[c]The values for I for MBBA, pyridine, and triphenyl phosphate are estimates.

[d]Source: Ref. 87.

[e]Source: Ref. 88.

[f]Source: Ref. 86.

[g]Source: Ref. 77.

Table 6.2. Kinetic theory values for small molecules

System[a]	R	B (Å)	C (Å)	ε	ρ^*	μ (amu)	I (amu Å^2)	κ_{dd}	T (°K)	Ψ_{13}	Ψ_{12}
CS_2	0.22	3.2	1.65	2.76	0.364	38.07	155.5	1.50	193	0.058	0.004
N_2	0.22	2.22	1.67	0.75	0.364	14.01	8.39	0.22	62.8	0.071	0.007
N_2	0.21	2.22	1.67	0.75	0.325	14.01	8.39	0.22	152.9	0.071	0.007
F_2	0.25	2.13	1.41	1.26	0.451	19.00	19.57	0.52	70	0.069	0.006
F_2	0.22	2.13	1.41	1.26	0.346	19.00	19.57	0.52	120	0.069	0.006
CO_2	0.20	2.68	1.50	2.19	0.329	22.01	43.21	0.87	273	0.054	0.004

[a]The geometries, temperatures, and reduced densities for these systems were taken from Tables 5.1 and 5.2.

VII. CHATTERING

In the previous chapters, various assumptions were made concerning the scattering dynamics of the system. First, it was assumed that the intermolecular potential can be modeled by a rigid convex core potential. Thus, a two body collision simply consists of free flight motion, interrupted by one or more impulsive hits. We will use the term "collision" to refer to the complete, two-body encounter (i.e., the totality of hits). The term, simple collisions, will be understood to denote events that involve a single hit (i.e., the molecules approach one another from an infinite separation, undergo a single impulsive hit, then freely stream apart to an infinite separation). More complicated collisions, involving two or more hits, will be termed chattering collisions. It is worth noting that chattering collisions only occur, in the strictest sense, for rigid molecules. However, there is a corresponding dynamical behavior for systems with soft interactions. A chattering collision for such systems can be defined as an event in which the molecules experience a harsh repulsive force more than once during their encounter. We expect the existence of a soft attractive core would encourage these generalized chattering events.

The second assumption made in the previous chapters, concerning the two-body scattering dynamics, was to ignore the existence of chattering collisions. Thus, each hit of the two body system is treated as a simple collision. This allows for the interpretation of the starred functions in Chapter II as functions of the precollisional

state. It is the validity of this last assumption that forms the central topic of this chapter.

The existence of chattering events is clearly a result of the anisotropy of the molecular interaction potential. As the geometry of the molecular models approaches that of a rigid (not loaded) sphere, the possibility of a chattering collision necessarily goes to zero.

Concern over the neglect of the chattering collisions first arose when Monte Carlo evaluation of certain transport coefficients for rigid ovaloids indicated that neglect of chattering events can give rise to significant errors when the molecules differ greatly from rigid spheres (89). These results suggest that a more accurate treatment of these complicated collisions is required.

The first section of this chapter is devoted to a formal analysis of chattering. This analysis divides naturally into two parts. First we discuss the dynamics of rigid ovaloid systems through a generalization of the pseudo-Liouville formalism commonly encountered in the analysis of rigid sphere systems (90). Next we utilize the pseudo-Liouville formalism for the analysis of the Boltzmann bracket integral. The result is a series expansion of the bracket integral, the leading term of which is the standard, simple collision bracket integral utilized in Chapters III-VI. Finally, in the second section, we present the results of some numerical work.

A. Formal Analysis

1. Dynamics of rigid ovaloid systems

For a system of hard ovaloids, the intermolecular potential is of the form

$$V_{ij} = \begin{cases} \infty & \text{if} \quad \ell_{ij} \leq 0 \\ 0 & \text{if} \quad \ell_{ij} > 0 \end{cases} . \tag{7.1}$$

Clearly the gradient of this potential is infinite at the point of contact, corresponding to an impulsive force, and so the Liouville operator is ill-defined for this interaction. However, the dynamics of this system is well-defined and, in fact, is comparatively simple.

We now confine our discussion to the dynamics of two isolated nonspherical bodies. The generalization to a many body system will be made later. We formally define the two particle interacting, L, and noninteracting, L_0, Liouville operators by

$$L = i\{H^{(2)}, \} \tag{7.2a}$$

and

$$L_0 = i\{H_0^{(2)}, \} \tag{7.2b}$$

respectively, where

$$H^{(2)} = H_0^{(2)} + V_{12} \tag{7.3}$$

is the two particle Hamiltonian. Here, $H_0^{(2)}$ is the noninteracting Hamiltonian and V_{12} is the interaction potential. With L and L_0

defined, we can express the time evolution operators by exp $\pm iLt$ and exp $\pm iL_0 t$. These exponential operators act on a two particle phase point, $\underline{x}^2$, and transform it to a new phase point at a time $\pm t$ later on the two particle trajectory determined by the dynamics of $H^{(2)}$ or $H_0^{(2)}$, respectively. Finally,

$$e^{\pm iLt} A(\underline{x}^2) = A(e^{\pm iLt} \underline{x}^2) \tag{7.4}$$

which is readily established for an analytic function by considering its Taylor series expansion.

The definitions of the preceding paragraph are formal and applicable to any pair potential. However, due to the simplicity of the dynamics for rigid ovaloids, we are able to write a more explicit form of the streaming operator. We begin by formally expanding the full streaming operator,

$$e^{\pm iLt} = e^{\pm iL_0 t} + \int_0^t dt' \, e^{\pm iLt'}(iL - iL_0)e^{\pm iL_0(t-t')} \quad . \tag{7.5}$$

This can be rewritten as

$$e^{\pm iLt} = e^{\pm iL_0 t} + \lim_{n\to\infty} \sum_{i=0}^{n} e^{\pm iLt_i} T^{(\pm)}(\varepsilon) \, e^{\pm iL_0(t-t_i)} \tag{7.6}$$

where

$$\begin{aligned} T^{(\pm)}(\varepsilon) &= \int_0^{\varepsilon} d\varepsilon' \, e^{\pm iL\varepsilon'}(iL - iL_0) \, e^{\mp iL_0\varepsilon'} \\ &= (\pm)[e^{\pm iL\varepsilon} e^{\mp iL_0\varepsilon} - 1] \quad . \end{aligned} \tag{7.7}$$

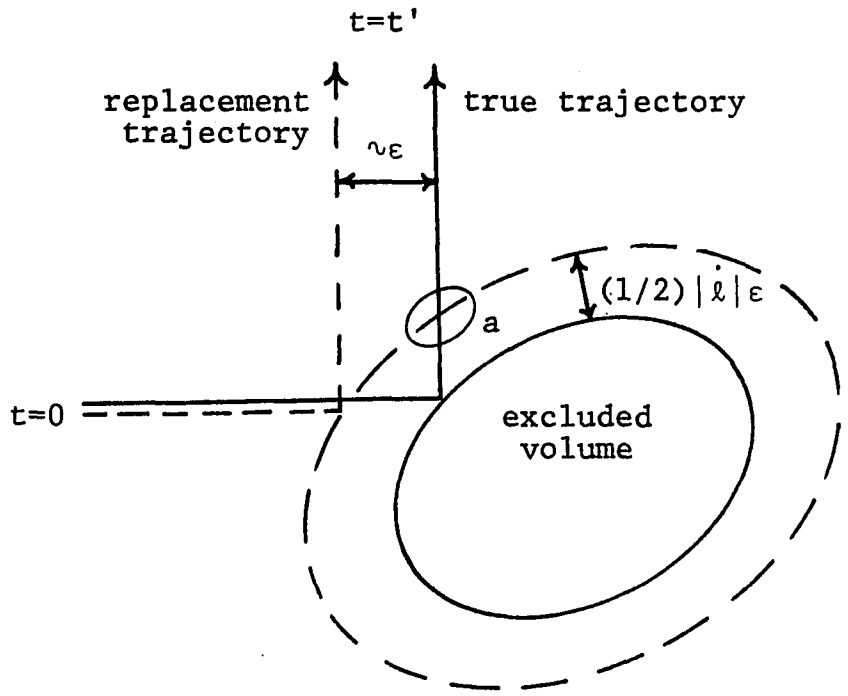

Figure 7.1. The true and the replacement dynamics at finite ε for forward streaming. As ε approaches zero, the two trajectories become indistinguishable. Region a, where the true trajectory breaks out of the thin shell, is the reason for the inclusion of the step function $\theta(-\dot{\ell})$ in the definition of $T^{(+)}$

Here, $t_0 = 0$, $t_n = t - \varepsilon$, and $\varepsilon = t/n$. The pseudo-Liouville formalism is obtained by making the following equivalent replacement (in the $\varepsilon \to 0$ limit) of $T^{(\pm)}(\varepsilon)$,

$$T^{(\pm)}(\varepsilon) \to \int_0^{\varepsilon} d\varepsilon' \, e^{\pm iL\varepsilon'} \, \delta(\ell - \tfrac{1}{2} |\dot{\ell}|\varepsilon) \times |\dot{\ell}|\theta(\dot{\ell})[\hat{b} - 1] e^{\mp iL_0\varepsilon'} \qquad (7.8)$$

where $\delta(x)$ is the Dirac delta function, $\theta(x)$ is the unit step function, and $\hat{b}$ reverses the sign of the relative contact velocity (equivalent to changing the pre or post collisional momenta to their post or pre collisional values). The difference (for finite ε) between $T^{(\pm)}(\varepsilon)$ and its replacement is illustrated in Fig. 7.1. From Fig. 7.1, it is obvious that the replacement becomes exact in the $\varepsilon \to 0$ limit. Defining $T^{(\pm)}(\varepsilon)$ by

$$T^{(\pm)}(\varepsilon) = \delta(\ell - \tfrac{1}{2} |\dot{\ell}|\varepsilon) |\dot{\ell}|\theta(\dot{\ell})[\hat{b} - 1] \quad , \qquad (7.9)$$

the full streaming operator can be written

$$\begin{aligned} e^{\pm iLt} &= e^{\pm iL^{(\pm)}t} = \lim_{\varepsilon \to 0} e^{\pm iL^{(\pm)}(\varepsilon)t} \\ &= e^{\pm iL_0 t} + \lim_{\varepsilon \to 0} \int_0^t dt' \, e^{\pm iLt'} \, T^{(\pm)}(\varepsilon) \, e^{\pm iL_0(t-t')} \end{aligned} \qquad (7.10)$$

where $L^{(\pm)}$, which is referred to as the pseudo-Liouville operator for reasons to become apparent below, is defined by the $\varepsilon \to 0$ limit of the RHS of Eq. (7.10). The streaming operators $\exp \pm iLt$ and $\exp \pm iL^{(\pm)}t$ are equivalent in the sense that $L^{(\pm)}$ reproduces the exact dynamics, determined by L. The operator, $T^{(\pm)}$, is defined to have the following

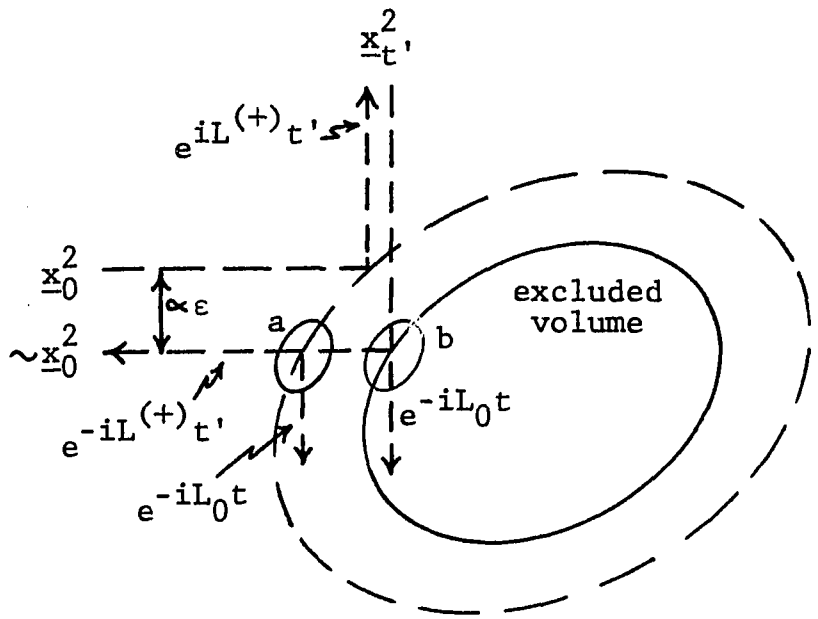

Figure 7.2. Action of the operator exp $iL^{(+)}t$ exp $-iL^{(+)}t$. The operator exp $iL^{(+)}t'$ propagates $\underline{x}^2_0$ to $\underline{x}^2_{t'}$. The operator exp $-iL^{(+)}t'$ streams $\underline{x}^2_{t'}$ back through the shell to region b where the full propagator, exp iLt, in the definition of exp $-iL^{(+)}t'$, Eq. (7.10), registers the interaction. Back streaming through region a, the conditions of the delta function are met, the $\hat{b}$ operator contribution cancels the original free streaming term in the $\varepsilon \to 0$ limit. Therefore, in the $\varepsilon \to 0$ limit, Eq. (7.11) holds

behavior. When the condition are such that a collision is to occur, the delta function conditions are met going into or leaving the collision by action of the operator exp $\pm iLt'$. Two contributions are obtained going into the collision. One involves $\hat{b}$ which transforms the momentum dependence to the pre or post collisional values, and the other, -1, which subtracts off the free streaming term. The Heavyside (θ) function results in a zero contribution when leaving the collision (see Fig. 7.1).

The operators $L^{(+)}$ and $L^{(-)}$ are interchangeable in physically allowed regions of phase space where the particles do not overlap. In this region, $L^{(+)}$ ($L^{(-)}$) can be used for backward (forward) streaming as well as forward (backward) streaming, i.e.,

$$e^{\pm iL^{(\pm)}t}\, e^{\mp iL^{(\pm)}t} = e^{\pm iL^{(\pm)}t}\, e^{\mp iL^{(\mp)}t} = 1 \quad . \tag{7.11}$$

This is illustrated for the $L^{(+)}$ operator in Fig. 7.2. Similar arguments apply as well for the $L^{(-)}$ operator.

It is often convenient to work with a binary collision expansion (bce) of the full evolution operator. For a two particle system, the bce is simply obtained by iteration of Eq. (7.10)

$$\begin{aligned} e^{\pm iLt} &= e^{\pm iL_0 t} + \lim_{\varepsilon\to 0} \lim_{\varepsilon'(<\varepsilon)\to 0} \int_0^t dt'\, e^{\pm iL^{(\pm)}(\varepsilon')t'}\, T^{(\pm)}(\varepsilon) \\ &\quad \times e^{\pm iL_0(t-t')} \\ &= e^{\pm iL_0 t} + \int_0^t dt'\, e^{\pm iL_0 t'}\, T^{(\pm)}\, e^{\pm iL_0(t-t')} \end{aligned}$$

$$+ \int_0^t dt' \int_0^{t'} dt'' \, e^{\pm iL_0 t''} T^{(\pm)} e^{\pm iL_0 (t'-t'')} T^{(\pm)} e^{\pm iL_0 (t-t')}$$

$$+ \ldots \quad . \tag{7.12}$$

Here,

$$T^{(\pm)} = \delta(\ell_+) |\dot{\ell}| \theta(\dot{\ell}) [\hat{b} - 1] \tag{7.13}$$

is the $\varepsilon \to 0$ limit of $T^{(\pm)}(\varepsilon)$ where $\delta(\ell_+) = \lim_{\varepsilon \to 0} \delta(\ell - \frac{1}{2} |\dot{\ell}| \varepsilon)$. The double limit ε and $\varepsilon'(<\varepsilon) \to 0$ ensures that the integrand is well-defined. There are two points of interest concerning this expansion. First, the expansion of Eq. (7.12) is identical to the formal expansion of the exponential operator $\exp \pm(iL_0 + T^{(\pm)})t$. In this sense, $\exp \pm iL^{(\pm)}t$ is equivalent to $\exp \pm(iL_0 + T^{(\pm)})t$ and, therefore, we will not hesitate in writing $iL^{(\pm)}$ as $iL_0 + T^{(\pm)}$. Second, if we wish to utilize this expansion, we are forced to extend the domain of definition of $T^{(\pm)}$ (and, therefore, also $L^{(\pm)}$) to include nonphysical, overlapping regions. This is due to the presence of the free streaming operator lying to the left of $T^{(\pm)}$ in various terms of the expansion. Because the regions of phase space where overlapping configurations exist are nonphysical (i.e., never penetrated by a real trajectory) and the dynamics in the overlapping regions never enter into any final results, the domain of definition of the $T^{(\pm)}$ operator can be extended arbitrarily to include these overlapping regions.

Van Leeuwen and Weyland (91) have chosen to retain the action of the $T^{(\pm)}$ operator as given by Eq. (7.13) for overlapping regions. Therefore, if two particles are initially overlapping, they simply free

stream apart. This behavior is termed semi-transparent action: molecules originally overlapping freely stream apart, but those originally nonoverlapping can never overlap. Hoegy (92) chooses an extension in which he assumes that the overlapping particles stream out of one another interactively. This is consistent with energy conservation and Eq. (7.1). The interaction kicks the two molecules apart with an infinite relative velocity. Since such contributions vanish due to the presence of normalized velocity distributions, Hoegy's extension, written $T^{(\pm)(H)}$, is

$$T^{(\pm)(H)} = T^{(\pm)} - \delta(\ell_-)\theta(\pm\dot{\ell})|\dot{\ell}| \quad . \tag{7.14}$$

Haines, Dorfman and Ernst (93) interpret overlapping configurations as the result of two particles approaching each other with an infinite relative velocity. Thus, they choose to immediately eliminate these contributions through the addition of a term which depends on the two particle phase at the initial time t = 0. Their (nonlocal) extension, denoted $T^{(\pm)(HDE)}$, is of the form

$$T^{(\pm)(HDE)} = T^{(\pm)} - \delta(t_+)\ (-\ell) \tag{7.15}$$

where $\delta(t_+) = \lim_{\eta\to 0} \delta(t - \eta)$. When the initial two particle phase lies in an overlapping region, $\theta(-\ell)$ is unity and the conditions for the delta function are met. The action of $\delta(t_+)\theta(-\ell)$ is then identical to the action of the -1 term in the definition of $T^{(\pm)}$, i.e., it cancels the free streaming term. Therefore, the action of $\exp \pm iL^{(\pm)(HDE)}t$ on any function of the two particle phase for overlapping configurations is

a) $T^{(+)}$

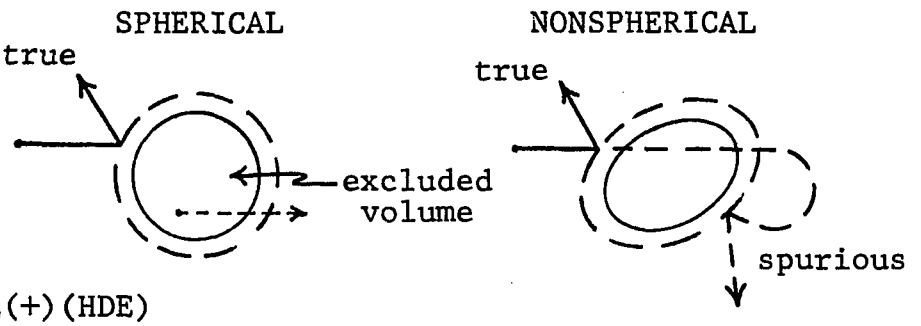

b) $T^{(+)(HDE)}$

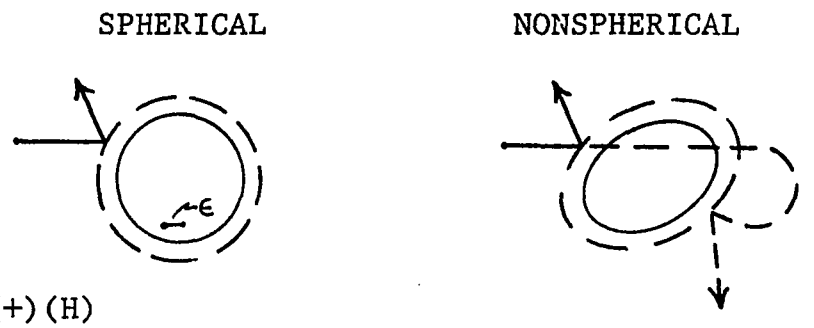

c) $T^{(+)(H)}$

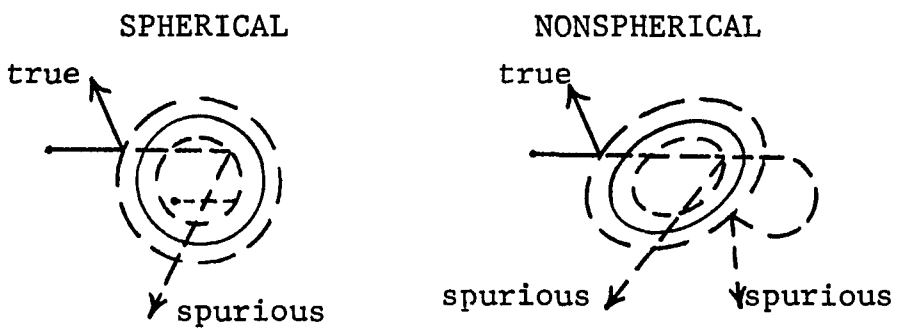

Figure 7.3. Existence of spurious trajectories in the bce for the three extensions of $T^{(+)}$ into the overlapping regions; a) $T^{(+)}$ b) $T^{(+)(HDE)}$, and c) $T^{(+)(H)}$. The interior trajectories, shown only for the spherical systems, also exist in the nonspherical systems

zero. However, when the initial two particle phase is nonoverlapping, the action of $T^{(\pm)(HDE)}$ is identical to $T^{(\pm)}$. This operator, $T^{(\pm)(HDE)}$, is nonlocal because it depends not only on the present two particle phase but also on the initial phase. The extension, $T^{(\pm)(HDE)}$, has also been used by other workers (94-97).

The differences between the extensions for $T^{(\pm)}$ do not manifest themselves outside the overlapping region. However, they do have different bce. That is, the expansions of exp $\pm iLt$ are not the same term for term. The extension, $T^{(\pm)(H)}$, contains spurious contributions to the second term of the bce for the case of rigid spheres, whereas the extensions $T^{(\pm)}$ and $T^{(\pm)(HDE)}$ do not. These spurious contributions are canceled off by contributions from the higher order terms in the binary collision expansion. However, for nonspherical molecules, all three extensions contain spurious contributions to the individual terms of the bce. These spurious trajectories are illustrated in Fig. 7.3. As required, the spurious contributions disappear when the bce is summed.

There exist three methods of dealing with these spurious contributions: (1) Handle them on the same footing as the true contributions at each level of the bce, comfortable with the knowledge that these ill-behaved trajectories cancel one another in the sum (in a relatively small number of terms since multiple chattering events are improbable). (2) Resum the contributions of (1) resulting from spurious collisions (which amounts to simply ignoring the spurious trajectories). (3) Introduce a nonlocal operator, dependent on the full two particle trajectory from the initial time to the present, as the extension of

the $T^{(\pm)}$ operator, which is zero on a trajectory with an ill-behaved history. This nonlocal operator is the formal result of the resummation in (2).

One further comment concerning the three alternative extensions of $T^{(\pm)}$ into the nonphysical, overlapping regions. We have already shown that the operators $L^{(+)}$ and $L^{(-)}$ are interchangeable in the forward and backward streaming operators when restricted to the physical, nonoverlapping regions of phase space (see Fig. 7.2). Thus, the operators, $L^{(+)}$ and $L^{(-)}$, preserve the time reversal symmetry of the dynamics. This property is also preserved by the two extensions $T^{(\pm)(H)}$ and $T^{(\pm)(HDE)}$, but is destroyed by the extension $T^{(\pm)}$ (this can be seen by first streaming just outside of the overlapping region and then attempt a back streaming). Due to this asymmetry, the distinction between the forward and the backward direction will be maintained when working with $L^{(+)}$ and $L^{(-)}$.

It is a simple matter to generalize the above formalism to an N-body system. First, define $L^{(N)}$ and $L_0^{(N)}$ by

$$L^{(N)} = i\{H^{(N)}, \} \tag{7.16a}$$

and

$$L_0^{(N)} = i\{H_0^{(N)}, \} \tag{7.16b}$$

where

$$H^{(N)} = \sum_{i=1}^{N} K_i + \sum_{\alpha} V_\alpha \tag{7.17}$$

is the N particle Hamiltonian, K_i is the kinetic energy of molecule i and V_α is the interaction potential between the molecular pair α. Splitting $H^{(N)}$ into two parts, $H^{(N)}(\alpha) + V_\alpha$, where

$$H^{(N)}(\alpha) = \sum_{i=1}^{N} K_i + \sum_{\beta \neq \alpha} V_\beta \quad , \tag{7.18}$$

allows the full evolution operator to be written as

$$e^{\pm iL^{(N)}t} = e^{\pm iL^{(N)}(\alpha)t} + \int_0^t dt' \, e^{\pm iL^{(N)}t'} \, iL_{V,\alpha} e^{\pm iL^{(N)}(\alpha)(t-t')} \quad . \tag{7.19}$$

Here,

$$iL^{(N)}_{(\alpha)} = i\{H^{(N)}(\alpha), \ \} \tag{7.20}$$

and

$$iL_{V,\alpha} = i\{H^{(N)} - H^{(N)}(\alpha), \ \} \quad . \tag{7.21}$$

At any instant in time, there is at most one hard collision. Therefore, the arguments made above for the two body case can be repeated, allowing us to replace $iL_{V,\alpha}$ with $T^{(\pm)}\alpha$ and to formally equate the expansions of $\exp \pm iL^{(N)}t$ and $\exp \pm(iL^{(N)}_{(\alpha)} + T^{(\pm)})t$. Furthermore, this argument can be repeated for each molecular pair with the result that

$$e^{\pm iL^{(N)}t} = e^{\pm(iL_0^{(N)} + \sum_\alpha T_\alpha^{(\pm)})t} \quad , \tag{7.22}$$

valid for nonoverlapping regions. Given this relation, we have that

$$A(\underline{x}^N_{\pm t}) = e^{\pm(iL_0^{(N)} + \sum_\alpha T_\alpha^{(\pm)})t} A(\underline{x}^N_0) \quad , \tag{7.23}$$

where

$$\underline{x}^N_{\pm t} = e^{\pm(iL_0^{(N)} + \sum_\alpha T_\alpha^{(\pm)})t} \underline{x}^N_0 \quad . \tag{7.24}$$

The results of Eqs. (7.22) and (7.23) can be extended to the nonphysical, overlapping regions. Clearly, $L_0^{(N)}$ and $T_\alpha^{(\pm)}$ are well-defined in the full phase space. Thus, we can extend the equivalence between $\exp \pm(iL_0^{(N)} + \sum_\alpha T_\alpha^{(\pm)})t$ and $\exp \pm iL^{(N)}t$ in Eq. (7.22) to include all phase space. Furthermore, Eq. (7.23), which is certainly valid for nonoverlapping regions, can be verified for overlapping regions as well. The operator, $iL_0^{(N)} + T_\alpha^{(\pm)}$, is a simple linear differential operator for overlapping regions of phase space. Therefore, Eq. (7.23) can be verified in the overlapping regions by expanding $A(\underline{x}^N)$ in its Taylor series expansion (identical to the method used in obtaining Eq. (7.4)). Upon differentiation with respect to time, Eq. (7.23) becomes

$$\frac{\partial}{\partial t} A(\underline{x}^N_{\pm t}) = \{iL_0^{(N)} + \sum_\alpha T_\alpha^{(\pm)}\} A(\underline{x}^N_{\pm t}) \quad . \tag{7.25}$$

Equation (7.25) is the equation of motion for the dynamic quantity $A(\underline{x}^N)$. This equation, with $iL^{(N)}$, expressed as $iL_0^{(N)} + \sum_\alpha T_\alpha^{(\pm)}$, is traditionally termed the pseudo-Liouville equation since Eq. (7.25) is equivalent to the equation of motion for A of Eq. (5.5), with $\sum_\alpha T_\alpha^{(\pm)}$ assuming the role of $iL^{(N)} - iL_0^{(N)}$.

The object of kinetic theory is not the calculation of $A(\underline{x}^N_{\pm t})$; for that is a problem of mechanics. Rather kinetic theory strives to determine the average behavior of A. This average, denoted A(t), is written

$$\overline{A}(\pm t) = \int d\underline{x}^N \, F^{(N)}(\underline{x}^N,0)A(\underline{x}^N_{\pm t}) \tag{7.26}$$

where $F^{(N)}$ is the N particle probability density at a time t = 0. Similarly, this can be written

$$\overline{A}(\pm t) = \int d\underline{x}^N \, A(\underline{x}^N)F^{(N)}(\underline{x}^N,\pm t) \tag{7.27}$$

where

$$F^{(N)}(\underline{x}^N,\pm t) = e^{\pm iL^{(N)\dagger}t} \, F^{(N)}(\underline{x}^N,0) \quad , \tag{7.28}$$

the dagger denoting the Hermitian conjugate. For an arbitrary operator, $\hat{X}$, the Hermitian conjugate is defined by

$$\int d\underline{x}^N \, B^* \, \hat{X} \, A = \int d\underline{x}^N (\hat{X}^\dagger B)^* A \tag{7.29}$$

where the superscript star denotes the complex conjugate. From Eq. (7.28), we see that the pseudo-Liouville equation for $F^{(N)}$ is

$$\frac{\partial}{\partial t} F^{(N)}(\underline{x}^N,\pm t) = \{-iL_0^{(N)} + T^{(\pm)\dagger}\}F^{(N)}(\underline{x}^N,\pm t) \tag{7.30}$$

where the result that $L_0^{(N)} = L_0^{(N)\dagger}$ was used, which results from a simple integration by parts argument. Note, however, that $iT^{(\pm)}$ is not self-adjoint. This is a result of the lack of time reversibility of the dynamics of $L^{(\pm)}$ in the overlapping regions. The equivalence, $L^{(\pm)} = L$, holds only in the nonoverlapping regions. Therefore, the self-adjointness

of L does not force $L^{(\pm)\dagger} = L^{(\pm)}$ due to the extension of the domain of definition of $L^{(\pm)}$ to include the overlapping regions. The Hermitian conjugate of $T^{(\pm)}$ is determined by the following arguments.

Consider first the conjugate of $T^{(+)}$. We know that

$$\int d\underline{x}_1 d\underline{x}_2 \; A \; T_{12}^{(+)\dagger} \; B \; = \; \int d\underline{x}_1 d\underline{x}_2 \; B \; T^{(+)} \; A \tag{7.31}$$

for the real functions A and B. Insertion of the explicit form for $T^{(+)}$ yields

$$\begin{aligned} &= \int d\underline{x}_1 d\underline{x}_2 \; B|\dot{\ell}|\delta(\ell_+)\theta(-\dot{\ell}) \; \hat{b} \cdot 1 \; A(\underline{x}_1,\underline{x}_2) \\ &= \int_{\dot{\ell}<0} d\underline{x}_1 d\underline{x}_2 \; B(\underline{x}_1,\underline{x}_2)|\dot{\ell}|\delta(\ell_+)A(\underline{x}_1^+,\underline{x}_2^+) \\ &\quad - \int_{\dot{\ell}<0} d\underline{x}_1 d\underline{x}_2 \; B(\underline{x}_1,\underline{x}_2)|\dot{\ell}|\delta(\ell_+)A(\underline{x}_1,\underline{x}_2) \end{aligned} \tag{7.32}$$

where $\underline{x}_i^+$ denotes the postcollision variables of body i. The integration variables of the first integral can be transformed to the postcollisional variables (denoted $d\underline{x}_1^+ d\underline{x}_2^+$). The Jacobian of this transformation is unity. Therefore, we obtain

$$\begin{aligned} &= \int_{\dot{\ell}^+>0} d\underline{x}_1^+ d\underline{x}_2^+ \; A(\underline{x}_1^+,\underline{x}_2^+)|\dot{\ell}^+|\delta(\ell_+^+)\hat{b} \; B(\underline{x}_1^+,\underline{x}_2^+) \\ &\quad - \int_{\dot{\ell}<0} d\underline{x}_1 d\underline{x}_2 \; A(\underline{x}_1,\underline{x}_2)|\dot{\ell}|\delta(\ell_+)B(\underline{x}_1,\underline{x}_2) \quad . \end{aligned} \tag{7.33}$$

By dropping the (+) superscripts in the first integral, we find that

$$= \int d\underline{x}_1 d\underline{x}_2 \; A\dot{\ell}\delta(\ell_+)\{\theta(\dot{\ell})\hat{b} + \theta(-\dot{\ell})\}B(\underline{x}_1,\underline{x}_2) \quad . \tag{7.34}$$

Comparison of Eqs. (7.32) and (7.34) yields

$$T^{(+)^\dagger} = \dot{\ell}\delta(\ell_+)[\theta(\dot{\ell})\hat{b} + \theta(-\dot{\ell})] \quad . \tag{7.35}$$

By identical methods, we can obtain the expression for $T^{(-)^\dagger}$. Combining the two results into a single expression, we have that

$$T^{(\pm)^\dagger} = \pm\dot{\ell}\delta(\ell_+)\{\theta(\pm\dot{\ell})\hat{b} + \theta(\mp\dot{\ell})\} \quad . \tag{7.36}$$

Note, it was necessary to first define the evolution and equations of motion for arbitrary (but analytic) functions of the phase (cf. Eq. (7.4)). The evolution of these functions is well-defined in terms of their Taylor series expansions. This is not true for $F^{(N)}$, which contains a discontinuity at $\ell_{ij} = 0$ for all i, j. However, the evolution and equation of motion for $F^{(N)}$ is well-defined in terms of the Hermitian conjugate of $L^{(N)}$.

The equation of motion for F is

$$\{\frac{\partial}{\partial t} + iL_0^{(N)}\}F^{(N)} = \sum_{i\neq j} T_{ij}^{(\pm)^\dagger} F^{(N)} \quad . \tag{7.37}$$

Defining the reduced distribution functions, $f^{(s)}$, in terms of $F^{(N)}$ (refer to Eq. (2.4))

$$f^{(s)} = [N!/(N - s)!]\int d\underline{x}_{s+1} \ldots d\underline{x}_N F^{(N)} \quad , \tag{7.38}$$

and integrating Eq. (7.37) over the phase variables of particles s + 1 through N, we obtain

$$\{ \frac{\partial}{\partial t} - iL^{(s)^\dagger} \} f^{(s)} = \sum_{j=1}^{s} \int d\underline{x}_{s+1} \, T_{j,s+1}^{(\pm)^\dagger} \, f^{(s+1)} \tag{7.39}$$

which represents the equation of motion for the reduced distribution functions. In deriving Eq. (7.39), we have made use of the result

$$\int d\underline{x}_i d\underline{x}_j \, T_{ij}^{(\pm)^\dagger} \, F^{(N)} = 0 \quad . \tag{7.40}$$

Equation (7.39) is the BBGKY hierarchy for rigid ovaloids. The first equation of this hierarchy is

$$\{ \frac{\partial}{\partial t} + iL_0^{(1)} \} f^{(1)} = \int d\underline{x}_2 \, T_{12}^{(+)^\dagger} \, f^{(2)} \quad . \tag{7.41}$$

Equation (7.41) represents the starting point for the derivations of the Enskog and Boltzmann equations in Chapter II (refer to Eq. (2.21)). The present derivation of Eq. (7.41) is alternative to that of Chapter II.

2. Chattering expansion of the bracket integral

In the reduction of Eq. (7.41) to the Boltzmann equation, $f^{(2)^*}$ is replaced with (98)

$$f^{(2)^*}(\underline{r}_1,\underline{1}; \underline{r}_1+\underline{\xi}_{12},\underline{2}; t) \rightarrow S \, f^{(1)^*}(\underline{r}_1,\underline{1},t) f^{(1)^*}(\underline{r}_1,\underline{2},t) \tag{7.42}$$

where

$$S = \lim_{\tau\to\infty} e^{-iL\tau} e^{+iL_0\tau} \quad . \tag{7.43}$$

The operator, S, streams the system back in time along interacting trajectories to the infinite past where the two particle distribution is

assumed to factor into a product of $f^{(1)}$'s. The operator, S, then streams this factored distribution forward along a noninteracting trajectory to the present. Making use of this replacement and utilizing the pseudo-Liouville formalism of the previous section, we are able to write the Boltzmann bracket integral of the function ϕ and ψ as

$$\{\phi,\psi\}^{ij} = V^{-1} \int d\underline{x}_1 d\underline{x}_2 \, \phi_i \, T^{(+)^\dagger} \, S \, f_0^{(1)} f_0^{(1)} \, \psi_j \tag{7.44}$$

where V is the volume of the system and i and j are molecular labels. The S operator, in the definition of the Boltzmann bracket integral, acts only on two particle phases in noninteracting regions of phase space. In this restricted region, the S operator conserves the kinetic energy of the two particles. Therefore, $f_0^{(1)} f_0^{(1)}$, which is a simple functional of the two particle kinetic energy, commutes with S. Utilizing the definition of the Hermitian conjugate and the commutability of $f_0^{(1)} f_0^{(1)}$ with S, the bracket integral can be recast in the form

$$\{\phi,\psi\}^{ij} = V^{-1} \int d\underline{x}_1 d\underline{x}_2 \, f_0^{(1)} f_0^{(1)} (T^{(+)} \phi_i) S \, \psi_j \quad . \tag{7.45}$$

Insertion of the bce for exp $-iL\tau$ into the expression for S yields

$$S = \lim_{\tau\to\infty} \{ e^{-iL_0\tau} + \int_0^\tau dt \, e^{-iL_0} \, T^{(-)} \, e^{-iL_0(\tau-t)} + \int_0^\tau dt \int_0^t dt' \, e^{-iL_0 t'}$$

$$\times \, T^{(-)} \, e^{-iL_0(t-t')} \, T^{(-)} \, e^{-iL_0(\tau-t)} + \ldots \} e^{+iL_0\tau}$$

$$= \{ 1 + \int_0^\infty dt \, e^{-iL_0 t} \, T^{(-)} \, e^{iL_0 t} + \int_0^\infty dt \int_0^t dt' \, e^{-iL_0 t'} \, T^{(-)}$$

$$x\, e^{-iL_0(t-t')}\, T^{(-)}\, e^{iL_0 t} + \ldots\} \tag{7.46}$$

which represents a bce of the S operator. When this expansion is substituted into the bracket integral, a series expansion of the bracket integral is generated. From Eqs. (7.42), (7.45), and (7.46), we see that the first approximation to S (setting S = 1) assumes that the molecules are hitting one another for the first time. The second term in the expansion corrects for two hit collision sequences. The next term corrects for three hit collisions and so on.

Insertion of Eq. (7.46) into Eq. (7.45) yields

$$\begin{aligned}\{\phi,\psi\}^{i,j} = V^{-1}\{ & \int d\underline{x}_1 d\underline{x}_2\, f_0^{(1)} f_0^{(1)} (T^{(+)}\phi_i)\psi_j + \int d\underline{x}_1 d\underline{x}_2\, f_0^{(1)} f_0^{(1)} (T^{(+)}\phi_i) \\ & \times \int_0^\infty dt\, e^{-iL_0 t}\, T^{(-)}\, e^{iL_0 t}\, \psi_j + \int d\underline{x}_1 d\underline{x}_2\, f_0^{(1)} f_0^{(1)} (T^{(+)}\phi_i) \\ & \times \int_0^\infty dt \int_0^t dt'\, e^{-iL_0 t'}\, T^{(-)}\, e^{-iL_0(t-t')}\, T^{(-)}\, e^{iL_0 t}\, \psi_j + \ldots\}.\end{aligned} \tag{7.47}$$

This is the chattering expansion of the Boltzmann bracket integral. Equation (7.46) will be written as

$$\{\phi,\psi\}^{ij} = \sum_{\ell=1}^{\infty} \{\phi,\psi\}_{(\ell)}^{ij} \tag{7.48}$$

with obvious definitions of the terms (cf. Eqs. (7.47) and (7.48)). The infinite upper limit on the summation in Eq. (7.48) is somewhat misleading since collisions rarely involve more than a few hits and infinite chattering sequences presumably appear in the phase space in a region of measure zero.

The first term of the chattering expansion is

$$\{\phi,\psi\}^{ij}_{(1)} = V^{-1} \int d\underline{x}_1 d\underline{x}_2 \, f_0^{(1)} f_0^{(1)} (T^{(+)}\phi_i)\psi_j \quad . \tag{7.49}$$

Using Eq. (7.9) for $T^{(+)}$ and integrating over the relative and center of mass coordinates, Eq. (7.49) becomes

$$\{\phi,\psi\}^{ij}_{(1)} = \int_{\hat{\ell}<0} d\underline{1} d\underline{2} d\hat{k} S f_0^{(1)} f_0^{(1)} \hat{\ell}\psi_j (\phi_i - \phi_i^+) \tag{7.50}$$

where, as above, the superscript (+) indicates the post-hit momenta. Furthermore, we will indicate the post-hit momenta following the nth future hit with a superscript (+n) and the momenta preceding n past hits with a superscript (-n).

An alternate form for $\{\phi,\psi\}^{ij}_{(1)}$ is obtained by utilizing the definition of the Hermitian conjugate of $T^{(+)}$. The alternate expression is

$$\{\phi,\psi\}^{ij}_{(1)} = \int d\underline{1} d\underline{2} d\hat{k} S f_0^{(1)} f_0^{(1)} \hat{\ell}\phi_i \psi_j^* \quad . \tag{7.51}$$

This is the familiar form of the simple collision bracket integral commonly encountered in dilute gas calculations and used in the previous four chapters.

The second term of Eq. (7.48) is

$$\{\phi,\psi\}^{ij}_{(2)} = V^{-1} \int d\underline{x}_1 d\underline{x}_2 \, f_0^{(1)} f_0^{(1)} (T^{(+)}\phi_i) \int_0^\infty dt \, e^{-iL_0 t} T^{(-)} e^{iL_0 t} \psi_j \, . \tag{7.52}$$

Using Eq. (7.9) in Eq. (7.52), we can immediately write $\{\phi,\psi\}^{ij}_{(2)}$ as

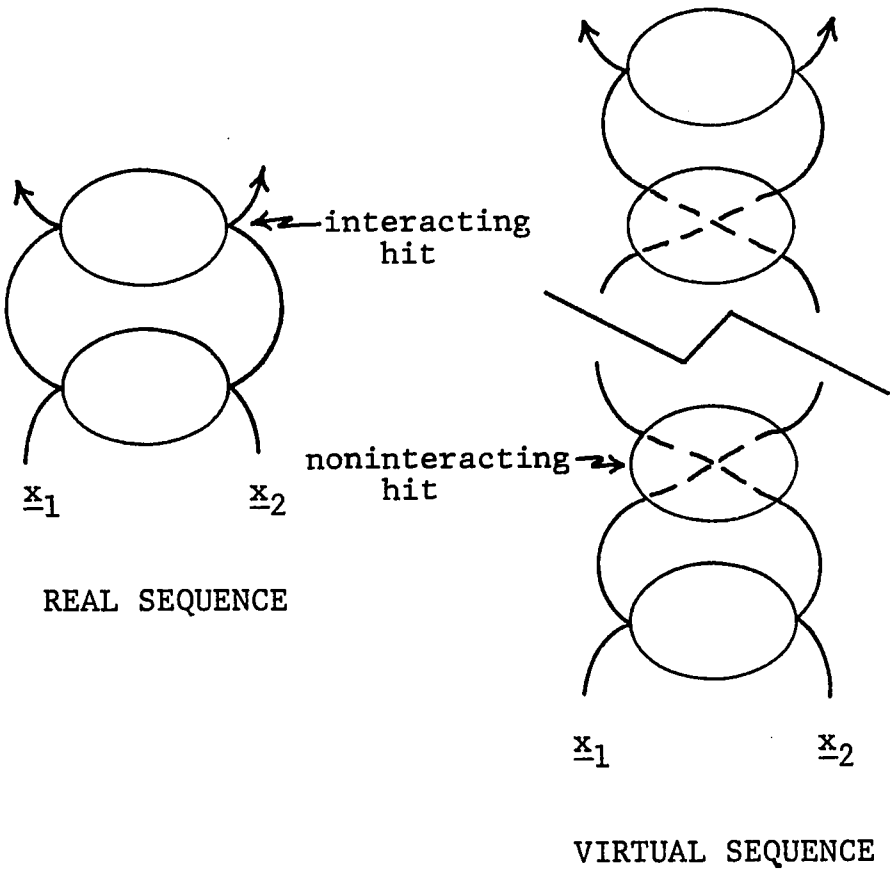

Figure 7.4. Real and partial collision sequences contributing to $\{\phi,\psi\}^{ij}_{(2)}$

$$\{\phi,\psi\}^{ij}_{(2)} = \int_{\hat{\ell}<0} d\underline{1}d\underline{2}d\hat{k}\; f_0^{(1)}f_0^{(1)}\hat{\ell}(\phi_i - \phi_i^+) \int_0^\infty dt\; e^{-iL_0t}\, T^{(-)}\, e^{iL_0t}\, \psi_j \quad . \tag{7.53}$$

Here, we have already integrated out the delta function. The operator

$$\int_0^\infty dt\; e^{-iL_0t}\, T^{(-)}\, e^{iL_0t} \tag{7.54}$$

in Eq. (7.53) introduces spurious contributions similar to those mentioned in context of the bce above. The operator exp $-iL_0t$ transforms the phase variables of the two interacting particles backwards along a noninteracting path in search of a past hit. For the smallest value of t, this past hit is part of a true collision sequence; for other than the smallest, it is part of a virtual collision sequence. Therefore, the operator of Eq. (7.54) incorporates collision sequences beginning and ending with an interacting hit between which are zero, one, or more "noninteracting hits", i.e., the molecules pass through each other. These collision sequences are illustrated in Fig. 7.4. We will incorporate these spurious collision sequences into the present discussion, and show that their contributions arising in the second term of the expansion of $\{\phi,\psi\}$ are canceled by contributions present in the third term of the expansion.

We define $\chi^{(n)}_{i_1,i_2,\ldots,i_{n-1}}$ as a characteristic function for a partial collision sequence consisting of n - 1 past interacting hits; the subscripts indicate the number of noninteracting hits immediately following each interacting hit of the sequence. This function is equal to unity when the present phase of molecules one and two lies on a trajectory

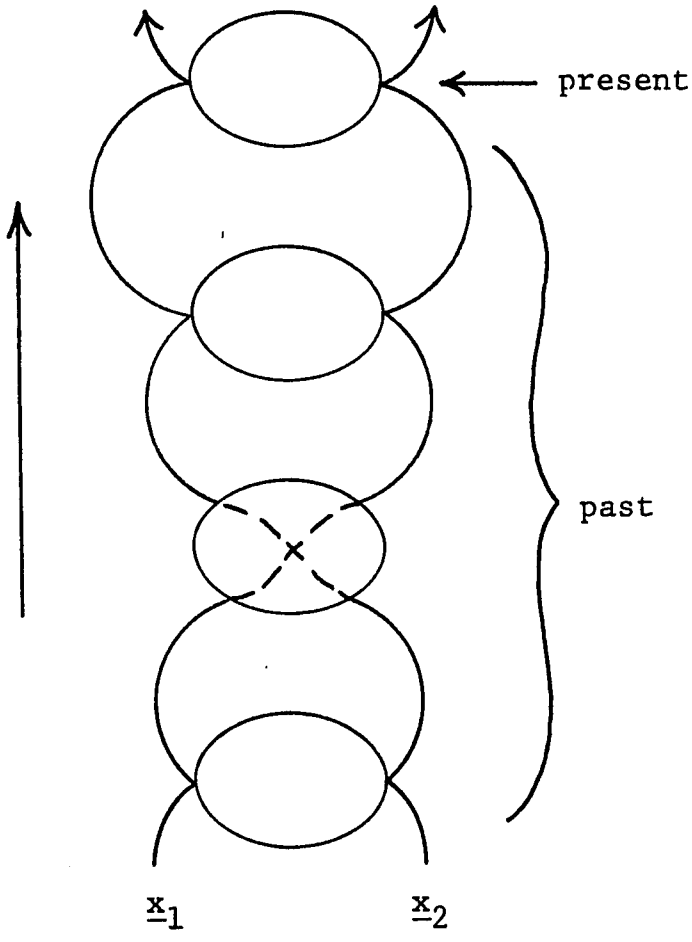

Figure 7.5. Partial collision sequence characterized by $\chi^{(3)}_{1,0}$

corresponding to a partial collision sequence of n interacting hits, with i_1 noninteracting hits immediately following the first interacting hit, i_2 noninteracting hits immediately following the second interacting hit, and so on; and is zero otherwise (refer to Fig. 7.5). The characteristic function $\chi^{(n)}_{i_1,i_2,\ldots,i_{n-1}}$ describes a virtual, partial collision sequence if any of the subscripts i_j are nonzero. If all subscripts are zero, then $\chi^{(n)}_{i_1,i_2,\ldots,i_{n-1}}$ describes a real, partial collision sequence.

We are now in a position to write out explicitly the form of the $\{\phi,\psi\}^{ij}_{(2)}$ term. Utilizing the above definitions, we find that

$$\{\phi,\psi\}^{ij}_{(2)} = \int_{\dot{\ell}<0} \underline{d1}\underline{d2}\hat{dk}Sf_0^{(1)}f_0^{(1)}\dot{\ell}(\phi_i - \phi_i^+)(\chi_0^{(2)} + \chi_1^{(2)} + \ldots)(\psi_j^- - \psi_j) \quad . \tag{7.55}$$

A comparison of Eqs. (7.55) and (7.50) shows us that the real collisions (determined by the $\chi_0^{(2)}$ characteristic function) in Eq. (7.55) correct the error made in $\{\phi,\psi\}^{ij}_{(1)}$, which treated the second hit of a multiple hit collision as if it were the first interaction. The higher order χ's (i.e., $\chi_1^{(2)}$, $\chi_2^{(2)}$, etc.) in Eq. (7.55) introduce spurious (or virtual) collision sequences. The summation in Eq. (7.55) does, in fact, truncate at some finite number. This truncation exists because eventually the relative velocity of the two interacting particles will separate the molecules to a distance where an interaction is no longer possible.

We will complete our discussion of the series expansion of Eq. (7.48) with an analysis of the $\{\phi,\psi\}^{ij}_{(3)}$ term. Explicitly, the term is

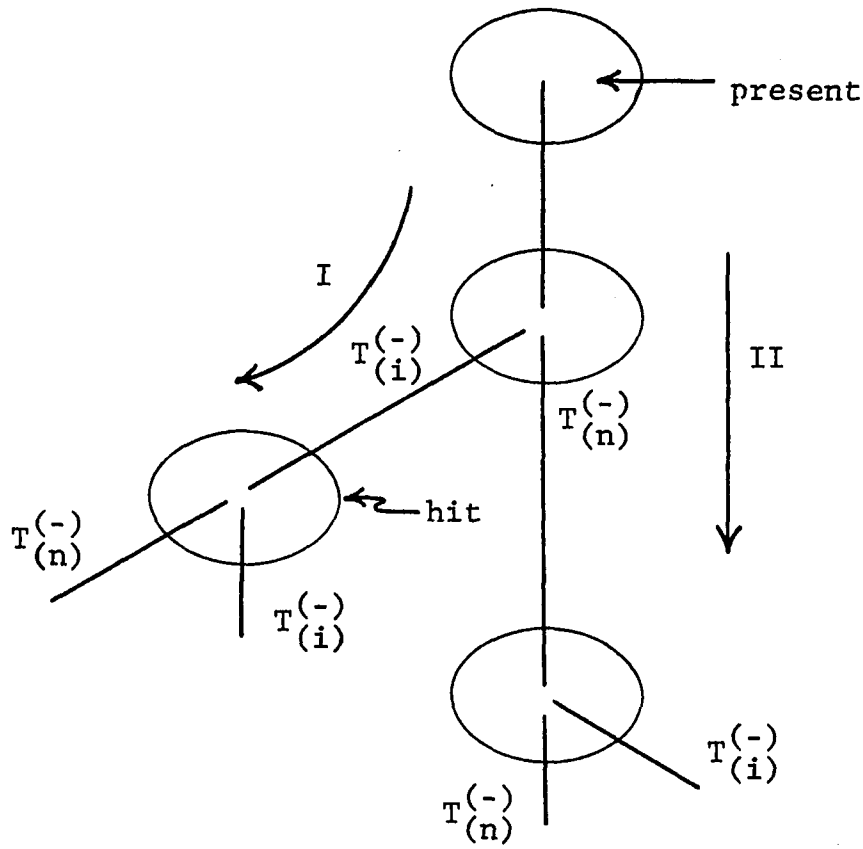

Figure 7.6. A branching process present in the $\{\phi,\psi\}^{ij}_{(3)}$ term

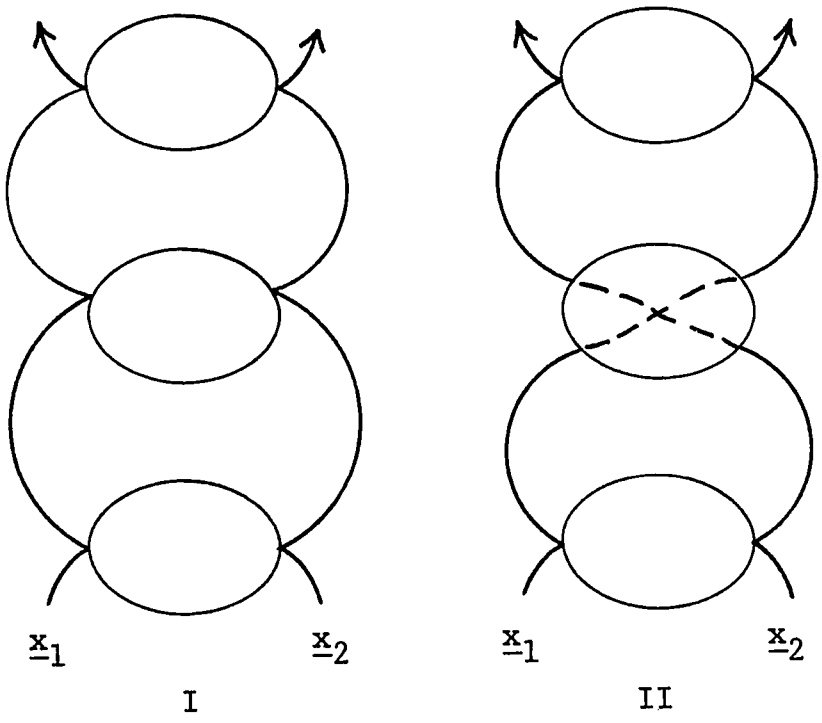

Figure 7.7. The two collision sequences comprising the branching process of Fig. 7.6

$$\{\phi,\psi\}^{ij}_{(3)} = \int_{\dot{\ell}<0} d\underline{1}d\underline{2}dk\hat{S}f_0^{(1)}f_0^{(1)}\dot{\ell}(\phi_i - \phi_i^+) \int_0^\infty dt \int_0^t dt' e^{-iL_0t'} T^{(-)}$$

$$\times e^{-iL_0(t-t')} T^{(-)} e^{iL_0t} \psi_j \quad . \tag{7.56}$$

This term incorporates sequences of three interacting hits. However, not so obvious is the fact that this term also contains expressions dealing with the existence (or nonexistence) of sequences with two interacting hits between which are one or more noninteracting hits. These two hit (interacting) partial collisions result from a branching process due to the form of the $T^{(\pm)}$ operators as a difference of interacting, $T^{(\pm)}(i)$, and noninteracting, $T^{(\pm)}(n)$, operators

$$T^{(\pm)} = T^{(\pm)}(i) - T^{(\pm)}(n)$$

$$= |\dot{\ell}|\delta(\ell_+)\theta(\mp\dot{\ell})\hat{b} - |\dot{\ell}|\delta(\ell_+)\theta(\mp\dot{\ell}) \quad . \tag{7.57}$$

This branching process is given a diagrammatic representation in Fig. 7.6. At this level in the chattering expansion, the branching process contains two separate partial collision sequences. The collision sequence denoted by I in Fig. 7.6 is the real sequence illustrated in Fig. 7.7. This type of collision sequence takes into account the existence of three interacting hit processes. The collision sequence denoted by II in Fig. 7.7 is a virtual collision sequence of the type introduced in $\{\phi,\psi\}^{ij}_{(2)}$. This term cancels the contribution of the virtual sequences to the previous $\{\phi,\psi\}^{ij}_{(2)}$ term. Sequences I and II represent the simplest examples of partial collision sequences contributing to the $\{\phi,\psi\}^{ij}_{(3)}$ term. More complicated partial collisions also contribute.

These higher order contributions are of two types. The first type (related to sequence I) consists of three interacting hits (beginning and ending with an interacting hit) between which are any number of noninteracting hits. The second type (related to sequence II) are similar to the first type except that the intermediate interacting hit of the first type is replaced with a noninteracting hit in the second type.

The discussion of the previous paragraph allows us to write Eq. (7.56) explicitly as

$$\{\phi,\psi\}^{ij}_{(3)} = \int_{\dot{\ell}<0} d\underline{1}d\underline{2}d\hat{k}Sf_0^{(1)}f_0^{(1)}\dot{\ell}(\phi_i - \phi_i^+)\{\sum_{r=0}^{\infty}\sum_{s=0}^{\infty}\chi^{(3)}_{r,s}(\psi_j^{-2} - \psi_j^-) - \sum_{r=1}^{\infty}\chi_r^{(2)}(\psi_j^- - \psi_j)\} \quad . \tag{7.58}$$

Here, the last summation is only over the virtual collision sequences.

The analysis of the higher order contributions to the exact bracket integral follows in a similar fashion. From the analysis of the first three terms, we can see a pattern emerging. The first term handles all hits as if they are the first hit of a collision. This is obviously wrong for chattering collisions. In the case of multiple hits, the second term corrects the error made in treating the second hit as if it were the first. However, in doing so, the $\{\phi,\psi\}^{ij}_{(2)}$ term introduces nonphysical, or virtual, collision sequences. The third order correction not only rectifies the error of assuming the third hit of a sequence to be the second hit (the error being made in the second term), it also

cancels out the contributions of the nonphysical collision sequences introduced in the previous term. In the process, it introduces still more complicated virtual collision processes.

It is now apparent that is is indeed possible to resume the chattering series of Eq. (7.48) (and, therefore, also the bce of Eq. (7.12)) in such a way to eliminate the virtual collision sequences. This resummation simply replaces $\Sigma\chi^{(n)}$ with $\chi^{(n)}_{0,0,\ldots,0}$ in the explicit expressions of the terms in the chattering expansion. This is precisely what we expected and is required if the true dynamics is to be reproduced by the bce. Therefore, the first correction to the simple collision bracket integral, $\{\phi,\psi\}^{ij}_{(1)}$, can be written

$$\{\phi,\psi\}^{ij}_{(2)} = \int_{\hat{k}<0} d\underline{1}d\underline{2}d\hat{k}Sf_0^{(1)}f_0^{(1)}\hat{k}(\phi_i^+ - \phi_i)\chi_0^{(2)}(\psi_j - \psi_j^-) \quad . \quad (7.59)$$

The higher order terms can be written in a similar fashion.

This concludes the formal results of this chapter. The Boltzmann bracket integral is expanded in a series as

$$\{\phi,\psi\}^{ij} = \sum_{n=1}^{\infty} \{\phi,\psi\}^{ij}_{(n)} \quad (7.60)$$

where the nth order term contains the details of a partial collision sequence of n real hits. The lowest order term is the commonly encountered, simple collision bracket integral used in the applications discussed in Chapters III through VI. As we shall see, only the two hit contribution to the bracket integral $\{\phi,\psi\}^{ij}_{(2)}$ of Eq. (7.59) gives an important correction to $\{\phi,\psi\}^{ij}_{(n)}$.

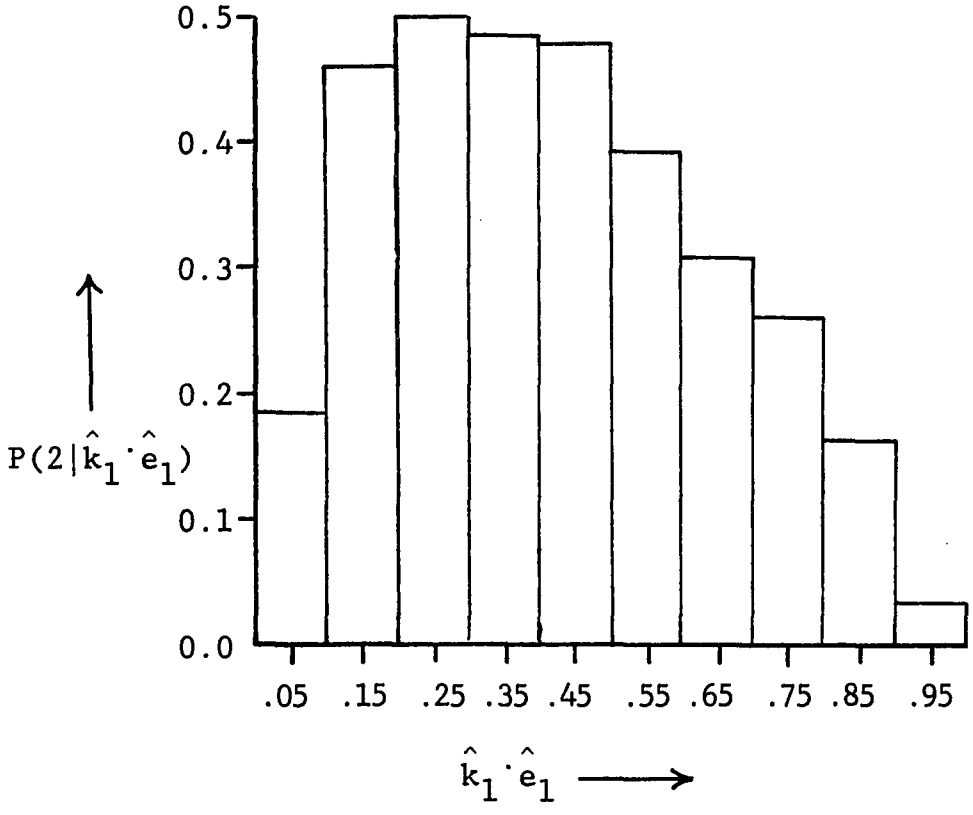

Figure 7.8. Bar graph representation of the conditional probability, $P(2|\hat{k}_1 \cdot \hat{e}_1)$

B. Numerical Work

In this section, we present an analysis of chattering collisions between a rigid sphere of radius 3.6 Bohr and a rigid ellipse with a major axis of 8.0 Bohr and a minor axis of 3.0 Bohr. Classical scattering trajectories for this system were calculated using the hard sphere-hard ellipse algorithm of Evans (89). The initial conditions for these trajectories were randomly chosen. The initial momenta of the atom-diatom system were sampled over a Boltzmann distribution at 300°K. The relative angles were sampled over a uniform distribution. Similarly, the impact plane was uniformly sampled.

A first indication of the importance of chattering collisions is found in Table 7.1. It can be seen that more than 25% of all collisions between the hard sphere and hard ellipse result in chattering; the vast majority of these chattering collisions are two hit events. Furthermore, from Table 7.1, it seems appropriate to ignore the existence of chattering collisions consisting of three or more hits, for these constitute only 1% of the total number of collisions. Therefore, we will focus our discussion towards the analysis of two hit chattering events.

Figure 7.8 is a bar graph of the function $P(2|\hat{k}_1 \cdot \hat{e}_1)$ versus $\hat{k}_1 \cdot \hat{e}_1$. The function $P(2|\hat{k}_1 \cdot \hat{e}_1)$ is the probability of a two hit chattering collision given that the sphere and ellipse first make contact at the point on the surface of ellipse specified by $\hat{k}_1 \cdot \hat{e}_1$ ($\hat{k}$ is the outward surface normal at contact and $\hat{e}$ is the symmetry axis of the ellipse). As such, $P(2|\hat{k}_1 \cdot \hat{e}_1)$ represents a conditional probability.

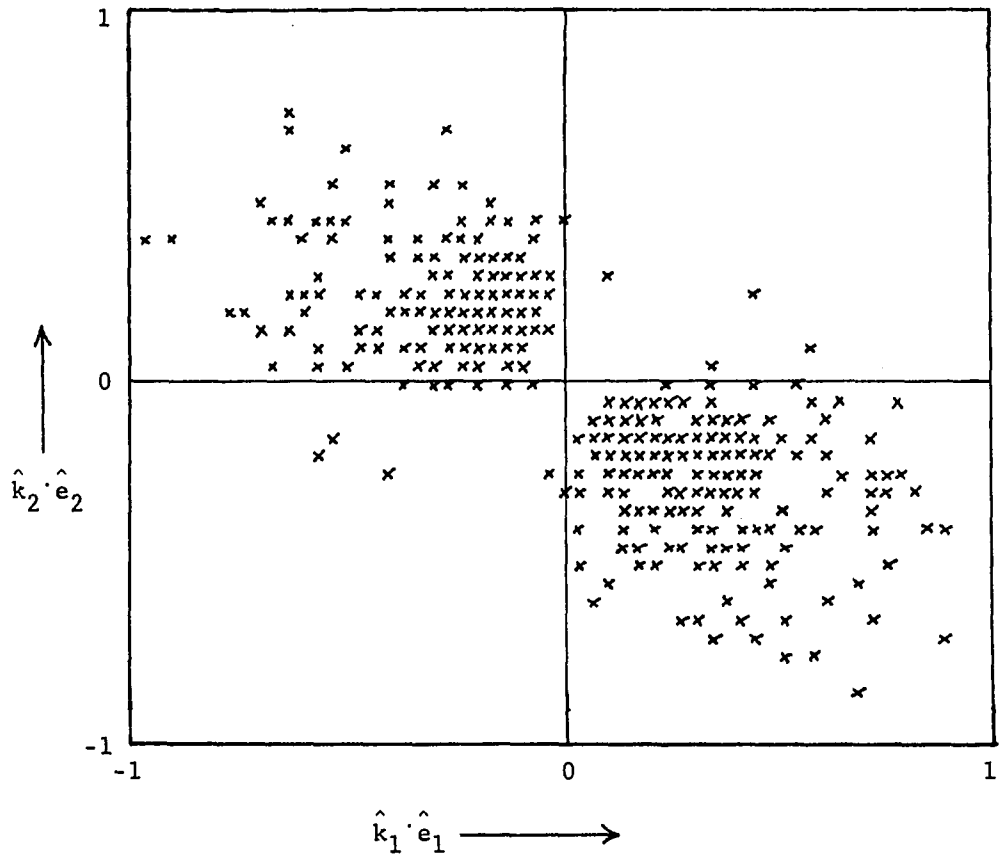

Figure 7.9. Sampling of two-hit chattering collisions on the surface of the ellipse

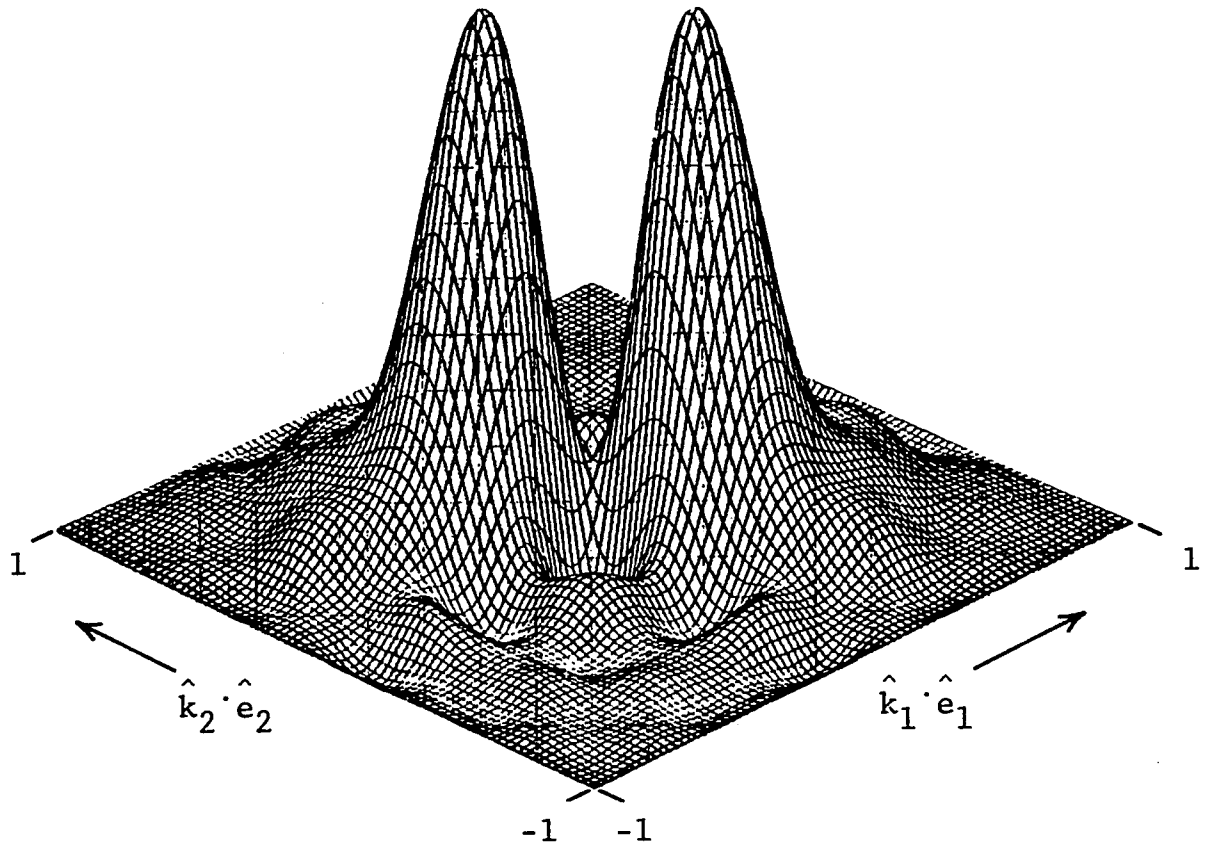

Figure 7.10. Density of two-hit chattering collisions on the surface of the ellipse

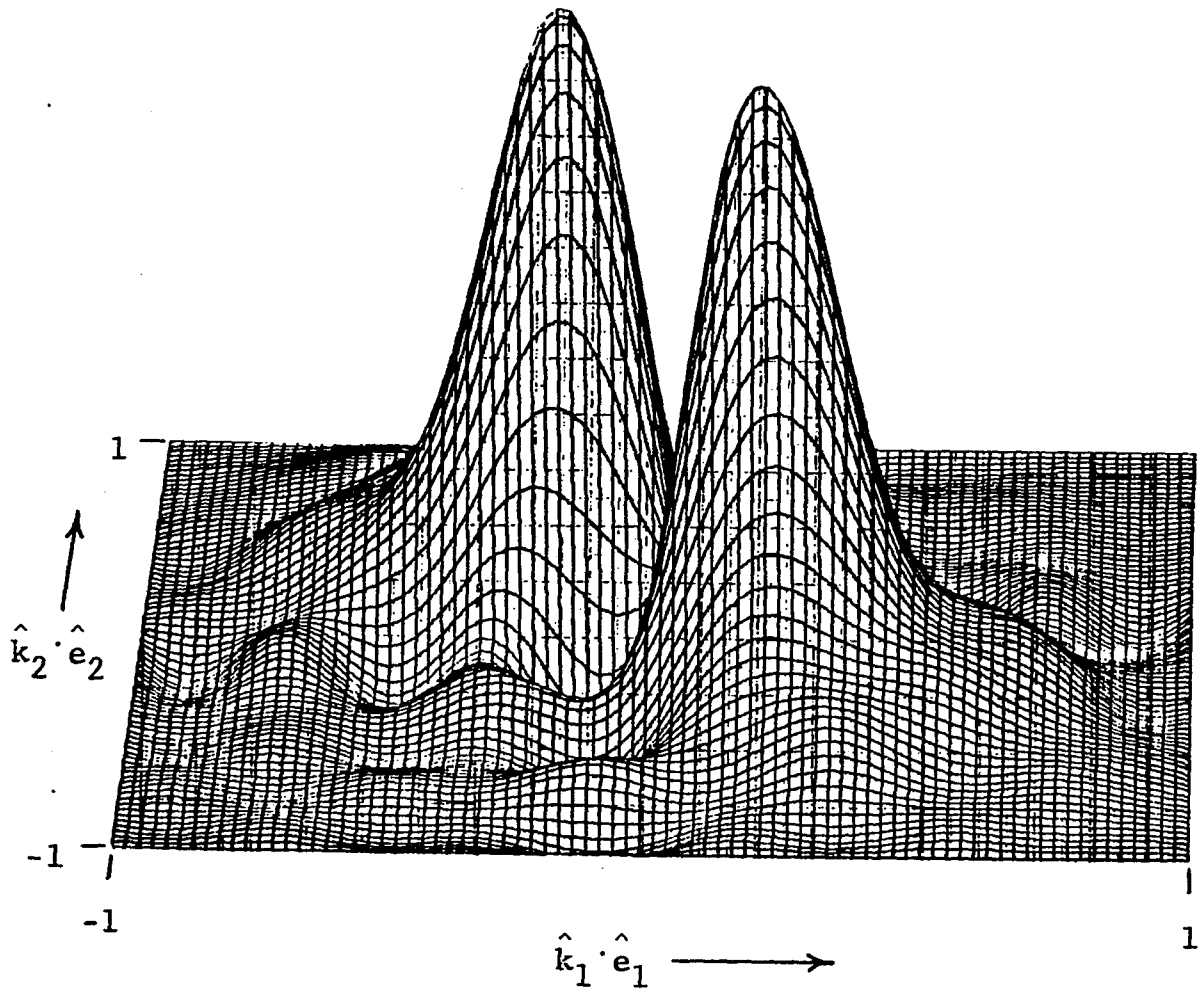

Figure 7.11. Density of two-hit chattering collisions on the surface of the ellipse

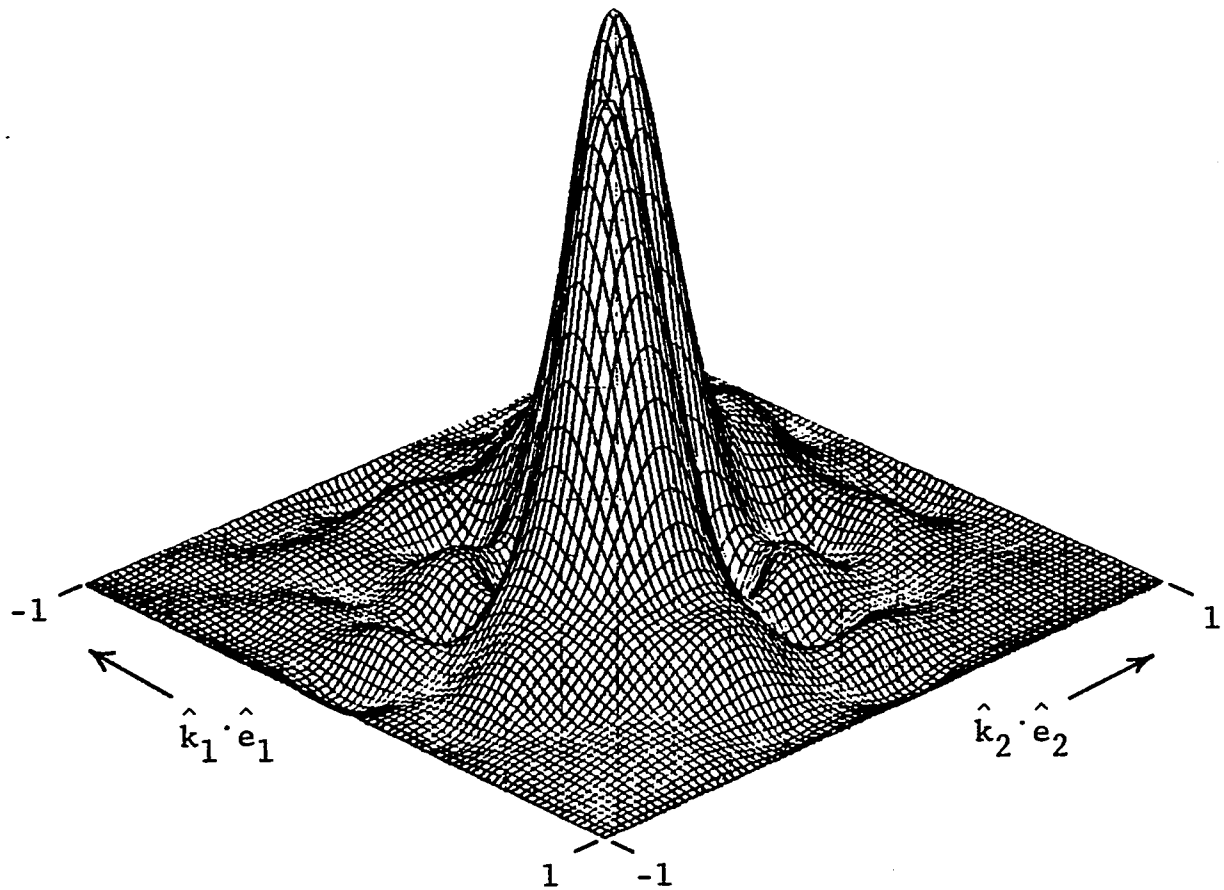

Figure 7.12. Density of two-hit chattering collisions on the surface of the ellipse

This condition probability is peaked at $\hat{k}_1 \cdot \hat{e}_1 \sim 0.25$ where its value is nearly 0.5 and drops off in the regions $\hat{k}_1 \cdot \hat{e}_1 \sim 0.05$ and 0.95.

Figure 7.9 is a plot of the "coordinates" of a representative sampling of the two hit chattering collisions. By "coordinates", we mean the values of $\hat{k} \cdot \hat{e}$ for the first $(\hat{k}_1 \cdot \hat{e}_1)$ and the second $(\hat{k}_2 \cdot \hat{e}_2)$ hits. From Fig. 7.9, it is obvious that, for the majority of two hit collisions, the values of $\hat{k}_1 \cdot \hat{e}_1$ and $\hat{k}_2 \cdot \hat{e}_2$ are of opposite sign. In other words, rarely do chattering collisions exist where both hits occur on the same end of the ellipse. Figures 7.10 through 7.12 are three dimensional representations of Fig. 7.9; the third dimension denoting the density of points.

Listed in Table 7.2 are the results of a statistical analysis of the density function plotted in Figs. 7.9 through 7.12. Expectation values, variances, standard deviations, covariances, and correlation coefficients are listed. The expectation value of the quantity x is defined by

$$E(x) = N^{-1} \sum_{i=1}^{N} x_i \tag{7.61}$$

where x_i is the value of x corresponding to the ith trajectory and N is the total number of trajectories. The variance, Var(x), and the standard deviation, $\sigma(x)$, of x are defined by

$$\mathrm{Var}(x) = E[(x - E(x))^2] \tag{7.62}$$

and

$$\sigma(x) = [\mathrm{Var}(x)]^{1/2} \quad . \tag{7.63}$$

Finally, the covariance, Cov(x,y), and correlation coefficient, $\rho(x,y)$, of the quantities x and y are given by

$$\mathrm{Cov}(x,y) = E[(x - E(x))(y - E(y))] \tag{7.64}$$

and

$$\rho(x,y) = \mathrm{Cov}(x,y)/\sigma(x)\sigma(y) \quad . \tag{7.65}$$

The final two entries in Table 7.2 are the expectation value and standard deviation of the quantity

$$\theta = \hat{k}_1 \times \hat{e}_1 \cdot \hat{k}_2/\sqrt{1 - (\hat{k}_1 \cdot \hat{e}_1)^2} \quad . \tag{7.66}$$

This quantity is an indication of how far out of plane are the vectors $\hat{k}_1$, $\hat{e}_1$, and $\hat{k}_2$. If, for example, $\rho(\theta)$ were equal to zero, all two hit chattering collisions would be planar (i.e., $\hat{k}_1$, $\hat{e}_1$, and $\hat{k}_2$ would lie in the same plane).

Our ultimate goal in studying chattering collisions is to improve the methods of calculating transport coefficients, or equivalently, bracket integrals. Table 7.3 is a list of the values of $\{\phi,\psi\}$, $[\phi,\psi]$, $\{\phi,\psi\} - [\phi,\psi]$, and $\{\phi,\psi\}_{(2)}$. Here, $\{\phi,\psi\}$, the exact bracket integral (cf. Eq. (7.45)), is evaluated via Monte Carlo techniques, as is the integral $\{\phi,\psi\}_{(2)}$. The Monte Carlo methods used here are discussed in detail in Ref. 89. The quantity $[\phi,\psi]$ is the simple collision bracket integral utilized in Chapters III through VI. In obtaining the results in Table 7.3, it was assumed that only two hit chattering events exist (this assumption being motivated by the results of Table 7.1). From

Table 7.3, it can be seen that the error made in neglecting chattering events is not uniform for the bracket integrals listed. For certain integrals (e.g., $\{\chi\chi; \chi\chi\}$), the error is negligible, whereas for others (e.g., $\{\gamma^2,\gamma^2\}$), the error is substantial. However, it is obvious that chattering events cannot be ignored if accurate calculation of the bracket integrals is desired. Furthermore, it is also obvious that consideration of only two hit chattering collisions is sufficient when calculating the bracket integrals.

In conclusion, the existence of chattering collisions should not be ignored for accurate calculation of transport coefficients. In fact, for the system studied here, approximately 25% of all collisions were chattering events. However, the majority of chattering collisions consist only of two hits and, therefore, it is sufficient to incorporate only two hit events into the calculation of the bracket integrals.

Table 7.1. A breakdown of the collisions

Collision Type	% of Total Collisions
1 hit	74.25
2 hits	24.62
3 hits	0.80
4 hits	0.20
5 or more hits	0.13

Table 7.2. Statistical analysis of two hit chattering collisions

Average	Value
$E(\hat{k}_1 \cdot \hat{e}_1)$	0.00
$E(\hat{k}_2 \cdot \hat{e}_2)$	-0.01
$E[\hat{k}_1 \cdot \hat{e}_1)^2]$	0.13
$E[(\hat{k}_2 \cdot \hat{e}_2)^2]$	0.12
$E[(\hat{k}_1 \cdot \hat{e}_1)(\hat{k}_2 \cdot \hat{e}_2)]$	-0.09
$\sigma(\hat{k}_1 \cdot \hat{e}_1)$	0.36
$\sigma(\hat{k}_2 \cdot \hat{e}_2)$	0.35
$Cov(\hat{k}_1 \cdot \hat{e}_1, \hat{k}_2 \cdot \hat{e}_2)$	-0.09
$\rho(\hat{k}_1 \cdot \hat{e}_1, \hat{k}_2 \cdot \hat{e}_2)$	-0.78
$E\left[\frac{\hat{k}_1 \times \hat{e}_1 \cdot \hat{k}_2}{\sqrt{1 - (\hat{k}_1 \hat{e}_1)^2}}\right]$	0.00
$\sigma\left[\frac{\hat{k}_1 \times \hat{e}_1 \cdot \hat{k}_2}{\sqrt{1 - (\hat{k}_i \cdot \hat{e}_i)^2}}\right]$	0.28

Table 7.3. Effects of chattering on various bracket integrals

$(\underset{,}{\xi}\ \circledcirc^n\ \underset{,}{\psi})$	$\{\underset{,}{\xi}\ \circledcirc^n\ \underset{,}{\psi}\}^a$ ($\AA^2$)	$[\underset{,}{\xi}\ \circledcirc^n\ \underset{,}{\psi}]$ ($\AA^2$)	Diff.[b] ($\AA^2$)	$\{\underset{,}{\xi}\ \circledcirc^n\ \underset{,}{\psi}\}_{(2)}$ ($\AA^2$)
$(\underset{,}{\Omega};\ \underset{,}{\Omega})$	82.04 ± 0.44	122.7	-40.66 ± 0.44	-40.09 ± 0.42
$(\underset{,}{\gamma};\ \underset{,}{\gamma})$	112.84 ± 0.57	92.4	20.44 ± 0.57	18.85 ± 0.18
$(\underset{,}{\gamma}\cdot\underset{,}{\Omega},\ \underset{,}{\gamma}\cdot\underset{,}{\Omega})$	103.00 ± 0.84	100.9	2.1 ± 0.84	1.54 ± 0.21
$(\underset{,}{\gamma\Omega};\ \underset{,}{\gamma\Omega})$	89.84 ± 0.69	100.9	-11.06 ± 0.69	-11.78 ± 0.33
$(\underset{,}{\gamma\Omega};\ \underset{,}{\Omega\gamma})$	166.26 ± 1.02	194.4	-28.14 ± 1.02	-28.29 ± 0.48
$(\gamma^2,\ \Omega^2)$	-27.26 ± 0.87	-82.1	54.84 ± 0.87	55.17 ± 0.80
$(\Omega^2,\ \gamma^2)$	-25.22 ± 0.65	-82.1	56.88 ± 0.65	55.16 ± 0.80
$(\gamma^2,\ \gamma^2)$	27.28 ± 0.87	82.1	-54.82 ± 0.87	-55.15 ± 0.80
$(\Omega^2,\ \Omega^2)$	25.23 ± 0.65	82.1	-56.87 ± 0.65	-55.17 ± 0.80
$(\underset{,}{\gamma\gamma};\ \underset{,}{\gamma\gamma})$	264.25 ± 1.99	266.9	-2.65 ± 1.99	-3.96 ± 0.50
$(\underset{,}{\gamma};\ \underset{,}{\gamma}\gamma^2)$	324.23 ± 2.77	256.7	67.53 ± 2.77	62.76 ± 0.93
$(\gamma^2\underset{,}{\gamma};\ \underset{,}{\gamma})$	324.20 ± 2.69	256.7	67.50 ± 2.69	63.04 ± 0.95
$(\underset{,}{\gamma};\ \underset{,}{\gamma}\Omega^2)$	125.42 ± 1.03	112.9	12.52 ± 1.03	12.19 ± 0.39
$(\Omega^2\underset{,}{\gamma};\ \underset{,}{\gamma})$	125.45 ± 0.96	112.9	12.55 ± 0.96	11.91 ± 0.37
$(\Omega^2\underset{,}{\gamma};\gamma\underset{,}{\Omega}^{\ 2})$	295.71 ± 3.55	352.6	-56.89 ± 3.55	-51.25 ± 1.45
$(\gamma^2\underset{,}{\gamma};\ \underset{,}{\gamma}\gamma^2)$	1282.99 ± 17.70	1071.2	211.79 ± 17.70	199.23 ± 5.23
$(\underset{,}{\Omega\Omega};\ \underset{,}{\Omega\Omega})$	114.72 ± 1.13	204.9	-90.18 ± 1.13	-87.65 ± 1.19
$(\gamma^2\underset{,}{\gamma};\ \underset{,}{\gamma}\Omega^2)$	330.53 ± 4.82	212.0	118.53 ± 4.82	113.41 ± 3.17
$(\Omega^2\underset{,}{\gamma};\ \underset{,}{\gamma}\gamma^2)$	328.01 ± 4.54	212.0	116.01 ± 4.54	109.55 ± 2.94

[a] Numerical values actually represent the bracket integral divided by $(2kT/\mu)^{1/2}$.

[b] Diff. equals $\{\underset{,}{\xi}\ \circledcirc^n\ \underset{,}{\psi}\} - [\underset{,}{\xi}\ \circledcirc^n\ \underset{,}{\psi}]$.

Table 7.3. Continued

$(\underline{\xi}, \odot^n \underline{\psi})$	$\{\underline{\xi}, \odot^n \underline{\psi}\}^a$ ($\mathring{A}^2$)	$[\underline{\xi}, \odot^n \underline{\psi}]$ ($\mathring{A}^2$)	Diff.[b] ($\mathring{A}^2$)	$\{\underline{\xi}, \odot^n \underline{\psi}\}_{(2)}$ ($\mathring{A}^2$)
$(\underline{\Omega}; \gamma)$	-0.05 ± 0.30	0	-0.50 ± 0.30	0.07 ± 0.09
$(\underline{\gamma}; \underline{\Omega})$	-0.87 ± 0.30	0	-0.87 ± 0.30	-0.10 ± 0.09
$(\underline{\gamma}^0\underline{\gamma}; \underline{\gamma}^0\underline{\gamma})$	255.16 ± 2.28	239.53	15.63 ± 2.28	14.42 ± 0.77
$(\underline{\Omega}^0\underline{\Omega}; \underline{\Omega}^0\underline{\Omega})$	106.31 ± 1.35	177.53	-71.22 ± 1.35	-69.26 ± 1.46

VIII. LITERATURE CITED

1. Boltzmann, L. Sitzungsber. Kaiserl. Akad. Wiss. 1982, 66(2), 275.

2. Chapman, S. Phil. Trans. R. Soc. A 1912, 213, 433; Chapman, S. Phil. Trans. R. Soc. A 1916, 216, 279; Chapman, S. Proc. R. Soc. A 1916, 98, 1.

3. Enskog, D. Phys. Zeit. 1911, 12, 56; Enskog, D. Phys. Zeit. 1911, 12, 533; Enskog, D. Annln. Phys. 1912, 38, 731; Enskog, D. Inaugural Dissertation, Uppsala (Sweden), 1917.

4. Chapman, S.; Cowling, T. G. "The Mathematical Theory of Non-Uniform Gases", 3rd ed.; Cambridge University Press: London, 1970.

5. Hirshfelder, J.; Curtiss, C; Bird, R. "Molecular Theory of Gases and Liquids", 1st ed.; Wiley: New York, 1954.

6. Enskog, D. K. Svensk. Vet.-Akad. Handl. 1921, 63, 4.

7. Curtiss, C. F. J. Chem. Phys. 1956, 24, 225; Curtiss, C. F.; Muckenfuss, C. J. Chem. Phys. 1957, 26, 1619; Curtiss, C. F.; Muchenfuss, C. J. Chem. Phys. 1958, 29, 1257.

8. Curtiss, C. F.; Dahler, J. S. J. Chem. Phys. 1963, 38, 2352.

9. Dahler, J. S.; Sather, N. F. J. Chem. Phys. 1961, 35, 1029; Dahler, J. S.; Sather, N. F. J. Chem. Phys. 1962, 38, 2363; Sandler, S. I.; Dahler, J. S. J. Chem. Phys. 1965, 43, 1750; Sandler, S. I.; Dahler, J. S. J. Chem. Phys. 1967, 47, 2621.

10. McCoy, B. J.; Sandler, S. I.; Dahler, J. S J. Chem. Phys. 1966, 45, 3485.

11. Hoffman, D. K. J. Chem. Phys. 1969, 50, 4823.

12. Klein, W. M.; Dahler, J. S.; Cooper, E.; Hoffman, D. K. J. Chem. Phys. 1970, 52, 4752; Cooper, E. R.; Hoffman, D. K. J. Chem. Phys. 1971, 55, 1016; Cooper, E. R.; Hoffman, D. K. J. Chem. Phys. 1973, 58, 3226.

13. Verlin, J. D.; Cooper, E. R.; Hoffman, D. K. J. Chem. Phys. 1971, 56, 3740.

14. Matzen, M. K.; Hoffman, D. C.; Dahler, J. S. J. Chem. Phys. 1972, 56, 1486; Matzen, M. K.; Hoffman, D. K. J. Chem. Phys. 1975, 62, 500; Matzen, M. K.; Hoffman, D. K. J. Chem. Phys. 1975, 62, 509.

15. Cooper, E. R.; Dahler, J. S.; Verlin, J. D.; Matzen, M. K.; Hoffman, D. K. J. Chem. Phys. 1973, 59, 403.

16. Dahler, J. S.; Theodosopulu, M. J. Chem. Phys. 1974, 60, 3567; Dahler, J. S.; Theodosopulu, M. J. Chem. Phys. 1974, 60, 4048.

17. Bogoliubov, N. N. In "Studies in Statistical Mechanics", 1st ed.; Uhlenbeck, G. E.; de Boer, J., Eds.; North Holland: Amsterdam, 1962; Vol. I, Part A.

18. Born, M.; Green, H. S. "A General Kinetic Theory of Fluids", 1st ed.; Cambridge University Press: Cambridge, 1952.

19. Kirkwood, J. G. J. Chem. Phys. 1946, 14, 180; Kirkwood, J. G. J. Chem. Phys. 1947, 15, 72.

20. Yvon, J. "La Theorie des fluides et de l'equation d'etat", 1st ed.; Hermann et Cie: Paris, 1935.

21. Cooper, E. R. Ph.D. Dissertation, Iowa State University, Ames, Iowa, 1972.

22. Cohen, E. G. D. Physica 1962, 28, 1025; Cohen, E. G. D. Physica 1962, 28, 1060.

23. Uhlenbeck, G. E.; Ford, G. W. In "Studies in Statistical Mechanics", 1st ed.; Uhlenbeck, G. E.; de Boer, J., Eds.; North Holland: Amsterdam, 1961; Vol. I, Part B.

24. Barajas, L.; Garcia-Colin, L. S.; Pina, E. J. Stat. Phys. 1973, 7, 161.

25. Van Beijeren, H.; Ernst, M. H. Physica 1973, 68, 437.

26. Morita, T.; Hiroike, K. Prog. Theor. Phys. 1960, 23, 385; Morita, T.; Hiroike, K. Prog. Theor. Phys. 1960, 23, 1003; Stell, G. In "The Equilibrium Theory of Classical Fluids", 1st ed.; Frisch, H. L.; Lebowitz, J. L., Eds.; W. A. Benjamin: New York, 1964; Chapter 2.

27. Van Beijeren, H.; Ernst, M. H. Physica 1973, 70, 225.

28. Ferziger, J. H.; Kaper, H. G. "Mathematical Theory of Transport Processes in Gases", 1st ed.; North Holland: Amsterdam, 1972.

29. Resibois, P.; De Leener, M. "Classical Kinetic Theory of Fluids", 1st ed.; John Wiley and Sons: New York, 1977.

30. Hoffman, D. K.; Dahler, J. S. J. Stat. Phys. 1969, 1, 521.

31. Grad. H. Commun. Pure Appl. Maths. 1949, 2, 331; Grad, H. Commun. Pure Appl. Maths. 1952, 5, 257.

32. For convenience, we have chosen $\underline{R}$ to equal 1/2 $\underline{\xi}_{12}$, although this is not necessary in principle. For the applications discussed in this work, the definition of $\underline{R}$ is academic, because we will only consider dense fluids of uniform density.

33. Hilbert, D. Math. Annalen. 1912, 72, 567.

34. See, e.g., Courant, R.; Hilbert, D. "Methods in Mathematical Physics", 2nd ed.; McGraw-Hill: New York, 1953.

35. The orthogonality of two functions, ψ and ϕ, is defined using the inner product

$$\langle\psi,\phi\rangle = n^{-1} \int d\underline{1} f_0^{(1)} \psi^* \phi \quad ;$$

the condition for orthogonality being $\langle\psi,\phi\rangle = 0$.

36. Typically the expansion set consists of Cartesian tensors and Sonine (or related) polynomials in the momentum variables (cf. Eq. (3.10)).

37. In practice, these matrix equations are solved using a nonsphericity expansion discussed in Refs. 38 and 39.

38. Cooper, E. R.; Hoffman, D. K. J. Chem. Phys. 1970, 54, 233.

39. Matzen, M. K. Ph.D. Dissertation, Iowa State University, Ames, Iowa, 1974.

40. Senftleben, H. Phys. Zeit. 1930, 31, 931.

41. Troutz, M.; Froschel, E. Ann. Phys. 1935, 22, 223.

42. Torwegge, H. Ann. Phys. 1938, 33, 459.

43. Beenakker, J. J. M.; Scoles, G.; Knaap, H. F. P.; Jonkman, R. M. Phys. Letts. 1962, 2, 5.

44. Gorter, C. J. Naturwissenschaften 1938, 26, 140.

45. Beenakker, J. J. M.; McCourt, F. R. Ann. Rev. Phys. Chem. 1970, 21, 47; Moraal, H. Phys. Rep. 1975, 17, 225.

46. Wang Chang, C. S.; Uhlenbeck, G. E. Ann Arbor, Michigan, 1951, University of Michigan Eng. Res. Inst. Report CM-681.

47. Coope, J. A. R.; Snider, R. F. J. Math. Phys. 1970, 11, 1003.

48. Townes, C. H.; Schawlow, A. L. "Microwave Spectroscopy", 1st ed.; McGraw-Hill: New York, 1955.

49. Thijsse, B. Ph.D. Dissertation, University of Leiden, Leiden (Netherlands), 1978.

50. Hermans, L. J. F.; Koks, J. M.; Hengeveld, A. F.; Knaap, H. F. P. Physica 1970, 50, 410.

51. Hermans, L. J. F.; Schutte, A.; Knaap, H. F. P.; Beenakker, J. J. M. Physica 1970, 46, 491.

52. Van Ditzhuyzen, P. G. Ph.D. Dissertation, University of Leiden, Leiden (Netherlands), 1976.

53. Curie, P. "Oeuvres de Pierre Curie", 1st ed.; Gauthier-Villars, Imprimeur-Libraire: Paris, 1908.

54. de Groot, S. R.; Mazur, P. "Non-Equilibrium Thermodynamics", 1st ed.; North Holland: Amsterdam, 1962; Chapter 3.

55. Onsager, L. Phys. Rev. 1931, 37, 405; Onsager, L. Phys. Rev. 1931, 38, 2265.

56. Casimir, H. B. G. Rev. Mod. Phys. 1945, 17, 102.

57. Weast, R. C., Ed. "Handbook of Chemistry and Physics", 56th ed.; CRC Press: Cleveland, 1975.

58. Evans, G. T.; Cole, R. G.; Hoffman, D. K. J. Chem. Phys. 1982, 77, 3209.

59. Debye, P. "Polar Molecules", 1st ed.; Dover Publications, Inc.: New York, 1929.

60. Perrin, F. J. Phys. Radium 1934, 5, 497; Perrin, F. J. Phys. Radium 1936, 7, 1.

61. Hu, C. M.; Zwanzig, R. J. Chem. Phys. 1974, 60, 4354; Youngren, G. K.: Acrivos, A. J. Chem. Phys. 1975, 63, 3846.

62. Chandler, D. J. Chem. Phys. 1974, 60, 3508.

63. Mori, H. Prog. Theor. Phys. 1965, 33, 423.

64. Kivelson, D.; Keyes, T. J. Chem. Phys. 1972, 57, 4599.

65. Cooper, E. R.; Hoffman, D. K. J. Chem. Phys. 1970, 53, 1100.

66. Hubbard, P. S. Phys. Rev. 1963, 131, 1155.

67. Carnahan, N. F.; Starling, K. E. J. Chem. Phys. 1969, 51, 635.

68. Cummings, P.; Nezbeda, I.; Smith, W. R.; Morisson, G. Molec. Phys. 1981, 43, 1471.

69. Steinhauser, O. Chem. Phys. Lett. 1981, 82, 153.

70. Battaglia, M. R.; Madden, P. A. Molec. Phys. 1978, 36, 1601.

71. Vold, R. R.; Vold, R. L.; Szevenyi, N. M. J. Chem. Phys. 1979, 70, 5213.

72. Barojas, J.; Levesque, D.; Quentrec, B. Phys. Rev. A 1973, 7, 1092.

73. Allen, M. P.; Kivelson, D. Molec. Phys. (in press).

74. Rebertus, D. W.; Sando, K. M. J. Chem. Phys. 1977, 47, 2585.

75. Chu, B. "Laser Light Scattering", 1st ed.; Academic Press: New York, 1977.

76. Berne, B. J.; Pecora, R. "Dynamic Light Scattering", 1st ed.; John Wiley and Sons: New York, 1976.

77. Tsay, S.-J.; Kivelson, D. Molec. Phys. 1975, 29, 1.

78. Stegeman, G. I. A.; Stoicheff, B. P. Phys. Rev. Lett. 1968, 21, 202; Stegeman, G. I. A.; Stoicheff, B. P. Phys. Rev. A 1973, 7, 1160.

79. Keyes, T.; Kivelson, D. J. Chem. Phys. 1971, 54, 1786; Keyes, T.; Kivelson, D. J. Chem. Phys. 1971, 55, 986.

80. For an up-to-date overview of the theory and experimental results for R, see Kivelson, D.; Madden, P. A. Ann. Rev. Phys. Chem. 1980, 31, 523.

81. Kivelson, D.; Hallum, R. Molec. Phys. 1979, 38, 1411.

82. Calef, D. F.; Wolynes, P. G. J. Chem. Phys. 1980, 72, 535.

83. Ernst, M. H.; Dorfman, J. R.; Cohen, E. G. D. Physica 1965, 31, 493; Ernst, M. H. Physica 1966, 32, 209; Ernst, M. H. Physica 1966, 32, 273.

84. Andersen, H. C.; Pecora, R. J. Chem. Phys. 1971, 54, 2584.

85. Dorfman, J. R.; Van Beijeren, H. In "Modern Theoretical Chemistry Series", 1st ed.; Berne, B. J., Ed.; Plenum: New York, 1977; Vol. 6, Part B.

86. Searly, G. M.; Bezot, P.; Sixou, P. J. Chem. Phys. 1976, 64, 1485.

87. Enright, G.; Stoicheff, B. P. J. Chem. Phys. 1974, 60, 2536.

88. Alms, G. R.; Gierke, T. D.; Patterson, G. D. J. Chem. Phys. 1977, 67, 5779.

89. Evans, D. R. Ph.D. Dissertation, Iowa State University, Ames, Iowa, 1981.

90. Ernst, M. H.; Dorfman, J. R.; Hoegy, W. R.; Van Leeuwen, J. M. J. Physica 1969, 45, 127.

91. Van Leeuwen, J. M. J.; Weyland, A. Physica 1967, 36, 457; Van Leeuwen, J. M. J ; Weyland, A. Physica 1968, 39, 35.

92. Hoegy, W. R. Ph.D. Dissertation, University of Michigan, Ann Arbor, Michigan, 1967.

93. Haines, L. K.; Dorfman, J. R.; Ernst, M. H. Phys. Rev. 1966, 144, 207.

94. Haines, L. K. Ph.D. Dissertation, University of Maryland, College Park, Maryland, 1966.

95. Sengers, J. V.; Cohen, E. G. D. Physica 1961, 27, 230.

96. Sengers, J. V. Phys. Fluids 1966, 9, 1333; Sengers, J. V. Phys. Fluids 1966, 9, 1685.

97. Choh, S. T. Ph.D. Dissertation, University of Michigan, Ann Arbor, Michigan, 1958.

98. Hollinger, H. B.; Curtiss, C. F. J. Chem. Phys. 1960, 33, 1386.

99. Green, M. S. J. Chem. Phys. 1951, 19, 1036.

100. Kubo, R. J. Phys. Soc. Japan 1957, 12, 570.

101. Evans, D. J.; Strett, W. B. Molec. Phys. 1978, 36, 161.

IX. ACKNOWLEDGMENTS

It is very difficult for me to know where to begin, because so many people have aided me during my graduate studies. First, I have enjoyed the company of all members of the research group, including Nick Wolf, Dave Burgess, and Ross Nord. To Chi-Keung Chan, I thank him for all his aid, especially after my departure; thank goodness he knew not for what he volunteered. Thanks to the Evans trio: To Dave Evans, for his helpful discussions relating to Chapters II through IV and for providing me with his trajectory programs used in the numerical work in Chapter VII. To Jim Evans, who was always open to and patient of my constant questioning. To Glenn Evans, who introduced me to the problems discussed in Chapters V and VI, who carried out a large part of the work in these two chapters, and more importantly who showed an interest in my future. And to my major professor, David Hoffman, I thank now for all his help, past, present, and future; I cannot think of a person with whom I would have enjoyed working for more than I did with him.

Finally, it is not difficult to know where to end this acknowledgment. To my wife, Melanie, who endured much more than anyone should be expected to tolerate, thank you with all my love.

X. APPENDIX A: REDUCTION OF THE BRACKET AND LAMBDA INTEGRALS

The first section of this appendix presents an outline of the procedure for carrying out the momentum integrations in the bracket integrals as developed by Hoffman (11). The second section presents a reduction of the lambda integrals, defined in Chapter VI, to a form similar to the bracket integrals.

A. Bracket Integrals

The collision, or bracket, integral of two functions ξ and ψ is defined by

$$[\xi,\psi]^{1j}_{\mu\nu} = -\frac{1}{n_\mu n_\nu}\int d\underline{1}_\mu f_0^{(1)}\xi\hat{K}\psi \tag{10.1}$$

where $\hat{K}$ represents either the Enskog or the Boltzmann collision operator defined by Eq. (2.54). Using the explicit form for $\hat{K}$ in Eq. (10.1), we obtain

$$[\xi,\psi]^{1j}_{\mu\nu} = -\frac{1}{n_\mu n_\nu}\int d\underline{1}_\mu d\underline{2}_\nu \times \Big[\int_{\hat{k}\cdot\underline{g}<0} d\hat{k}S_{\mu\nu}\chi_{\mu\nu}\hat{k}\cdot\underline{g}f^{(1)}_{\mu,0}f^{(1)}_{\nu,0}\xi(1)\psi(j) + \int_{\hat{k}\cdot\underline{g}>0} d\hat{k}S_{\mu\nu}\chi_{\mu\nu}\hat{k}\cdot\underline{g}f^{(1)}_{\mu,0}f^{(1)}_{\nu,0}\xi(1)\psi(j')\Big] \quad , \tag{10.2}$$

where μ and ν refer to species types, j equals either 1 or 2, the primes refer to the precollisional state, and the remaining functions are defined in Chapter II. Inserting the explicit forms for the $f_0^{(1)}$'s (which are local Maxwellians normalized to the local number density) and transforming to the dimensionless relative and center of mass momenta

$$\underline{\gamma} = \sqrt{\frac{\mu_{\mu\nu}}{m_\nu}}\ \underline{W}_\nu - \sqrt{\frac{\mu_{\mu\nu}}{m_\mu}}\ \underline{W}_\mu \tag{10.3a}$$

and

$$\underline{\Gamma} = \sqrt{\frac{\mu_{\mu\nu}}{m_\mu}}\ \underline{W}_\nu + \sqrt{\frac{\mu_{\mu\nu}}{m_\nu}}\ \underline{W}_\mu \quad , \tag{10.3b}$$

respectively, the bracket integral becomes

$$[\xi,\psi]^{1j}_{\mu\nu} = -B^{(n)} \int \hat{de}_\mu \hat{de}_\nu \times d\underline{\gamma} d\underline{\Gamma} \exp-[\gamma^2 + \Gamma^2 + \Omega_\mu^2 + \Omega_\nu^2]$$
$$\times \left[\int_{\hat{k}\cdot\underline{g}<0} d\hat{k} S_{\mu\nu} \chi_{\mu\nu} \hat{k} \cdot \underline{g} \xi(1)\psi(j) \right.$$
$$\left. + \int_{\hat{k}\cdot\underline{g}>0} d\hat{k} S_{\mu\nu} \chi_{\mu\nu} \hat{k} \cdot \underline{g} \xi(1)\psi(j') \right] \quad . \tag{10.4}$$

Here, $\underline{W}$ and $\underline{\Omega}$ are the linear and angular momentum, respectively, and n denotes the number of active degrees of freedom for the collisional pair. For the atom-diatom system, n = 8 and $B^{(8)} = 1/4\pi^5$, for the diatom-diatom system n = 10 and $B^{(10)} = 1/16\pi^7$, and for the general top-general top system, n = 12 and $B^{(12)} = 1/64\pi^{10}$. We now define an n-dimensional momentum vector, $\underline{\eta}$, with components

$$\underline{\eta} = [\underline{\Omega}_\mu, \underline{\Omega}_\nu, \underline{\Gamma}, \underline{\gamma}_\perp, \gamma_\parallel] \tag{10.5}$$

where $\gamma_\parallel$ is $\hat{k} \cdot \underline{\gamma}$ and $\underline{\gamma}_\perp$ is $\underline{\gamma} - \gamma_\parallel \hat{k}$. In terms of the generalized momentum vector $\underline{\eta}$, the bracket integral becomes

$$[\xi,\psi]^{1j}_{\mu\nu} = -B^{(n)} \int d\hat{e}_\mu d\hat{e}_\nu d\underline{\eta} e^{-\eta^2} \times \left[\int_{\hat{k}\cdot\underline{g}<0} d\hat{k} S_{\mu\nu}\chi_{\mu\nu}\hat{k}\cdot\underline{g}\xi_1\psi_j \right.$$

$$\left. + \int_{\hat{k}\cdot\underline{g}>0} d\hat{k} S_{\mu\nu}\chi_{\mu\nu}\hat{k}\cdot\underline{g}\xi_1\psi_j' \right] \quad . \tag{10.6}$$

Now, $\hat{k}\cdot\underline{g}$ can be expressed as

$$\hat{k}\cdot\underline{g} = \sqrt{2kT/\mu_{\mu\nu}}\,[\gamma_\parallel - \underline{a}_\mu\cdot\underline{\Omega}_\mu - a_\nu\cdot\underline{\Omega}_\nu] \quad , \tag{10.7}$$

where $\underline{a}_i = \sqrt{\mu_{\mu\nu}/I}\;\underline{\xi}_i \times \hat{k}$. Since Eq. (10.7) is linear in the components of $\underline{\eta}$, there exists a unit vector $\hat{\varepsilon}$ in the n-dimensional momentum space such that

$$\sqrt{2kT/\mu_{\mu\nu}}\; D_{\mu\nu}\varepsilon\cdot\underline{\eta} = \hat{k}\cdot\underline{g} \quad . \tag{10.8}$$

This unit vector is

$$\hat{\varepsilon} = D^{-1}_{\mu\nu}[-\underline{a}_\mu, -\underline{a}_\nu, 0, 0, 1] \tag{10.9}$$

where

$$D^2_{\mu\nu} = 1 + \underline{a}_\mu\cdot\underline{a}_\mu + \underline{a}_\nu\cdot\underline{a}_\nu \quad . \tag{10.10}$$

At this point, we introduce an orthogonal matrix $\underline{\underline{\delta}}$, defined by

$$\underline{E} = \underline{\underline{\delta}}^\dagger\cdot\underline{\eta} \quad , \tag{10.11}$$

where $\underline{E}$ represents the generalized momentum vector expressed in the new coordinate frame which has $\hat{\varepsilon}_n$ as the nth unit vector (i.e., $\varepsilon_n = \hat{\varepsilon}\cdot\underline{\eta}$). The collision dynamics in the rotated frame assumes the simple form (11)

$$\varepsilon_n' = -\varepsilon_n \tag{10.12a}$$

and

$$\underline{E}_{\perp}' = \underline{E}_{\perp} \quad , \tag{10.12b}$$

where $\underline{E}_{\perp}$ is the part of $\underline{E}$ perpendicular to $\hat{\varepsilon}_n$. Transforming to the new coordinate frame allows us to write the bracket integrals as

$$[\xi,\psi]^{1j}_{\mu\nu} = \sqrt{\frac{2kT}{\mu_{\mu\nu}}}\, B^{(n)} \int d\hat{k} d\hat{e}_\mu d\hat{e}_\nu \times S_{\mu\nu}\chi_{\mu\nu}D_{\mu\nu}\underline{\underline{S}}_{\xi_1}\underline{\underline{S}}_{\psi_j}\, \circledcirc_n^{u+v}(\underline{u},\underline{v}) \tag{10.13}$$

where

$$(u,v) = -\int_{\varepsilon_n<0} d\underline{E}\, e^{-E^2}\, \varepsilon_n \underline{E}^u \underline{E}^v - \int_{\varepsilon_n>0} d\underline{E}\, e^{-E^2}\, \varepsilon_n \underline{E}^u \underline{E}'^v \quad . \tag{10.14}$$

Here, the symbol $\circledcirc_n^m$ denotes a sequential contraction of the m indices in the n-dimensional space, and $\underline{\underline{S}}_{\xi(\psi)}$ represents a projection operator (dependent on orientational variables alone) which projects from the polyad $\underline{E}^u$ ($\underline{E}^v$) the quantity ξ (ψ) where u and v represent the tensor rank of the momentum variables in ξ and ψ, respectively. For example, $\underline{\underline{S}}_{\underline{W}_i^0\underline{W}_i}$ is

$$\underline{\underline{S}}_{\underline{W}_i^0\underline{W}_i} = \underline{\underline{S}}^{\,0}_{\underline{W}_i}\,\underline{\underline{S}}_{\underline{W}_i} \tag{10.15}$$

where

$$\underline{\underline{S}}_{\underline{W}_i} = \begin{pmatrix} 0 & | & 0 \\ \hline & | & \\ 0 & | & \underline{\underline{U}}^{(3)} \end{pmatrix} \circledcirc'^{\Delta}_{n\equiv} \quad . \tag{10.16}$$

The momentum integrations in Eq. (10.14) can now be carried out yielding

tensor functions of rank u + v. The tensor functions thus obtained are dependent on the orientation variables $\hat{k}$, $\hat{e}_\mu$, and $\hat{e}_\nu$ through the quantity $\hat{\varepsilon}_n$. For example, the $(\underline{1},\underline{1})$ integral equals

$$(\underline{1},\underline{1}) = \pi^{1/2(n-1)}\hat{\varepsilon}_n\hat{\varepsilon}_n \quad . \tag{10.17}$$

Therefore, the momentum integrations in the bracket integrals can be carried out analytically. The remaining integrations in Eq. (10.13) are simple orientation integrals which can be evaluated using simple numerical quadratures.

B. Lambda Integrals

The lambda integrals defined in Chapter VI are given by

$$\lambda_V(\underline{\underline{\psi}}) = (5VnkT)^{-1} \int d\underline{x}_1 d\underline{x}_2 \chi \times f_0^{(1)} f_0^{(1)} \overset{0}{\underline{\underline{g}}}_{V,12} : (\underline{\underline{\psi}}^*(\underline{x}_1) + \underline{\underline{\psi}}^*(\underline{x}_2)) \tag{10.18}$$

For our purposes, we choose to deal with the integral

$$I = \int d\underline{x}_1 d\underline{x}_2 \chi f_0^{(1)} f_0^{(1)} \underline{\underline{G}}(\underline{x}_1,\underline{x}_2) : \overset{0}{\underline{\underline{g}}}_{V,12} \tag{10.19}$$

instead, which equals $\lambda_V(\underset{0}{\underline{\underline{\psi}}})$ when the appropriate $\underline{\underline{G}}$ function is inserted into this integral. Here, $\underline{\underline{g}}_{V,12}$ is related to the potential part of the stress tensor (cf. Eq. (6.7)). Furthermore, we will confine our discussion to the case of two identical colliding particles. A detailed discussion of the techniques used in this section may be found in Ref. 8 (see also Chapter II).

First, the following form for $\underline{\underline{G}}^{0}_{V,12}$

$$\underline{\underline{G}}^{0}_{V,12} = \frac{1}{4}\,\underline{r}^{o}_{12}\{iL_V^{(2)}(\underline{p}_2 - \underline{p}_1)\} \quad , \tag{10.20}$$

where $L_V^{(2)}$ is the interacting part of the two particle Liouville operator, is inserted into Eq. (10.19). The resulting expression is then rewritten as

$$I = \lim_{\varepsilon\to 0_+} (8\varepsilon)^{-1} \int d\underline{x}_1 d\underline{x}_2 \chi f_0^{(1)} f_0^{(1)} \underline{\underline{G}}: \underline{r}^{o}_{12}\{(e^{iL^{(2)}\varepsilon} - e^{iL_0^{(2)}\varepsilon})$$

$$- (e^{-iL^{(2)}\varepsilon} - e^{-iL_0^{(2)}\varepsilon})\}(\underline{p}_2 - \underline{p}_1) \tag{10.21}$$

where, by definition, $L^{(2)} = L_0^{(2)} + L_V^{(2)}$. The operators $\exp \pm iL^{(2)}\varepsilon$ and $\exp \pm iL_0^{(2)}\varepsilon$ are the two particle interacting and noninteracting streaming operators, respectively. The +(-) sign refers to forward (backwards) streaming. Transforming the $\underline{r}_1$ and $\underline{r}_2$ integrations to the center of mass, $\underline{R}$, and relative, $\underline{r}_{12}$, variables defined by

$$\underline{R} = \frac{1}{2}(\underline{r}_1 + \underline{r}_2) \tag{10.22a}$$

and

$$\underline{r}_{12} = \underline{r}_2 - \underline{r}_1 \quad , \tag{10.22b}$$

and realizing that χ vanishes for overlapping configurations of particles one and two; the integral in Eq. (10.21) is conveniently written as

$$I = \lim_{0_+} (8\varepsilon)^{-1} \int d\underline{R}d\underline{1}d\underline{2}d\ell_{12} \times \{ \int_{\hat{k}\cdot g>0} dkS\chi f_0^{(1)} f_0^{(1)} \underline{\underline{G}}: \overset{\circ}{\underline{r}}_{12}$$

$$\times [(e^{iL^{(2)}\varepsilon} - e^{iL_0^{(2)}\varepsilon}) - (e^{-iL^{(2)}\varepsilon} - e^{iL_0^{(2)}\varepsilon})](\underline{p}_2 - \underline{p}_1)$$

$$+ \int_{\hat{k}\cdot\underline{g}<0} dk\hat{S}\chi f_0^{(1)} f_0^{(1)} \underline{\underline{G}}: \overset{\circ}{\underline{r}}_{12}[(e^{iL^{(2)}\varepsilon} - e^{iL_0^{(2)}\varepsilon})$$

$$- (e^{-iL^{(2)}\varepsilon} - e^{-iL_0^{(2)}\varepsilon})](\underline{p}_2 - \underline{p}_1)\} \quad . \tag{10.23}$$

Here, the variables ℓ_{12} and $\hat{k}$, and the S function are defined in Chapter II.

We are now in a position to carry out the ℓ_{12} integration. Because the action of the operators $L^{(2)}$ and $L_0^{(2)}$ differs only in the vicinity of the interaction, the only nonzero contribution to the ℓ_{12} integral is in the region $0 \leq \ell_{12} \leq |\dot{\ell}_{12}|\varepsilon$, for a vanishingly short time ε. On the postcollisional surface, i.e., $\dot{\ell}_{12} > 0$, the contribution of the forward streaming operators to the integral is zero; whereas the effect of the backward streaming operators in the region $0 \leq \ell_{12} \leq |\dot{\ell}_{12}|\varepsilon$ is

$$-(e^{-iL^{(2)}\varepsilon} - e^{-iL_0^{(2)}\varepsilon})(\underline{p}_2 - \underline{p}_1) = (\underline{p}_1^- - p_1^+) - (p_2^- - p_2^+) \quad , \tag{10.24}$$

where, in this region, $p_i^+ = \underline{p}_i$. The superscipt -(+) refers to the pre (post) collisional value. Similarly, on the precollisional surface, the action of the streaming operators is

$$(e^{iL^{(2)}\varepsilon} - e^{iL_0^{(2)}\varepsilon})(\underline{p}_2 - \underline{p}_1) = (\underline{p}_1^- - \underline{p}_1^+) - (\underline{p}_2^- - \underline{p}_2^+) \quad , \quad (10.25)$$

where, in this region, $\underline{p}_i^- = \underline{p}_i$. By using Eqs. (10.23) and (10.24), and the Mean Value Theorem of Calculus, Eq. (10.22) becomes

$$I = (1/8) \int d\underline{R}d\underline{1}d\underline{2}\{ \int_{\dot{\ell}>0} d\hat{k}S|\dot{\ell}|\chi f_0^{(1)} f_0^{(1)} \underline{\underline{G}}: \overset{o}{\underline{\xi}}_{12}[(\underline{p}_1^- - \underline{p}_1^+) - (\underline{p}_2^- - \underline{p}_2^+)]$$

$$+ \int_{\dot{\ell}<0} d\hat{k}S|\dot{\ell}|\chi f_0^{(1)} f_0^{(1)} \underline{\underline{G}}: \underline{\xi}_{12}[(p_1^- - \underline{p}_1^+) - (\underline{p}_2^- - \underline{p}_2^+)]\} \quad . \quad (10.26)$$

The pre and post collisional momenta are related through the relations

$$\underline{p}_i^- - \underline{p}_i^+ = \hat{k}_i K^+ = -\hat{k}_i K^- \quad , \quad i = 1, 2 \quad (10.27)$$

where

$$K^{\pm} = mD^{-2}\hat{k} \cdot \underline{g}^{\pm} \quad (10.28)$$

and $\hat{k}_i$ denotes the outward surface normal of the ith body at the point of contact. Equations (10.27) and (10.28) allow us to rewrite Eq. (10.26) as

$$I = \frac{m}{4} \int d\underline{R}d\underline{1}d\underline{2} \int dkS\chi f_0^{(1)} f_0^{(1)} (\hat{k} \cdot \underline{g})^2 D^{-2} \underline{\underline{G}}: \overset{o}{\underline{\xi}}_{12}\hat{k} \quad . \quad (10.29)$$

Therefore, the lambda integral is equal to

$$\lambda_V(\underline{\underline{\psi}}) = \frac{m}{20nkT} \int d\underline{1}d\underline{2} \int d\hat{k}S\chi f_0^{(1)} f_0^{(1)} (\hat{k} \cdot \underline{g})^2 D^{-2} \overset{o}{\underline{\xi}}_{12} k: (\underline{\underline{\psi}}^*(1) + \underline{\underline{\psi}}^*(2)) \quad (10.30)$$

where the trivial R integration has been carried out. Rewriting

Eq. (10.30) in the form

$$\lambda_V(\underline{\underline{\psi}}) = -\frac{nm}{20kT}\{-\frac{1}{n^2}\int d\underline{1}d\underline{2}d\hat{k}S\chi f_0^{(1)}f_0^{(1)}(\hat{k}\cdot\underline{g})D^{-2}\overset{\circ}{\underline{\underline{\xi}}}_{12}\hat{k}:\ (\underline{\underline{\psi}}^*(1)+\underline{\underline{\psi}}^*(2))\quad , \tag{10.31}$$

it becomes evident that the lambda integral is very similar to the standard kinetic theory bracket integrals for rigid convex molecules, Eq. (10.2). (The main difference between the two is the presence of an additional $\hat{k}\cdot\underline{g}$ term in the integrand of Eq. (10.31).) Therefore, we can reproduce step for step the method outlined in the previous section to evaluate the momentum integrations, with the result that

$$\lambda_V(\underline{\underline{\psi}}) = -(n/5)B^{(n)}\int d\hat{k}d\hat{e}_1d\hat{e}_2S\chi\overset{\circ}{\underline{\underline{\xi}}}_{12}k:\ \{(\underline{\underline{S}}_{\psi_1}+\underline{\underline{S}}_{\psi_2})\circledast_n^v[\underline{0},\underline{v}] \tag{10.32}$$

where

$$\begin{aligned}[\underline{u},\underline{v}] &= -\int_{\varepsilon_n>0} d\underline{E}\, e^{-E^2}\,\varepsilon_n^2[\underline{E}'^u+\underline{E}^u]\underline{E}'^v \\ &= -\frac{1}{2}\left(\frac{-1}{\sqrt{2}}\right)^{u+v}\pi^{(n-1)/2}\,\hat{P}_{(u,v)} \\ &\quad\times\sum_{j=0\ (\text{even})}^{u}\ \sum_{k=j\ (\text{even,odd})}^{v+j} 2^{k/2}(k+1)\left(\frac{k+1}{2}\right) \\ &\quad\times(\hat{\varepsilon}_n)^j\,\underline{\underline{J}}^{(n-1)}_{(u+v-k)}\,(\hat{\varepsilon}_n)^{k-j}\quad .\end{aligned} \tag{10.33}$$

Here, $\hat{P}_{(u,v)}$ denotes the permutation operator which forms the sums of all distinct permutations of the first u and the last v indices. We will only require $[\underline{0},\underline{0}]$, $[\underline{0},\underline{1}]$, and $[\underline{0},\underline{2}]$, which, from Eq. (10.33), are

$$[\underline{0},\underline{0}] = -\frac{1}{2}\pi^{n/2} \tag{10.34a}$$

$$[\underline{0},\underline{1}] = \pi^{(n-1)2}\,\hat{\varepsilon}_n \tag{10.34b}$$

and

$$[\underline{0},\underline{2}] = -\frac{1}{4}\pi^{n/2}\,\underline{\underline{U}}^{(n)} + 2\hat{\varepsilon}_n\hat{\varepsilon}_n \quad . \tag{10.34c}$$

With the above mentioned modifications, the lambda integrals can be evaluated in the same manner as the bracket integrals.

XI. APPENDIX B: MORI FORMALISM

In this appendix, we present a brief outline of the projection operator techniques developed by Mori. A more complete discussion of the following results are found in Refs. 63 and 76.

Mori's theory relies on the existence of distinct, well-separated, relaxation times in the fluid. For example, we know that the angular momentum of a highly anisotropic molecule in a dense medium relaxes on a much faster time scale than does its orientation (see the discussion of the parameter ε_ω in Chapter II). This separation of the angular momentum and orientational relaxation times is capitalized upon in Chapter V. Thus, the first task in the implementation of the Mori formalism is identification of the slowly relaxing dynamical quantities. Let A_i, i = 1 to n, represent the n slowly relaxing quantities in the fluid under consideration. For convenience, they will be written in vector form as

$$|\underline{A}\rangle = \begin{pmatrix} A_1 \\ A_2 \\ \cdot \\ \cdot \\ \cdot \\ A_n \end{pmatrix} \tag{11.1}$$

where $|\underline{A}\rangle$ represents a Dirac vector. Furthermore, we define the operators

$$P = |\underline{A}\rangle \cdot \langle\underline{A}|\underline{A}\rangle^{-1} \cdot \langle\underline{A}| \tag{11.2a}$$

and

$$Q = 1 - P \tag{11.2b}$$

where P projects Dirac vectors onto the subspace spanned by the slowly relaxing vectors and Q onto the rapidly relaxing subspace. With the aid of the above definitions, we can recast the equations of motion for $|\underline{A}\rangle$ into the form of a generalized Langevin equation.

The equation of motion for $|\underline{A}\rangle$ is

$$\frac{d}{dt}|\underline{A}(t)\rangle = iL^{(N)}|\underline{A}(t)\rangle \quad , \tag{11.3}$$

where

$$|\underline{A}(t)\rangle = e^{iL^{(N)}t}|\underline{A}(0)\rangle \quad ;$$
$$|\underline{A}(0)\rangle = |\underline{A}\rangle \quad . \tag{11.4}$$

Equation (11.2) is equivalent to Eq. (2.2) above. Using the definition of the projection operator, Eq. (11.3) becomes

$$\frac{d}{dt}|\underline{A}(t)\rangle = e^{iL^{(N)}t}\, iPL^{(N)}|\underline{A}\rangle + e^{iL^{(N)}t}\, iQL^{(N)}|\underline{A}\rangle$$
$$= |\underline{A}(t)\rangle \cdot i\underline{\underline{\Omega}}^{\dagger} + e^{iL^{(N)}t}\, iQL^{(N)}|\underline{A}\rangle \tag{11.5}$$

where the frequency matrix is

$$i\underline{\underline{\Omega}}^{\dagger} = \beta\underline{\underline{\chi}}^{-1} \cdot \langle\underline{A}|iL^{(N)}|\underline{A}\rangle \quad . \tag{11.6}$$

Here, the dagger denotes an Hermitian conjugate,

$$\underline{\underline{\chi}} = \langle\underline{A}|\underline{A}\rangle \tag{11.7}$$

is the static susceptibility, and $\beta = 1/kT$. The second term on the RHS of Eq. (11.5) can be rewritten, using the operator identity

$$e^{iL^{(N)}t} = e^{iQL^{(N)}t} + \int_0^t dt' \, e^{iL^{(N)}(t-t')} \, iPL^{(N)} \, e^{iQL^{(N)}t'} \quad , \tag{11.8}$$

in the form

$$e^{iL^{(N)}t} \, iQL^{(N)} |\underline{A}\rangle = - \int_0^t dt' |\underline{A}(t-t')\rangle \cdot \underline{\underline{K}}^{\dagger}(t') + |\underline{F}_p(t)\rangle \tag{11.9}$$

where

$$|\underline{F}\rangle = iQL^{(N)} |\underline{A}\rangle \tag{11.10}$$

and

$$\underline{\underline{K}}^{\dagger}(t) = \beta \underline{\underline{\chi}}^{-1} \cdot \langle \underline{F} | \underline{F}_p(t)\rangle \quad . \tag{11.11}$$

Here, the subscript, p, on the function indicates that the time evolution of that particular quantity is governed by the projected propagator $\exp iQL^{(N)}t$, i.e.,

$$|\underline{F}_p(t)\rangle = e^{iQL^{(N)}t} \, |\underline{F}\rangle \quad . \tag{11.12}$$

The ket $|\underline{F}_p(t)\rangle$ is the random fluxuating force. By definition $|\underline{F}_p(t)\rangle$ lies in the subspace spanned by the rapidly varying quantities. Using Eqs. (11.5) and (11.9), Eq. (11.3) becomes

$$\frac{d}{dt} |A(t)\rangle = |\underline{A}(t)\rangle \cdot i\underline{\underline{\Omega}}^{\dagger} - \int_0^t dt' |\underline{A}(t-t')\rangle \cdot \underline{\underline{K}}^{\dagger}(t') + |\underline{F}_p(t)\rangle \, . \tag{11.13}$$

This equation is the generalized Langevin equation.

Finally, from the expression for the time rate of change of $|\underline{A}\rangle$, we can obtain an equation of motion for the matrix of time correlation functions. Taking the Dirac product of Eq. (11.13) with $\langle\underline{A}|$, we obtain

$$\frac{d}{dt}\langle\underline{A}(t)|\underline{A}\rangle = i\underline{\underline{\Omega}} \cdot \langle\underline{A}(t)|\underline{A}\rangle - \int_0^t dt' \, \underline{\underline{K}}(t') \cdot \langle\underline{A}(t-t')|\underline{A}\rangle \quad . \quad (11.14)$$

The random force drops out of this expression because of its orthogonality to $\langle\underline{A}|$. Equation (11.14) is an exact result of the Liouville equation. Equation (11.14)'s simple appearance is somewhat deceiving because we have buried the N-body dynamics of the system in the memory kernal, $\underline{\underline{K}}(t')$.

One approximation which is often invoked when encountering equations similar to Eq. (11.14) is known as a Markovian approximation. Relying on the existence of a time scale separation, one argues that because $|\underline{A}\rangle$ contains the complete set of slow variables, then $\underline{\underline{K}}$ must decay to zero on the rapid time scale due to its definition as a tcf of the rapid fluxuating force, Eq. (11.11). Therefore, Eq. (11.14) can be approximated by

$$\frac{d}{dt}\langle\underline{A}(t)|\underline{A}\rangle = \{i\underline{\underline{\Omega}} - \underline{\underline{\Gamma}}\} \cdot \langle\underline{A}(t)|\underline{A}\rangle \quad (11.15)$$

where

$$\underline{\underline{\Gamma}} = \int_0^\infty dt' \, \underline{\underline{K}}(t') \quad (11.16)$$

is the relaxation matrix. Because the memory kernal, $\underline{\underline{K}}(t)$, is defined as a product of a static (time independent) part times a kinetic (time

dependent) part (refer to Eq. (11.11)), the quantity $\underline{\underline{\Gamma}}$ is also divided into a static part, $\underline{\underline{\chi}}$ (defined by Eq. (11.7)), and a kinetic part, $\underline{\underline{L}}$, as

$$\underline{\underline{\Gamma}} = \underline{\underline{L}} \cdot \underline{\underline{\chi}}^{-1} \quad . \tag{11.17}$$

Here, the kinetic part is defined by

$$\begin{aligned} \underline{\underline{L}} &= \beta \int_0^\infty dt' \langle \underline{F}_p(t') | \underline{F} \rangle \\ &= \beta \int_0^\infty dt' \langle \dot{\underline{A}} | e^{iQL^{(N)}t'} | \dot{\underline{A}} \rangle \quad . \end{aligned} \tag{11.18}$$

The kinetic part of $\underline{\underline{\Gamma}}$, $\underline{\underline{L}}$, represents a matrix of transport coefficients defined through the Green (99)-Kubo (100) relations.

We wish to discuss one last point. Mori showed that the transport coefficients, $\underline{\underline{L}}$, of the form

$$\underline{\underline{L}} = \beta \int_0^\infty dt' \langle \dot{\underline{A}} | e^{iQL^{(N)}t'} | \dot{\underline{A}} \rangle \quad , \tag{11.19}$$

is equivalent to the form

$$\underline{\underline{L}} = \beta \int_0^{\tau^+} dt' \langle \dot{\underline{A}} | e^{iL^{(N)}t'} | \dot{\underline{A}} \rangle \quad . \tag{11.20}$$

Here, τ^+ is a time which satisfies the inequality

$$\tau_{\dot{A}} \lesssim \tau^+ << \tau_A \tag{11.21}$$

where τ_A and $\tau_{\dot{A}}$ represent the typical relaxation times for the $|\underline{A}\rangle$ and the $|\dot{\underline{A}}\rangle$ variables, respectively (assumed to be widely separated). Consider the single variables case. Let this single slow variable be

denoted by $|a\rangle$, and further require (for convenience) that $\langle a|iL^{(N)}|a\rangle = 0$. Then, Eq. (11.14) for $|a\rangle$ is

$$\frac{d}{dt}\langle a|a(t)\rangle = -\int_0^t dt'(\langle \dot{a}|e^{iQL^{(N)}t'}|\dot{a}\rangle/\langle a|a\rangle)\langle a|a(t-t')\rangle \quad . \tag{11.22}$$

This reduces, in the Markovian limit, to

$$\frac{d}{dt}\langle a|a(t)\rangle = -\frac{1}{\tau_a}\langle a|a(t)\rangle \tag{11.23}$$

where

$$\frac{1}{\tau_a} = \int_0^\infty dt'\langle \dot{a}|e^{iQL^{(N)}t'}|\dot{a}\rangle/\langle a|a\rangle \quad . \tag{11.24}$$

By definition, the time rate of change of $\langle a|a(t)\rangle$ can also be written as

$$\frac{d}{dt}\langle a|a(t)\rangle = -\int_0^t dt'\langle \dot{a}|\dot{a}(t')\rangle \quad . \tag{11.25}$$

Equating Eqs. (11.21) and (11.24) at the time τ^+, we find that

$$\int_0^{\tau^+} dt'\langle \dot{a}|e^{iL^{(N)}t'}|\dot{a}\rangle\langle \dot{a}|\dot{a}\rangle^{-1} = \langle \dot{a}|\dot{a}\rangle^{-1}\int_0^{\tau^+} dt'\langle \dot{a}|e^{iQL^{(N)}t'}|\dot{a}\rangle\langle a|a\rangle^{-1} \times \langle a|a(\tau^+ - t')\rangle \quad . \tag{11.26}$$

Expanding the function $\langle a|a(\tau^+ - t')\rangle$ in a Taylor series

$$\langle a|a(\tau^+ - t')\rangle = \langle a|a\rangle - \frac{1}{2}(\tau^+ - t')^2\langle \dot{a}|\dot{a}\rangle + \ldots \quad , \tag{11.27}$$

and inserting this expansion into Eq. (11.25), we obtain

$$\int_0^{\tau^+} dt' \langle \dot{a}|e^{iL^{(N)}t'}|\dot{a}\rangle\langle\dot{a}|\dot{a}\rangle^{-1} = \int_0^{\infty} dt' \langle \dot{a}|e^{iQL^{(N)}t'}|\dot{a}\rangle\langle\dot{a}|\dot{a}\rangle^{-1} \times \{1 - (\frac{\tau^+}{\tau_a}) + \ldots\} \quad . \tag{11.28}$$

Therefore, the value of the transport coefficient for the Mori form,

$$L = \beta \int_0^{\infty} dt' \langle \dot{a}|e^{iQL^{(N)}t'}|\dot{a}\rangle\langle\dot{a}|\dot{a}\rangle^{-1} \quad , \tag{11.29}$$

can be gotten by integrating the true tcf of $|\dot{a}\rangle$ over a short initial period,

$$L = \beta \int_0^{\tau^+} dt' \langle \dot{a}|e^{iL^{(N)}t'}|\dot{a}\rangle\langle\dot{a}|\dot{a}\rangle^{-1} \quad . \tag{11.30}$$

The error made in this replacement is related to the ratio τ^+/τ_a, which is much less than unity for widely separated time scales.

The results listed here are extensively used in Chapters V and VI.

XII. APPENDIX C: THE TIME CORRELATION FUNCTION EXPRESSION FOR THE R PARAMETER

In this appendix, we discuss the Tsay and Kivelson (77) derivation of an expression for R using the Mori formalism. The final expression for R is Eq. (6.4a), which is used as the starting point in the work of Chapter VI. A similar derivation to the one discussed here can be found in Ref. 84.

We choose to examine a fluid whose only slowly relaxing quantities are

$$\mathcal{D}_{xz} = \sum_j [\hat{e}_j]^{(2)}_{xz} e^{ikx_j} \tag{12.1a}$$

and

$$g_z = \sum_j P_{zj} e^{ikx_j} \tag{12.1b}$$

where $\underline{\underline{\mathcal{D}}}$ and $\underline{g}$ represent the spatial Fourier transforms of the orientation and linear momentum densities, respectively. Here, P_{zj} is the z component of the linear momentum of particle j and $\mathcal{D}_{xz}$ is the xz component of $\underline{\underline{\mathcal{D}}}$. The wavevector, $\underline{k}$, is defined as the difference between the propagation vectors of the incoming beam ($\underline{k}_i$) and that of the scattered beam ($\underline{k}_f$), i.e., $\underline{k} = \underline{k}_f - \underline{k}_i$. Furthermore, $\underline{k}$ defines the $\hat{x}$ direction and $\underline{k}_i \times \underline{k}_f$ defines the $\hat{z}$ axis. Given this geometry, the only variables required for the calculation of R are those found in Eqs. (12.1a) and (12.1b) (77).

Because P_z is a conserved quantity, it can be shown that (in the small k limit)

$$\dot{g}_z = \frac{d}{dt} g_z = ik \sum_j \sigma_j e^{ikx_j} \tag{12.2}$$

where σ_j, which is related to the stress tensor, is given by

$$\begin{aligned} \sigma_j &= \frac{d}{dt} (\underline{r}_j \underline{p}_j)_{xz} \\ &= (\underline{\underline{\sigma}}_{K,j})_{xz} + \sum_q (\underline{\underline{\sigma}}_{V,jq})_{xz} \quad . \end{aligned} \tag{12.3}$$

Here, $\underline{\underline{\sigma}}_{K,j}$ and $\underline{\underline{\sigma}}_{V,jq}$ are given by

$$\underline{\underline{\sigma}}_{K,j} = m^{-1} \underline{p}_j \underline{p}_j \tag{12.4a}$$

and

$$\underline{\underline{\sigma}}_{V,jq} = \frac{1}{2} \underline{r}_{jq} \frac{\partial}{\partial \underline{r}_j} V_{jq} \tag{12.4b}$$

where $\underline{r}_{jq} = \underline{r}_q - \underline{r}_j$, and V_{jq} is the interaction potential between particles j and q.

Following the Mori method (outlined in Appendix B), using $\mathcal{D}_{xz}$ and g_z as the primary variables, we obtain the pair of transport equations for the tcfs

$$\begin{bmatrix} \langle \mathcal{D}_{xz} | \dot{\mathcal{D}}_{xz}(\omega) \rangle \\ \langle \mathcal{D}_{xz} | \dot{g}_z(\omega) \rangle \end{bmatrix} = \underline{\underline{T}}(\omega)^{-1} \begin{bmatrix} \langle \mathcal{D}_{xz} | \mathcal{D}_{xz}(\omega) \rangle \\ \langle \mathcal{D}_{xz} | g_z(\omega) \rangle \end{bmatrix} \tag{12.5}$$

where the Laplace transform, $A(\omega)$, is defined by

$$A(\omega) = \int_0^\infty dt\, e^{-\omega t} A(t) \quad . \tag{12.6}$$

Tsay and Kivelson show that the elements of the transport matrix, $\underline{\underline{T}}(\omega)$, in the small k and Markovian limits, reduce to:

$$T_{11}^{-1} = \Gamma_0 = \lim_{k\to 0} \sum_{j,q} \int_0^\infty dt \langle \dot{\mathcal{D}}_{xz,q} | e^{iQ_2 L^{(N)} t} | \dot{\mathcal{D}}_{xz,j} \rangle / \langle \mathcal{D}_{xz} | \mathcal{D}_{xz} \rangle \quad , \tag{12.7}$$

$$T_{22}^{-1} = k^2 \eta_{22}/\rho \quad , \tag{12.8}$$

$$T_{12}^{-1} = ik(\Gamma_0 \eta R/\rho)^{1/2} \gamma^{1/2} \quad , \tag{12.9}$$

and

$$T_{21}^{-1} = ik(\Gamma_0 \eta R/\rho)^{1/2} \gamma^{-1/2} \quad . \tag{12.10}$$

Here, ρ is the mass density, γ is the ratio

$$\gamma = \langle \mathcal{D}_{xz} | \mathcal{D}_{xz} \rangle / \langle g_z | g_z \rangle \quad , \tag{12.11}$$

and the quantity η_{22}, which is related to the viscosity, is given by

$$\eta_{22} = \lim_{k\to 0} (Vk_B T)^{-1} \sum_{j,q} \int_0^\infty dt \langle \sigma_q | e^{iQ_2 L^{(N)} t} | \sigma_j \rangle \tag{12.12}$$

where V is the volume of the system and k_B is Boltzmann's constant. The quantity η, the viscosity, is given by

$$\eta = \lim_{k\to 0} (Vk_B T)^{-1} \sum_{j,q} \int_0^\infty dt \langle \sigma_q | e^{iQ_g L^{(N)} t} | \sigma_j \rangle \quad . \tag{12.13}$$

The difference between η and η_{22} lies in their projected propagators, $\exp(iQ_g L^{(N)} t)$ versus $\exp(iQ_2 L^{(N)} t)$, where Q_g and Q_2 are

$$Q_g = 1 - P_g \tag{12.14a}$$

and

$$Q_2 = 1 - P_g - P_D \tag{12.14b}$$

and P_g and P_D are

$$P_g = |g_z\rangle\langle g_z|g_z\rangle^{-1}\langle g_z| \tag{12.15a}$$

and

$$P_D = |\mathcal{D}_{xz}\rangle\langle\mathcal{D}_{xz}|\mathcal{D}_{xz}\rangle^{-1}\langle\mathcal{D}_{xz}| \quad . \tag{12.15b}$$

Finally, the R parameter is given by

$$R = \lim_{k\to 0} |\{\sum_{jq}\int_0^\infty dt\langle\sigma_j|e^{iQ_2L^{(N)}t}|\dot{\mathcal{D}}_{xz,q}\rangle\}\{\sum_{jq}\int_0^\infty dt\langle\dot{\mathcal{D}}_{xz,q}|e^{iQ_2L^{(N)}t}|\sigma_j\rangle\}|$$

$$\times [\Gamma_0 n V k_B T\langle\mathcal{D}_{xz}|\mathcal{D}_{xz}\rangle]^{-1} \quad . \tag{12.16}$$

This is the final form for R. We choose to write Eq. (12.16) as

$$R = I_{13}I_{31}/\tilde{I}_{11}I_{33} \tag{12.17}$$

where

$$I_{13} = \int_0^\infty dt\langle\sigma_{xz}|e^{iQ_2L^{(N)}t}|\dot{\mathcal{D}}_{xz}\rangle \tag{12.18a}$$

$$I_{31} = \int_0^\infty dt \langle \dot{\mathcal{D}}_{xz} | e^{iQ_2 L^{(N)} t} | \sigma_{xz} \rangle \tag{12.18b}$$

$$\tilde{I}_{11} = \int_0^\infty dt \langle \sigma_{xz} | e^{iQ_g L^{(N)} t} | \sigma_{xz} \rangle \tag{12.18c}$$

$$I_{33} = \int_0^\infty dt \langle \dot{\mathcal{D}}_{xz} | e^{iQ_2 L^{(N)} t} | \dot{\mathcal{D}}_{xz} \rangle \tag{12.18d}$$

and

$$I_{11} = \int_0 dt \langle \sigma_{xz} | e^{iQ_2 L^{(N)} t} | \sigma_{xz} \rangle \quad . \tag{12.18e}$$

Here and after, all time correlation functions will be understood to be evaluated in the k→0 limit. The tilde on $\tilde{I}_{11}$ is a reminder that it is Q_g and not Q_2 which is contained in its definition.

Due to the isotropy of space, the shear-orientation coupling, as measured by R, is independent of the particular choice of the $\hat{z}$ (or $\hat{x}$) direction. Therefore, we can replace the I_{ij} integrals of Eq. (12.18), written

$$I_{ij} = \hat{z}\hat{x}\hat{x}\hat{z} \circledcirc^4 \int_0^\infty dt \langle \underline{\chi} \, e^{iQL^{(N)} t} \, \underline{\chi} \rangle \quad , \tag{12.19}$$

with their isotropic average, defined by

$$I_{ij} \quad \frac{1}{8\pi^2} \int d\hat{z} \int_{\perp \hat{z}} d\hat{x} \, I_{ij} \quad . \tag{12.20}$$

Here, the $\hat{x}$ integration is confined to lie in the plane perpendicular

to $\hat{z}$; the $\hat{z}$ integration is over the unit sphere. The result of averaging the $\hat{z}\hat{x}\hat{x}\hat{z}$ polyad is

$$\frac{1}{8\pi^2}\int d\hat{z}\int_{\perp\hat{z}} d\hat{x}\,\hat{z}\hat{x}\hat{x}\hat{z} = \frac{1}{10}\underline{\underline{\delta}}^{(2)} + \frac{3}{2}\underline{\underline{I}}^{(a)} \qquad (12.21)$$

where

$$(\underline{\underline{\delta}}^{(2)})_{ijk\ell} = \frac{1}{2}(\delta_{i\ell}\delta_{jk} + \delta_{ik}\delta_{j\ell}) - \frac{1}{3}\delta_{ij}\delta_{k\ell} \qquad (12.22a)$$

and

$$(\underline{\underline{I}}^{(a)})_{ijk\ell} = \frac{1}{2}(\delta_{i\ell}\delta_{jk} - \delta_{ik}\delta_{j\ell}) \quad . \qquad (12.22b)$$

By definition, $\underline{\underline{\delta}}^{(2)}$ projects out the traceless and symmetric part of a second rank tensor and $\underline{\underline{I}}^{(a)}$ projects out the antisymmetric part. We will ignore the term $3/2\ \underline{\underline{I}}^{(a)}$ in Eq. (12.21) for the following reason. The only I_{ij} integral where this term yields a nonvanishing contribution is the viscosity integral, $\tilde{I}_{11}$. Here, the integral resulting from $1/10\ \underline{\underline{\delta}}^{(2)}$ is the shear viscosity (η_s), whereas the integral resulting from $3/2\ \underline{\underline{I}}^{(a)}$ is the rotational viscosity (η_r). The ratio η_r/η_s is known to be small, on the order 10^{-3} (101). Therefore, we will neglect the rotational viscosity at this point to obtain

$$I_{13} = \int_0^\infty dt \langle \underline{\underline{\sigma}}^0 \circledcirc^2 e^{iQ_2 L^{(N)} t}\, \dot{\underline{\underline{D}}} \rangle \qquad (12.23a)$$

$$I_{31} = \int_0^\infty dt \langle \dot{\underline{\underline{D}}} \circledcirc^2 e^{iQ_2 L^{(N)} t}\, \underline{\underline{\sigma}}^0 \rangle \qquad (12.23b)$$

$$\tilde{I}_{11} = \int_0^\infty dt \langle \underline{\underline{\sigma}}^0 \circledast^2 e^{iQ_g L^{(N)} t} \underline{\underline{\sigma}}^0 \rangle \tag{12.23c}$$

$$I_{33} = \int_0^\infty dt \langle \dot{\underline{\underline{D}}} \circledast^2 e^{iQ_2 L^{(N)} t} \dot{\underline{\underline{D}}} \rangle \tag{12.23d}$$

and

$$I_{11} = \int_0^\infty dt \langle \underline{\underline{\sigma}}^0 \circledast^2 e^{iQ_2 L^{(N)} t} \underline{\underline{\sigma}}^0 \rangle \tag{12.23e}$$

where the 1/10 factors out of the expression for R. Equations (12.17) and (12.23) constitute the expression for R studied in Chapter VI.

An alternate expression for R, discussed in Chapter VI, is also given by Tsay and Kivelson (77) and Andersen and Pecora (84) in the small k limit. The alternate form,

$$R = (\eta - \eta_{22})/\eta \tag{12.24}$$

expresses R in terms of the shear viscosities, η and η_{22}. This is rewritten in terms of the I_{ij} integrals as

$$R = (\tilde{I}_{11} - I_{11})/\tilde{I}_{11} \quad . \tag{12.25}$$

In order to establish the equivalence of the two forms for R in the small k limit, it is most natural to proceed from Eq. (12.24)

$$\tilde{I}_{11} R = \tilde{I}_{11} - I_{11} \tag{12.26}$$

where $\tilde{I}_{11}$ and I_{11} are defined by Eqs. (12.18c) and (12.18e). Inserting the operator identity

$$e^{iQ_2L^{(N)}t} - e^{iQ_gL^{(N)}t} = -\int_0^t dt'\, e^{iQ_gL^{(N)}(t-t')}\, iP_DL^{(N)}\, e^{iQ_2L^{(N)}t'}, \tag{12.27}$$

into Eq. (12.16), we find that

$$\tilde{I}_{11}^R = \langle \mathcal{D}_{xz}|\mathcal{D}_{xz}\rangle^{-1}\{\int_0^\infty dt\langle \dot{\mathcal{D}}_{xz}|e^{iQ_2L^{(N)}t}|\sigma_{xz}\rangle\}\{\int_0^\infty dt\langle\sigma_{xz}|e^{iQ_gL^{(N)}t}|\mathcal{D}_{xz}\rangle\}. \tag{12.28}$$

Use of the definition of the P_D projection operator was made in writing the above relation. Already, this equation is very similar in form to Eq. (12.16). What remains is to relate

$$\int_0^\infty dt\langle\sigma_{xz}|e^{iQ_gL^{(N)}t}|\mathcal{D}_{xz}\rangle \tag{12.29}$$

to

$$\int_0^\infty dt\langle\sigma_{xz}|e^{iQ_2L^{(N)}t}|\dot{\mathcal{D}}_{xz}\rangle \quad . \tag{12.30}$$

Using the operator identity, Eq. (12.27), in the following form

$$e^{iQ_2L^{(N)}t}|\dot{\mathcal{D}}_{xz}\rangle = e^{iQ_gL^{(N)}t}|\dot{\mathcal{D}}_{xz}\rangle - \int_0^t dt'\, e^{iQ_gL^{(N)}(t-t')}\, iP_DL^{(N)} \times e^{iQ_2L^{(N)}t'}|\dot{\mathcal{D}}_{xz}\rangle \quad , \tag{12.31}$$

and taking the Markovian limit of this equation, we obtain

$$\int_0^\infty dt\langle\sigma_{xz}|e^{iQ_gL^{(N)}t}|\mathcal{D}_{xz}\rangle = \Gamma_0^{-1}\{\int_0^\infty dt\langle\sigma_{xz}|e^{iQ_2L^{(N)}t}|\dot{\mathcal{D}}_{xz}\rangle$$

$$- \int_0^\infty dt\langle\sigma_{xz}|e^{iQ_gL^{(N)}t}|\dot{\mathcal{D}}_{xz}\rangle \qquad (12.32)$$

where Γ_0 is defined by Eq. (12.7). In the small k limit, the second term on the RHS of Eq. (12.32) vanishes. This can be seen by first rewriting this term, with the aid of the identity

$$e^{iQ_gL^{(N)}t} = e^{iL^{(N)}t} - \int_0^t dt'\, e^{iL^{(N)}(t-t')}\, iP_gL^{(N)}\, e^{iQ_gL^{(N)}t}, \qquad (12.33)$$

as

$$\int_0^\infty dt\langle\sigma_{xz}|e^{iQ_gL^{(N)}t}|\dot{\mathcal{D}}_{xz}\rangle = \int_0^\infty dt\langle\sigma_{xz}|e^{iL^{(N)}t}|\dot{\mathcal{D}}_{xz}\rangle - \int_0^\infty dt \int_0^t dt'$$

$$\times \langle\sigma_{xz}|e^{iL^{(N)}(t-t')}\, iP_gL^{(N)}\, e^{iQ_gL^{(N)}t'}|\dot{\mathcal{D}}_{xz}\rangle \quad . \qquad (12.34)$$

Now, as Tsay and Kivelson have pointed out, $P_g iL^{(N)}|X\rangle \sim O(k)$ and, therefore, the second term on the RHS of Eq. (12.34) vanishes in the k = 0 limit. That the remaining term in this equation is zero follows from

$$\int_0^\infty dt\langle\sigma_{xz}|e^{iL^{(N)}t}|\dot{\mathcal{D}}_{xz}\rangle = -\int_0^\infty dt\langle iLr_xp_z|\dot{\mathcal{D}}_{xz}(t)\rangle$$

$$= \int_0^\infty dt\langle r_xp_z|\frac{d}{dt}\dot{\mathcal{D}}_{xz}(t)\rangle$$

$$= \langle r_x p_z | \dot{\mathcal{D}}_{xz}(0) \rangle - \langle r_x p_z | \dot{\mathcal{D}}_{xz}(\infty) \rangle = 0 \quad . \tag{12.35}$$

Here, the first term decays to zero and the second term is odd in the linear momentum. Thus,

$$\lim_{k \to 0} \int_0^\infty dt \langle \sigma_{xz} | e^{iQ_g L^{(N)} t} | \dot{\mathcal{D}}_{xz} \rangle = 0 \quad . \tag{12.36}$$

With the aid of Eqs. (12.36) and (12.32), Eq. (12.28) becomes

$$R = I_{13} I_{31} / \tilde{I}_{11} I_{33}$$

which is the alternate expression for R. Therefore, in the small k limit, the two forms for R are equivalent.

XIII. APPENDIX D: TABULATION OF THE INTEGRALS REQUIRED FOR THE CALCULATION OF THE R PARAMETER

This appendix consists of a listing of the integrals required for the calculation of the R parameter of Chapter VI. The reduced quantities and integrals are denoted with a tilde. The quantities $\tilde{S}$, $\tilde{h}_i$, $\tilde{h}_i'$, $\tilde{h}_i''$ are defined by

$$S = C^2 \tilde{S} \tag{13.1a}$$

$$h_i = C \tilde{h}_i \tag{13.1b}$$

$$h_i' = C \varepsilon \tilde{h}_i' \tag{13.1c}$$

and

$$h_i'' = C \varepsilon \tilde{h}_i'' \tag{13.1d}$$

where h_i is the supporting function of the ith body, and $h_i'(x)$ and $h_i''(x)$ are the first and second derivatives of the supporting function with respect to x. Here B and C are the major and minor axes of the ellipse modeling the diatom,

$$\varepsilon = (B^2 - C^2)/C^2 \quad , \tag{13.2}$$

is the shape anisotropy of the diatom,

$$\rho^* = n(4\pi C^2 B/3) \quad , \tag{13.3}$$

is the reduced density, and

$$\kappa_{dd} = I/\mu C^2 \quad . \tag{13.4}$$

The reduced integrals, defined to be unitless and nonvanishing in the limit $\varepsilon \to 0$, are

$$(1)\quad K_{11} = (2kT/\mu)^{1/2} C^2 \{(1/30\sqrt{\pi}) \int dx_1 dx_2 d\alpha \chi \tilde{S}(5D^{-1} - 2D^{-3})\}$$

$$= (2kT/\mu)^{1/2} C^2 \tilde{K}_{11} \tag{13.5}$$

$$(2)\quad K_{12} = (2kT/\mu)^{1/2} C^2 \varepsilon^2 \kappa_{dd}^{-1} \{(1/30\sqrt{\pi}) \int dx_1 dx_2 d\alpha \chi S D^{-3} [\tilde{h}_1'^2 (1 - x_1^2)$$

$$+ \tilde{h}_2'^2 (1 - x_2^2)]\}$$

$$= (2kT/\mu)^{1/2} C^2 \varepsilon^2 \kappa_{dd}^{-1} \tilde{K}_{12} \tag{13.6}$$

$$(3)\quad K_{13} = (2kT/\mu)^{1/2} C^2 \varepsilon \kappa_{dd}^{-1} \{-(1/40) \int dx_1 dx_2 d\alpha \chi \tilde{S} D^{-2} [\tilde{h}_1' x_1 (1 - x_1^2)$$

$$+ \tilde{h}_2' x_2 (1 - x_2^2)]$$

$$= (2kT/\mu)^{1/2} C^2 \varepsilon \kappa_{dd}^{-1} \tilde{K}_{13} \tag{13.7}$$

$$(4)\quad K_{22} = (2kT/\mu)^{1/2} D^2 \varepsilon^2 \kappa_{dd}^{-1} \{(1/30\sqrt{\pi}) \int dx_1 dx_2 d\alpha \chi \tilde{S} D^{-1} \tilde{h}_1'^2 (1 - x_1^2)$$

$$\times [7 + \varepsilon^2 \kappa_{dd}^{-1} D^{-2} (2\tilde{h}_2'^2 (1 - x_2^2)(1 - 3\cos^2\alpha) - 4\tilde{h}_1'^2 (1 - x_1^2))]\}$$

$$= (2kT/\mu)^{1/2} C^2 \varepsilon^2 \kappa_{dd}^{-1} \tilde{K}_{22} \tag{13.8}$$

$$(5)\quad K_{23} = (2kT/\mu)^{1/2} C^2 \varepsilon^3 \kappa_{dd}^{-3/2} \{(1/20) \int dx_1 dx_2 d\alpha \chi \tilde{S} D^{-2}$$

$$\times \tilde{h}_1'^2 \tilde{h}_2' x_1 (1 - x_1^2)(1 - x_2^2) \sin^2\alpha\}$$

$$= (2kT/\mu)^{1/2} C^2 \varepsilon^3 \kappa_{dd}^{-3/2} \tilde{K}_{23} \tag{13.9}$$

$$(6)\quad K_{33} = (2kT/\mu)^{1/2}C^2\varepsilon^2\kappa_{dd}^{-1}\{(1/20\sqrt{\pi})\int dx_1dx_2d\alpha\chi\tilde{S}D^{-1}[\tilde{h}_1'^2(1-x_1^2)$$

$$+ 2\tilde{h}_1'\tilde{h}_2'x_1x_2(1-x_1^2)(1-x_2^2)(1+\cos^2\alpha) + \tilde{h}_1'\tilde{h}_2'(2x_1^2-1)(2x_2^2-1)$$

$$\times\sqrt{(1-x_1^2)(1-x_2^2)}\cos\alpha]\}$$

$$= (2kT/\mu)^{1/2}C^2\varepsilon^2\kappa_{dd}^{-1}\tilde{K}_{33} \qquad (13.10)$$

$$(7)\quad \lambda_V(\underline{W}^0\underline{W}) = (\rho^*/\sqrt{1+\varepsilon})\{(1/40\pi)\int dx_1dx_2d\alpha\chi\tilde{S}D^{-2}(\tilde{h}_1+\tilde{h}_2)\}$$

$$= (\rho^*/\sqrt{1+\varepsilon})\tilde{\lambda}_V(\underline{W}^0\underline{W}) \qquad (13.11)$$

$$(8)\quad \lambda_V(\underline{\Omega}^0\Omega) = (\rho^*/\sqrt{1+\varepsilon})\{-(3/80\pi)\int dx_1dx_2d\alpha\chi\tilde{S}[(\tilde{h}_1+\tilde{h}_2)$$

$$\times(x_1^2 - 1/3 + (1/3)\varepsilon^2\kappa_{dd}^{-1}D^{-2}\tilde{h}_1'^2(1-x_1^2) + \varepsilon x_1(\tilde{h}_1'(1-x_1^2)$$

$$+ \tilde{h}_2'\sqrt{(1-x_1^2)(1-x_2^2)}\cos\alpha)]\}$$

$$= (\rho^*/\sqrt{1+\ })\tilde{\lambda}_V(\underline{\Omega}^0\underline{\Omega}) \qquad (13.12)$$

$$(9)\quad \lambda_V(\underline{\Omega}x\hat{e}^0\hat{e}) = (\rho^*/\sqrt{1+\varepsilon})\varepsilon\kappa_{dd}^{-1/2}\{-(3/40\pi^{3/2})\int dx_1dx_2d\alpha\chi\tilde{S}D^{-1}$$

$$\times\tilde{h}_1'[-2x_1(1-x_1^2)(\tilde{h}_1+\tilde{h}_2) + \varepsilon(2x_1^2-1)(\tilde{h}_1'(1-x_1^2)$$

$$+ \tilde{h}_2'\sqrt{(1-x_1^2)(1-x_2^2)}\cos\alpha]\}$$

$$= (\rho^*/\sqrt{1+\varepsilon})\varepsilon\kappa^{-1/2}\tilde{\lambda}_V(\underline{\Omega}x\hat{e}^0\hat{e}) \qquad (13.13)$$

$$(10)\quad \lambda_V(\underline{r}^0\underline{p}) = (\rho^*/\sqrt{1+\varepsilon})C\sqrt{mkT}\{(3/40\pi^{3/2})\int dx_1dx_2d\alpha\chi\tilde{S}D^{-3}$$

$$\times\,[(2/3)(\tilde{h}_1+\tilde{h}_2)^2 + \varepsilon^2(1/2)(\tilde{h}_1'^2(1-x_1^2) + \tilde{h}_2'^2(1-x_2^2)$$

$$+\,2\tilde{h}_1'\tilde{h}_2'\sqrt{(1-x_1^2)(1-x_2^2)}\,\cos\alpha)]\}$$

$$= (\rho^*/\sqrt{1+\varepsilon})C\sqrt{mkT}\;\tilde{\lambda}_V(\underline{r}^0\underline{p}) \qquad (13.14)$$

$$(11)\quad h_u^{(1)} = (\rho^*/\sqrt{1+\varepsilon})\{(1/40\pi)\int dx_1dx_2d\alpha\chi\tilde{S}D^{-2}(\tilde{h}_1+\tilde{h}_2)$$

$$= (\rho^*/\sqrt{1+\varepsilon})\tilde{h}_u^{(1)} \qquad (13.15)$$

$$(12)\quad h_u^{(2)} = (\rho^*/\sqrt{1+\varepsilon})\varepsilon^2\kappa_{dd}^{-1}\{-(1/40\pi)\int dx_1dx_2d\alpha\tilde{S}\chi D^{-2}(\tilde{h}_1+\tilde{h}_2)\tilde{h}_1'^2(1-x_1^2)\}$$

$$= (\rho^*/\sqrt{1+\varepsilon})\varepsilon^2\kappa_{dd}^{-1}\tilde{h}_u^{(2)} \quad . \qquad (13.16)$$